



**Synthesis of Limonene and Styrene Carbonate via  
CO<sub>2</sub> Cycloaddition.**

A thesis presented for the degree of

*Doctor of Philosophy*

by

**Abdul Rehman**

School of Engineering,  
Newcastle University, United Kingdom

November 2019



## Abstract

Global concerns about high CO<sub>2</sub> levels and the dwindling supply of fossil resources are increasing. As a consequence, the utilization of CO<sub>2</sub> and waste biomass as renewable resources into valuable products is highly desirable as part of a sustainable future of the chemical process industry. Synthesis of cyclic carbonates by CO<sub>2</sub> cycloaddition to epoxides is a highly promising reaction in terms of “green chemistry” due to its 100% atom-economy.

This work reports bio-based limonene carbonate (LC) synthesis by CO<sub>2</sub> cycloaddition to terpene-derived limonene oxide (LO). The reaction was carried out with high stereoselectivity using commercially available, inexpensive tetrabutylammonium chloride (TBAC) as a homogeneous catalyst. High yield (86%) of limonene carbonate (LC) was obtained at 140 °C, 40 bar CO<sub>2</sub> pressure using 6 mol% TBAC after 20 h. Moreover, the detailed study of reaction kinetics revealed first order dependence with respect to LO, CO<sub>2</sub> and TBAC concentrations. Bio-derived cyclic carbonates are of significant research interest as building blocks for non-isocyanate polyurethanes (NIPUs).

Synthesis of cyclic carbonate from epoxide and CO<sub>2</sub> is a typical gas-liquid multiphase catalytic process involving a gas-liquid mass transfer in the reactor and catalytic cycloaddition reaction in the liquid phase. Therefore, it was anticipated that an efficient reactor design and a continuous flow approach could mitigate many of the limitations observed in the batch reactor. In this study, a continuous styrene carbonate (SC) synthesis from styrene oxide (SO) and CO<sub>2</sub> was demonstrated in a ‘tube-in-tube’ gas-liquid reactor. The exceptionally high permeation of CO<sub>2</sub> through the membrane, combined with the high surface area to volume ratio resulted in the quantitative conversion of SO in a significantly reduced reaction time i.e. 45 min at 120 °C and 6 bar *p* (CO<sub>2</sub>) using a 1:4 ZnBr<sub>2</sub>/TBAB catalyst ratio.

Synthesis of SC was also investigated in the presence of pyrrolidinopyridinium iodide (PPI) in combination with zinc halides (ZnX<sub>2</sub>) as a binary homogeneous catalyst system. The synergistic effect between PPI and ZnI<sub>2</sub> resulted in a ~10-fold increase in the reaction rate compared to using PPI alone as a catalyst. The potential for the carbonation reaction was further intensified by heterogenising the PPI onto silica. An increase in catalytic activity was observed due to the synergistic effect between halide anion and acidic Si–OH (silanol) surface. In all cases, the detailed studies of reaction kinetics were carried out to determine the corresponding kinetic values (*k* and *E<sub>a</sub>*) and thermodynamic activation parameters ( $\Delta H^\ddagger$ ,  $\Delta S^\ddagger$  and  $\Delta G^\ddagger$ ).



## Acknowledgments

First and foremost, I would like to express my sincere gratitude and appreciation to my supervisors Prof. Adam Harvey, Dr. Valentine C. Eze and Dr. Ana María López-Fernández for their kind supervision and continuous support throughout my Ph.D. Their immense knowledge in the design of experiments, critical analysis of data and vast experience of scientific writing and communication were invaluable for my development during the Ph.D. I could not have imagined better advisors and mentors.

I would like to express my special thanks to my parents (Muhammad Ashraf and Parveen Akhtar), my siblings (Irfan Ashraf and Wardah Ashraf), my beloved wife (Bushra Shaheen) and my son (Aksam Rehman) for their enormous support, prayers, and encouragement throughout this period. My special thanks to all of my friends for their continuous support.

I would also like to acknowledge:

- University of Engineering and Technology, Lahore, Pakistan for providing financial support to complete my Ph.D. at Newcastle University, UK.
- Engineering and Physical Science Research Council (EPSRC), UK for funding the ‘Sustainable Polymers’ project (grant no. EP/L017393).
- Dr. Michael Carrol, School of Chemistry, Newcastle University for giving me the opportunity to perform a part of my experimental work in his lab.
- Dr. Corrine Wills, School of Chemistry, Newcastle University for her support to perform NMR analysis.
- Dr. Andrea Laybourn, Nanoscale and Microscale Research Centre at the University of Nottingham for her support in the characterisation of heterogeneous catalyst
- Process Intensification Group, Newcastle University for their support and feedback.
- Dr. Ian Ingram, Department of Chemistry, York University, for his insightful comments.
- CEAM technical and IT staff for their support.



## Table of Contents

Abstract.....	i
Acknowledgments .....	iii
List of Publications and Conferences .....	x
List of Schemes .....	xii
List of Figures.....	xvi
List of Tables .....	xxii
List of Abbreviations .....	xxvi
List of Nomenclature .....	xxx
Chapter 1 Introduction .....	1
1.1 Background.....	1
1.2 Cyclic carbonate synthesis by CO <sub>2</sub> cycloaddition to epoxides .....	2
1.3 Catalyst systems for CO <sub>2</sub> cycloaddition to epoxides.....	3
1.4 Bio-based cyclic carbonate synthesis .....	5
1.5 Cyclic carbonate synthesis in continuous flow reactors.....	6
1.6 Kinetics study of cyclic carbonate synthesis .....	7
1.7 Aims and objectives .....	8
Chapter 2 Literature review.....	9
2.1 Introduction .....	9
2.2 Organic carbonates .....	10
2.2.1 Acyclic carbonate synthesis .....	10
2.2.2 Polycarbonates synthesis .....	11
2.3 Cyclic carbonate synthesis .....	13
2.3.1 Cyclic carbonates synthesis from CO <sub>2</sub> and epoxides .....	15
2.3.2 Cyclic carbonate synthesis from CO <sub>2</sub> and 1,2-diols .....	16

2.3.3	Cyclic carbonate synthesis by oxidative carboxylation of alkenes.....	17
2.4	Applications of cyclic carbonates .....	20
2.5	Epoxides as substrates for cyclic carbonate synthesis .....	21
2.6	Reaction conditions for cyclic carbonates synthesis.....	22
2.6.1	Temperature .....	23
2.6.2	CO <sub>2</sub> pressure .....	23
2.6.3	Co-catalyst .....	23
2.6.4	Solvent .....	26
2.7	Stereochemical information of cyclic carbonates .....	26
2.8	Catalytic systems for CO <sub>2</sub> cycloaddition to epoxides .....	28
2.9	Organocatalysts .....	29
2.9.1	Ammonium salt-based catalysts.....	30
2.9.2	Phosphonium salts as homogeneous and heterogeneous catalysts .....	35
2.9.3	Imidazolium salts as homogeneous and heterogeneous catalysts.....	37
2.9.4	Hydrogen bond donor-based organocatalysts .....	40
2.9.5	Metal-based complexes.....	42
2.10	Cyclic carbonate synthesis from internal epoxides.....	51
2.11	Cyclic carbonates synthesis from bio-based epoxides.....	54
2.12	Kinetics study of cyclic carbonates synthesis using heterogeneous catalysts .....	56
2.13	Kinetics study of cyclic carbonate synthesis using homogeneous catalysts.....	57
2.13.1	Eley-Rideal (ER) mechanism.....	59
2.13.2	Langmuir-Hinshelwood (LH) mechanism .....	61
2.13.3	Diffusion limitations in heterogeneous catalysis .....	62
2.14	Flow chemistry.....	63
2.15	Cyclic carbonate synthesis under continuous flow conditions .....	64
2.16	Teflon <sup>®</sup> AF-2400-based ‘tube-in-tube’ gas-liquid reactor.....	67
2.17	Summary .....	70
Chapter 3	Materials and methods .....	73

3.1	Introduction .....	73
3.2	Materials .....	74
3.3	Experimental setup .....	76
3.3.1	Semi-batch reactor .....	76
3.3.2	Tube-in-tube gas-liquid reactor .....	77
3.4	Experimental procedures .....	79
3.4.1	Cyclic carbonate synthesis in a semi-batch reactor .....	79
3.4.2	Cyclic carbonate synthesis in a 'tube-in-tube' gas/liquid reactor .....	80
3.4.3	Kinetic experiments for CO <sub>2</sub> cycloaddition to epoxides .....	80
3.4.4	General procedure for epoxidation of ( <i>R</i> )-(+)-limonene .....	81
3.4.5	Preparation of homogeneous pyrrolidinopyridinium iodide catalyst .....	83
3.4.6	Preparation of silica-supported pyrrolidinopyridinium iodide catalyst .....	84
3.5	Characterization of silica-supported pyrrolidinopyridinium iodide (SiO <sub>2</sub> -PPI) .....	84
3.5.1	Solid-state <sup>13</sup> C CP MAS NMR .....	85
3.5.2	BET analysis .....	86
3.5.3	Elemental analysis .....	87
3.5.4	XRD analysis .....	88
3.6	Homogeneous kinetics for CO <sub>2</sub> cycloaddition to epoxide .....	89
3.7	Heterogeneous kinetics for CO <sub>2</sub> cycloaddition to epoxides .....	90
3.8	Determination of kinetic and thermodynamic activation parameters .....	92
3.9	Analytical techniques .....	94
3.9.1	FTIR spectroscopy .....	94
3.9.2	Gas chromatography (GC) .....	97
3.9.3	<sup>1</sup> H NMR spectroscopy .....	101
Chapter 4 Bio-based cyclic carbonates synthesis from limonene oxide (LO) and CO <sub>2</sub> catalysed by tetrabutylammonium chloride (TBAC) .....		
4.1	Introduction .....	103
4.2	Effect of halide anion on CO <sub>2</sub> cycloaddition to LO .....	103
4.3	Stereoselective epoxidation of ( <i>R</i> )-(+)-limonene .....	105

4.4	Effect of reaction parameters on CO <sub>2</sub> cycloaddition to LO .....	105
4.5	Selection of solvent .....	107
4.6	Kinetics study of CO <sub>2</sub> cycloaddition to LO catalysed by TBAC .....	109
4.6.1	Reaction order with respect to [LO] .....	110
4.6.2	Reaction order with respect to [TBAC] .....	112
4.6.3	Reaction order with respect to [CO <sub>2</sub> ] .....	113
4.6.4	Temperature dependence and determination of activation parameters .....	114
4.7	Proposed reaction mechanism .....	117
4.8	Summary .....	118
Chapter 5 Continuous styrene carbonate (SC) synthesis from styrene oxide (SO) and CO <sub>2</sub> in a 'tube-in-tube' gas-liquid flow reactor .....		
5.1	Introduction .....	119
5.2	Effect of halide anion activity and catalyst loading .....	119
5.3	Effect of reaction parameters in a continuous flow reactor .....	121
5.4	Kinetics study of CO <sub>2</sub> cycloaddition to SO catalysed by TBAB/ZnBr <sub>2</sub> .....	122
5.4.1	Reaction order with respect to [TBAB] .....	125
5.4.2	Reaction order with respect to [CO <sub>2</sub> ] .....	126
5.4.3	Reaction order with respect to [ZnBr <sub>2</sub> ] .....	128
5.4.4	Temperature dependence and determination of activation parameters .....	129
5.5	Proposed reaction mechanism .....	131
5.6	Summary .....	132
Chapter 6 Styrene carbonate (SC) synthesis by CO <sub>2</sub> cycloaddition to styrene oxide (SO) using pyrrolidinopyridinium iodide (PPI) and zinc halides (ZnX <sub>2</sub> ) .....		
6.1	Introduction .....	133
6.2	Effect of zinc halide anions activity on CO <sub>2</sub> cycloaddition to SO .....	133
6.3	Kinetics study of CO <sub>2</sub> cycloaddition to SO catalysed by PPI/ZnI <sub>2</sub> catalyst .....	135
6.3.1	Reaction order with respect to epoxide .....	136
6.3.2	Reaction order with respect to catalyst .....	138

6.3.3	Reaction order with respect to CO <sub>2</sub> .....	140
6.3.4	Temperature dependence and determination of activation parameters .....	142
6.4	Proposed reaction mechanism .....	144
6.5	Summary.....	145
Chapter 7 Styrene carbonate (SC) synthesis from styrene oxide (SO) and CO <sub>2</sub> using silica-supported pyrrolidinopyridinium iodide (SiO <sub>2</sub> -PPI) .....		146
7.1	Introduction .....	146
7.2	Mixing dependence.....	146
7.3	Reusability of SiO <sub>2</sub> -PPI.....	147
7.4	Effect of internal mass transfer limitations.....	148
7.5	Kinetics study of CO <sub>2</sub> cycloaddition to SO using SiO <sub>2</sub> -PPI catalyst .....	149
7.6	Determination of the reaction orders with respect to SO, CO <sub>2</sub> and SiO <sub>2</sub> -PPI.....	152
7.7	Proposed reaction mechanisms.....	155
7.8	Summary.....	156
Chapter 8 Conclusions and Further Work .....		157
8.1	Conclusions .....	157
8.2	Further work .....	162
References .....		165
Chapter 9 Appendices .....		193
Appendix A.....		193
Appendix B.....		197
Appendix C.....		200
Appendix D .....		202

## List of Publications and Conferences

### Publications

- 1- **Rehman, A.**, Fernández, A.M.L., Resul, M.F.M.G. and Harvey, A. (2019) 'Highly selective, sustainable synthesis of limonene cyclic carbonate from bio-based limonene oxide and CO<sub>2</sub>: A kinetic study', *Journal of CO<sub>2</sub> Utilization*, 29, pp. 126-133.
- 2- **Rehman, A.**, Fernandez, A.M.L., Resul, M.F.M.G. and Harvey, A. (2018) 'Kinetic investigations of styrene carbonate synthesis from styrene oxide and CO<sub>2</sub> using a continuous flow tube-in-tube gas-liquid reactor', *Journal of CO<sub>2</sub> Utilization*, 24, pp. 341-349.
- 3- **Rehman, A.**, Eze, V.C., Resul, M.F.M.G. and Harvey, A. (2018) 'Kinetics and mechanistic investigation of epoxide/CO<sub>2</sub> cycloaddition by a synergistic catalytic effect of pyrrolidinopyridinium iodide and zinc halides', *Journal of Energy Chemistry*.
- 4- Resul, M.F.M.G., Fernández, A.M.L., **Rehman, A.**, and Harvey, A.P. (2018) 'Development of a selective, solvent-free epoxidation of limonene using hydrogen peroxide and a tungsten-based catalyst', *Reaction Chemistry & Engineering*, 3(5), pp. 747-756.
- 5- Durkin, A., Tapygin, I., Mukhtar, G.R.M.F., **Rehman, A.**, Kong, Q., Lopez, F.A.M., Harvey, A., Shah, N. and Guo, M. 'Scale-up and sustainability evaluation of biopolymer production from citrus waste offering carbon capture and utilisation pathway', *ChemistryOpen*, ISSN: 2191-1363.
- 6- **Rehman, A.**, Eze, V.C., Resul, M.F.M.G. and Harvey, A. (2019) 'A kinetic study of Zn halide/TBAB-catalysed fixation of CO<sub>2</sub> with styrene oxide in propylene carbonate', *Green processing and synthesis*, (8) pp. 719–729.

### Conference Presentations

- 1- **Rehman, A.**, Fernández, A.M.L. and Harvey, A. 'Synthesis of cyclic carbonates from epoxides and CO<sub>2</sub> in a continuous tube-in-tube flow reactor'. Poster presented at 5<sup>th</sup> Conference on Carbon Dioxide as Feedstock for Fuels, Chemistry and Polymers, 6-7 December 2016, Maternushaus, Cologne, Germany.

- 2- **Rehman, A.**, Fernández, A.M.L., and Harvey, A. ‘Intensification of cyclic carbonate synthesis from epoxides and CO<sub>2</sub> using tube-in-tube gas/liquid microreactor’. Oral communication presented at the 10<sup>th</sup> World Congress of Chemical Engineering (WCCE), 1<sup>st</sup> –5<sup>th</sup> October 2017, Barcelona, Spain.
- 3- **Rehman, A.**, Fernández, A.M.L. and Harvey, A. ‘Catalytic synthesis of cyclic carbonates from CO<sub>2</sub> and renewable terpene-based epoxides: Batch to Continuous?’. Oral communication presented at the 4<sup>th</sup> International Symposium on Green Chemistry (ISGC), 2017, La Rochelle, France.
- 4- **Rehman, A.**, Fernández, A.M.L. and Harvey, A. ‘Synthesis of cyclic carbonates from epoxides and CO<sub>2</sub> in a continuous tube-in-tube flow reactor’. Poster presented at 5<sup>th</sup> Conference on Carbon Dioxide as Feedstock for Fuels, Chemistry and Polymers, 6-7 December 2016, Maternushaus, Cologne, Germany.
- 5- **Rehman, A.**, Fernández, A.M.L., and Harvey, A. ‘on “Kinetic study of cyclic carbonate synthesis from epoxides and CO<sub>2</sub> in the presence of propylene carbonate as a green solvent”’. Oral communication presented at the 6<sup>th</sup> international congress on Green Process Engineering (GPE), 3-6 June 2018, Toulouse, France.

## List of Schemes

### Chapter 1

Scheme 1.1 Synthesis of cyclic carbonates from epoxides and CO<sub>2</sub>. ..... 3

### Chapter 2

Scheme 2.1 Synthesis of acyclic carbonates via cyclic carbonates route. .... 10

Scheme 2.2 Synthesis of polycarbonates from epoxides and CO<sub>2</sub>. .... 12

Scheme 2.3 General reaction mechanism of polycarbonate synthesis from epoxides and CO<sub>2</sub> (Martin *et al.*, 2015). .... 12

Scheme 2.4 Synthesis of cyclic carbonates from (1) diols and phosgene (2) diols and dialkyl carbonates/urea (3) epoxides and CO<sub>2</sub>. .... 14

Scheme 2.5 Different routes for cyclic carbonate formation with CO<sub>2</sub> emitted per unit of carbonate produced (Aresta *et al.*, 2013). .... 14

Scheme 2.6 General mechanism of cyclic carbonate synthesis using an acid-base catalyst system (Cokoja *et al.*, 2015). .... 15

Scheme 2.7 Cyclic carbonate synthesis from 1,2-diols and CO<sub>2</sub> using benzonitrile as a solvent. .... 16

Scheme 2.8 Oxidative carboxylation of alkenes to form cyclic carbonates. .... 17

Scheme 2.9 Reaction mechanism of oxidative carboxylation of styrene (Sun *et al.*, 2004a). 18

Scheme 2.10 Oxidative carboxylation of cyclohexene to form cyclohexene carbonate. .... 18

Scheme 2.11 General reaction of alkenes epoxidation in the presence of an oxidant. .... 21

Scheme 2.12 Petroleum-based epoxides as substrates for cyclic carbonate synthesis. .... 22

Scheme 2.13 Terpene-based epoxides as substrates for bio-based cyclic carbonates synthesis. .... 22

Scheme 2.14 Structures of some commonly used co-catalysts for cyclic carbonate and polycarbonate synthesis. .... 24

Scheme 2.15 Epoxide ring-opening positions in case of terminal epoxide and possible back-biting reactions resulting in a cyclic carbonate formation. .... 27

Scheme 2.16 General reaction mechanism for CO <sub>2</sub> cycloaddition to 2,3-disubstituted epoxide with formal retention of configuration (Martin <i>et al.</i> , 2015).....	28
Scheme 2.17 General mechanism for cyclic carbonate synthesis by CO <sub>2</sub> cycloaddition to epoxide catalysed by tetrabutylammonium halides (TBAX). .....	31
Scheme 2.18 General mechanism for cyclic carbonate synthesis catalysed by TBAX in conjunction with HBDs. ....	32
Scheme 2.19 Structure of nitrogen donor bases used as catalysts for cyclic carbonate synthesis. ....	33
Scheme 2.20 Proposed reaction mechanism for cyclic carbonate synthesis using SiO <sub>2</sub> -supported phosphonium salt as a heterogeneous catalyst (Takahashi <i>et al.</i> , 2006).....	36
Scheme 2. 21 Proposed reaction mechanisms for cyclic carbonate synthesis using ILs as catalysts (Jutz <i>et al.</i> , 2010). ....	37
Scheme 2.22 Structures of some commonly used imidazolium-based ILs as catalysts for cyclic carbonate synthesis. ....	38
Scheme 2.23 General reaction mechanism for CO <sub>2</sub> cycloaddition to epoxides catalysed by the monometallic complex. ....	42
Scheme 2.24 Structure of Al (III) salen complex as a catalyst for cyclic carbonate synthesis.	44
Scheme 2.25 Structure of bimetallic Al (III) salen complex as a catalyst for cyclic carbonate synthesis (Melendez <i>et al.</i> , 2007). ....	44
Scheme 2.26 Structure of bimetallic Al (III) salen complex as a one-component bifunctional catalyst (Melendez <i>et al.</i> , 2009).....	45
Scheme 2.27 Structure of Al (III) amino triphenolate complex as a catalyst for cyclic carbonate synthesis. ....	47
Scheme 2.28 General reaction mechanism for CO <sub>2</sub> cycloaddition to epoxides catalysed by Zn-salts in combination with ILs.....	50
Scheme 2.29 Switch in selectivity towards CHC and PCHC using Zn (II) salphen complex under different reaction conditions. ....	52

Scheme 2.30 Reaction scheme for terpene-based NIPUs formation from limonene (Bähr <i>et al.</i> 2012). .....	55
Scheme 2.31 Reaction mechanism for CO <sub>2</sub> cycloaddition to epoxides catalysed by bimetallic Al (III) salen complex in combination with TBAB (Clegg <i>et al.</i> (2010a)). .....	58
Scheme 2.32 Chemical structure of Teflon <sup>®</sup> AF-2400 membrane. ....	67
Scheme 2.33 General mechanism of CO <sub>2</sub> cycloaddition to epoxides by two possible pathways: (Cycle 1) epoxide activation as an initial step, (Cycle 2) CO <sub>2</sub> activation as an initial step (Shaikh <i>et al.</i> , 2017). .....	71
<b>Chapter 3</b>	
Scheme 3.1 Stereoselective epoxidation of ( <i>R</i> )-(+)-limonene using N-bromosuccinimide (NBS). .....	81
Scheme 3.2 Preparation of homogeneous pyrrolidinopyridinium iodide (PPI) catalyst. ....	83
Scheme 3.3 Preparation of silica-supported pyrrolidinopyridinium iodide (SiO <sub>2</sub> -PPI) catalyst. ....	84
<b>Chapter 4</b>	
Scheme 4.1 Epoxidation of ( <i>R</i> )-(+)-limonene and subsequent limonene carbonate (LC) synthesis via CO <sub>2</sub> cycloaddition to limonene oxide (LO). ....	104
Scheme 4.2 Stereoselective epoxidation of ( <i>R</i> )-(+)-limonene using N-bromosuccinimide. .	105
Scheme 4.3 Proposed reaction mechanism of cyclic carbonate synthesis from tri-substituted epoxide and CO <sub>2</sub> . .....	117
<b>Chapter 5</b>	
Scheme 5.1 Chemical reaction for styrene carbonate (SC) synthesis from styrene oxide (SO) and CO <sub>2</sub> . ....	124
Scheme 5.2 Proposed reaction mechanism of styrene carbonate (SC) formation from styrene oxide (SO) and CO <sub>2</sub> catalysed by TBAB/ZnBr <sub>2</sub> as an acid-base binary homogeneous catalyst. ....	131
<b>Chapter 6</b>	
Scheme 6.1 Styrene carbonate (SC) synthesis by CO <sub>2</sub> cycloaddition to styrene oxide (SO) in the presence of PPI/ZnX <sub>2</sub> as a binary homogeneous catalyst. ....	133

Scheme 6.2 Proposed reaction mechanism for styrene carbonate (SC) formation catalysed by PPI and ZnI <sub>2</sub> . .....	144
---	-----

## **Chapter 7**

Scheme 7.1 Proposed mechanism of SC formation based on the reaction of adsorbed SO with CO <sub>2</sub> in the bulk stream. ....	155
--	-----

## List of Figures

### Chapter 2

Figure 2.1 Teflon<sup>®</sup> AF-2400 based ‘tube-in-tube’ gas-liquid reactor..... 67

### Chapter 3

Figure 3.1 Experimental setup for cyclic carbonate synthesis in a semi-batch reactor. .... 76

Figure 3.2 Schematic diagram of the semi-batch reactor for cyclic carbonate synthesis. .... 77

Figure 3.3 Flow configuration in a ‘tube-in-tube’ gas-liquid reactor..... 78

Figure 3.4 Uniqsis Flowsyn system used to operate the ‘tube-in-tube’ gas-liquid reactor. .... 78

Figure 3.5 Schematic diagram of the continuous flow reactor for cyclic carbonate synthesis. 79

Figure 3.6 Experimental setup for stereoselective epoxidation of (*R*)-(+)-limonene. .... 82

Figure 3.7 <sup>13</sup>C NMR spectrum of pyrrolidinopyridinium iodide (PPI) in DMSO (\*) 500 MHz at 298K..... 83

Figure 3.8 (a) Solid-state <sup>13</sup>C CP MAS NMR spectrum of functionalised silica (SiO<sub>2</sub>-C<sub>3</sub>H<sub>6</sub>-I) (b) <sup>13</sup>C NMR spectrum of 3-iodopropyltrimethoxysilane (c) Solid-state <sup>13</sup>C CP MAS NMR spectrum of silica-supported pyrrolidinopyridinium iodide (SiO<sub>2</sub>-PPI) (d) <sup>13</sup>C NMR spectrum of the homogeneous analogue (PPI) (\* solvent peaks). .... 86

Figure 3.9 Nitrogen (N<sub>2</sub>) gas adsorption and desorption isotherms of silica-supported pyrrolidinopyridinium iodide (SiO<sub>2</sub>-PPI)..... 87

Figure 3.10 XRD patterns of the functionalised silica (SiO<sub>2</sub>-C<sub>3</sub>H<sub>6</sub>-I) and silica-supported pyrrolidinopyridinium iodide (SiO<sub>2</sub>-PPI) catalyst. .... 88

Figure 3.11 FTIR spectra of styrene carbonate (SC) synthesis by CO<sub>2</sub> cycloaddition to styrene oxide (SO). .... 95

Figure 3.12 FTIR spectra of limonene carbonate (LC) synthesis by CO<sub>2</sub> cycloaddition to limonene oxide (LO). .... 96

Figure 3.13 FTIR calibration curves for (a) Styrene oxide (SO) peak area at 876 cm<sup>-1</sup> against [SO] M (b) Limonene oxide (LO) peak area at 841 cm<sup>-1</sup> against [LO] M. .... 97

Figure 3.14 Example GC spectra of SO and SC using naphthalene (internal standard) before and after the reaction. ....	98
Figure 3.15 GC spectra of LO obtained as a result of stereoselective epoxidation of ( <i>R</i> )-(+)-limonene. ....	99
Figure 3.16 GC calibration curves for different concentrations of (a) Styrene oxide (SO) (b) Limonene oxide (LO). ....	100
Figure 3.17 <sup>1</sup> H-NMR spectra to determine the conversion and yield of limonene carbonate (LC). ....	101
<b>Chapter 4</b>	
Figure 4.1 (a) Effect of temperature over the range of (100–140) °C at 40 bar <i>p</i> (CO <sub>2</sub> ), 6 mol% TBAC and 10 h reaction time (b) Effect of <i>p</i> (CO <sub>2</sub> ) over the range of (5–40) bar at 120 °C, 6 mol% TBAC and 10 h reaction time (c) Effect of catalyst loading over the range of (1.5–7.5) mol% at 120 °C, 40 bar <i>p</i> (CO <sub>2</sub> ) and 10 h reaction time (d) Effect of reaction time over the range of (0–20) hr at 140 °C, 40 bar <i>p</i> (CO <sub>2</sub> ) and 6 mol% TBAC. ....	107
Figure 4.2 Plot of ln ([LO <sub>0</sub> ] / [LO]) against reaction time (hr) showing the change in the reaction rate using different solvents, (reaction conditions: 4.5 M LO, 120 °C, 40 bar <i>p</i> (CO <sub>2</sub> ) and 6 mol% TBAC). ....	108
Figure 4.3 Comparison of the rate constants for limonene carbonate (LC) formation using commercial and <i>trans</i> -enriched limonene oxide (LO) as substrates at (a) 120 °C (b) 140 °C, (reaction conditions: LO (solvent-free), 6 mol % TBAC and 40 bar <i>p</i> (CO <sub>2</sub> )). ....	110
Figure 4.4 (a) Decrease in [LO] M as a function of reaction time (hr) for five different concentrations of LO (1.5–5.5) M (b) First-order kinetics plot i.e. ln [LO] against the reaction time (hr) showing the conversion of LO to LC (c) Plot of ln ( <i>k</i> <sub>obs</sub> ) against ln [LO] showing the first-order dependence of the reaction w.r.t [LO] (d) Plot of ( <i>k</i> <sub>obs</sub> ) against [LO] showing a linear-correlation, (reaction conditions: 120 °C, <i>p</i> (CO <sub>2</sub> ) = 40 bar and 6 mol% TBAC). ....	111
Figure 4.5 (a) First-order kinetics plot of ln [LO] against reaction time (hr) for five different concentrations of TBAC (1.5–7.5) mol % (b) Plot of ln ( <i>k</i> <sub>obs</sub> ) against ln [TBAC] showing the first-order dependence of the reaction w.r.t [TBAC], (reaction condition: 4.5 M LO, 120 °C and <i>p</i> (CO <sub>2</sub> ) = 40 bar). ....	112

Figure 4.6 Plot showing a linear-correlation between ( $k_{obs}$ ) and [TBAC], (reaction conditions: 4.5 M LO, (1.5–7.5) mol% TBAC, 120 °C, 40 bar $p$ (CO <sub>2</sub> )).	113
Figure 4.7 (a) First-order kinetics plot of ln [LO] against reaction time (hr) for four different $p$ (CO <sub>2</sub> ) ranging from (10–40) bar (b) Plot of ln ( $k_{obs}$ ) against the ln $p$ (CO <sub>2</sub> ) showing a linear correlation (c) Plot showing a linear-correlation between ( $k_{obs}$ ) and $p$ (CO <sub>2</sub> ), (reaction condition: 4.5 M LO, 120 °C and $p$ (CO <sub>2</sub> ) = (10–40) bar).	114
Figure 4.8 (a) First-order kinetics plot of ln [LO] against reaction time (hr) over the range of (100–140) °C (b) Curve fitting of ln ( $k_{obs}$ ) against the reciprocal absolute temperature (1/T) to determine the activation energy ( $E_a$ ), (reaction conditions: 4.5 M LO at $p$ (CO <sub>2</sub> ) = 40 bar and 6 mol% TBAC).	115
Figure 4.9 Eyring plot of ln ( $k_{obs}$ ) / T against the reciprocal of absolute temperature (1/T) over the range of (100–140) °C to determine the activation parameters.	116

## Chapter 5

Figure 5.1 (a) Decrease in [SO] M as a function of reaction time (min) using four different concentrations of TBAB (0.025–0.1) M and ZnBr <sub>2</sub> (6.5 mM) at 100 °C and 6 bar $p$ (CO <sub>2</sub> ) (b) First-order kinetic plots i.e. ln [SO] against reaction time (min) (c) Curve fitting of ln ( $k_{obs}$ ) against ln [TBAB] to determine the order of the reaction (d) Plot of the observed rate constant ( $k_{obs}$ ) against [TBAB] showing a linear correlation.	126
Figure 5.2 (a) First-order kinetic plots i.e. ln [SO] against reaction time (min) for four different $p$ (CO <sub>2</sub> ) (2-8 bar) at 100 °C, [TBAB] (0.1M) and [ZnBr <sub>2</sub> ] (6.5 mM) (b) Curve fitting of ln ( $k_{obs}$ ) against ln $p$ [CO <sub>2</sub> ] to determine the order of the reaction w.r.t. CO <sub>2</sub> (c) Plot of the observed rate constant ( $k_{obs}$ ) against $p$ (CO <sub>2</sub> ) showing a linear correlation.	127
Figure 5.3 (a) First-order kinetics plot i.e. ln [SO] against reaction time (min) for four different concentrations of ZnBr <sub>2</sub> (3.25–26) mM and [TBAB] (0.1M) at 100 °C and 6 bar $p$ (CO <sub>2</sub> ) (b) Curve fitting of ln $k_{obs}$ against ln [ZnBr <sub>2</sub> ] to determine the order of the reaction w.r.t ZnBr <sub>2</sub> .	128
Figure 5.4 (a) Decrease in [SO] M as a function of reaction time (min) over the range of (90–120) °C using [TBAB] (0.1 M) and [ZnBr <sub>2</sub> ] (6.5 mM) at 6 bar $p$ (CO <sub>2</sub> ) (b) First-order kinetic plots i.e. ln [SO] against reaction time (min) (c) Arrhenius plot for SC formation over the	

range of (90–120) °C using TBAB (alone) and TBAB/ZnBr<sub>2</sub> as a binary catalyst (d) Eyring plot for SC formation using TBAB/ZnBr<sub>2</sub> over the range of (90–120) °C. .... 130

## Chapter 6

Figure 6.1 Relative catalytic activity of PPI catalyst for SC formation with and without ZnX<sub>2</sub>, (reaction conditions SO, [PPI] 76 mM, [ZnX<sub>2</sub>] 38 mM, 100 °C and 10 bar *p* (CO<sub>2</sub>)). ..... 134

Figure 6.2 (a) Decrease in [SO] M as a function of reaction time (min) for five different concentrations of SO (1.5–5.5) M (b) Plot of initial reaction rate (mol L<sup>-1</sup> min<sup>-1</sup>) against initial [SO] M showing a linear correlation, (reaction conditions: (2.5–5.5) M SO, 76 mM [PPI], 38 mM [ZnI<sub>2</sub>], 100 °C and 10 bar CO<sub>2</sub>). ..... 137

Figure 6.3 First-order kinetics plot showing a linear fit of all the data points (reaction conditions: 1.5 M SO, 76 mM [PPI], 38 mM [ZnI<sub>2</sub>], 100 °C and 10 bar *p* (CO<sub>2</sub>)). ..... 138

Figure 6.4 (a) Double logarithmic plot between (*k*<sub>obs</sub>) and PPI concentrations (76–304) mM to determine the order w.r.t [PPI] (b) Double logarithmic plot between (*k*<sub>obs</sub>) and ZnI<sub>2</sub> concentrations (38–152) mM to determine the order of the reaction w.r.t [ZnI<sub>2</sub>] (c) First-order kinetics Plot showing a linear fit of all data points into first-order kinetics plot (19–76) mM (d) Double logarithmic plot between (*k*<sub>obs</sub>) and PP<sup>+</sup> ZnI<sub>3</sub><sup>-</sup> concentrations to determine the order w.r.t catalyst, (reaction conditions: 3.5 M SO, PPI/ZnI<sub>2</sub> (1:1), 100 °C and 10 bar *p* (CO<sub>2</sub>)). 139

Figure 6.5 (a) Double logarithmic plot between (*k*<sub>obs</sub>) and *p* (CO<sub>2</sub>) over the range of (2–10) bar (b) Plot showing a linear-correlation between (*k*<sub>obs</sub>) and *p* (CO<sub>2</sub>), (c) Double logarithmic plot between (*k*<sub>obs</sub>) and *p* (CO<sub>2</sub>) over the range of (10–40) bar (reaction conditions: 3.5 M SO, 76 mM [PPI], 38 mM [ZnI<sub>2</sub>], and 100 °C). ..... 141

Figure 6.6 (a) Arrhenius plot for SC formation using PPI catalyst with and without ZnI<sub>2</sub> (b) Eyring plot for SC formation using PPI catalyst with and without ZnI<sub>2</sub>, (reaction conditions 3.5 M [SO], 76 mM [PPI], 38 mM [ZnI<sub>2</sub>], (100–140) °C and 10 bar *p* (CO<sub>2</sub>)). ..... 142

## Chapter 7

Figure 7.1 Effect of stirring speed on reaction rate (SO (Solvent-free), 76 mM [SiO<sub>2</sub>-PPI], 140 °C and 10 bar *p* (CO<sub>2</sub>)). ..... 147

Figure 7.2 Reusability of the SiO<sub>2</sub>-PPI catalyst at 120 °C, 1 bar *p* (CO<sub>2</sub>), 76 mM [SiO<sub>2</sub>-PPI], 20 h. .... 148

Figure 7.3 Kinetic models and experimental data for the conversion of SO to SC (a) Pseudo-homogeneous model (b) LH model (c) ER model with combined SO and CO <sub>2</sub> adsorption (d) Arrhenius plot to determine the activation energy for SC formation (dots: experimental data, lines: model), (reaction conditions: solvent-free SO, 76 mM [SiO <sub>2</sub> -PPI], (100–180) °C, 10 bar of <i>p</i> (CO <sub>2</sub> ) for (0–360) min reaction time). .....	150
Figure 7.4 Eyring plot for SC formation over the range of (100–180) °C using SiO <sub>2</sub> -PPI catalyst. ....	151
Figure 7.5 (a) Plot showing the linear correlation between initial reaction rate (mol L <sup>-1</sup> min <sup>-1</sup> ) and initial [SO] over the range of (1.5–5.5) M SO (b) Plot showing a linear fit of all the data points to first-order kinetics for 1.5 M SO, (reaction conditions: 76 mM [SiO <sub>2</sub> -PPI], 140 °C and 10 bar <i>p</i> (CO <sub>2</sub> )). .....	152
Figure 7.6 (a) First-order kinetic plots i.e. ln [SO] against reaction time (min) over the pressure range of (2.5–10) bar <i>p</i> (CO <sub>2</sub> ) (b) Double logarithmic plot between ( <i>k</i> <sub>obs</sub> ) and <i>p</i> (CO <sub>2</sub> ) to determine the order of reaction w.r.t CO <sub>2</sub> (c) Plot of the observed rate constant ( <i>k</i> <sub>obs</sub> ) against <i>p</i> (CO <sub>2</sub> ) showing a linear correlation, (reaction conditions: SO, 76 mM [SiO <sub>2</sub> -PPI], 140 °C). .....	153
Figure 7.7 (a) First-order kinetic plots i.e. ln [SO] against reaction time (min) over the range of (38–152) mM [SiO <sub>2</sub> -PPI], (b) Double logarithmic plot between ( <i>k</i> <sub>obs</sub> ) and [SiO <sub>2</sub> -PPI] to determine the order of reaction w.r.t SiO <sub>2</sub> -PPI, (reaction conditions: 3.5 M SO, 140 °C and 10 bar <i>p</i> (CO <sub>2</sub> )). .....	154



## List of Tables

### Chapter 2

Table 2.1 Summary of catalysts used for cyclic carbonate synthesis from 1,2-diols and CO <sub>2</sub> .	17
Table 2.2 Summary of catalysts used for oxidative carboxylation of alkenes.....	19
Table 2.3 Summary of HBDs based ammonium salts as homogeneous catalysts. ....	32
Table 2.4 Summary of ammonium salts as heterogeneous catalyst systems. ....	34
Table 2.5 Summary of phosphonium salts as homogeneous catalysts.....	35
Table 2.6 Summary of phosphonium salt as heterogeneous catalysts. ....	36
Table 2.7 Summary of imidazolium salts as heterogeneous catalysts. ....	40
Table 2.8 Summary of two-component HBDs based catalyst systems. ....	41
Table 2.9 Summary of Cr (III)-based salen and salphen complexes as homogeneous catalysts. .....	48
Table 2.10 Summary of Zn-based complexes as homogeneous catalysts.....	49
Table 2.11 Summary of Zn-salts based binary homogeneous catalysts.....	51
Table 2.12 Summary of catalytic systems used for CO <sub>2</sub> cycloaddition to internal epoxides...	53
Table 2.13 Gas permeability of different gases through Teflon <sup>®</sup> AF-2400 membrane.....	68
Table 2.14 Applications of the ‘tube-in-tube’ gas-liquid reactor in organic synthesis.....	69

### Chapter 3

Table 3.1 List of the chemicals used in this study.....	75
Table 3.2 Summary of reaction conditions for cyclic carbonates synthesis by CO <sub>2</sub> cycloaddition to styrene oxide (SO) and limonene oxide (LO) in a semi-batch reactor.....	80
Table 3.3 Summary of BET analysis of the parent SiO <sub>2</sub> and SiO <sub>2</sub> -PPI catalyst. ....	87
Table 3.4 Elemental analysis (CN) of fresh and recovered SiO <sub>2</sub> -PPI samples showing catalyst loading over SiO <sub>2</sub> . ....	88

Table 3.5 Summary of FTIR epoxide peak intensity data for calibration curve using different concentrations of SO (0.5–5) M in PC as a solvent. ....	95
Table 3.6 Summary of FTIR epoxide peak intensity data for the calibration curve using different concentrations of LO (0.5–4.5) M in PC as a solvent. ....	96
Table 3.7 Summary of GC peak areas against different concentrations of SO using chloroform as a solvent. ....	99
Table 3.8 Summary of GC peak areas against different concentrations of limonene oxide (LO) using chloroform as a solvent. ....	100
<b>Chapter 4</b>	
Table 4.1 Catalytic activities of TBAX for LC synthesis by CO <sub>2</sub> cycloaddition to commercial LO, (reaction conditions: 120 °C, <i>p</i> (CO <sub>2</sub> ) = 40 bar, 3 mol% TBAX, 20 h). ....	104
Table 4.2 Rate constants of limonene carbonate (LC) synthesis using different reaction solvents. ....	109
Table 4.3 Summary of activation parameters of limonene carbonate (LC) synthesis determined from Eyring equation. ....	116
<b>Chapter 5</b>	
Table 5.1 Catalyst screening for styrene carbonate (SC) synthesis in a semi-batch reactor, (reaction conditions: SO (35 mmol), 100 °C, 1bar <i>p</i> (CO <sub>2</sub> ) and 3 h). ....	121
Table 5.2 Study of reaction parameters for styrene carbonate (SC) formation in a continuous flow reactor. ....	122
Table 5.3 Rate constants for the conversion of SO to SC as a function of reaction temperature in both batch and continuous flow reactor, (reaction conditions: 4.5 M SO, 1:4 ZnBr <sub>2</sub> /TBAB, 6 bar <i>p</i> (CO <sub>2</sub> )). ....	123
Table 5.4 Summary of activation parameters of SC formation from SO and CO <sub>2</sub> catalysed by TBAB/ZnBr <sub>2</sub> determined from Eyring equation. ....	130
<b>Chapter 6</b>	
Table 6.1 Relative catalytic activity for SC formation from SO and CO <sub>2</sub> in terms of the initial reaction rate. ....	135

Table 6.2 Summary of activation parameters for SC formation using PPI catalyst with and without zinc halides as co-catalysts determined from Eyring equation..... 143

**Chapter 7**

Table 7.1 Summary of activation parameters for SC formation from SO and CO<sub>2</sub> using SiO<sub>2</sub>-PPI catalyst determined from the Eyring equation. .... 151



## List of Abbreviations

ATR	Attenuated total reflectance
AF	Amorphous fluoroplastics
BET	Brunauer-Emmett-Teller
BPA	Bisphenol-A
CCS	Carbon capture and sequestration
CCU	Carbon capture and utilization
CHC	Cyclohexene carbonate
CHO	Cyclohexene oxide
CP MAS	Cross-polarization magic angle spinning
DFT	Density functional theory
DMC	Dimethyl carbonate
EC	Ethylene carbonate
EO	Ethylene oxide
ER	Eley-Rideal
FFV	Fractional free volume
FID	Flame ionization detector
FTIR	Fourier-transform infrared spectroscopy
GC	Gas chromatography
HBD	Hydrogen bond donor
ID	Inner diameter
ILs	Ionic liquids
LC	Limonene carbonate
LDC	Limonene dicarbonate

LDO	Limonene dioxide
LH	Langmuir-Hinshelwood
LO	Limonene oxide
MOFs	Metal organic frameworks
NBS	N-bromosuccinimide
NIPUs	Non-isocyanate polyurethanes
NMR	Nuclear magnetic resonance
OD	Outer diameter
PC	Propylene carbonate
PG	Propylene glycol
PH	Pseudo-homogeneous
PID	Proportional integral derivative
PO	Propylene oxide
PPC	Polypropylene carbonate
PPI	Pyrrolidinopyridinium iodide
ppm	parts per million
PS	Polystyrene
REACH	Registration, Evaluation, Authorisation and Restriction of Chemicals
rpm	revolutions per minute
SC	Styrene carbonate
SO	Styrene oxide
SiO <sub>2</sub> -PPI	Silica-supported pyrrolidinopyridinium iodide
TBAX	Tetrabutylammonium halides
TBAB	Tetrabutylammonium bromide

TBAC	Tetrabutylammonium chloride
TBAI	Tetrabutylammonium iodide
TBAF	Tetrabutylammonium fluoride
TOF	Turnover frequency
TON	Turnover number
XRD	X-ray diffraction



## List of Nomenclature

$\rho$	Density ( $\text{Kg m}^{-3}$ )
$\epsilon_p$	Porosity of catalyst particle
$\mu_L$	Liquid viscosity (m Pa. sec)
$\emptyset$	Catalyst active site
$\emptyset_j$	Fraction of the catalytic sites that remain unoccupied
$\tau_p$	Tortuosity of the catalyst particles
$\Delta H^\ddagger$	Enthalpy of activation ( $\text{KJ mol}^{-1}$ )
$\Delta S^\ddagger$	Entropy of activation ( $\text{J mol}^{-1} \text{K}^{-1}$ )
$\Delta G^\ddagger$	Gibbs free activation energy ( $\text{kJ mol}^{-1}$ )
$\text{\AA}$	Angstrom ( $10^{-10} \text{ m}$ )
$A_{is}$	Peak area of internal standard
C	Carbon content (%)
cB	centiBarrer ( $10^{-8} (\text{cm}^2 - \text{cm}) / (\text{cm} - \text{Hg} - \text{sec} - \text{cm}^2)$ )
Cis	Concentration of internal standard (mg/L)
$^{13}\text{C-NMR}$	Carbon (13) nuclear magnetic resonance
$De$	Effective diffusivity ( $\text{cm}^2 \text{sec}^{-1}$ )
$D_L$	Gas diffusivity in the liquid ( $\text{cm}^2 \text{sec}^{-1}$ )
$E_a$	Activation energy ( $\text{kJ mol}^{-1}$ )
$h$	Planck's constant ( $6.62608 \times 10^{-34} \text{ J s}$ )
$^1\text{H-NMR}$	Proton nuclear magnetic resonance
$I_{x \text{ cis}}$	Intensity of <i>cis</i> -isomer before the reaction
$I_{x' \text{ cis}}$	Intensity of <i>cis</i> -isomer after the reaction
$k$	Pseudo-first-order rate constant

$k_B$	Boltzmann constant ( $1.38065 \times 10^{-23} \text{ J K}^{-1}$ )
$k_s$	Rate constant for the forward surface reaction
$k_{\text{obs}}$	Observed rate constant
$K_A$	Adsorption-desorption equilibrium constant for reactant A
$K_B$	Adsorption-desorption equilibrium constant for reactant B
$K_C$	Adsorption-desorption equilibrium constant for product C
$M$	Molar concentration (mol/L)
$\text{Me}$	Methyl group
$M_T$	Thiele's modulus
$M_w$	Molecular weight (g/mol)
$N$	Nitrogen content (%)
$n$	Number of moles
$\text{Nu}$	Nucleophile
$P$	Pressure (bar)
$p(\text{CO}_2)$	$\text{CO}_2$ pressure (bar)
$R$	Universal gas constant ( $8.314 \text{ J mol}^{-1} \text{ K}^{-1}$ )
$T$	Temperature ( $^{\circ}\text{C}$ )
$T_g$	Glass transition temperature ( $^{\circ}\text{C}$ )
$t$	Reaction time
$t\text{Bu}$	tert-butyl
$V_{bA}$	Molar volume of solute at boiling point ( $\text{cm}^3 \text{ mol}^{-1}$ )



# Chapter 1 Introduction

## 1.1 Background

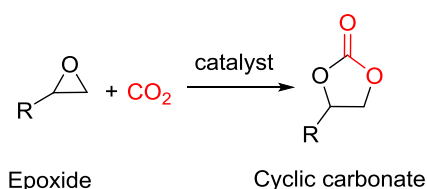
Global concerns about high CO<sub>2</sub> levels and dwindling supplies of fossil resources are increasing. The diminishing national and global reserves of crude oil, coupled with fluctuating supplies of fossil resources, means that long-term supply and economic viability for petroleum-derived value-added products are at considerable risk. Additionally, many of the processes used to convert crude oil into valuable products utilise auxiliary chemical elements with their own sustainability issues (e.g. rare-earth and platinum group metals), therefore it is likely that the ability of the chemical industry to supply petroleum-derived products will come under ever-increasing threat. Moreover, the concentration of CO<sub>2</sub> in the environment has been dramatically increased over the last two decades, causing severe climatic changes due to global warming. The anthropogenic emission of CO<sub>2</sub> into the atmosphere now exceeds 36 Gt, which is 43% above the level since the beginning of the industrial revolution (IPCC, (2018)). Alternatively, CO<sub>2</sub> has the benefits of availability in abundance, inexpensive, non-toxic and non-flammable (Sakakura *et al.*, 2007). Therefore, the utilization of CO<sub>2</sub> and waste biomass as renewable resources for valuable products is highly desirable in order to meet the growing and to make various supply chains 'greener'. This will not only help to reduce the anthropogenic emission of CO<sub>2</sub> into the atmosphere, but also decrease the dependence on depleting resources of fossil fuel.

Currently, the utilization of a renewable source of CO<sub>2</sub> for the production of other valuable products has attracted the attention of the scientific community. The utilization of CO<sub>2</sub> as a C1-building block for organic synthesis will certainly not enable industry to significantly reduce the anthropogenic CO<sub>2</sub> emissions. However, it can be used as a renewable, non-toxic and economical source for the production of many high-value products. Therefore, significant efforts have been devoted in academia and industry to develop the methodologies for effective CO<sub>2</sub> utilization. The utilization of CO<sub>2</sub> as a C1-building block is challenging due to its high thermodynamic stability and kinetic inertness i.e. owing to its low standard heat of formation i.e.  $\Delta H_f = -394 \text{ kJ mol}^{-1}$ ) and standard Gibbs energy of formation i.e.  $\Delta G_f = -395 \text{ kJ mol}^{-1}$  ('NIST database,' 2018). Due to the low reactivity of CO<sub>2</sub>, this alternative approach of CO<sub>2</sub> utilisation as feedstock for organic synthesis requires high energy input and may result in the

exhaust of more CO<sub>2</sub> than consumed by the reaction. Therefore, the reaction of CO<sub>2</sub> should be with those compounds which have relatively high free energy to provide a thermodynamically feasible process. For instance, synthesis of urea from ammonia and CO<sub>2</sub> is a highly exothermic reaction i.e.  $\Delta H_r = -101 \text{ kJ mol}^{-1}$  (Barzagli *et al.*, 2011). Currently, the annual production of urea is around 157 Mt, corresponding to 115 Mt/year direct CO<sub>2</sub> utilisation (Omae, 2012). Similarly, another example of effective CO<sub>2</sub> utilization is the production of salicylic acid by the reaction of phenolates and CO<sub>2</sub> i.e.  $\Delta H_r = -31 \text{ kJ mol}^{-1}$ , which is the first step in the industrial production of aspirin (Aresta and Dibenedetto, 2004). This process was commercialised since the 19<sup>th</sup> century (Federsel *et al.*, 2010). Currently, the annual production of salicylic acid is around 90 Kt, corresponding to 29 Kt/year direct CO<sub>2</sub> utilisation (Kleij *et al.*, 2017). Among these processes, synthesis of cyclic carbonate via CO<sub>2</sub> cycloaddition to epoxide is another thermodynamically favourable reaction i.e.  $\Delta H_r = -144 \text{ kJ mol}^{-1}$  for ethylene carbonate (EC) synthesis from ethylene oxide (EO) and CO<sub>2</sub> ('NIST database,' 2018). The energy required for this reaction is provided by the discharge of ring-strain energy enclosed in the three-membered epoxide used as a substrate.

## 1.2 Cyclic carbonate synthesis by CO<sub>2</sub> cycloaddition to epoxides

Synthesis of cyclic carbonates by the cycloaddition of CO<sub>2</sub> to epoxides is a promising reaction in terms of sustainability and green chemistry due to its 100% atom economic conversion (Scheme 1.1) (Yoshida and Ihara, 2004). 'Cycloaddition' is defined as a type of addition reaction in which two (or more) unsaturated molecules combine to form a cyclic product. For instance, Diels-elder reaction is a chemical reaction, in which an olefin combines with a diene to form a substituted derivative of cyclohexene is called a cycloaddition reaction. Synthesis of cyclic carbonates from epoxide and CO<sub>2</sub> has been commonly used as cycloaddition reaction in literature (Hirose *et al.*, 2018; Anthofer *et al.*, 2014). In this thesis, 'cycloaddition' has been used for the reaction between epoxide and CO<sub>2</sub> to form cyclic carbonate. The formation of cyclic carbonate from epoxide and CO<sub>2</sub> involves fewer hazardous species, as it incorporates CO<sub>2</sub> as a C1 feedstock source rather than the conventional highly toxic and corrosive phosgene route (Martin and Kleij, 2011). As CO<sub>2</sub> is available in excess, non-toxic and non-flammable, it can be used as a renewable source for the production of cyclic carbonates.



Scheme 1.1 Synthesis of cyclic carbonates from epoxides and CO<sub>2</sub>.

Organic cyclic carbonates have a broad range of applications, such as high boiling point green polar aprotic solvents, electrolytes in Li-ion batteries, monomer for polycarbonates and polyurethanes synthesis, intermediates for the manufacturing of pharmaceuticals and many other fine chemicals (Comerford *et al.*, 2015). Synthesis of cyclic carbonates from epoxides and CO<sub>2</sub> has been commercialized since the 1950s (Peppel, 1958). Currently, the annual production of cyclic carbonates is around 80 Kt, corresponding to 40 Kt/year direct CO<sub>2</sub> utilisation (Kleij *et al.*, 2017). However, the demand for cyclic carbonates has been increasing rapidly due to their applications in Li-ion batteries that are an important part of our modern life. Similarly, cyclic carbonates are being increasingly used as intermediates for the preparation of many other useful products. For instance, synthesis of ethylene carbonate (EC) by CO<sub>2</sub> cycloaddition to ethylene oxide (EO) and subsequent production of ethylene glycol (EG) via hydrolysis has been already industrialised on large scale by Shell omega (Han *et al.*, 2012). Similarly, the reaction between methanol and ethylene carbonate to form ethylene glycol and dimethyl carbonate has been commercialised by Asahi Kasei (Fukuoka *et al.*, 2003). Organic cyclic carbonates are highly stable compounds that can ensure long-term CO<sub>2</sub> sequestration compared to other CO<sub>2</sub> based products such as urea which readily releases CO<sub>2</sub> on its utilisation as fertilizer (Aresta *et al.*, 2013).

### 1.3 Catalyst systems for CO<sub>2</sub> cycloaddition to epoxides

As described earlier, synthesis of cyclic carbonates from epoxides and CO<sub>2</sub> was determined to be a highly exothermic reaction i.e.  $\Delta H_r = -144 \text{ kJ mol}^{-1}$  for EC synthesis from EO and CO<sub>2</sub> ('NIST database,' 2018). However, unlike urea and salicylic acid synthesis, this reaction does not occur spontaneously due to the high activation barrier of the uncatalysed reaction i.e. (209–251) kJ mol<sup>-1</sup> depending on the type of epoxide used (Wang *et al.*, 2012). Currently, quaternary ammonium and phosphonium salts are being used as catalysts for commercial cyclic carbonate synthesis (Castro-Osma *et al.*, 2016). These catalysts have relatively low catalytic activity, causing cyclic carbonates formation at elevated reaction temperature and

CO<sub>2</sub> pressure. As a result, the current commercial production of cyclic carbonate is emitting CO<sub>2</sub> into the atmosphere rather than consuming i.e. 0.92 tonnes CO<sub>2</sub> emitted per each tonne of cyclic carbonate produced (Aresta *et al.*, 2013). Therefore, a highly efficient catalyst system is required which can substantially decrease the activation energy, allowing the reaction to take place at mild reaction conditions. During the last two decades, significant research has been conducted to develop various homogeneous and heterogeneous catalyst systems. These mainly include organocatalysts such as ammonium salts, phosphonium salts, imidazolium salts, ionic liquids and metal complexes (Buettner *et al.*, 2017). Among these metal complexes such as bimetallic Al (III) salen complexes in combination with nucleophilic co-catalysts have attracted considerable attention due to their ability to catalyse the reaction under ambient conditions i.e. 25 °C and 1 bar *p* (CO<sub>2</sub>) (Melendez *et al.*, 2007). The use of these catalysts on a commercial scale can help in significant reduction of CO<sub>2</sub> emissions related to cyclic carbonate synthesis.

Heterogeneous catalysts offer substantial advantages, such as easy separation and reusability, thereby avoiding extensive use of solvents involved in downstream processes (Cokoja *et al.*, 2015). To facilitate catalyst separation and recycling, high surface area inorganic supports, such as silica (SiO<sub>2</sub>), polymeric materials, and metal-organic frameworks (MOFs) are commonly used for heterogenisation. However, reduced catalytic activity due to leaching, or other forms of deactivation, associated with heterogeneous catalysts is a key issue. Most of the heterogeneous catalysts for epoxide/CO<sub>2</sub> cycloaddition reported in the literature require harsh reaction conditions, such as high temperature, pressure and catalyst loading (Yasuda *et al.*, 2006). Various catalysts have been prepared by grafting ammonium, phosphonium and aminopyridinium based halides onto high surface area silica supports (Motokura *et al.*, 2009). Some of these catalysts have unexpectedly exhibited higher catalytic activity than their homogeneous analogues, due to the synergistic effect of the halide anions with Si–OH (silanol) groups (Takahashi *et al.*, 2006). Conversely, most catalyst systems still lack commercial applicability at the industrial scale from an ecological and/or economic viewpoint. Furthermore, these catalyst systems have exhibited a high activity for terminal epoxides, but little or none towards di- and tri-substituted internal epoxides (Shaikh *et al.*, 2017).

#### 1.4 Bio-based cyclic carbonate synthesis

Synthesis of cyclic carbonates is mostly carried out with petrochemical-based terminal epoxides such as ethylene oxide (EO), propylene oxide (PO) and styrene oxide (SO). Nevertheless, in order to satisfy the demands of green chemistry, recent efforts have been focused on the utilisation of renewable resources as potential raw materials instead of using crude oil as feedstock. The use of petroleum-based cyclic carbonate as a monomer for the production of polymers is also associated with various environmental and health issues (Geueke *et al.*, 2014). Moreover, the growing demand for polymers in modern society is under threat due to depleting global reserves of fossil fuel, environmental issues and supply security risks as many of the main oil producers are located in politically unstable regions. Evidently, there is a requirement to seek sustainable substitutes to petroleum-derived polymers with naturally available feedstocks, especially from waste biomass.

Naturally occurring terpenes have been identified as key starting materials for the production of bio-based epoxides (Kristufek *et al.*, 2017). For instance, d-limonene is a monocyclic unsaturated terpene, mainly extracted from the peel of citrus fruits (90 wt %) (Firdaus *et al.*, 2011). It is a principal component of many essential oils and obtained as a waste product during harvesting and orange juice production. The global production of d-limonene (also known as (+)-Limonene) was approximately 70,000 tonnes, which is gradually increasing every year (Ciriminna *et al.*, 2014). Due to its abundance as a waste by-product and suitability for organic synthesis due to the presence of two double bonds, it can be used as a sustainable replacement for petrol-based epoxides without competing with food crops. The synthesis of cyclic carbonates from d-limonene oxide, in particular, is of significant interest, as it can be used as a bio-renewable monomer for the production of fully bio-based polymers such as non-isocyanate polyurethanes (NIPUs), which have potential applications as thermoset materials, elastomers, or thermoplastics (Bähr *et al.*, 2012). The use of bio-based epoxides derived from renewable resources such as waste biomass and CO<sub>2</sub> can provide a sustainable basis for the future polymer industry (Zhu *et al.*, 2016).

## 1.5 Cyclic carbonate synthesis in continuous flow reactors

Flow chemistry has many advantages over conventional batch reactors, typically including enhanced rates of heat and mass transfer (due to higher surface area to volume ratios and efficient mixing), improved safety (lower inventories), easy and highly reproducible screening of reaction parameters, which may improve the reliability of scale-up and process optimisation (Kozak *et al.*, 2013). Most of the studies on cyclic carbonate synthesis from non-volatile epoxides such as styrene oxide (SO) and other commercially important epoxides have been carried out in high-pressure batch reactors (Cokoja *et al.*, 2015; Buettner *et al.*, 2017). However, the use of a continuous flow reactor for cyclic carbonate synthesis is considered as the most promising approach for large scale production (North *et al.*, 2009b).

Synthesis of cyclic carbonates from epoxides and CO<sub>2</sub> is a typical gas-liquid reaction involving a gas-liquid mass transfer in a reactor and the catalytic cycloaddition reaction in the liquid phase (Zhao *et al.*, 2013). Previous studies on cyclic carbonate synthesis performed in batch reactors suggested that the rate of reaction was controlled by the rate of CO<sub>2</sub> mass transfer from the gaseous phase to the reaction mixture (Metcalf *et al.*, 2013). Thus, it was anticipated that an efficient reactor design in terms of the high rate of heat/mass transfer and a continuous flow approach could mitigate many of the shortcomings observed in a traditional batch reactor. Moreover, the reactor design can affect the rate of the gas-liquid catalytic reaction (Lokhat *et al.*, 2016). Recently, microreactor technology is being increasingly used in flow chemistry due to its wide range of applications in chemical synthesis (Yao *et al.*, 2017). Among the various reactions studied at the microscale, the gas/liquid biphasic reaction is an important category (Su *et al.*, 2009). In this study, synthesis of cyclic carbonates has been carried out in ‘tube-in-tube’ gas-liquid microreactor with the aim to increase the effective (interfacial) surface area, and thus to increase the gas availability in the solution. The inner tube of this reactor is made of Teflon<sup>®</sup> AF-2400 fluoropolymer semi-permeable membrane through which only gas can permeate. These reactors have a higher surface area to volume ratios than conventional batch reactors and exceptionally high permeation of CO<sub>2</sub> across membrane compared to other gases i.e. (280,000 cB) (Biogeneral). This can lead to, significantly improved gas/liquid reaction efficiency due to increased mass transfer from gas to the liquid phase. This concentric tube reactor design has the ability to form microbubbles of gas which are rapidly dissolved into the counterflowing liquid. Diffusion-controlled formation of homogeneous saturated gas solutions is thus obtained under continuous flow conditions

(Koos *et al.*, 2011). Over the last decade, this novel concept of reactor design has found a wide range of applications in organic chemistry (Brzozowski *et al.*, 2015).

## 1.6 Kinetics study of cyclic carbonate synthesis

Synthesis of cyclic carbonates by CO<sub>2</sub> cycloaddition to epoxides was extensively studied using various catalyst systems leading to high conversion and product yields (Shaikh *et al.*, 2017). However, a detailed study of kinetics is required to investigate the reaction mechanism and to determine the general rate law (North and Pasquale, 2009). Mechanistic investigations are necessary to increase the activity of catalyst systems and to control the selectivity of the reaction (Martín and Kleij, 2014). The study of reaction kinetics provides basic information to design a chemical reactor.

Several kinetic studies of cyclic carbonate synthesis by CO<sub>2</sub> cycloaddition to epoxides based on the pseudo-first-order kinetic model have been reported in the literature. In most of the homogeneous kinetic studies, the reaction exhibited first-order dependence with respect to epoxide and CO<sub>2</sub> concentrations. Nevertheless, the reaction order with respect to catalyst varied depending on the type of the catalyst used. The order of reaction in the presence of a monometallic catalyst was mostly reported as first-order. However, a second-order reaction with respect to catalyst was also reported in the presence of bifunctional and binary catalyst systems (Pescarmona and Taherimehr, 2012).

North *et al.*, (2012) reported cyclic carbonate synthesis from terminal epoxides and CO<sub>2</sub> in the presence of bi-metallic aluminium-salen complex [ $\{Al-(salen)\}_2O$ ] in combination with tetrabutylammonium bromide (TBAB) as a highly efficient binary homogeneous catalyst at mild reaction conditions (25 °C and 1 bar *p* (CO<sub>2</sub>)). The detailed study of reaction kinetics revealed first-order dependence of the reaction with respect to epoxide, CO<sub>2</sub> and metallic complex concentrations. Remarkably, the order of the reaction with respect to TBAB was determined to be second order due to the participation of two molecules of TBAB in the rate-determining step. Similarly, Kleij *et al.*, (2014) also reported second-order dependence of the reaction with respect to catalyst when the cycloaddition reaction was carried out using Zn(salen) complex in combination with TBAI suggesting a bimetallic reaction mechanism.

## 1.7 Aims and objectives

The aim of this study is to investigate cyclic carbonate synthesis by CO<sub>2</sub> cycloaddition to both bio-based limonene oxide (LO) and petroleum-based styrene oxide (SO).

The objectives of this research project are:

1. To study cyclic carbonate synthesis by CO<sub>2</sub> cycloaddition to bio-based limonene oxide (LO) in the presence of tetrabutylammonium chloride (TBAC) as a monofunctional homogenous catalyst.
2. To study cyclic carbonate synthesis by CO<sub>2</sub> cycloaddition to styrene oxide (SO) in a continuous flow 'tube-in-tube' gas-liquid reactor in the presence of tetrabutylammonium bromide (TBAB) and zinc bromide (ZnBr<sub>2</sub>) as an acid-base binary homogeneous catalyst.
3. To study cyclic carbonate synthesis by CO<sub>2</sub> cycloaddition to epoxide in the presence of pyrrolidinopyridinium iodide (PPI) and zinc iodide (ZnI<sub>2</sub>) as an acid-base binary homogeneous catalyst.
4. To study cyclic carbonate synthesis by CO<sub>2</sub> cycloaddition to epoxide in the presence of silica-supported pyrrolidinopyridinium iodide (SiO<sub>2</sub>-PPI) as a bifunctional heterogeneous catalyst.
5. To perform kinetic studies of cyclic carbonate synthesis by CO<sub>2</sub> cycloaddition to epoxides in the presence of both homogeneous and heterogeneous catalysts.

## Chapter 2 Literature review

### 2.1 Introduction

Despite various efforts to develop alternative renewable energy resources, fossil fuels are still considered as the major source of power generation, transportation fuel and raw materials for the production of many other value-added products and likely to remain so for next (20–40) years (North, 2012). The demand for these products is continuously increasing due to the increased population. At present, 85% of global energy production is based on the fossil resources such as coal, oil and gas whereas the remaining 15% is produced by nuclear and renewable energy sources such as solar, wind and waste biomass etc. (Aresta *et al.*, 2013). As a matter of fact, only (30–35)% of the chemical energy produced by burning fossil fuel has been converted into other forms of energies such as electrical, mechanical and others and the remaining (65–70)% is going directly into the atmosphere as waste heat (Aresta and Dibenedetto, 2007). Consequently, the resources of fossil fuels are going to deplete at a much faster rate. Moreover, the concentration of CO<sub>2</sub> in the environment has been dramatically increased over the last two decades, causing severe climatic changes due to global warming.

Currently, many technologies have been developed to reduce anthropogenic CO<sub>2</sub> emission. Generally, these include ‘Carbon Capture and Storage’ (CCS) and ‘Carbon Capture and Utilization’ (CCU). CCS involves highly energy-intensive methods of CO<sub>2</sub> injection into exhausted oil and gas reservoirs under supercritical conditions. Due to high energy requirements and possible leakage of concentrated CO<sub>2</sub>, CCS is not considered to be economically and ecologically feasible method (Singh *et al.*, 2011). The utilisation of CO<sub>2</sub> in production of organic carbonates is, therefore, counts towards reducing global emissions. The development of the less energy-intensive methodologies for the utilization of CO<sub>2</sub> has gained much attention in both academia and the chemical process industry. This chapter covers the synthesis of organic carbonates particularly cyclic carbonates by CO<sub>2</sub> cycloaddition to epoxides. Recent developments in catalytic systems for this reaction, kinetics and mechanistic investigations and the parameters affecting their activity and selectivity has been particularly focused. Moreover, the recent efforts on the utilization of renewable resources as potential raw materials for the cyclic carbonate synthesis have also been discussed. Mostly, the production of cyclic carbonates has been carried out in batch reactors which were designed to

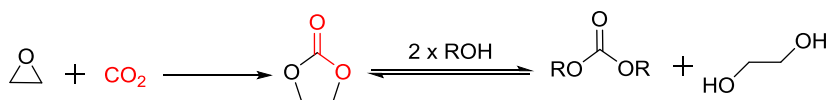
meet the requirements of reaction conditions under traditional catalytic systems. Nonetheless, in order to satisfy the demands of a multi-scale approach for industrial transformation, the use of flow chemistry and novel reactor designs for the synthesis of these carbonates has been also discussed.

## 2.2 Organic carbonates

CO<sub>2</sub> has the benefits of availability in abundance, inexpensive, non-toxic and non-flammable (Sakakura *et al.*, 2007). Therefore, it can be utilized as a potential C1-building block for the synthesis of many organic compounds. Particularly, the utilization of CO<sub>2</sub> for the synthesis of organic carbonates has attracted considerable attention. Synthesis of organic carbonates has the potential to be industrialized on large scale due to their wide range of applications (Sakakura and Kohno, 2009). Organic carbonates can be classified on a structural basis such as cyclic, acyclic and polycarbonates.

### 2.2.1 Acyclic carbonate synthesis

The conventional method for the production of acyclic carbonate consists of two steps involving phosgene synthesis from CO and Cl<sub>2</sub>, followed by the reaction of phosgene with alcohols in the presence of concentrated NaOH (Shaikh and Sivaram, 1996). However, this method has some major drawbacks such as the use of highly volatile and toxic phosgene, handling a large amount of HCl generated as a by-product and the limited yield of the product. Acyclic carbonates such as dimethyl carbonate (DMC), have many applications in the chemical process industry. It has been increasingly used as a 'green' solvent and fuel additive (Schaffner *et al.*, 2010). An alternative method for the production of acyclic carbonates is via cyclic carbonates. This process involves ethylene carbonate (EC) synthesis by the cycloaddition of CO<sub>2</sub> to ethylene oxide (EO) followed by reaction with alcohols (Scheme 2.1). Despite multi-step processing and the production of ethylene glycol as a major by-product, this process was commercialized in 1986 (Duranleau *et al.*, 1987).



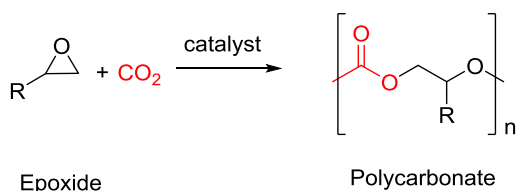
Scheme 2.1 Synthesis of acyclic carbonates via cyclic carbonates route.

Direct reaction of CO<sub>2</sub> with alcohols in the presence of metal catalysts was also investigated as a promising method for the synthesis of acyclic carbonates. This process also has some potential short-comings such as high reaction temperature and pressure requirement, catalyst decomposition and poor selectivity due to hydrolysis as a major side reaction. Nevertheless, recent developments in the catalyst systems such as the use of titanium and tin-based catalysts have significantly improved the product yield (Choi *et al.*, 2008). Moreover, a dehydrating condensation of alcohols and CO<sub>2</sub> was also proposed using zeolites as dehydrating agents to avoid these side reactions (George *et al.*, 2009). At the present time, dehydrating condensation of methanol (CH<sub>3</sub>OH) and CO<sub>2</sub> in the presence of a titanium-based catalyst at 180 °C and 300 atm *p* (CO<sub>2</sub>) was considered to be a most effective method for the production of dimethyl carbonate (Sakakura and Kohno, 2009).

### 2.2.2 Polycarbonates synthesis

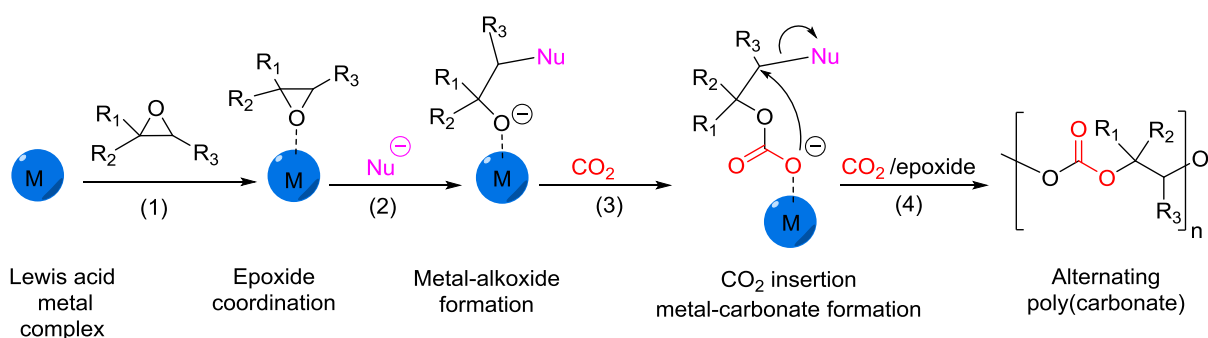
Polycarbonates are a major class of industrially important organic carbonates. These can be defined as a class of engineering thermoplastics having carbonate group (–O–(C=O)–O–) in their molecular structures. Aromatic polycarbonates have a broad range of applications in our daily life such as in medical applications, construction materials, automotive, electronic devices, and data storage materials such as CDs and DVDs (Sakakura and Kohno, 2009). The conventional method of commercial aromatic polycarbonate synthesis involves the condensation of phosgene and bisphenol-A (BPA) (Hudgin and Bendler, 2000). These polycarbonates exhibit excellent physical and mechanical properties such as high impact strength, high-temperature resistance, good electric insulation, high rigidity, transparent to light and amorphous nature. However, the process involving the use of highly volatile and toxic raw materials such as phosgene and BPA has potential drawbacks related to health issues (Geueke *et al.*, 2014).

An alternative route for the production of aliphatic polycarbonates via copolymerization of epoxides and CO<sub>2</sub> using zinc-based catalyst was first proposed by Inoue *et al.* (1969) (Scheme 2.2). The reaction between epoxide and CO<sub>2</sub> can be controlled to form either polycarbonates or cyclic carbonates depending on the reaction conditions and the catalyst system used. Aliphatic polycarbonates are kinetic products, whereas cyclic carbonates are thermodynamic products of the reaction between epoxide and CO<sub>2</sub> (Kember *et al.*, 2011).



Scheme 2.2 Synthesis of polycarbonates from epoxides and CO<sub>2</sub>.

This reaction involves the direct use of CO<sub>2</sub> as an alternative building block compared to the traditional use of toxic chemicals such as phosgene and BPA. Synthesis of polycarbonate from epoxide and CO<sub>2</sub> has recently gained much attention in both academia and industry due to its 100% atom economy. Significant research has been focused to develop an efficient catalyst system to overcome the kinetic stability of CO<sub>2</sub> and to make this process commercially viable. A broad range of catalyst systems has been developed with the aim to carry out this reaction under mild reaction conditions. These involve the use of rare earth metals (Wang *et al.*, 2005), metal-based salen complexes (Darensbourg, 2007), metal macrocycles (Aida *et al.*, 1986) and zinc β-diiminiate complexes (Moore *et al.*, 2003). These catalysts are mainly used for CO<sub>2</sub> copolymerization with petroleum-based epoxides e.g. propylene oxide (PO) and cyclohexene oxide (CHO) etc. The generally accepted reaction mechanism for polycarbonates formation via alternating copolymerization of epoxides and CO<sub>2</sub> using a Lewis acid metal complex in combination with nucleophile additive involves the following steps (Scheme 2.3):



Scheme 2.3 General reaction mechanism of polycarbonate synthesis from epoxides and CO<sub>2</sub> (Martin *et al.*, 2015).

- 1) Initially, the epoxide activation takes place by the interaction of the metal centre with the oxygen atom of epoxide.
- 2) The activated epoxide further undergoes a nucleophilic attack by the halide anion on the least substituted carbon atom of the epoxide to form a metal-bonded alkoxide intermediate.

3) Subsequently, the ring-opened epoxide intermediate undergoes CO<sub>2</sub> insertion to form a carbonate.

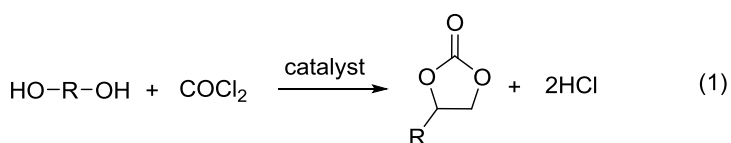
4) Finally, the carbonate undergoes successive addition (propagation) of epoxide and CO<sub>2</sub> to form a polycarbonate.

Among other types of polycarbonates, synthesis of poly(propylene) carbonate (PPC) has been already commercialized (Fukuoka *et al.*, 2003). However, these polycarbonates have a limited range of applications due to their low glass transition temperatures (T<sub>g</sub>) i.e. 40 °C and low thermal stability. The physical and mechanical properties of the polycarbonates also depend on the type of epoxides used as substrates. T<sub>g</sub> of the polycarbonate can be increased using high molecular weight epoxides such as cyclohexene oxide (CHO) (Kember *et al.*, 2011). However, this polymer still has poor mechanical properties due to its brittle nature (Coates and Moore, 2004). Therefore, polycarbonates produced via copolymerization of CO<sub>2</sub> and epoxides are facing challenges to compete with commercial BPA-polycarbonates having superior properties such as high T<sub>g</sub> i.e. 150 °C, high mechanical strength and good thermal stability.

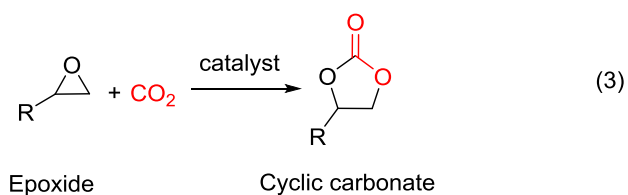
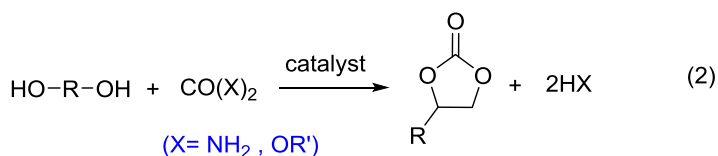
### 2.3 Cyclic carbonate synthesis

Another important class of organic carbonates is five-membered cyclic carbonates. Cyclic carbonate formation via CO<sub>2</sub> cycloaddition to epoxides is a highly promising and desirable reaction in terms of “green chemistry” due to its 100% atom economy and sustainable transformation of CO<sub>2</sub>. Conventionally, the formation of cyclic carbonates was carried out by the reaction of diols with phosgene (Reaction 1, Scheme 2.4) (Aresta and Quaranta, 1997). However, this reaction is no longer considered desirable due to the toxic and corrosive nature of phosgene and high cost involved in the disposal of HCl generated as a by-product. Therefore, various alternative methods for cyclic carbonate synthesis have been proposed to replace phosgene with DMC (Selva *et al.*, 2014), urea (Kuznetsov *et al.*, 2013) or CO (Gabriele *et al.*, 2011) as alternative carbon source (Reaction 2). However, these reactions are not considered as ecologically and economically feasible due to the additional steps involved in downstream processing such as separation and handling of the by-products. Conversely, synthesis of cyclic carbonate by CO<sub>2</sub> cycloaddition to epoxides is a promising reaction due to its 100% atom economy (Reaction 3). Moreover, a life-cycle-assessment study reveals that the amount of CO<sub>2</sub> emitted by the traditional methods of cyclic carbonate synthesis is

significantly higher than the sustainable route of cyclic carbonate synthesis via CO<sub>2</sub> cycloaddition to epoxides (Scheme 2.5) (Aresta *et al.*, 2013).

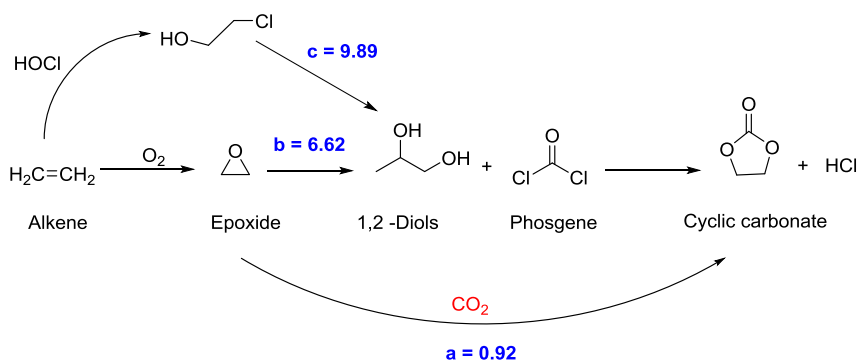


Diols                      Phosgene                      Cyclic carbonate



Scheme 2.4 Synthesis of cyclic carbonates from (1) diols and phosgene (2) diols and dialkyl carbonates/urea (3) epoxides and CO<sub>2</sub>.

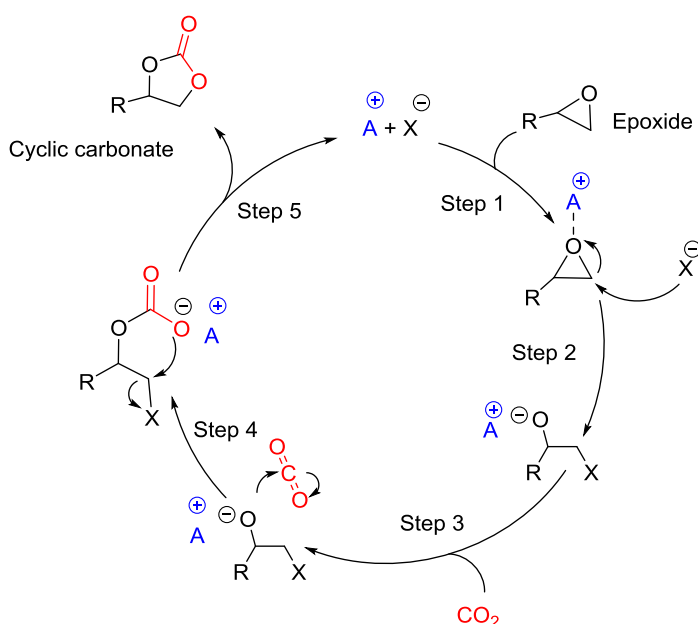
$t_{\text{CO}_2 \text{ emitted}} / t_{\text{carbonate produced}}$



Scheme 2.5 Different routes for cyclic carbonate formation with CO<sub>2</sub> emitted per unit of carbonate produced (Aresta *et al.*, 2013).

### 2.3.1 Cyclic carbonates synthesis from CO<sub>2</sub> and epoxides

The generally accepted reaction mechanism of cyclic carbonate synthesis catalysed by an acid-base catalyst involves the following steps in Scheme 2.6 (Comerford *et al.*, 2015):



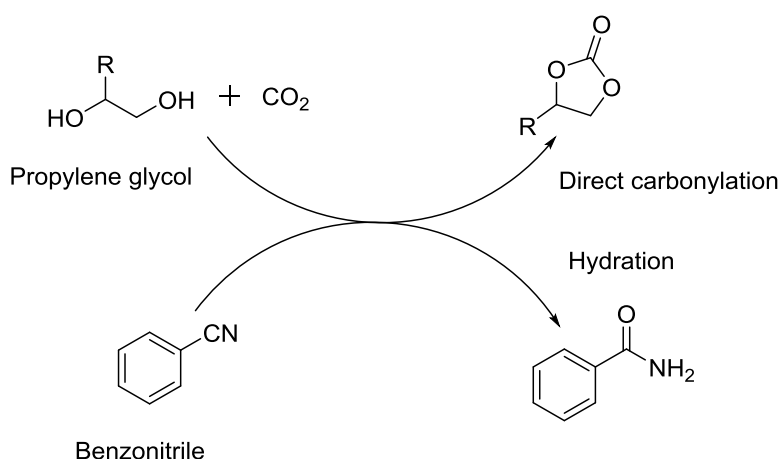
Scheme 2.6 General mechanism of cyclic carbonate synthesis using an acid-base catalyst system (Cokoja *et al.*, 2015).

- 1) Epoxide activation by the interaction of Lewis acid (A) with an oxygen atom.
- 2) Ring-opening of activated epoxide by the nucleophilic attack of halide anion ( $X^-$ ) on the least hindered C atom of the epoxide to form an alkoxide intermediate. The stability to this ring-opened epoxide was provided by the counter cation.
- 3) Subsequently, CO<sub>2</sub>-insertion takes place by the nucleophilic attack of negatively charged oxygen of alkoxide on an electrophilic carbon atom of CO<sub>2</sub> to form a carbonate intermediate. CO<sub>2</sub> is a linear apolar molecule with two polar C=O bonds resulting in a partial positive and partial negative charge on carbon and oxygen atoms respectively. Therefore activation of CO<sub>2</sub> can be carried out by both nucleophilic and electrophilic attack.
- 4) The resulting open-chain carbonate further undergoes intramolecular cyclic elimination (back-biting reaction).
- 5) Finally, a five-membered cyclic carbonate is formed by the displacement of the  $X^-$  and the catalyst is regenerated. The nucleophile (halide anion) provided by the catalyst should have

good nucleophilicity and leaving group abilities so that it helps to open the epoxide ring and finally be displaced to allow cyclic carbonate formation. Similarly, to facilitate the CO<sub>2</sub> insertion, the cation should also have favourable interactions with an alkoxide to provide greater stability to ring opened epoxide (Sakakura *et al.*, 2007).

### 2.3.2 Cyclic carbonate synthesis from CO<sub>2</sub> and 1,2-diols

Direct use of CO<sub>2</sub> with 1,2-diols is also a promising approach for cyclic carbonate synthesis. The use of diols e.g. ethylene glycol and propylene glycol as substrates have the advantage of lower toxicity and easier handling of diols than epoxides (Yue *et al.*, 2012). Da Silva *et al.* (2012) reported propylene carbonate (PC) synthesis from 1,2-propylene glycol and CO<sub>2</sub> catalyzed by K<sub>2</sub>CO<sub>3</sub>. The reaction was performed in the presence of benzonitrile to absorb the water formed as a by-product during this reaction (Scheme 2.7). Various catalyst systems for cyclic carbonate synthesis from 1,2-diols and CO<sub>2</sub> were reported such as organotin compounds and metal acetates to increase the yield of the product (Table 2.1). Particularly, the reactions catalysed by organotins have shown relatively high product yield (%) and selectivity towards cyclic carbonates. However, this process has some short-comings such as low product yield (%) due to water formation as a by-product as well as requiring high temperature, pressure and a large amount of catalyst due to low reactivity of both diols and CO<sub>2</sub> (Tamura *et al.*, 2014). To improve the product yield, continuous removal of water is required using suitable dehydrating agents.



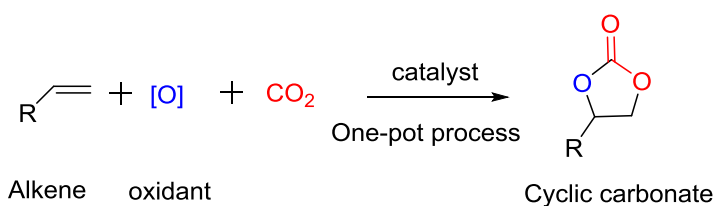
Scheme 2.7 Cyclic carbonate synthesis from 1,2-diols and CO<sub>2</sub> using benzonitrile as a solvent.

Entry	Substrate	Catalyst system	Solvent	Reaction conditions	Yield (%)	References
1	1,2-propylene glycol	Bu <sub>2</sub> Sn(OMe) <sub>2</sub>	DMF	180 °C, 150 bar <i>p</i> (CO <sub>2</sub> ), 12 h	2	(Du <i>et al.</i> , 2005)
2	1,2-glycerol	Dibutyltin dimethoxide Bu <sub>2</sub> Sn(OMe) <sub>2</sub>	-	180 °C, 50 bar <i>p</i> (CO <sub>2</sub> ), 12 h	7	(Aresta <i>et al.</i> , 2006)
3	1,2-propylene glycol	K <sub>2</sub> CO <sub>3</sub>	benzo nitrile	175 °C, 100 bar <i>p</i> (CO <sub>2</sub> ), 18 h	20	(Da Silva <i>et al.</i> , 2012)
4	1,2-glycerol	Dibutyltin oxide (Bu <sub>2</sub> SnO) and zeolite	Methanol (CH <sub>3</sub> OH)	80 °C, 35 bar <i>p</i> (CO <sub>2</sub> ), 4 h	35	(George <i>et al.</i> , 2009)
5	1,2-propylene glycol	anhydrous zinc acetate Zn(OAc) <sub>2</sub>	acetonitrile (CH <sub>3</sub> CN)	170 °C, 100 bar <i>p</i> (CO <sub>2</sub> ),	24.2	(Huang <i>et al.</i> , 2007)
6	1,2-propylene glycol	1,5,7-triazabicyclo[4.4.0]dec-5-ene	(CH <sub>3</sub> CN)	170 °C, 100 bar <i>p</i> (CO <sub>2</sub> ),	22	(Huang <i>et al.</i> , 2008)

Table 2.1 Summary of catalysts used for cyclic carbonate synthesis from 1,2-diols and CO<sub>2</sub>.

### 2.3.3 Cyclic carbonate synthesis by oxidative carboxylation of alkenes

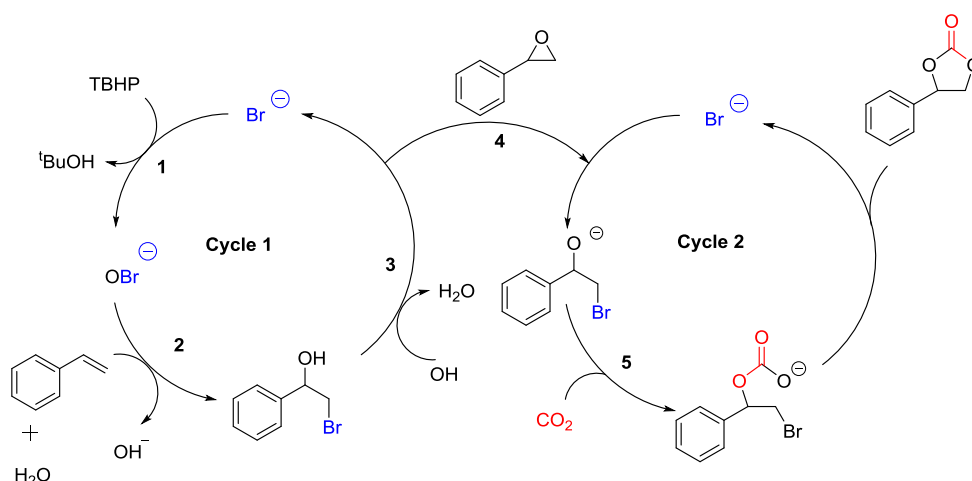
Another possible route of cyclic carbonate synthesis is the one-step oxidative carboxylation of alkenes (Scheme 2.8). Oxidative carboxylation is the combination of two reactions involving epoxidation of alkenes and cycloaddition of CO<sub>2</sub> to the *in situ* formed epoxides.



Scheme 2.8 Oxidative carboxylation of alkenes to form cyclic carbonates.

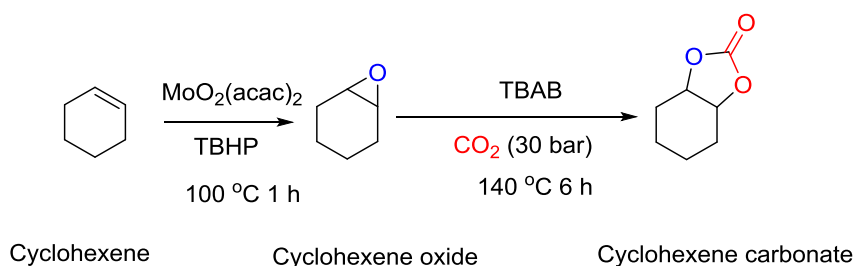
Cyclic carbonate synthesis by this method was first reported by Aresta *et al.* (1987). The formation of styrene carbonate (SC) from styrene and molecular oxygen was carried out in the presence of rhodium salts as a homogeneous catalyst at (40–80) °C and 50 bar *p* (CO<sub>2</sub>). As a result, a low yield of SC (20.5–30) % was obtained due to poor catalyst stability under these reaction conditions. To increase the catalytic activity, it is important to understand the

mechanism involved in oxidative carboxylation of alkenes. Sun *et al.* (2004a) reported SC synthesis catalysed by imidazolium ionic liquids in combination with TBAB using tert-butylhydroperoxide (TBHP) as an oxidant, resulting in 38% SC yield at 80 °C, 10 bar *p* (CO<sub>2</sub>) after 6 h. Moreover, a possible reaction mechanism was proposed showing the reaction of TBHP with TBAB to produce an oxybromide species (OBr<sup>-</sup>) which further reacts with styrene and water to form bromohydrin (cycle 1) (Scheme 2.8). Finally, affording SO in the catalytic cycle in cycle 2. The epoxide ring-opening takes place by the halide anion (Br<sup>-</sup>) and the resulting intermediate undergoes CO<sub>2</sub> cycloaddition to form SC.



Scheme 2.9 Reaction mechanism of oxidative carboxylation of styrene (Sun *et al.*, 2004a).

Similarly, two separate non-interfering catalysts were also used to catalyse both epoxidation and CO<sub>2</sub> cycloaddition reactions individually. For instance, Chen *et al.* (2011) reported oxidative carboxylation of cyclohexene in the presence of TBHP as an oxidant. Here, molybdenyl acetylacetonate MoO<sub>2</sub>(acac)<sub>2</sub> was used as a catalyst for the epoxidation step to produce CHO. Subsequently, the cycloaddition of CO<sub>2</sub> to CHO was performed using TBAB catalyst resulting in 84% yield at 140 °C and 30 bar *p* (CO<sub>2</sub>) after 6 h (Scheme 2.9).



Scheme 2.10 Oxidative carboxylation of cyclohexene to form cyclohexene carbonate.

Formation of cyclic carbonates via oxidative carboxylation is considered to be a cost-effective and environmentally friendly process due to the direct use of less expensive alkenes thereby avoiding additional steps involved in the epoxidation of alkenes, separation and handling of epoxides. However, this process is still lacking in commercial applications due to low product yield and competitive side reactions leading to benzaldehyde and benzoic acid formation as major by-products. Therefore, a highly efficient catalyst system is required which can catalyse epoxidation of alkenes and CO<sub>2</sub> cycloaddition reactions simultaneously. Future research should focus on the development of a highly efficient catalyst system and process technology for this reaction. Some other studies related to oxidative carboxylation of alkenes using different catalyst systems and oxidants are summarized in Table 2.2.

Entry	Substrate	Catalyst system	Oxidant	Reaction conditions	Yield (%)	Reference
1	Styrene	Niobium oxide in the presence of DMF solvent	Molecular oxygen	125 °C, 50 bar <i>p</i> (CO <sub>2</sub> ), 5 h	17	(Aresta <i>et al.</i> , 2000)
2	Styrene	Immobilization of gold over silica TBAB and ZnBr <sub>2</sub>	TBHP	80 °C, 80 bar <i>p</i> (CO <sub>2</sub> ) 4 h	35	(Sun <i>et al.</i> , 2005b)
3	Styrene	NBS and 1,8-diazabicycloundecene-7-ene (DBU)	H <sub>2</sub> O <sub>2</sub>	60 °C, 20 bar <i>p</i> (CO <sub>2</sub> ) 3 h	89	(Eghbali and Li, 2007)
4	Styrene	Sodium phosphotungstate in combination with TBAB	H <sub>2</sub> O <sub>2</sub>	50 °C, 24 bar <i>p</i> (CO <sub>2</sub> ), 12 h	57	(Wang <i>et al.</i> , 2008)
5	Propylene	TBAB grafted over the titanosilicate	H <sub>2</sub> O <sub>2</sub>	40 °C, 20 bar <i>p</i> (CO <sub>2</sub> ) 12 h	48	(Zhang <i>et al.</i> , 2008)
6	Cyclohexene	Molybdenyl acetylacetonate MoO <sub>2</sub> (acac) <sub>2</sub> TBAB	TBHP	140 °C, 30 bar <i>p</i> (CO <sub>2</sub> ) 6 h	84	(Chen <i>et al.</i> , 2011)
7	Styrene	Imidazolium-based ionic liquids (ILs)	TBHP	150 °C, 5 bar <i>p</i> (CO <sub>2</sub> ), 12 h	40	(Girard <i>et al.</i> , 2014)

Table 2.2 Summary of catalysts used for oxidative carboxylation of alkenes.

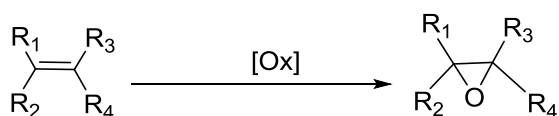
## 2.4 Applications of cyclic carbonates

Organic cyclic carbonates have a wide range of applications:

1. Cyclic carbonates are being increasingly used as ‘green’ polar aprotic solvents in chemical process industry due to their high boiling point, high dipole moment, high flash point, less toxicity and biodegradability (North *et al.*, 2009a). These organic solvents are considered as a potential replacement of traditionally used toxic polar aprotic solvents e.g. DMF which is likely to be banned according to European REACH regulations due to its impact on human health such as acute toxicity and reproductive toxicity (Comerford *et al.*, 2015).
2. Cyclic carbonates can be used as electrolytes in the Li-ion batteries due to their high dielectric properties (Etacheri *et al.*, 2011). The demand for lithium-ion batteries has been increasing rapidly due to their applications in many portable devices (Aravindan *et al.*, 2011).
3. Cyclic carbonates can be used as monomers for polymers synthesis such as polycarbonate and non-isocyanate polyurethanes (Gillis *et al.*, 1997; Clements, 2003). The use of organic cyclic carbonates as raw material for the production of these polymers have recently gained much attention in both academia and the chemical process industry. These processes have the advantage of offering alternative routes for the production of polymers by avoiding the traditional use of highly volatile and toxic chemicals such as BPA and phosgene (Geueke *et al.*, 2014).
4. Cyclic carbonates can also be used as intermediates for the production of pharmaceuticals and many other industrially important chemicals such as glycol or pyrimidines and carbamates (Laugel *et al.*, 2013; Comerford *et al.*, 2015).
5. Moreover, cyclic carbonates can also be used as substrates for the production of dimethyl carbonate (DMC) by transesterification with CH<sub>3</sub>OH (Fukuoka *et al.*, 2003). Despite the challenges associated with the production of ethylene glycol (EG) as a by-product, the production of DMC by this method has been already commercialized (Han *et al.*, 2012). Similarly, ethylene carbonate (EC) is also used for the production of EG on a commercial scale (Fukuoka *et al.*, 2003).

## 2.5 Epoxides as substrates for cyclic carbonate synthesis

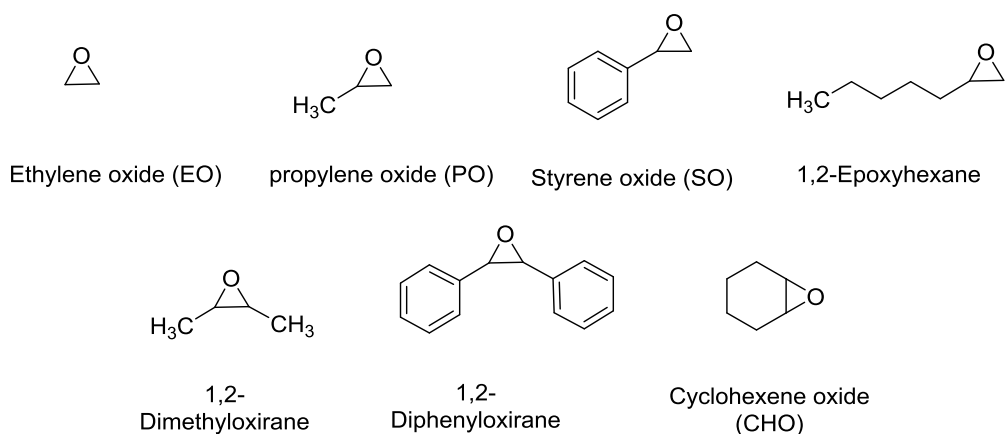
Epoxides are three-membered rings of cyclic ethers containing high strain energy. The epoxidation of alkenes is a well-known reaction (Scheme 2.11) with high commercial importance due to a wide range of applications (Astruc, 2007). Epoxides are commonly used as an intermediate for the production of many valuable polymers such as polyester, polyether, polycarbonates, and polyurethanes (Cavani and Teles, 2009).



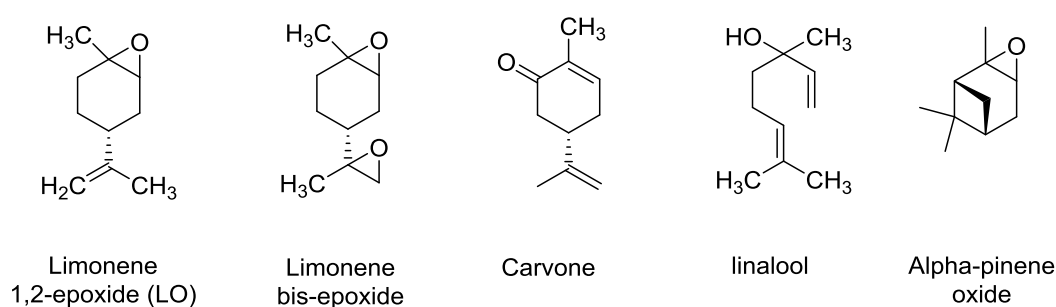
Scheme 2.11 General reaction of alkenes epoxidation in the presence of an oxidant.

Mono-substituted epoxides such as EO, PO and SO etc. also known as terminal epoxides are commonly used as substrates for cyclic carbonate synthesis (Scheme 2.12). Conversely, the use of di- and tri-substituted (internal) epoxides was relatively less studied due to low reactivity of these epoxides under mild reaction conditions. The type of epoxide can also affect the rate of cycloaddition reaction and selectivity of the product. For instance, internal epoxides offer high resistance to the nucleophilic attack of halide anion due to their high steric hindrance (Decortes *et al.*, 2010). Therefore, internal epoxides like CHO show less reactivity than terminal epoxides under the same reaction conditions. Synthesis of cyclohexene carbonates (CHC) by CO<sub>2</sub> cycloaddition to CHO is generally considered to be more challenging under mild reaction conditions due to strain offered by the adjacent cyclohexene ring to the five-membered cyclic carbonate ring (Darensbourg and Phelps, 2005).

Most of the epoxides used for cyclic carbonate synthesis are derived from petroleum-based chemicals. However, in order to satisfy the growing demands of these green chemistry, recent efforts have been focused on the utilization of renewable resources as potential raw materials for cyclic and poly(carbonate) synthesis. Particularly, the epoxidation of terpenes to form bio-based epoxides such as limonene oxide, pinene oxide, carvone, linalool and menthene oxide has recently gained much attention as substrates for the production of sustainable polymers (Scheme 2.13) (Fiorani *et al.*, 2016). This approach will not only help to overcome the threat of an increasing shortage of fossil resources but also eliminate the production of toxic intermediates in the polymer industry.



Scheme 2.12 Petroleum-based epoxides as substrates for cyclic carbonate synthesis.



Scheme 2.13 Terpene-based epoxides as substrates for bio-based cyclic carbonates synthesis.

## 2.6 Reaction conditions for cyclic carbonates synthesis

Synthesis of cyclic carbonates via  $\text{CO}_2$  cycloaddition to epoxides is strongly influenced by the reaction conditions. In order to achieve high efficiency of any catalytic system, the maximum contact between all the components of a reaction mixture is highly desirable under the given reaction conditions. For instance, solvent-free cyclic carbonate synthesis catalysed by a metal complex in combination with nucleophile additive requires a uniform reaction mixture of all the components for high catalytic performance. However, this can be a challenging task due to a different range of polarities of all the species in the reaction mixture. Reaction conditions can affect  $\text{CO}_2$  dissolution in the reaction mixture due to a change in the density of the epoxide. The density of epoxide can be increased with an increase in  $\text{CO}_2$  pressure or decrease in reaction temperature. The decrease in reaction temperature can increase the  $\text{CO}_2$  solubility, but at the same time, it may decrease the solubility of catalyst and co-catalyst in the reaction mixture. Similarly, high  $\text{CO}_2$  dissolution in the reaction mixture could also result in the decrease of catalyst solubility and it may precipitate.

### 2.6.1 Temperature

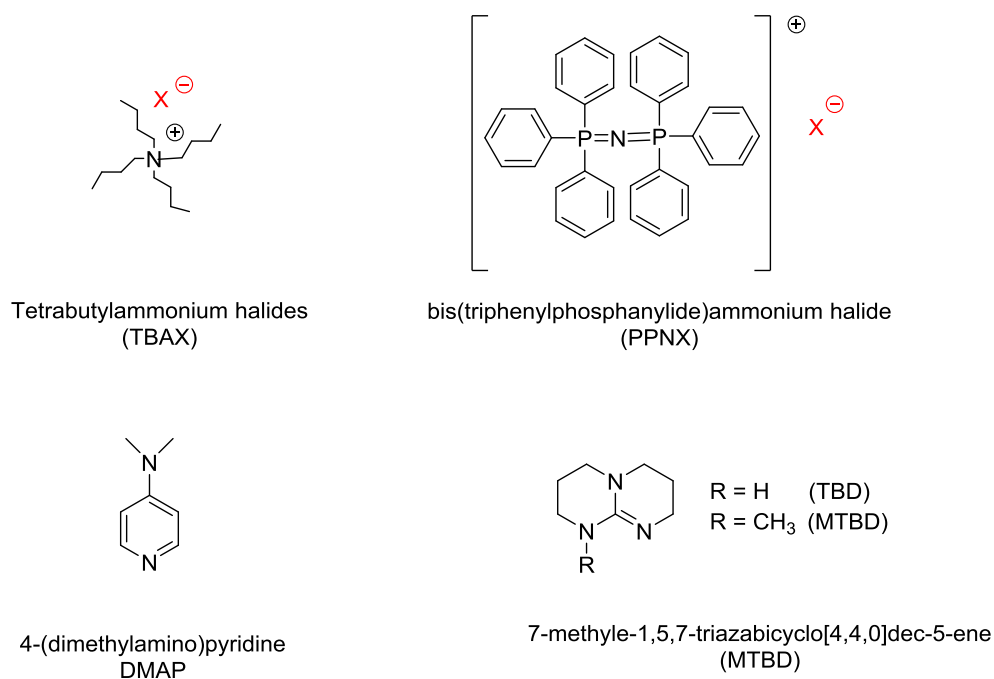
It is very difficult to predict the influence of temperature on the solubility of all components. However, the rate of catalytic CO<sub>2</sub> cycloaddition to epoxides generally increases with temperature due to an increase in catalyst activity at a higher temperature. Moreover, the mass transfer coefficient in a gas-liquid reaction can also be influenced by the gas diffusivity in the liquid ( $D_L$ ) and the liquid viscosity ( $\mu_L$ ) (Ferreira *et al.*, 2010). Increasing the temperature increases  $D_L$  and decreases  $\mu_L$ , both of which act to increase the gas-liquid mass transfer coefficient. Similarly, an increase in the reaction temperature can enhance the selectivity towards cyclic carbonates as these are thermodynamically benign products for a reaction between epoxide and CO<sub>2</sub> (Sakakura and Kohno, 2009). The activation energy required for cyclic carbonate synthesis is significantly higher than for polycarbonate formation (Pescarmona and Taherimehr, 2012).

### 2.6.2 CO<sub>2</sub> pressure

The effect of CO<sub>2</sub> pressure on cyclic carbonate synthesis catalysed by various homogeneous and heterogeneous catalyst systems was extensively studied resulting in an increase in reaction rate with the increase in CO<sub>2</sub> pressure up to a certain limit. However, a further increase in CO<sub>2</sub> pressure after a certain limit (i.e.  $p_c = 0.47 \text{ g mL}^{-1}$ ) where the CO<sub>2</sub> insertion is not a rate-limiting step anymore, a sudden decrease in reaction rate was commonly observed due to dilution effect causing a decrease in epoxide and catalyst concentration in the reaction mixture (Guadagno and Kazarian, 2004). Moreover, an increase in catalytic activity of longer alkyl chain ionic liquids for cyclic carbonates formation under supercritical CO<sub>2</sub> conditions was also reported (Taherimehr *et al.*, 2012). The use of CO<sub>2</sub> under supercritical conditions has the advantage of providing a homogeneous CO<sub>2</sub>-rich gas phase which maximizes the contact between all the components of the reaction mixture. This change in phase behaviour for cyclic carbonate synthesis was investigated using high-pressure reactors containing a viewing window.

### 2.6.3 Co-catalyst

The use of co-catalysts has been extensively studied in cyclic carbonate synthesis. Most commonly used co-catalyst for this reaction are nucleophile additives such as quaternary ammonium and phosphonium salts and other Lewis bases as shown in (Scheme 2.14).



Scheme 2.14 Structures of some commonly used co-catalysts for cyclic carbonate and polycarbonate synthesis.

The use of co-catalyst generally results in significant enhancement of reaction rate (Lu *et al.*, 2006). The role of co-catalyst during cyclic carbonate formation is to provide a nucleophile (mostly halide anion) required to open the ring of the epoxide. Moreover, co-catalyst is an essential part of the non-nucleophilic catalyst systems e.g. Zn salts and Zn-salphen complexes which shows no catalytic activity in the presence of catalyst alone (Decortes *et al.*, 2010). The use of TBAX as co-catalyst exhibited variable catalytic activities depending on the nature of catalyst and reaction conditions. For example, the order of catalytic activity of TBAX in combination with bimetallic Al(III)-salen complexes was observed as  $\text{Br}^- > \text{I}^- > \text{Cl}^- > \text{F}^-$  which was suggested as a good balance between nucleophilicity and leaving group ability of halide anions (Clegg *et al.*, 2010a). Similarly, when TBAX immobilized over chitosan supporting material were used as a heterogeneous catalyst for CO<sub>2</sub> cycloaddition to terminal epoxides, the order of halide anion activity was observed to be  $\text{I}^- > \text{Br}^- > \text{Cl}^-$  which is consistent with leaving group abilities of the halide anions (Zhao *et al.*, 2007). Similarly, the change in halide anion activity was also observed by changing the type of epoxide. The order of halide anion activity for terminal epoxides was found to be consistent with the order of leaving group ability of the halide anions i.e.  $\text{I}^- > \text{Br}^- > \text{Cl}^- > \text{F}^-$ . However, the use of  $\text{Br}^-$  has shown higher catalytic activity than  $\text{I}^-$  under the same reaction conditions in case of sterically

hindered internal epoxides. This increase in activity was attributed due to the smaller size of  $\text{Br}^-$  than  $\text{I}^-$  (Whiteoak *et al.*, 2012b).

Synthesis of PC from PO and  $\text{CO}_2$  in the presence of TBAX as co-catalysts has shown a change in selectivity by changing the halide anion ( $\text{X}^-$ ) (Lu and Wang, 2004). This was observed due to the replacement of higher leaving group ability anions such as  $\text{I}^-$  and  $\text{Br}^-$  with poor leaving group ability anions such as  $\text{Cl}^-$ ,  $\text{F}^-$  and  $\text{CH}_3\text{COO}^-$  which favours the polycarbonate formation by avoiding the back-biting reaction required to close the ring of the carbonate intermediate. However, the reaction rate can be decreased significantly by the use of poor leaving group ability anions due to reduced catalytic activity.

Similarly, the use of bis(triphenylphosphoranylide) ammonium halides (PPNX) as co-catalyst was preferred for polycarbonate synthesis. For instance, PPNCI has poor leaving group ability, thus promotes polycarbonate synthesis by avoiding back-biting reaction to close the ring of carbonate intermediate (Chisholm and Zhou, 2004). Moreover, in case of the binary catalyst system, the molar ratio between catalyst and co-catalyst, type of co-catalyst and reaction conditions can also play an important role to decide the selectivity of reaction between epoxide and  $\text{CO}_2$ . For instance,  $\text{CO}_2$  cycloaddition to CHO catalyzed by Fe (III) complex (0.1 mol%) without the use of co-catalyst favours the formation of poly(cyclohexene) carbonate (PCHC) at high  $p$  ( $\text{CO}_2$ ) (10 bar). However, the use of higher loading of Fe (III) complex (1 mol%) in combination with PPNCI (2 mol%) as nucleophile additive resulted in the switch of product selectivity from polycarbonate to cyclic carbonate and cyclohexene carbonate (CHC) was achieved with high selectivity at low  $p$  ( $\text{CO}_2$ ) (1 bar) (Buchard *et al.*, 2011). Similarly, the reaction carried out in the presence of Fe (III) amino triphenolate complex in combination with PPNCI using equimolar ratio (0.5/0.5 mol%) resulted in complete selectivity towards PCHC at 85 °C, 80 bar  $p$  ( $\text{CO}_2$ ) after 3 h. However, the change in the molar ratio between catalyst and co-catalyst (0.5/5 mol%) has switched the selectivity towards cyclic carbonates under the same reaction conditions. The use of the higher molar ratio of co-catalyst (nucleophile) helps to displace the metal-bond carbonate intermediate favouring back-biting reaction to form cyclic carbonates (Taherimehr *et al.*, 2013).

#### 2.6.4 Solvent

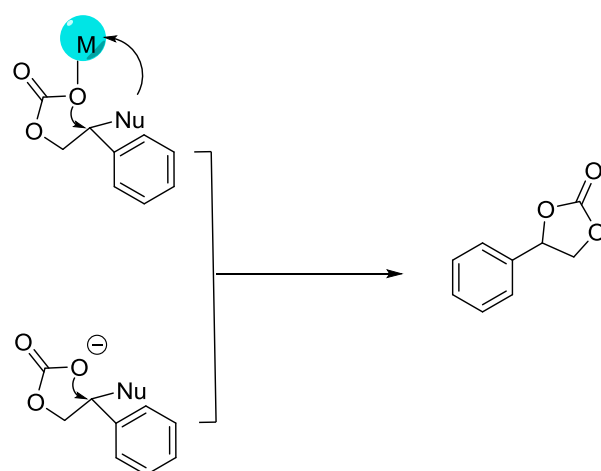
The use of a reaction solvent is generally avoided for cyclic carbonate synthesis if the catalyst is soluble in the epoxide under the reaction conditions. However, in some cases, a reaction solvent is required to avoid mass transfer limitations if the catalyst or co-catalyst is not completely soluble in the given concentration of epoxide. However, the dilution of the reaction mixture may also affect the rate of reaction due to poor contact between the components of the reaction mixture. For instance, the catalytic activity of the Zn-salphen complex in combination with TBAI was higher under solvent-free conditions than using dichloromethane ( $\text{CH}_2\text{Cl}_2$ ) as reaction solvent under the same reaction conditions (Decortes and Kleij, 2011).

#### 2.7 Stereochemical information of cyclic carbonates

Synthesis of five-membered cyclic carbonates with high stereoselectivity has recently gained much attention (Whiteoak *et al.*, 2013b). The use of enantiopure cyclic carbonates as intermediates are of high commercial importance due to their versatile reactivity. These can be used as substrates for the synthesis of optically pure *cis*-diols which are of particular interest in pharmaceutical applications (Sun *et al.*, 2013). For instance, the use of the drug in the enantiopure form can avoid unexpected side effects of consuming undesired isomer (Archelas and Furstoss, 1997). Similarly, cyclic carbonates with high *trans*-isomers have also shown high reactivity and better properties of limonene-based non-isocyanate polyurethane (NIPU) formation (Schimpf *et al.*, 2017). Therefore, the synthesis of enantiopure cyclic carbonates from low-cost racemic epoxides with high kinetic resolution is highly desirable from the commercial point of view. In this system, the use of a chiral complex (Lewis acid) selectively reacts with one of the enantiomers of the racemic oxirane. Subsequently, the activated epoxide undergoes enantioselective, nucleophilic epoxide ring-opening by the attack of halide anion or activated  $\text{CO}_2$  to form the corresponding cyclic carbonate in enantiomerically pure form (Wu *et al.*, 2016).

In case of  $\text{CO}_2$  cycloaddition to terminal epoxides, the epoxide ring-opening was mostly carried out by the nucleophilic attack on the least sterically hindered  $\beta$  (methine) carbon atom of the epoxide due to its high accessibility (Scheme 2.15) (Darensbourg, 2007). Similarly, the nature of the groups attached with epoxides may also affect the selectivity of the product formation. For instance, SO has more affinity to make cyclic carbonates than CHO due to its

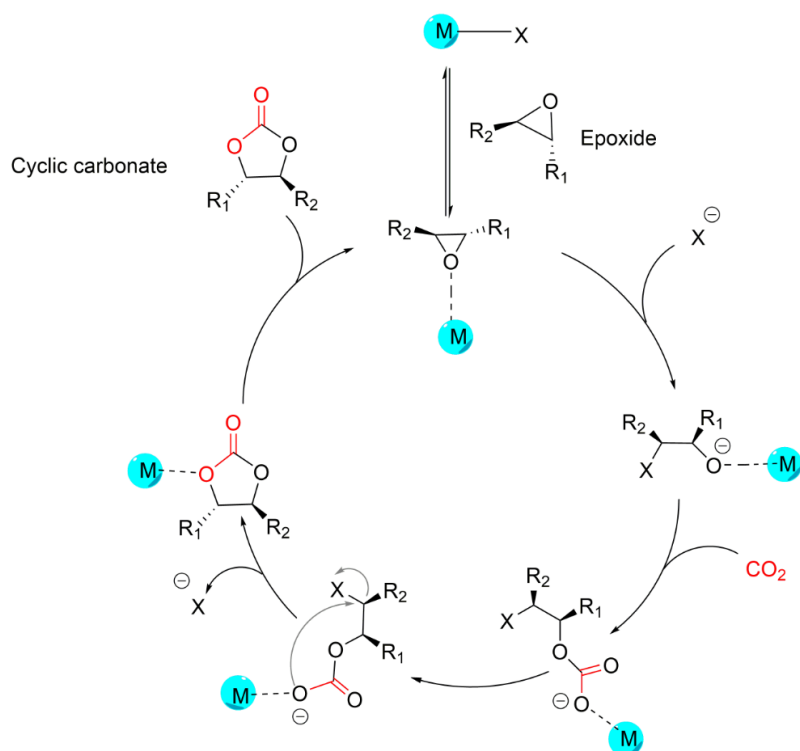
electron withdrawing nature which favours the back-biting reaction required for cyclic carbonate synthesis (Wu *et al.*, 2010). Although  $\beta$ -carbon is the most favourable position for ring-opening in case of terminal epoxides, the nucleophilic attack can also take place on the  $\alpha$ -carbon (methylene) as suggested in case of terminal epoxides having electron-withdrawing groups (Chisholm and Zhou, 2004). Moreover, the stereochemical information may partially change if the attack of the nucleophile is on the  $\alpha$ -position (Castro-Gómez *et al.*, 2013).



Scheme 2.15 Epoxide ring-opening positions in case of terminal epoxide and possible back-biting reactions resulting in a cyclic carbonate formation.

The cycloaddition of  $\text{CO}_2$  to di-substituted epoxides with high stereoselectivity can be achieved using an appropriate metal-based catalyst system in combination with nucleophile additive.  $\text{CO}_2$  cycloaddition to 2,3-disubstituted epoxide (a mixture of *cis*- and *trans*-isomers) with formal retention of configuration via a double inversion mechanism can be shown as Scheme 2.16 (Martin *et al.*, 2015). Here, activation of epoxide takes place by the interaction of metal (Lewis acid) with the oxygen atom of epoxide. The activated epoxide undergoes nucleophilic attack by the halide anion to form a metal-bonded alkoxide intermediate causing an inversion of configuration at this C centre. Subsequently, the  $\text{CO}_2$  insertion takes place by the nucleophilic attack of alkoxide on electrophilic C atom of  $\text{CO}_2$  to form a carbonate intermediate. The resulting carbonate further undergoes ring closure by intramolecular disassociation of halide anion by  $\text{S}_{\text{N}}1$  mechanism resulting inversion of configuration again

on the same C centre. Finally, a cyclic carbonate is formed with formal retention of configuration.



Scheme 2.16 General reaction mechanism for CO<sub>2</sub> cycloaddition to 2,3-disubstituted epoxide with formal retention of configuration (Martin *et al.*, 2015).

## 2.8 Catalytic systems for CO<sub>2</sub> cycloaddition to epoxides

In the last 17 years, significant research has been focused on the development of highly efficient catalytic systems for CO<sub>2</sub> cycloaddition to epoxides with the aim to carry out the reaction under mild reaction conditions. To develop a commercially viable catalytic system, the properties of the catalyst system such as stability, recyclability, upscaling, ecologic and economic feasibility and sustainability are important factors to evaluate the performance of a catalytic system. For homogeneous catalysis, the catalyst separation from the reaction mixture involved different solvent extraction techniques and subsequent highly energy-intensive distillation processes. Organic cyclic carbonates are high boiling point products e.g. PC having boiling point > 240 °C, leading to high energy requirements in separation processes. In order to make the process sustainable, the use of heterogeneous catalysis with high catalytic activity is of high commercial importance.

From the past few years, heterogeneous catalysts for cyclic carbonate synthesis have gained much attention due to ease of separation and recyclability, thereby avoiding extensive use of solvents in downstream processes. To facilitate catalyst separation and to reuse the catalyst for consecutive runs, the immobilizing of active homogeneous catalysts on high surface area inorganic supports such as silica and polymer-based materials was considered as a promising approach. To avoid leaching of the active catalytic species and to improve the catalyst life, the grafting of the active homogeneous catalyst over the supporting material was carried out through strong covalent bonding. However, a decrease in CO<sub>2</sub> cycloaddition reaction rate was generally observed using heterogeneous catalysts compared to their homogeneous counterparts due to mass-transfer (diffusion) limitations between reactants and active catalytic sites (Yu and Jones, 2003). To minimize this effect, a uniform distribution of the active catalytic species on high surface area materials is highly desirable. The supporting materials can also play an important catalytic role by providing active catalytic sites in combination with grafted catalytic species. The catalytic systems employed in both homogenous and heterogeneous phases for cyclic carbonate synthesis via CO<sub>2</sub> cycloaddition to epoxides can be classified into three major classes:

- 1) Organocatalysts
- 2) Metal-based complexes
- 3) Zinc salt based catalysts

## **2.9 Organocatalysts**

The use of organocatalysts for CO<sub>2</sub> cycloaddition to epoxides were extensively studied in both homogeneous and heterogeneous phases. Organocatalysts have advantages such as inexpensive commercial availability, non-toxicity and stable nature under the reaction conditions. Organocatalysts can be further classified as:

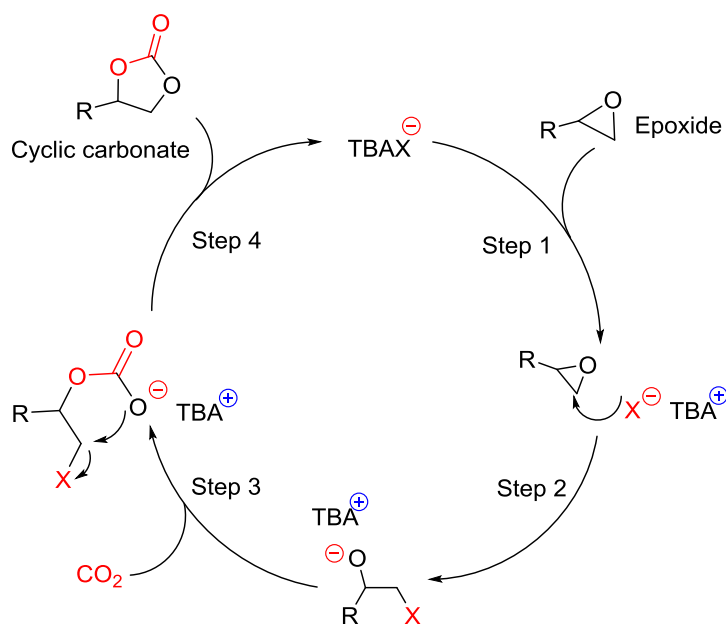
- i. Ammonium salt-based catalysts
- ii. Phosphonium salt-based catalysts
- iii. Imidazolium salt-based catalysts
- iv. Hydrogen bond donor-based organocatalysts.

### 2.9.1 Ammonium salt-based catalysts

#### *Tetrabutylammonium halides*

Tetrabutylammonium halides (TBAX) are most commonly used catalysts/co-catalysts for CO<sub>2</sub> cycloaddition to epoxides due to their strong nucleophilic and leaving group abilities. However, the use of TBAX alone as catalysts for cyclic carbonate formation generally requires harsh reaction conditions due to the lack of an acidic group required for the activation of epoxide. The first use of TBAX as catalysts for CO<sub>2</sub> cycloaddition to terminal epoxides was reported by Calo *et al.* (2002). In this study, synthesis of SC from SO and CO<sub>2</sub> was carried out by two methods (a) using 10 wt % TBAI as catalyst resulting in 80% SC yield at 60 °C and 1 bar *p* (CO<sub>2</sub>) after 22 h (b) using 1:1 wt % mixture of TBAB and TBAI resulting in 83% yield at 120 °C and atmospheric pressure after 4 h. Moreover, the reaction mechanism of cyclic carbonate synthesis using TBAX catalyst was suggested for the first time (Scheme 2.17). According to this mechanism, reaction takes place in four steps: (1) The halide anion (X) provided by the catalyst attacks nucleophilically on the least hindered carbon atom of the epoxide, (2) Epoxide ring-opening to form an alkoxide intermediate, (3) CO<sub>2</sub>-insertion occurs in the ring-opened epoxide and (4) finally, a five-membered ring of corresponding cyclic carbonate was formed by intramolecular elimination of the halide anion due to its leaving group ability. Later on, this mechanism was also supported by the density functional theory (DFT) (Wang *et al.*, 2012). The epoxide ring-opening was determined as the rate-determining step due to the high activation barrier. For EC synthesis from EO and CO<sub>2</sub>, the E<sub>a</sub> required for epoxide ring opening was determined to be 121 kJ mol<sup>-1</sup> using tetraethylammonium bromide (Et<sub>4</sub>NBr) as a catalyst rather than 243 kJ mol<sup>-1</sup> required for the uncatalysed reaction. The catalytic activity of the TBAX varies depending on the nucleophilicity and leaving group ability of the halide anions. When TBAX were used as catalysts alone, the order of the reactivity of these halide anions was observed as Cl<sup>-</sup> > Br<sup>-</sup> > I<sup>-</sup> > F<sup>-</sup> which is in agreement to the order of nucleophilicity of halide anions, except F<sup>-</sup>. Whereas, the less catalytic activity of F<sup>-</sup> was explained by its poor leaving group ability (Steinbauer *et al.*, 2018). Similarly, the chain length of cations also plays an important role in the catalytic activity of the alkylammonium halides for CO<sub>2</sub> cycloaddition to terminal epoxides causing an increase in catalytic activity with the increase in the chain length. This increase in catalytic activity was explained by the weak electrostatic forces between the halide anion and bulkier cation chain

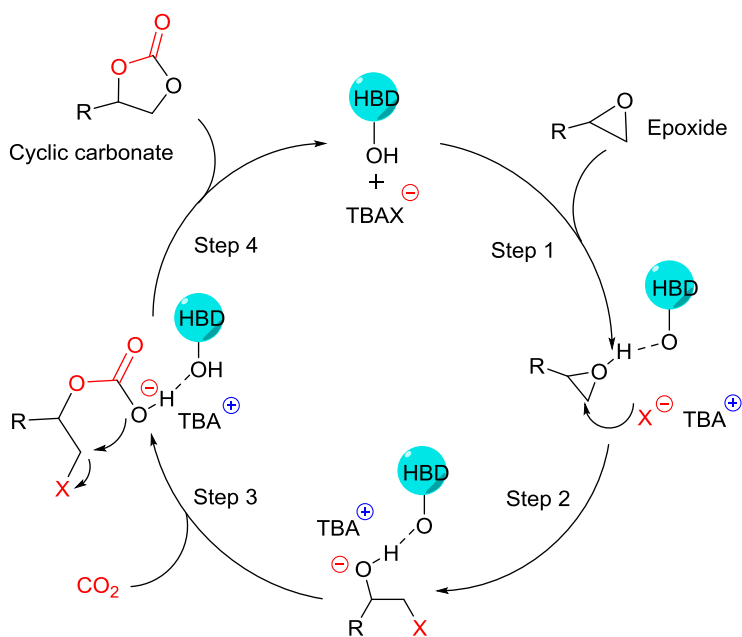
length leading to higher nucleophilicity of halide anion which in turn favours the epoxide ring opening (Jutz *et al.*, 2010).



Scheme 2.17 General mechanism for cyclic carbonate synthesis by CO<sub>2</sub> cycloaddition to epoxide catalysed by tetrabutylammonium halides (TBAX).

### ***Hydrogen bond donor ammonium-based catalysts***

Recently, considerable attention has been focused to increase the activity of TBAX using hydrogen bond donors (HBDs) such as OH-functional groups as co-catalyst. HBDs cause epoxide activation by the interaction with its oxygen atom through hydrogen bonding resulting in polarization of the C–O–C bond and making it energetically less demanding. The activated epoxide facilitates ring opening by the nucleophilic attack of halide anions followed by rapid CO<sub>2</sub> insertion (Scheme 2.18). Wang *et al.* (2006) reported an OH-functionalised ammonium salts such as hydroxyethyl tributylammonium bromide (HETBAB) as an active catalyst for cycloaddition reaction. The presence of an OH-group significantly enhance the rate of epoxide ring opening by the nucleophilic attack of the halide anion resulting in an improved yield of 96% PC rather than 74% product yield when the reaction was catalysed by TBAB alone under same reaction conditions. The presence of HBD in the catalyst system has two advantages: 1) epoxide activation through hydrogen bonding which favours epoxide ring-opening, 2) provides stability to the ring-opened epoxide intermediate which is a key factor for rapid CO<sub>2</sub> insertion. Some other OH-group functionalized ammonium salts as HBD based homogenous catalyst for cyclic carbonate synthesis have been summarized in Table 2.3.



Scheme 2.18 General mechanism for cyclic carbonate synthesis catalysed by TBAX in conjunction with HBDs.

Sr. No.	Catalyst	Substrate	Reaction conditions	Yield (%)	Reference
1 <sup>a</sup>	Choline iodide (6.08 mol %)	SO	85 °C, 10 bar <i>p</i> (CO <sub>2</sub> ), 6 h	99	(Amaral <i>et al.</i> , 2013)
2	Tri-methylammonium histidine iodide (0.28 mol %)	SO	120 °C, 1 bar <i>p</i> (CO <sub>2</sub> ), 6 h	95	(Roshan <i>et al.</i> , 2014)
3	Tetrabutylammonium hydroxide (1 mol %)	SO	120 °C, 10 bar <i>p</i> (CO <sub>2</sub> ), 24 h	88	(Ema <i>et al.</i> , 2015)
4	Bifunctional ammonium salts (2.15 mol %)	SO	90 °C, 5 bar <i>p</i> (CO <sub>2</sub> ), 2 h	95	(Büttner <i>et al.</i> , 2015)

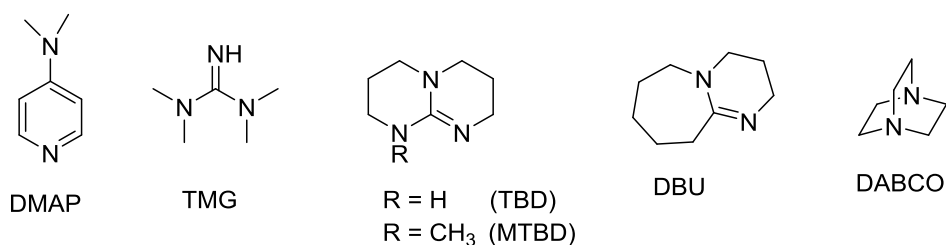
<sup>a</sup> Ethanol was used as the reaction solvent.

Table 2.3 Summary of HBDs based ammonium salts as homogeneous catalysts.

### ***Nitrogen donor bases as catalysts***

Another class of nitrogen donor bases such as 4-(dimethylamino)pyridine (DMAP), 1,4-(diazabicyclo)octane (DABCO), 1,1,3,3-tetramethylguanidine (TMG) and 1,5,7-(triazabicyclo)decene (TBD) were reported as active catalysts for the cyclic carbonate synthesis (Scheme 2.19). Barbarini *et al.* (2003) reported the SC synthesis from SO and CO<sub>2</sub> in the presence of methyl-1,5,7-(triazabicyclo)decene (MTBD) in both homogeneous phase

and heterogeneous phase prepared by covalent grafting over silica ( $\text{SiO}_2$ ). As a result, a 95% yield of SC was obtained using homogeneous catalysts at 140 °C and 50 bar  $p$  ( $\text{CO}_2$ ) for 20 h. Although heterogeneous analogue of the catalyst has the advantage of recycling, the catalytic activity decreased significantly and a 90% yield of SC was achieved after 70 h under the same reaction conditions. Zhang *et al.* (2006) reported  $\text{SiO}_2$ -supported TBD and  $\text{SiO}_2$ -supported DBU as heterogeneous catalysts for PC formation by  $\text{CO}_2$  cycloaddition to PO. The quantitative yield of PC was achieved at 150 °C and 15 bar  $p$  ( $\text{CO}_2$ ) for 10 h. Both heterogeneous catalysts can be used up to 5 cycles with an appreciable decrease in activity and selectivity. Similarly, some other TMG, DBU and DMAP based catalysts were also reported for  $\text{CO}_2$  cycloaddition to terminal epoxides (Cokoja *et al.*, 2015). However, the reduced catalytic activity, harsh reaction conditions, and recycling problems were the key issues to limit the applications of these catalysts on a commercial scale.



Scheme 2.19 Structure of nitrogen donor bases used as catalysts for cyclic carbonate synthesis.

### ***Ammonium salt-based heterogeneous catalysts***

Alkylammonium halides as heterogeneous catalyst prepared by immobilizing on high surface area inorganic supports were extensively studied. The catalysts have exhibited higher catalytic activities for  $\text{CO}_2$  cycloaddition to terminal epoxides (Table 2.4). The activity of immobilised alkylammonium halides was further enhanced by grafting OH-functionalized ammonium salts. These heterogeneous catalysts have the advantages of easy separation and good recyclability. However, cyclic carbonate formation in the presence of these catalysts still requires high temperature, pressure and catalyst loading, which can result in the negative carbon footprint of the reaction. Moreover, the catalytic activities were found to be significantly lower than their homogeneous analogues. Motokura *et al.* (2009) reported  $\text{SiO}_2$ -supported aminopyridinium halides as a highly active catalyst for  $\text{CO}_2$  cycloaddition to epoxides under mild reaction conditions i.e. 100 °C and 1 bar  $p$  ( $\text{CO}_2$ ) (entry 5, Table 2.4).  $\text{SiO}_2$ -supported aminopyridinium halides catalysts have unexpectedly exhibited higher catalytic activity than their homogeneous counterparts. The enhancement in catalytic activity

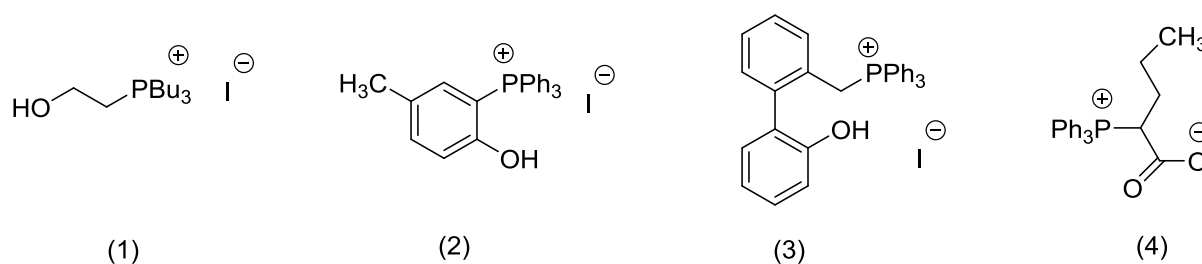
was observed due to the synergistic effect of the halide anions with Si–OH (silanol) groups acting as weak acidic sites to activate epoxide. SiO<sub>2</sub>-supported aminopyridinium halides also have several advantages over other alkylammonium halide based catalysts, such as the presence of a long chain of delocalized cations in resonance form, facile methods of preparation and high stability in the air. Moreover, the catalyst exhibited good recyclability, with up to 3 cycles without a decrease in catalytic activity. The synergistic effect between hydroxyl and amino group over the surface of the catalyst exhibited high catalytic activity. In addition to the grafting of OH-functionalized groups, naturally occurring OH-group based biopolymers such as chitosan (CS) and cellulose (CL) were also used as supporting materials for the immobilization of ammonium salts (entry 4 and 7, Table 2.4).

Sr. No.	Catalyst	Support	Reaction conditions	Yield (%)	Reusability (runs)	Reference
1	hexaalkylguanidinium chloride (1 mol%)	SiO <sub>2</sub>	120 °C, 45 bar <i>p</i> (CO <sub>2</sub> ), 4 h	99	5	(Xie <i>et al.</i> , 2005)
2	Quaternary ammonium salts (1 mol%)	SiO <sub>2</sub>	150 °C, 80 bar <i>p</i> (CO <sub>2</sub> ), 6 h	97	8	(Wang <i>et al.</i> , 2006)
3	PEG-supported quaternary ammonium salts (5 mol%)	PS	100 °C, 80 bar <i>p</i> (CO <sub>2</sub> ), 12 h	95.2	5	(Du <i>et al.</i> , 2006)
4	3-chloro-2-(hydroxypropyl) trimethylammonium chloride (1.7 mol%)	CS	160 °C, 40 bar <i>p</i> (CO <sub>2</sub> ), 6 h	88	5	(IPCC, (2018))
5	4-pyrrolidinopyridinium iodide	SiO <sub>2</sub>	100 °C, 1 bar <i>p</i> (CO <sub>2</sub> ), 20.5 h	89	3	(Motokura <i>et al.</i> , 2009)
6	Diethanolamine based ammonium halides (2 mol%)	PS	110 °C, 1 bar <i>p</i> (CO <sub>2</sub> ), 6 h	96	6	(Chen <i>et al.</i> , 2012)
7	hydroxypropyl trimethylammonium iodide (0.4 mol%)	CL	120 °C, 12 bar <i>p</i> (CO <sub>2</sub> ), 6 h	88	6	(Tharun <i>et al.</i> , 2013)

Table 2.4 Summary of ammonium salts as heterogeneous catalyst systems.

## 2.9.2 Phosphonium salts as homogeneous and heterogeneous catalysts

Phosphonium salts as catalysts in both homogeneous and heterogeneous phase were also studied for cyclic carbonate formation due to their high thermal stability (Del Sesto *et al.*, 2005). Although the catalytic activity of phosphonium salts was found to be identical with ammonium counterparts, the use of phosphonium halides as catalysts was less commonly studied. The catalytic activity of phosphonium salts in conjunction with Co (II) salts was even found to be higher than ammonium and imidazolium-based ionic liquids (Sibaouih *et al.*, 2009). The HBDs based bifunctional phosphonium halides exhibited higher catalytic activity compared to monofunctional counterparts due to their ability of epoxide activation. The use of phosphonium based homogeneous catalyst for CO<sub>2</sub> cycloaddition to epoxides is summarised in Table 2.5.

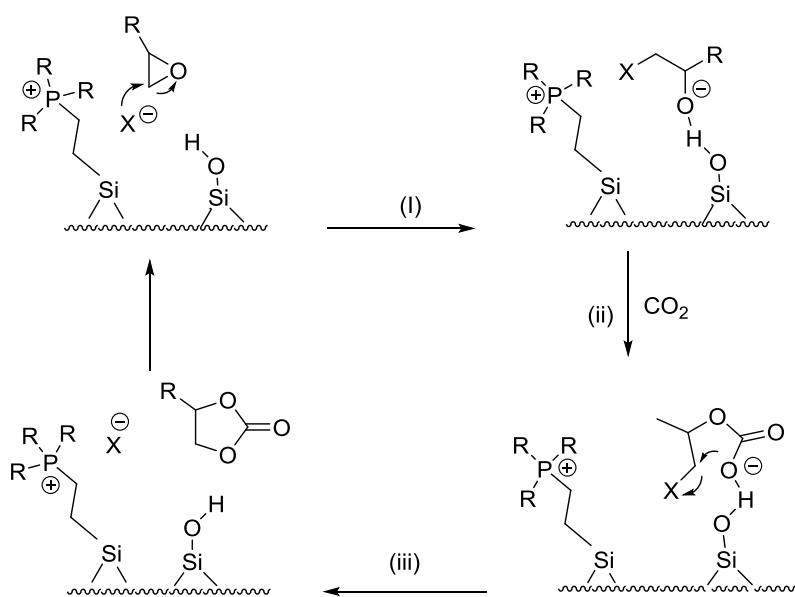


Sr. No.	Catalyst	Substrate	Reaction conditions	Yield (%)	Reference
1	butyl-triphenylphosphonium Iodide (PPh <sub>3</sub> BuI) (0.5 mol%)	SO	125 °C, 20 bar <i>p</i> (CO <sub>2</sub> ), 1 h	83	(Sun <i>et al.</i> , 2009)
2	phosphorus ylides (4)	SO	25 °C, 1 bar <i>p</i> (CO <sub>2</sub> ), 6 h	62	(Zhou <i>et al.</i> , 2015)
3	Tetraarylphosphonium Salt (2) (15 mol%)	SO	120 °C, 1 bar <i>p</i> (CO <sub>2</sub> ), 12 h	91	(Toda <i>et al.</i> , 2016)
4	Bifunctional quaternary phosphonium iodide (3) (1 mol%)	SO	60 °C, 1 bar <i>p</i> (CO <sub>2</sub> ), 24 h	92	(Liu <i>et al.</i> , 2016a)

Table 2.5 Summary of phosphonium salts as homogeneous catalysts.

Similarly, cyclic carbonates synthesis catalysed by phosphonium salts in the heterogeneous phase were summarized in Table 2.6. Among these catalyst systems, SiO<sub>2</sub>-supported phosphonium salts were also reported as highly efficient heterogeneous catalysts under mild reaction conditions i.e. 100 °C, 10 bar *p* (CO<sub>2</sub>) (Takahashi *et al.*, 2006). The synergistic effect

between phosphonium halides and silanol groups (Si–OH) over the surface of SiO<sub>2</sub> acting as weak acids resulted in higher catalytic activity. This heterogeneous catalyst system was also investigated under continuous flow conditions and the catalyst has shown good catalytic activity even after 1000 h of reaction time. Moreover, a reaction mechanism was proposed (Scheme 2.20). Here, Si–OH groups over the surface of SiO<sub>2</sub> act as weak acids to activate the epoxide and the halide anion provided by the catalyst open the ring of activated epoxide by nucleophilic attack on least hindered carbon (I). The ring-opened epoxide further interacts with CO<sub>2</sub> to form carbonate (II). Finally, a five-membered cyclic carbonate is formed as a result of back-biting reaction (III).



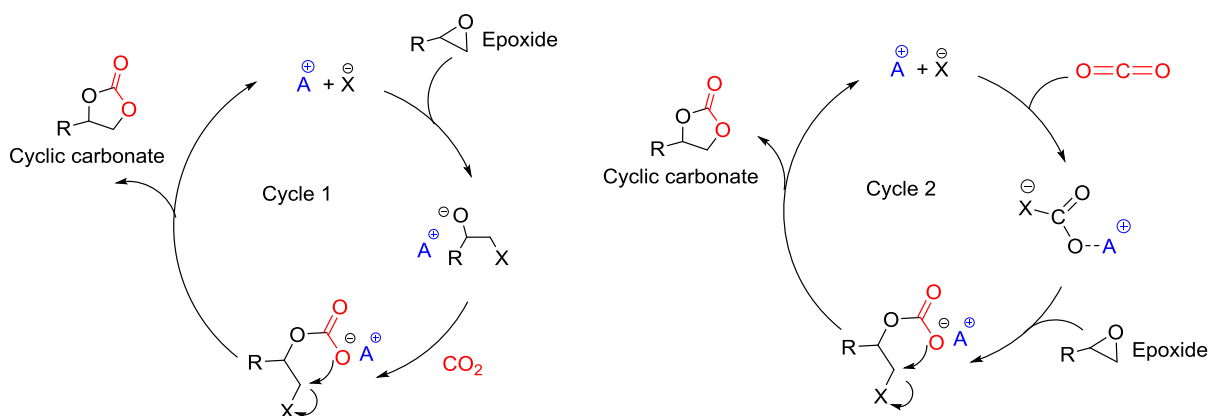
Scheme 2.20 Proposed reaction mechanism for cyclic carbonate synthesis using SiO<sub>2</sub>-supported phosphonium salt as a heterogeneous catalyst (Takahashi *et al.*, 2006).

Sr. No.	Catalyst	Support	Reaction conditions	Yield (%)	Reusability (runs)	Reference
1	Tributyl phosphonium iodide (PBU <sub>3</sub> I) (1 mol%)	SiO <sub>2</sub>	100 °C, 10 bar <i>p</i> (CO <sub>2</sub> ), 1 h	>99	Fixed bed (1000 h)	(Takahashi <i>et al.</i> , 2006)
2	3-(triethoxysilyl) propyltriphenyl phosphonium bromide (1 mol%)	SiO <sub>2</sub>	90 °C, 10 bar <i>p</i> (CO <sub>2</sub> ), 1 h	86	10	(Sakai <i>et al.</i> , 2008)
3	Tributyl phosphonium chloride (PBU <sub>3</sub> Cl) (5 mol%)	PS	150 °C, 50 bar <i>p</i> (CO <sub>2</sub> ), 10 h	95.8	5	(Xiong <i>et al.</i> , 2013)

Table 2.6 Summary of phosphonium salt as heterogeneous catalysts.

### 2.9.3 Imidazolium salts as homogeneous and heterogeneous catalysts

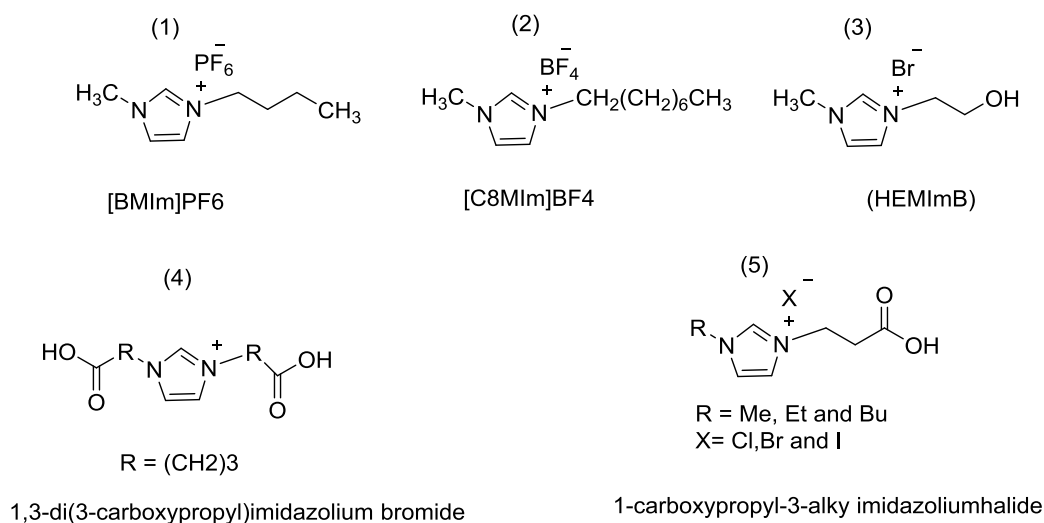
The cycloaddition of CO<sub>2</sub> to epoxides catalysed by imidazolium-based ionic liquids (ILs) was also studied in both homogeneous and heterogeneous phase. ILs in the homogeneous phase can play a double role as it can be used both as catalyst and solvent due to their ability to dissolve a considerable amount of CO<sub>2</sub>. Cyclic carbonate formation using ILs alone was mostly carried out at > 80 °C to achieve higher product yields. The reaction mechanism of CO<sub>2</sub> cycloaddition to epoxides in the presence of non-metallic ILs depends on the nature of cation and anion. Two types of reaction mechanisms for cyclic carbonate synthesis catalysed by ILs, were proposed (Scheme 2.21) (Pescarmona and Taherimehr, 2012).



Scheme 2. 21 Proposed reaction mechanisms for cyclic carbonate synthesis using ILs as catalysts (Jutz *et al.*, 2010).

The first reaction mechanism is in agreement with a generally accepted mechanism for cyclic carbonate synthesis as discussed previously in the presence of an acid-base catalyst, explaining ring-opening of epoxides by nucleophilic attack of halide anion followed by CO<sub>2</sub> insertion into the ring opened epoxide and finally the closure of the ring to generate cyclic carbonate (Cycle 1). Another possible pathway for cyclic carbonate formation was proposed using ILs containing bulky anions such as BF<sub>4</sub><sup>-</sup> and PF<sub>6</sub><sup>-</sup>. These bulky anions interact with CO<sub>2</sub> directly to form a new ionic intermediate [X-CO<sub>2</sub>]<sup>-</sup> rather than weaker interaction with the epoxides. Due to more basicity of the ionic species compared to halide anion (X), this further interacts with an epoxide to form a carbonate intermediate. Finally, the cyclic carbonate was obtained as the product (Cycle 2) (Jutz *et al.*, 2010). This mechanism was also supported by the mechanistic investigation carried out using *in-situ* ATR-FTIR spectroscopy

(Seki *et al.*, 2008). Some commonly known ILs used as catalysts for CO<sub>2</sub> cycloaddition to terminal epoxides are shown in Scheme 2.22.



Scheme 2.22 Structures of some commonly used imidazolium-based ILs as catalysts for cyclic carbonate synthesis.

Peng and Deng (2001) reported the first use of IL-based catalysts such as 1-n-butyl-3-methylimidazolium halides (BMImX) for CO<sub>2</sub> cycloaddition to epoxides resulting quantitative conversion of terminal epoxides with 100% selectivity. Formation of PC from PO and CO<sub>2</sub> was carried out using [BMIm] PF<sub>6</sub> (**1**) at 110 °C and 25 bar *p* (CO<sub>2</sub>) for 6 h. Moreover, the catalyst can be recycled after separation by distillation. PC synthesis by CO<sub>2</sub> cycloaddition to PO was also reported in the presence of 1-octyl-3-methylimidazolium tetrafluoroborate [C<sub>8</sub>-MIm]<sup>+</sup> BF<sub>4</sub> (**2**) as a homogeneous catalyst at supercritical conditions i.e. 100 °C and 140 bar *p* (CO<sub>2</sub>). The high solubility of the epoxide and CO<sub>2</sub> under supercritical conditions resulted in enhanced catalytic activity and a 100% yield of PC in less than 2 h (Kawanami *et al.*, 2003).

The use of hydroxyl-functionalized (OH) ionic liquids such as 1-(2-hydroxyethyl)-3-methylimidazolium bromide (HEMImBr) (**3**) has also shown higher catalytic activities than their non-hydroxyl functionalized analogues (Sun *et al.*, 2008). The quantitative yield of SC was achieved using HEMImBr at 125 °C and 20 bar *p* (CO<sub>2</sub>) after 1 h. Wang *et al.* (2014a) also reported several hydroxymethyl-functionalized ILs as homogeneous catalysts for cyclic carbonate synthesis under solvent-free conditions resulting in 90% yield of SC at 120 °C and 20 bar *p* (CO<sub>2</sub>) for 2 h. Similarly, the use of carboxyl-functionalized (COOH) Imidazolium halides (**4**) were also reported (Sun *et al.*, 2011). The activation of epoxide due to the HB

donor ability of the COOH group resulted in higher catalytic activity. Synthesis of PC in the presence of carboxylic-acid functionalized imidazolium salt as an acid-base bifunctional catalyst was achieved with 95% yield at 100 °C and 20 bar  $p$  (CO<sub>2</sub>) for 1 h.

Anthofer *et al.* (2014) also proposed hydroxyl-functionalized mono and bis-imidazolium halides (**5**) as most active one-component catalysts for CO<sub>2</sub> cycloaddition to SO at 70 °C and 4 bar  $p$  (CO<sub>2</sub>) resulting in 96% yield after 22 h. The presence of the proton at the C2 position of the imidazolium ring causes epoxide activation and hence facilitates the epoxide ring-opening by the nucleophilic attack of halide anion. Furthermore, the presence of HB donors in the bifunctional structure of the catalyst provides the stability of the ring opened epoxide in the transition state.

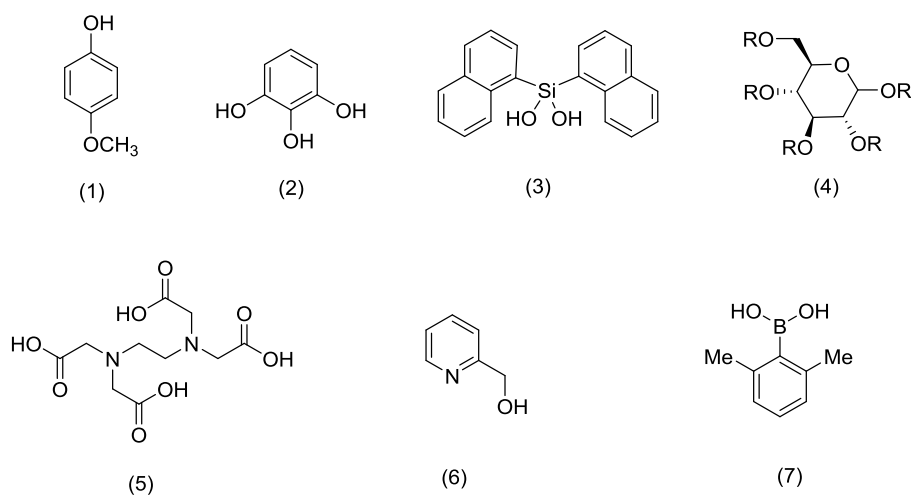
Due to high product solubility of ILs in the homogeneous phase, highly energy-intensive downstream processes are required for the separation of the catalyst. In order to make the process more economical and environment-friendly, the immobilizing of ILs over the various supporting materials was studied as a promising approach towards heterogeneous catalysis. Particularly, the immobilization of –OH and –COOH group-containing ionic liquids are highly advantageous for CO<sub>2</sub> cycloaddition to epoxides under mild reaction conditions. SC formation from SO and CO<sub>2</sub> using various heterogeneous imidazolium-based ionic liquids are summarized in Table 2.7. These mainly include PS, The heterogenisation of imidazolium-based ILs was mostly carried out by copolymerization with divinylbenzene (DVB), and by immobilizing the active species of PS, SiO<sub>2</sub> and biopolymeric (e.g. chitosan (CS), carboxymethylcellulose (CMC) supporting materials.

Sr. No.	Catalyst	Support	Reaction conditions	Yield (%)	Reusability (runs)	Reference
1	1-butyl-3-methylimidazolium tetrafluoroborate (BMImBF <sub>4</sub> ) (1.8 mol%)	SiO <sub>2</sub>	160 °C, 80 bar <i>p</i> (CO <sub>2</sub> ), 4 h	96	3	(Wang <i>et al.</i> , 2007)
2	3-butyl-1-vinylimidazolium chloride (0.7 mol %)	DVB	110 °C, 60 bar <i>p</i> (CO <sub>2</sub> ), 7 h	79	5	(Xie <i>et al.</i> , 2007)
3	1-(2-hydroxyethyl)-imidazolium bromide 1.6 mol%	PS	120 °C, 25 bar <i>p</i> (CO <sub>2</sub> ), 4 h	93	6	(Sakai <i>et al.</i> , 2008)
4	1-carboxyethyl imidazolium bromide (CSEImBr) (0.45 mol%)	SiO <sub>2</sub>	110 °C, 16.2 bar <i>p</i> (CO <sub>2</sub> ), 5 h	96	4	(Han <i>et al.</i> , 2011)
5	2-3-(hydroxypropyl)-imidazolium bromide (13.8 wt %)	PS	130 °C, 20 bar <i>p</i> (CO <sub>2</sub> ), 1 h	98	3	(Watile <i>et al.</i> , 2012)
6	1-ethyl-3-methyl imidazolium bromide (MImBr) (1 mol%)	CS	120 °C, 20 bar <i>p</i> (CO <sub>2</sub> ), 4 h	85	5	(Sun <i>et al.</i> , 2012)
7	1-butyl-3-triethoxysilylpropyl imidazolium iodide (BImI) (1.2 mol%)	CMC	110 °C, 18 bar <i>p</i> (CO <sub>2</sub> ), 4 h	92	3	(Roshan <i>et al.</i> , 2012)
8	1-vinyl-3-carboxyethylimidazolium bromide (1 mol%)	DVB	130 °C, 25 bar <i>p</i> (CO <sub>2</sub> ), 6 h	90	5	(Shi <i>et al.</i> , 2013)

Table 2.7 Summary of imidazolium salts as heterogeneous catalysts.

#### 2.9.4 Hydrogen bond donor-based organocatalysts

Hydrogen bond donors (HBDs) in combination with TBAX as binary catalyst systems were also reported as efficient homogeneous catalytic systems for cyclic carbonate formation (Buettner *et al.*, 2017). The reaction carried out using HB-donor organocatalysts alone have shown no or little catalytic activity. However, the presence of nucleophile additives in combination with HBDs have resulted in a significant increase in catalytic activity under mild reaction conditions due to the synergistic effect (Shen *et al.*, 2003). Alkylammonium halides, KI, DMAP and DBU were most commonly used as nucleophile additives in combination with HBD organocatalysts for cyclic carbonates synthesis (Table 2.8).

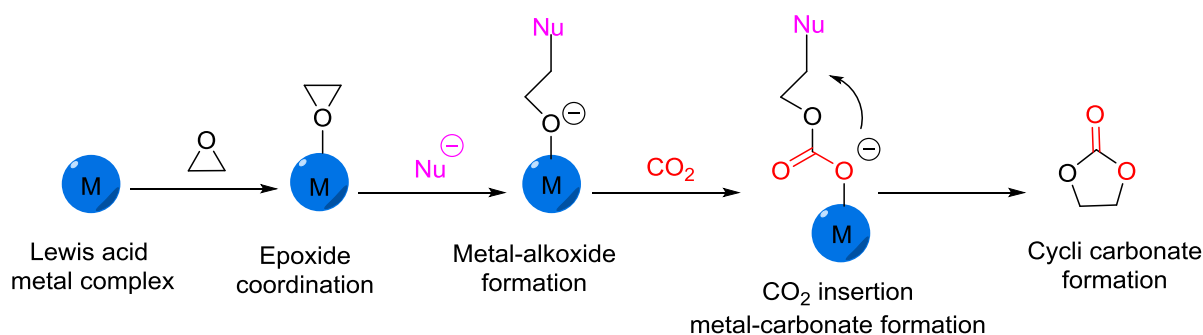


Entry	Catalyst	Co-Catalyst	Reaction conditions	Yield %	References
1	<i>p</i> -methoxyphenol (1)	DMAP	120 °C, 23 bar <i>p</i> (CO <sub>2</sub> ), 48 h	96	(Shen <i>et al.</i> , 2003)
2	Pyrogallol Ph(OH) <sub>3</sub> (2)	TBAI	45 °C, 10 bar <i>p</i> (CO <sub>2</sub> ), 18 h	52	(Whiteoak <i>et al.</i> , 2012c)
3	dinaphthylsilanediol (Si-diol) (3)	TBAI	23 °C, 1 bar <i>p</i> (CO <sub>2</sub> ), 7 h	93	(Hardman- Baldwin and Mattson, 2014)
4	Tannic acid (4)	TBAI	80 °C, 10 bar <i>p</i> (CO <sub>2</sub> ), 18 h	76	(Wilhelm <i>et al.</i> , 2014)
5	Cellulose	DBU	120 °C, 20 bar <i>p</i> (CO <sub>2</sub> ), 2 h	85	(Sun <i>et al.</i> , 2014)
6	Ethylenediaminetetraacetic acid (EDTA) (5)	TBAI	50 °C, 5 bar <i>p</i> (CO <sub>2</sub> ), 18 h	94	(Liu <i>et al.</i> , 2016b)
7	2-pyridine methanol (6)	TBAI	45 °C, 1 bar <i>p</i> (CO <sub>2</sub> ), 20 h	85	(Wang <i>et al.</i> , 2016)
8	(2,6-dimethyl phenyl) boronic acid and water (7)	TBAI	50 °C, 10 bar <i>p</i> (CO <sub>2</sub> ), 7 h	88	(Wang and Zhang, 2016)
9	ascorbic acid	TBAI	60 °C, 1 bar <i>p</i> (CO <sub>2</sub> ), 23 h	96	(Arayachukiat <i>et al.</i> , 2017)

Table 2.8 Summary of two-component HBDs based catalyst systems.

### 2.9.5 Metal-based complexes

Metal-based salen and salphen complexes are widely recognized as highly efficient catalysts for the cyclic carbonate synthesis under mild reaction conditions. Salen ligands can be prepared by the condensation of salicylaldehyde with a chiral or achiral diamine (Martin *et al.*, 2015). The use of metal-based salen complexes for cyclic carbonate synthesis has several advantages such as the facile method of preparation in enantiomerically pure form and easy availability. Due to their tunable structures, salen complexes are highly desirable catalysts for kinetic resolution and asymmetric cyclic carbonate formation (Canali and Sherrington, 1999). The metal-based complexes can be used as catalysts alone or in a combination with the nucleophile additive co-catalyst. The reaction mechanism involved in cyclic carbonate synthesis in the presence of metal complexes in combination with nucleophile has been generally well established (Scheme 2.23) (Pescarmona and Taherimehr, 2012).



Scheme 2.23 General reaction mechanism for CO<sub>2</sub> cycloaddition to epoxides catalysed by the monometallic complex.

The reaction mechanism of cyclic carbonate synthesis in the presence of monometallic complexes involves the activation of epoxide by the interaction of a metal centre with oxygen (M–O interaction), followed by epoxide ring opening by the nucleophilic attack of the halide anion on least hindered C atom of the epoxide to form a metal-bonded alkoxide intermediate. This ring-opened intermediate further undergoes CO<sub>2</sub> insertion by the nucleophilic attack of metal-bonded alkoxide on the carbon atom to form a metal-bonded carbonate. Finally, the carbonate undergoes back-biting reaction to form five-membered cyclic carbonate. This mechanism was also supported by the *in-situ* IR kinetic analysis and most likely to occur using low epoxide/catalyst molar ratio (Darensbourg and Yarbrough, 2002). The bimetallic reaction mechanism involving the activation of both epoxide and CO<sub>2</sub> simultaneously was also reported for the reactions carried out using metal complexes containing two neighboring

metal centres. The simultaneous activation of CO<sub>2</sub> helps to promote CO<sub>2</sub> insertion to a ring-opened epoxide by making this step energetically less demanding. This dual activation of epoxide and CO<sub>2</sub> has resulted in the higher catalytic activity of bimetallic complexes than monometallic complexes (Melendez *et al.*, 2007).

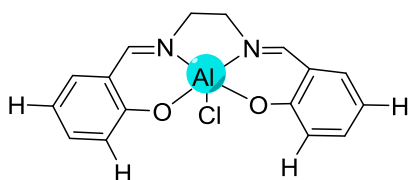
The nature of the metal centre and the ligand connected with the metal centre plays an important role to decide the catalytic activity of the metal complexes. Moreover, the strength of the M–O bond of alkoxide and carbonate intermediates also play a key role to determine the activity of the catalyst (Srivastava *et al.*, 2005). For instance, a strong M–O bond makes the alkoxide challenging to interact with CO<sub>2</sub> to form carbonate. Conversely, a weak M–O bond can be easily replaced by the nucleophile or a solvent molecule resulting in low catalytic activity, but also promoting the back-biting reaction at the same time to form cyclic carbonates. Therefore, intermediate bond strength is more favoured for the better performance of the catalyst.

Similarly, the steric and electronic properties of the complexes also affect the catalytic activity and selectivity of the metal complexes. These properties are mostly defined by the type of ligand attached to the metal centre. For instance, the use of ligands having high electron-donor ability favours cyclic carbonate formation by promoting the back-biting reaction (Pescarmona and Taherimehr, 2012). Similarly, the steric properties of the complexes also affect the catalytic activity of metal complexes and can be varied by the replacement of substituents attached on the aromatic rings of the ligands (Wu *et al.*, 2011).

Various types of metal-based salen and salphen complexes with tuneable properties have been examined as highly efficient catalysts for CO<sub>2</sub> cycloaddition to epoxides. These were generally used in conjunction with nucleophile additives as an essential part of the catalyst or to increase the catalytic activity of a nucleophile containing metal complex. The role of the nucleophile is defined as to open the epoxide ring by providing the halide anion. Moreover, it can also interact with the metal centre of the complex to provide an electron-rich environment leading to rapid epoxide or CO<sub>2</sub> insertion. The properties of the metal complexes can be further changed by the choice of metal centre.

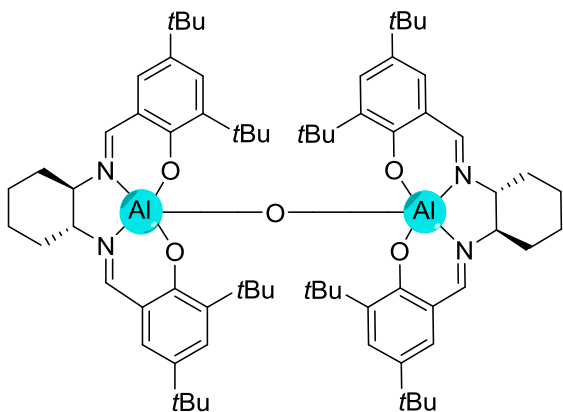
### Al (III) salen complexes

The use of Al (III) salen complex in combination with TBAX as a binary catalyst system for CO<sub>2</sub> cycloaddition to epoxides was initially reported by Lu *et al.* (2004). Synthesis of SC carried out using Al (III) salen complex (0.125 mol%) in combination with TBAI (0.125 mol%) has resulted in quantitative yields of cyclic carbonates from terminal epoxides at 25 °C and 6 bar *p* (CO<sub>2</sub>) after 15 h (Scheme 2.24).



Scheme 2.24 Structure of Al (III) salen complex as a catalyst for cyclic carbonate synthesis.

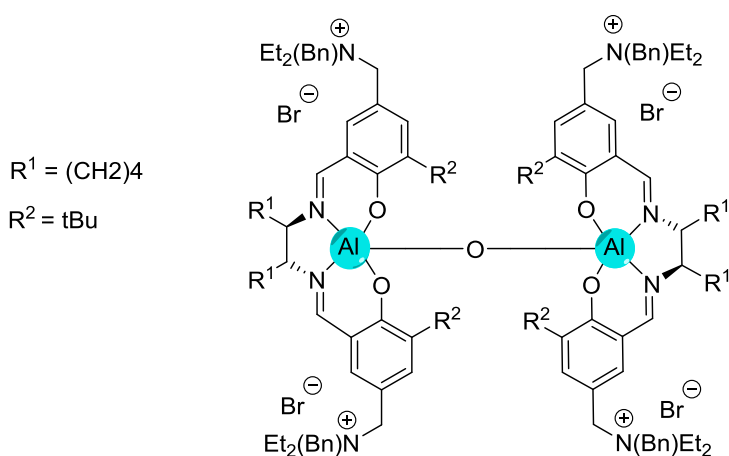
Later on, Melendez *et al.* (2007) reported bimetallic Al (III) salen complex (Scheme 2.25) in combination with TBAB as a highly effective binary homogeneous catalyst for the CO<sub>2</sub> cycloaddition to terminal epoxides at ambient conditions i.e. at 25 °C and 1 bar *p* (CO<sub>2</sub>). SC formation from SO and CO<sub>2</sub> using this binary homogeneous catalyst has resulted in almost quantitative conversion after 24 h reaction time. The presence of two metallic centres in the catalyst structure facilitates the simultaneous interaction with one or both of the reactants and intermediates leading to a higher reaction rate and product selectivity.



Scheme 2.25 Structure of bimetallic Al (III) salen complex as a catalyst for cyclic carbonate synthesis (Melendez *et al.*, 2007).

Subsequently, to avoid the use of TBAB as co-catalyst, the use of one-component bifunctional catalyst was also reported by covalent bonding of the TBAB with Al (III) salen complex (Scheme 2.26) (Melendez *et al.*, 2009). The use of one-component bifunctional catalyst has

shown comparable results to binary catalyst system i.e. quantitative conversion of SO to SC at 25 °C and 1 bar  $p$  ( $\text{CO}_2$ ) after 24 h. However, the use of one-component catalyst has a drawback of high catalyst loading due to its high molecular weight i.e. about 1600 g/mol. For example, 2.5 mol% catalyst loading means 4 g of the one-component catalyst is required for each 12 g (100 mmol) of SO. To reduce the molecular weight of the one-component catalyst prepared by the replacement of tert-butyl groups ( $t\text{Bu}$ ) attached to each phenyl ring with H was also investigated. However, the catalyst has shown less catalytic activity due to solubility issues (North and Young, 2011). Similarly, the presence of  $\text{Br}^-$  anion on the salen scaffold has shown higher catalytic activity than  $\text{Cl}^-$  due to a good balance of its nucleophilicity and leaving group ability.



Scheme 2.26 Structure of bimetallic Al (III) salen complex as a one-component bifunctional catalyst (Melendez *et al.*, 2009).

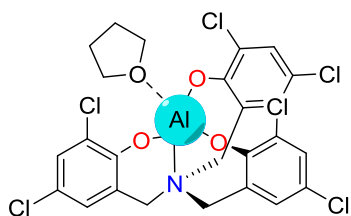
To make the process sustainable, the use of one-component catalysts in the heterogeneous phase was considered as a promising approach towards its commercial applications. It can be prepared by grafting of ammonium moiety of the one-component bifunctional catalyst over high surface areas inorganic supports such as a polymer (Merrifield resin) and amorphous  $\text{SiO}_2$  (Melendez *et al.*, 2009). The supported catalysts have shown comparable results to their homogenous analogues. For instance, the use of 2.5 mol% polymer-supported catalyst has shown 100% SO conversion to SC at 25 °C, 1 bar  $p$  ( $\text{CO}_2$ ) and 24 h. The heterogeneous catalysts can be easily separated and recycled. However, a significant decrease in the catalytic activity of the immobilised catalyst was observed and the product yield was decreased to 70% after two successive runs. To improve the recyclability of the heterogeneous catalyst, another one-component catalyst having four quaternary ammonium groups attached with the scaffold

of Al (III) salen complex was prepared by immobilizing over the polymer resin. However, no significant improvement in the reusability of the heterogeneous catalyst was observed.

The heterogeneous catalysts were also prepared by the immobilization of bimetallic catalysts over amorphous SiO<sub>2</sub> and MCM-41 supports. SiO<sub>2</sub>-supported catalyst has shown 78% conversion of SO to SC under an ambient condition (Meléndez *et al.*, 2011). Moreover, the catalyst has shown good recyclability up to 11 runs with a progressive decrease in catalytic activity. The reduction in catalytic activity was observed due to dequaternization of quaternary ammonium groups connected with the complex scaffold. This heterogeneous catalyst has shown high-temperature stability and can be used up to 170 °C. Due to these properties, the heterogeneous catalyst was also tested in a flow reactor for cyclic carbonate synthesis under continuous flow conditions (North *et al.*, 2011). The catalyst has also shown a reasonable conversion of SO to SC using simulated flue gases under continuous flow conditions. Moreover, the catalyst deactivation was observed after extended use which can be reversed by the quaternization of the deactivated catalyst by the addition of benzyl bromide.

Another one-component Al (III) salen complex based homogeneous catalyst with the covalent bonding of quaternary phosphonium halides instead of quaternary ammonium halides was also reported by the same group (North *et al.*, 2012). The use of this catalyst for CO<sub>2</sub> cycloaddition to terminal epoxide has also shown comparable conversion at mild reaction conditions. Recently, Wu and North (2017) proposed Al (III) salphen complex made by the connection of two salen scaffolds with the phenyl ring. This catalyst was prepared with the aim to increase in activity and to further reduce the amount of catalyst used during the reaction. The experimental results have shown that only 0.25 mol % of the complex in combination with 0.5 mol% TBAB has resulted in 90% conversion of SO to SC at 50 °C and 10 bar *p* (CO<sub>2</sub>).

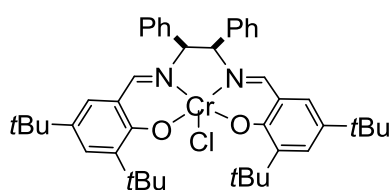
Whiteoak *et al.* (2013a) reported amino triphenolate based Al (III) complex (0.5 mol%) (Scheme 2.27) in combination with TBAI (2.5 mol%) as being highly effective for CO<sub>2</sub> cycloaddition to several terminal epoxides. Remarkably, this catalyst has shown high activity for cyclic carbonate synthesis from terminal epoxides (initial TOF= 36000 h<sup>-1</sup>). Formation of PC catalysed by this binary catalyst has shown a 94% yield at 90 °C and 10 bar *p* (CO<sub>2</sub>) after 2 h. Due to its trigonal geometry, this catalyst has also shown higher catalytic activity for cyclic carbonates formation from more sterically congested internal epoxides.



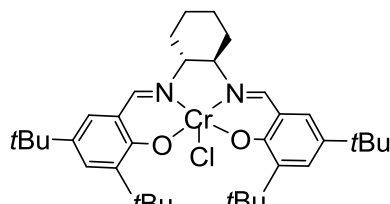
Scheme 2.27 Structure of Al (III) amino triphenolate complex as a catalyst for cyclic carbonate synthesis.

### *Cr (III)-based complexes*

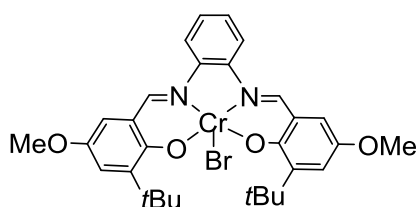
Cr (III) salen and salphen complexes in conjunction with nucleophile additives were identified as highly active catalysts for cyclic carbonate formation at low  $p$  ( $\text{CO}_2$ ) ( $< 10$  bar). Moreover, these complexes have the ability to easily tuneable structure which can be efficiently used for asymmetric cyclic carbonate synthesis with high stereoselectivity. The use of Cr (III) salen and salphen complexes for cyclic carbonate synthesis is summarized in Table 2.9.



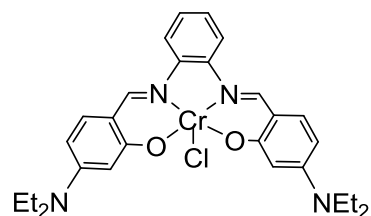
(1)



(2)



(3)



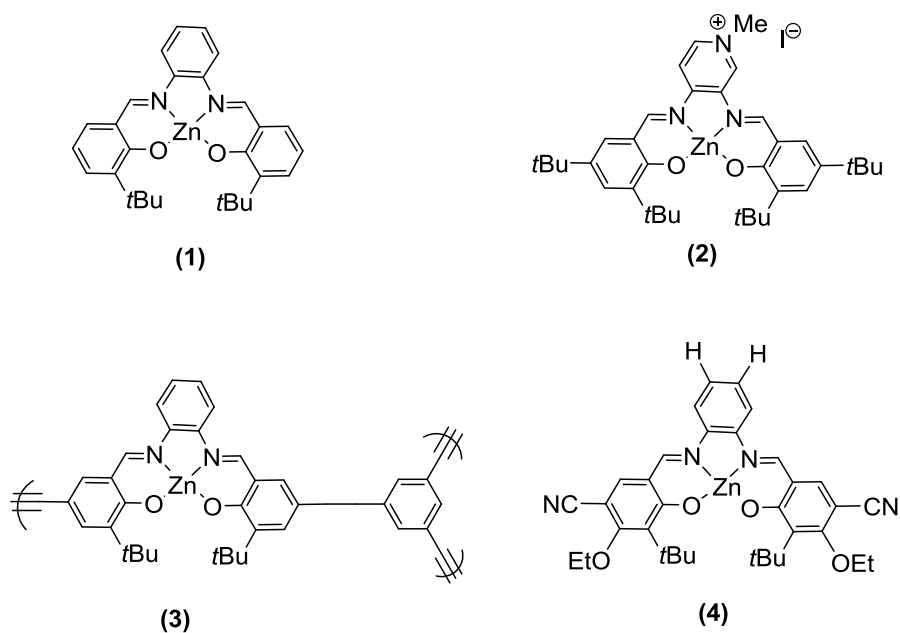
(4)

Entry	Catalyst	Co-catalyst	Substrate	Reaction conditions	Yield (%)	References
1	Cr (III) salen complex <b>(1)</b> 1 mol%	DMAP 1 mol%	SO	85 °C, 3.4 bar <i>p</i> (CO <sub>2</sub> ), 7 h		(Paddock and Nguyen, 2001)
2	Cr (III) salphen complex <b>(4)</b> 1 mol%	DMAP 2 mol%	PO	100 °C, 2 bar <i>p</i> (CO <sub>2</sub> ), 1.4 h	100	(Paddock and Nguyen, 2004)
3	Cr (III) salphen complex <b>(2)</b> 2.5 mol %	TBAB 2.5 mol%	SO	25 °C, 1 bar <i>p</i> (CO <sub>2</sub> ), 24 h	92%	(Castro-Osma <i>et al.</i> , 2016)
4	Cr (III) salphen complex <b>(3)</b> 1.5 mol %	TBAB 1.5 mol%	SO	25 °C, 1 bar <i>p</i> (CO <sub>2</sub> ), 24 h	100	(Castro-Osma <i>et al.</i> , 2016)

Table 2.9 Summary of Cr (III)-based salen and salphen complexes as homogeneous catalysts.

### ***Zinc (II)-based complexes***

Decortes *et al.* (2010) reported zinc based monometallic complexes with high catalytic activity at mild reaction conditions i.e. (25–45 °C and 2–10 bar *p* (CO<sub>2</sub>)). These complexes have the advantage of bulky groups connected with salphen scaffolds on *ortho*-positions that prevent catalytic deactivation due to unwanted dimerization of the complex. Nevertheless, the use of these complexes in combination with TBAX was limited for cyclic carbonate synthesis from terminal epoxides. The use of some zinc based salphen complexes as catalysts for cycloaddition of CO<sub>2</sub> to epoxides is summarised in Table 2.10. The catalytic activity of Zn (II) salphen complex was attributed to its unique structure offering increased Zn ion Lewis acid properties in combination with bulky tert-butyl (*t*Bu) substituents to stabilize the ring-opened epoxide. The reaction was performed using dichloromethane CH<sub>2</sub>Cl<sub>2</sub> as a solvent. The synthesis of SC from SO and CO<sub>2</sub> in the presence of the above-mentioned binary catalyst system has shown 80% yield at 45 °C and 10 bar *p* (CO<sub>2</sub>) after 18 h. However, the use of solvent was omitted under supercritical conditions i.e. 80 °C and 80 bar *p* (CO<sub>2</sub>) and reaction time was decreased from 18 to 3 h. The use of a solvent in this reaction has shown a decrease in the reaction rate as compared to a CO<sub>2</sub> rich solvent-free environment. Later on, it was observed that reaction can be further optimized using methyl ethyl ketone (MEK) as the reaction solvent. The synthesis of SC carried out in the presence of MEK has resulted in 89% isolated yield at 25 °C and 2 bar *p* (CO<sub>2</sub>) after 18 h reaction (Decortes *et al.*, 2010).



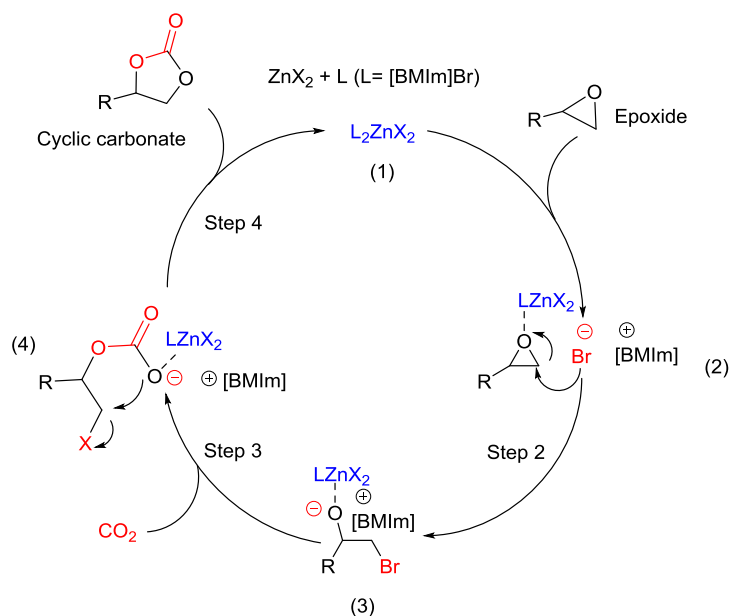
Entry	Catalyst	Co-catalyst	Substrate	Reaction conditions	Yield (%)	Reference
1	Zn (II) salphen complex <b>(1)</b> 2.5 mol %	TBAI 2.5 mol %	SO	80 °C, 80 bar <i>p</i> (CO <sub>2</sub> ), 3 h	80	(Decortes <i>et al.</i> , 2010)
2	Zn(salpyr) catalyst <b>(2)</b> 0.5 mol%	–	SO	80 °C, 10 bar <i>p</i> (CO <sub>2</sub> ), 18 h	88	(Martin <i>et al.</i> , 2014)
3	Salen-based zinc-coordinated complex <b>(3)</b> (0.1 mol%)	TBAB 3.6 mol %	SO	120 °C, 30 bar <i>p</i> (CO <sub>2</sub> ), 1 h	96	(Xie <i>et al.</i> , 2014)
4	Zn-based complex <b>(4)</b> 0.2 mol %	TBAI 0.2 mol %	PO	40 °C, 20 bar <i>p</i> (CO <sub>2</sub> ), 20 h	88	(Fuchs <i>et al.</i> , 2014)

Table 2.10 Summary of Zn-based complexes as homogeneous catalysts.

### ***Zinc salt-based catalysts***

The use of commercially available zinc salts in combination with onium salts was also reported as a simple acid-base bifunctional homogeneous catalyst for CO<sub>2</sub> cycloaddition to epoxides. Zn-salts such as ZnX<sub>2</sub> ( where X= I<sup>-</sup>, Br<sup>-</sup> or Cl<sup>-</sup> ) provides a Lewis acidic site to activate the epoxide which readily undergoes ring opening by nucleophilic attack of halide anion provided by the ammonium salts (Sun *et al.*, 2005a). The catalytic role of imidazolium-based ionic liquids in combination with Lewis acid compounds such as zinc halides have been also investigated as binary homogeneous catalysts for cyclic carbonate synthesis. PC

synthesis carried out using BMImBr alone has shown TOF  $37 \text{ h}^{-1}$  at  $100 \text{ }^\circ\text{C}$  and  $35 \text{ bar } p$  ( $\text{CO}_2$ ) after 1 h. However, a significant enhancement in catalytic activity was reported (TOF  $1679 \text{ h}^{-1}$ ) using  $\text{ZnBr}_2$  as co-catalyst at the same reaction conditions. The reaction mechanism for  $\text{CO}_2$  cycloaddition to epoxides using Zn-salts in combination with ionic liquids was also proposed (Scheme 2.28).



Scheme 2.28 General reaction mechanism for  $\text{CO}_2$  cycloaddition to epoxides catalysed by Zn-salts in combination with ILs.

The Lewis acid site provided by the Zn salts activates the epoxide by the interaction with the oxygen atom of epoxide. Subsequently, the ring-opening of the activate epoxide takes place by the  $\text{Br}^-$  provided by the ionic liquid catalyst. Li *et al.* (2004) also described the increase in catalytic activity using imidazolium-based ionic liquids in combination with zinc halides. PC synthesis carried out in the presence of BMImBr in a combination of  $\text{ZnCl}_2$  has shown 86% yield ( $3015 \text{ h}^{-1}$ ) at  $100 \text{ }^\circ\text{C}$  and  $15 \text{ bar } p$  ( $\text{CO}_2$ ) after 1 h. Moreover, a reaction mechanism was proposed explaining the synergistic effect between ionic liquids and zinc salts. Similarly, the use of TBAX in combination with zinc halides as a highly effective acid-base binary homogeneous catalyst was also reported. SC formation from SO and  $\text{CO}_2$  catalysed by TBAI/ $\text{ZnBr}_2$  has shown a 98% yield of SC with a turnover frequency (TOF) of  $6861 \text{ h}^{-1}$  using 1:2 molar ratio under supercritical conditions i.e.  $90 \text{ }^\circ\text{C}$  and  $80 \text{ bar } p$  ( $\text{CO}_2$ ) after 30 min (Sun *et al.*, 2005a). This enhanced catalytic activity was attributed to the supercritical reaction conditions where a homogeneous mixture of epoxide,  $\text{CO}_2$  and catalyst was achieved resulting in good mixing. The effect of a change in  $\text{CO}_2$  pressure on cyclic carbonate synthesis was also

investigated. The results have shown that SC yield increases gradually by increasing pressure from 20 to 80 bar. However, the change in  $p$  ( $\text{CO}_2$ ) from 80 bar to 100 bar resulted in a sharp decrease in product yield which was explained by the dilution effect leading to decrease in epoxide concentration around the catalyst in the expanded reaction medium at higher pressure i.e. > 80 bar. The decrease in the rate of reaction due to the similar dilution effect at very high pressure was also observed by some other authors. Moreover, a reaction mechanism was proposed explaining the increase in catalytic activity due to a synergistic effect between  $\text{ZnBr}_2$  and TBAI. The use of zinc salts in conjunction with onium salts for cyclic carbonate synthesis has been summarized in Table 2.11.

Entry	Catalyst	Co-catalyst	Substrate	Reaction conditions	Yield (%)	Reference
1	$\text{ZnCl}_2$ 0.02 mol %	BMIImBr 0.11 mol %	SO	100 °C, 15 bar $p$ ( $\text{CO}_2$ ), 1 h	86	(Li <i>et al.</i> , 2004)
2	$\text{ZnBr}_2$ 0.4 mol %	BMIImCl 0.8 mol %	SO	80 °C, 40 bar $p$ ( $\text{CO}_2$ ), 1 h	93	(Sun <i>et al.</i> , 2004b)
3	$\text{ZnBr}_2$ 0.3 mol %	TBAI 0.6 mol %	SO	90 °C, 80 bar $p$ ( $\text{CO}_2$ ), 30 min	98	(Sun <i>et al.</i> , 2005a)
4	$\text{ZnBr}_2$ 0.015 mol %	Tetraphenylphosphonium iodide [ $\text{Ph}_4\text{P}$ ]I 0.09 mol %	PO	120 °C, 25 bar $p$ ( $\text{CO}_2$ ), 1 h	90	(Wu <i>et al.</i> , 2008)
5	$\text{ZnI}_2$ 0.3 mol %	Dicationic ionic liquid 0.14 mol %	SO	110 °C, 15 bar $p$ ( $\text{CO}_2$ ), 3 h	94	(Sun <i>et al.</i> , 2004b)
6	$\text{ZnBr}_2$ 1 mol %	Poly(4- vinylimidazolium) 1 mol% DBU 2 mol %	SO	80 °C, 1 bar $p$ ( $\text{CO}_2$ ), 10 h	94	(Seo and Chung, 2014)
7	$\text{ZnBr}_2$ 1 mol %	Methylimidazole (MIm) based heterocyclic compounds	PO	160 °C, 25 bar $p$ ( $\text{CO}_2$ ), 48 min	99	(Liu <i>et al.</i> , 2015b)
8	Imidazolium zinc tetrahalide 0.02 mol%	-	EO	100 °C, 35 bar $p$ ( $\text{CO}_2$ ), 1 h	72	(Kim <i>et al.</i> , 2003)

Table 2.11 Summary of Zn-salts based binary homogeneous catalysts.

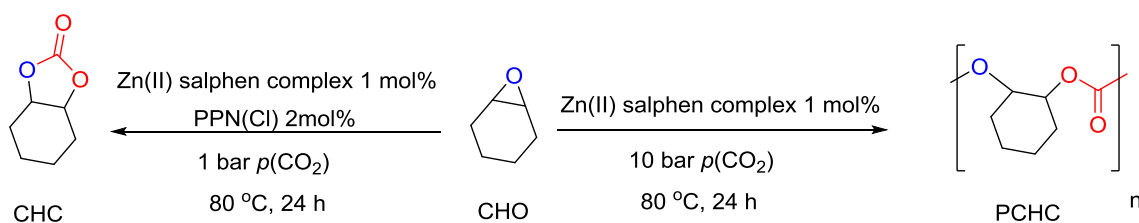
## 2.10 Cyclic carbonate synthesis from internal epoxides

Although  $\text{CO}_2$  cycloaddition to terminal epoxides has been extensively studied in the presence of various catalyst systems, the  $\text{CO}_2$  cycloaddition to sterically congested di- and tri-substituted internal epoxides with high stereoselectivity is still challenging. The cycloaddition of  $\text{CO}_2$  to internal epoxides is of particular interest, as they can be derived from naturally

occurring renewable sources, such as bio-based olefinic compounds extracted from terpenes and unsaturated fatty acids (Byrne *et al.*, 2004; Langanke *et al.*, 2013). These bio-based olefinic compounds can be easily converted to corresponding epoxides using standard epoxidation methods.

Naturally occurring terpenes have been identified as key starting materials for the production of bio-based epoxides (Villa de P *et al.*, 1999b). In particular, cyclic carbonates formation from limonene epoxides i.e. limonene oxide (LO) and limonene dioxide (LDO) is of significant interest as these can be used as a non-toxic monomer for the production of fully bio-based polymers such as NIPUs, which have promising applications as thermoset materials, elastomers, or thermoplastics (Bähr *et al.*, 2012). Similarly, the by-products of bio-refineries can also be used as raw materials. One example is 1,4-cyclohexadiene, derived from unsaturated fatty acids, which can be converted into mono- or bis-epoxides to give sustainable CHO. Synthesis of CHC is generally considered to be more challenging than polycarbonate synthesis due to the strain offered by the CHO ring to five-membered cyclic carbonate ring and high activation energy barrier i.e.  $> 80 \text{ kJ mol}^{-1}$  compared to poly(cyclohexene) carbonate (PCHC) (Darensbourg *et al.*, 2003).

Some catalyst systems for CO<sub>2</sub> coupling with internal epoxides have been reported in the literature. Taherimehr *et al.* (2012) stated synthesis of CHC using Zn(II) salphen complex (0.05 mol%) in combination with TBAI (0.25 mol%) under supercritical conditions where all the reactants coexist in a single CO<sub>2</sub>-rich phase resulting in a 38% yield at 80 °C, 80 bar *p* (CO<sub>2</sub>) after 5 h. Similarly, Buchard *et al.* (2011) reported a bimetallic Fe (III) complex (1 mol%) in combination with PPNCl (2 mol%), that can selectively transform CHO to CHC (90% conversion) at 80 °C, 1 bar *p* (CO<sub>2</sub>) after 24 h. Interestingly, the selectivity can be switched to PCHC synthesis (70% conversion) using 0.1 mol% of the complex without any co-catalyst at 80 °C and higher *p* (CO<sub>2</sub>) i.e. 10 bar after 24 h (Scheme 2.29).



Scheme 2.29 Switch in selectivity towards CHC and PCHC using Zn (II) salphen complex under different reaction conditions.

Moreover, in the case of CO<sub>2</sub> cycloaddition to internal epoxides, the use of TBAB as nucleophile additive has been preferred over TBAI due to the reduced size of Br<sup>-</sup> compared to I<sup>-</sup>. Notably, MEK was used as a reaction solvent in case of both Fe (III) trisphenolate and Al (III) triphenolate complexes as catalysts. Some other studies related to cyclic carbonates synthesis from internal epoxides such as 1,2-dimethyloxirane and 1,2-diphenyloxirane using various homogeneous catalyst systems have been summarized in Table 2.12.

Epoxide	Catalyst (mol %)	Co-Catalyst (mol %)	Solvent	Reaction conditions	Conversion (%)	Ref.
2,3-dimethyloxirane	Fe(III) amino (trisphenolate) complex (0.5)	TBAB (2.5)	MEK	85 °C 10 bar <i>p</i> (CO <sub>2</sub> ) and 18 h	83	(Whiteoak <i>et al.</i> , 2012a)
1,2-Dimethyloxirane	Fe(III) amino (trisphenolate) complex (0.5)	TBAB (0.5)	MEK	85 °C 2 bar <i>p</i> (CO <sub>2</sub> ) and 18 h	53	(Whiteoak <i>et al.</i> , 2012b)
1,2-Diphenyloxirane	Al (III) salen complex (2.5)	TBAB (2.5)	No solvent	85 °C, 10 bar <i>p</i> (CO <sub>2</sub> ) and 72 h	>99	(Beattie <i>et al.</i> , 2013)
1,2-Dimethyloxirane	Al (III) salen complex (2.5)	TBAB (2.5)	No solvent	85 °C, 10 bar <i>p</i> (CO <sub>2</sub> ) and 24 h	49	(Beattie <i>et al.</i> , 2013)
1,2-Dimethyloxirane	Al (III) amino triphenolate complex (0.5)	TBAB (5)	MEK	90 °C, 10 bar <i>p</i> (CO <sub>2</sub> ) and 42 h	99	(Whiteoak <i>et al.</i> , 2013a)
1,2-Diphenyloxirane	Al (III) amino triphenolate complex (0.5)	TBAB (5)	MEK	90 °C, 10 bar <i>p</i> (CO <sub>2</sub> ) and 42 h	82	(Whiteoak <i>et al.</i> , 2013a)
1,2-Dimethyloxirane	Cu(II) complex (2.5)	TBAB (5)	No solvent	25 °C, 1 bar <i>p</i> (CO <sub>2</sub> ) and 24 h	36	(Vignesh and Muralidharan, 2013)
1,2-Dimethyloxirane	Zn(II) complex (2.5)	TBAB (5)	No solvent	25 °C, 1 bar <i>p</i> (CO <sub>2</sub> ) and 24 h	42	(Vignesh and Muralidharan, 2013)
Cyclo(octane) oxide	Co(III) based bisamino-bisamide complex	DMAP	No solvent	150 °C, 20 bar <i>p</i> (CO <sub>2</sub> ) and 5 h	83	(Ramidi <i>et al.</i> , 2013)
1,2-Dimethyloxirane (22:78 <i>cis/trans</i> )	Polyphenolate complex (0.2)	TBAB (8)	No solvent	85 °C, 10 bar <i>p</i> (CO <sub>2</sub> ) and 45 h	66 (19:81 <i>cis/trans</i> )	(Qin <i>et al.</i> , 2014)

Table 2.12 Summary of catalytic systems used for CO<sub>2</sub> cycloaddition to internal epoxides.

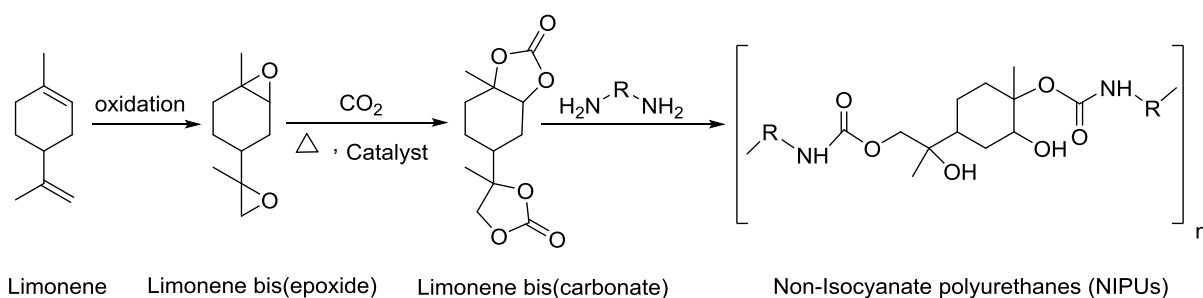
## 2.11 Cyclic carbonates synthesis from bio-based epoxides

Synthesis of cyclic carbonates from bio-based epoxides is a promising approach for sustainable production of cyclic carbonates. The utilization of CO<sub>2</sub> and waste biomass to valuable products is highly desirable as part of a sustainable future of the chemical process industry (Ampelli *et al.*, 2015). Naturally occurring terpenes have been identified as key starting materials for the production of bio-based epoxides (Villa de P *et al.*, 1999a). Terpenes, derived from ‘Turpentine’, are naturally occurring compounds. They are mostly produced by coniferous plants. Terpenes are mainly cyclic compounds containing highly unsaturated hydrocarbons with one or more C–C double bonds. Terpenes are readily available at large scale, with worldwide production of about 350,000 tonnes/year (de Jong *et al.*, 2012).

Among these unsaturated hydrocarbon monoterpenes (C<sub>10</sub>H<sub>16</sub>), d-limonene has been extensively studied as a possible renewable platform chemical for the production of biopolymers. (+)-Limonene is a monocyclic unsaturated terpene, mainly extracted from the peel of citrus fruits (90 wt. %) (Firdaus *et al.*, 2011). It is a principal component of many essential oils and can be obtained as a waste product during harvesting and orange juice production (Ciriminna *et al.*, 2014). Due to its abundance as a waste by-product and its high reactivity, it can be used as a sustainable replacement for petrol-based epoxides without competing with food crops. Formation of cyclic carbonates from d-limonene, in particular, is of significant interest as it is a non-toxic, biodegradable and bio-renewable monomer for the production of fully bio-based polymers such as NIPUs, which have potential applications as thermoset materials, elastomers, or thermoplastics.

Bähr *et al.* (2012) reported the synthesis of limonene dicarbonate (LDC) from commercially available limonene dioxide (LDO) and CO<sub>2</sub> catalysed by TBAB alone resulting in almost complete conversion of LDO using 3 mol% TBAB at 140 °C and 30 bar *p* (CO<sub>2</sub>) after 55 h. The reaction was also performed using SiO<sub>2</sub>-supported pyrrolidinopyridinium iodide (SiO<sub>2</sub>-PPI) as a bifunctional heterogeneous catalyst. However, the heterogeneous catalyst has exhibited a significantly lower reaction rate than TBAB i.e. 78% epoxy group conversion after 120 h at the same reaction conditions. The decrease in reaction rate was due to the steric hindrance of LDO which shows less conversion in the presence of a bulky heterogeneous catalyst. LDC obtained from cycloaddition reaction was further used as a monomer for the synthesis of NIPUs by the reaction with polyfunctional amines (Scheme 2.30). The resulting NIPU has shown good mechanical and thermal properties. This novel approach for the

production of cyclic carbonates not only provides a substitute for the traditional phosgene-based toxic isocyanate monomers with 'green' renewable monomers but also reduces the strong reliability on petroleum-based raw materials.



Scheme 2.30 Reaction scheme for terpene-based NIPUs formation from limonene (Bähr *et al.* 2012).

Another study from the same group reported cyclic carbonate synthesis from bio-based epoxides derived from linseed oil (ELSO) and soybean oil (ESBO) (Bähr and Mülhaupt, 2012). The reaction was carried out using both homogeneous TBAB and heterogeneous SiO<sub>2</sub>-PPI catalysts. Again, the higher reaction rate was observed using homogeneous TBAB (3 mol%) resulting in complete conversion of ELSO at 140 °C, 30 bar *p* (CO<sub>2</sub>) after 20 h than 45 h using SiO<sub>2</sub>-PPI under the same reaction conditions. Similar results have been also reported for CO<sub>2</sub> coupling to ESBO. The cyclic carbonates obtained from these reactions were further used for the production of NIPUs.

Recently, Fiorani *et al.* (2016) reported bio-based cyclic carbonate synthesis from terpene-based epoxides and CO<sub>2</sub> in the presence of Al (III) triphenolate complex in conjunction with bis(triphenylphosphine)iminium chloride (PPNCl) as an active binary homogeneous catalyst system. For instance, synthesis of limonene carbonates (LC) from LO and CO<sub>2</sub> was successfully carried out using 1 mol% Al (III) triphenolate complex and 3 mol% PPNCl. Interestingly, the same catalyst system was used for poly(limonene) carbonate (PLC) synthesis at low temperature (40–70) °C with no cyclic carbonate as a by-product. However, a further rise in temperature up to 85 °C resulted in a change of catalyst selectivity and cyclic carbonate was found as the only product. These findings were consistent with previously reported DFT study describing the formation of LC as a thermodynamically more favourable product due to higher kinetic energy barrier than PLC synthesis. This catalyst system exhibited a 57% yield of LC using *trans*-limonene oxide as a substrate at 85 °C and 10 bar *p* (CO<sub>2</sub>) after 66 h. The requirement of long reaction time was due to the slow rate of reaction caused by the sterically hindered nature of tri-substituted internal epoxides. Similarly, the

catalyst has shown 27% isolated yield of limonene dicarbonate from limonene dioxide at 120 °C and otherwise constant reaction conditions. This reaction was performed at a higher temperature to enhance the mass-transfer between CO<sub>2</sub> and highly viscous limonene dioxide. Moreover, a double inversion reaction mechanism was proposed explaining the complete retention of stereochemical information obtained as a result of experimental observation.

Most recently, Martínez *et al.* (2017) reported lanthanum heteroscorpionate based complex in conjunction with TBAX (1:4 molar ratio) as an effective catalyst system for LC synthesis via cycloaddition reaction of CO<sub>2</sub> and limonene oxide under solvent-free conditions. The reaction was carried out using commercially available limonene oxide (40:60 *cis/trans* isomer) at 100 °C and 10 bar *p* (CO<sub>2</sub>) resulting in 43% yield of LC after 16 h. Similarly, the synthesis of LDC from LDO and CO<sub>2</sub> was also carried resulting 69% product yield at the same reaction conditions.

## 2.12 Kinetics study of cyclic carbonates synthesis using heterogeneous catalysts

Synthesis of cyclic carbonates by CO<sub>2</sub> cycloaddition to epoxides has been carried out in the presence of various heterogeneous catalyst systems. However, to the best of our knowledge, no kinetic study for cycloaddition reaction using a heterogeneous catalyst has been reported. Synthesis of cyclic carbonate in the presence of a heterogeneous catalyst is a three-phase (liquid-gas-solid) reaction. Heterogeneous kinetics for this reaction is complicated by the diffusion, adsorption and desorption properties of the reactants and products on the surface of a solid catalyst. The elementary steps involved in the overall heterogeneous catalytic reaction are given below:

- 1- Diffusion of the reactants from the bulk reaction medium to the external surface of the catalyst particles.
- 2- Intraparticle diffusion of the reactants from the external surface to the pores of the catalyst.
- 3- Adsorption of the reactants on the active sites of the catalyst.
- 4- Formation of the activated complex by the reaction of adsorbed reactants.
- 5- Product formation by the decomposition of the activated complex.
- 6- Diffusion of the products from the active site to the external surface.
- 7- Desorption of the products from the external surface to the bulk reaction medium.

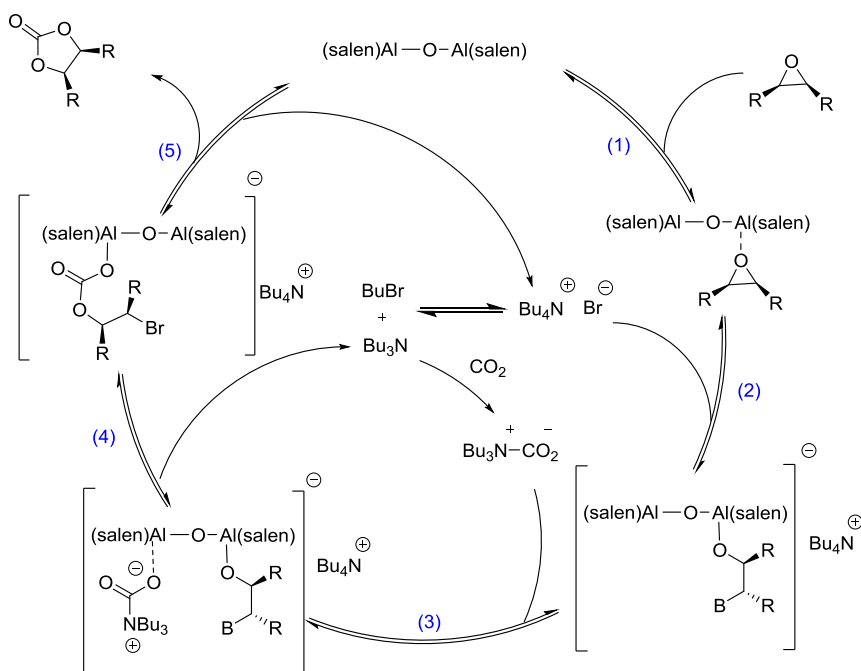
Therefore, the rate-determining step could be either mass transfer limitations (Steps 1, 2, 6 and 7) or the intrinsic kinetics of the reaction (Steps 3–5). Generally, the heterogeneous catalytic reactions are modelled by either Eley-Rideal (ER) or Langmuir-Hinshelwood (LH) mechanisms (Satterfield, 1991). However, the reaction was carried out in the presence of a heterogeneous catalyst, which can leach significantly into the reaction medium, so could not be modelled by heterogeneous kinetic mechanism and followed a pseudo-homogeneous mechanism as in case of homogeneous catalysis.

### **2.13 Kinetics study of cyclic carbonate synthesis using homogeneous catalysts**

To investigate the reaction mechanism involved in cyclic carbonate synthesis and to determine the general equation of the rate law, several kinetic studies of cyclic carbonates synthesis by CO<sub>2</sub> cycloaddition to epoxides have been reported.

Clegg *et al.* (2010a) reported a detailed kinetic study of SC synthesis from SO and CO<sub>2</sub> in the presence of bimetallic Al (III) salen complex and TBAB as the binary homogeneous catalyst system. The reaction has shown first-order dependence on the epoxide, CO<sub>2</sub> and salen complex concentrations. However, an unexpected second order reaction with respect to TBAB was observed suggesting a dual role of TBAB in the catalytic cycle as shown in the reaction mechanism (Scheme 2.31). According to this mechanism, the activation of the epoxide was carried out by one of the metal centres due to its Lewis acidic properties (Step 1). The activated epoxide undergoes nucleophilic attack by the Br<sup>-</sup> anion provided by the TBAB (first role) to form a metal-bound alkoxide intermediate (Step 2). The *in-situ* tributylamine formation by the decomposition of TBAB (second role) was observed leading to CO<sub>2</sub> activation by carbamate formation which further coordinates with one of the metal centres of the dimeric Al (III) complex at a much faster rate than with CO<sub>2</sub> only (Step 3). This results in the formation of two reaction intermediates on the same side of the salen complex which easily combine to form the corresponding carbonate (Step 4). Finally, the cyclic carbonate was formed and the catalyst was regenerated (Step 5). The inactivity of the mono-metallic salen complex under the same reaction conditions also validates the participation of the two metallic centres in the reaction mechanism. Al (III) complex has shown remarkably high catalytic stability and can be recycled up to 60 times without a decrease in catalytic activity. However, TBAB needs to be replaced during recycling experiments. The effect of halide anion on the catalytic activity was also examined. As a result, the order of halide anion

activity was found to be  $\text{Br}^- > \text{I}^- > \text{Cl}^- > \text{F}^-$ , which was described due to a balance between the leaving group ability and nucleophilicity of halide anions.



Scheme 2.31 Reaction mechanism for  $\text{CO}_2$  cycloaddition to epoxides catalysed by bimetallic Al (III) salen complex in combination with TBAB (Clegg *et al.* (2010a).

Later on, Supasitmongkol and Styring (2014) reported the synthesis of cyclic carbonates using Al (III) salenac complex in conjunction with TBAB as an active binary homogenous catalyst. The effect of a change in temperature on the rate constants was studied by performing the experiments over the range of (80–150) °C. The  $E_a$  for SC formation catalyzed by Al (III)-salenac complex alone was determined to be  $34 \text{ kJ mol}^{-1}$  which was further reduced to  $23 \text{ kJ mol}^{-1}$  using TBAB as co-catalyst.

Luo *et al.* (2015) reported a kinetic study of SC synthesis from SO and  $\text{CO}_2$  using ionic liquid ([BMIm]Br) in combination with graphite oxide (GO) as a binary homogeneous catalyst. The experiments of the kinetic study were performed in the presence of the PC as the reaction solvent. The progress of the reaction was monitored by *in-situ* IR spectroscopy. The effect of reaction temperature was studied over the range of (75–95) °C and  $E_a$  for SC synthesis was determined using the Arrhenius equation. The  $E_a$  for SC synthesis was determined to be  $80.74 \text{ kJ mol}^{-1}$  using (BMIm)Br as catalyst alone. However, it was reduced by  $25.38 \text{ kJ mol}^{-1}$  using GO as co-catalyst. Moreover, the order of reaction w.r.t epoxide (SO) and catalyst (BMIm)Br was determined to be first-order.

Cuesta-Aluja *et al.* (2016) reported CO<sub>2</sub> cycloaddition to terminal epoxides at 80 °C and 10 bar *p* (CO<sub>2</sub>) using Al (III)-salabza complexes in conjunction with TBAB as a binary homogeneous catalyst. Moreover, a detailed study of reaction kinetics was performed suggesting first-order reaction dependence on epoxide, CO<sub>2</sub>, TBAB and Al-salabza complex concentrations. Moreover, the E<sub>a</sub> for SC formation was determined to be 38 kJ mol<sup>-1</sup> by performing experiments over the range of (40–100) °C and 10 bar *p* (CO<sub>2</sub>).

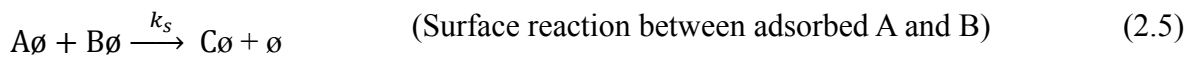
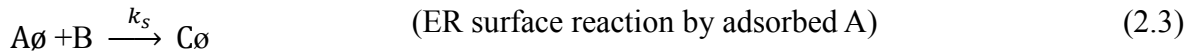
Castro-Osma *et al.* (2016) reported a kinetic study of SC synthesis from SO and CO<sub>2</sub> catalysed by Cr (salphen) complex in combination with TBAB which was performed at solvent-free conditions. The conversion of SO to SC was determined by taking the sample from the reaction mixture after a regular interval of 30 min followed high-performance liquid chromatography (HPLC) analysis. The order of reaction with respect to TBAB was determined to be first-order by performing the experiment over the range (175–437) mM TBAB concentrations. The order of the reaction with respect to Cr (salphen) complex in combination with TBAB was determined to be zero-order under the conditions when [TBAB] < [Complex] and first-order when [TBAB] > [Complex]. Moreover, the reaction mechanism was proposed suggesting the formation of six-coordinate anionic [Cr(salphen)-Br<sub>2</sub>]<sup>-</sup> as an active catalytic species.

Recently, Luo *et al.* (2017) also reported CO<sub>2</sub> cycloaddition to epoxides using ionic liquid-functionalized Al (III) salen oligomers as an effective bifunctional homogeneous catalyst. The activity of the catalyst system can be further increased by using Al (III) salen oligomers in conjunction with ionic liquid ([BMIm]Cl) as the binary catalyst system. The kinetic study of SC synthesis has been investigating using *in-situ* IR spectroscopy. As a result, the reaction was found to be first order with respect to epoxide and bifunctional catalyst. However, the order of the reaction with respect to the binary catalyst system was found to non-first order, suggesting the formation of a six-coordinated transition complex in the catalytic cycle as an active species. Moreover, the E<sub>a</sub> for SC formation catalysed by the binary catalyst was determined to be 64.9 kJ mol<sup>-1</sup> over the range of (80–140) °C.

### **2.13.1 Eley-Rideal (ER) mechanism**

The ER mechanism of heterogeneous catalysis is based on the assumption that reaction takes place between one of the reactants species (A) adsorbed over the catalyst surface with another reactant species (B) present in the bulk reaction medium to form a product C and desorbs.

Assuming ER kinetics mechanism, the elementary steps for the heterogeneous catalysis for reaction between A and B to form C can be given as Eq (2.1–2.6), where  $\emptyset$  is the vacant catalyst site,  $K_A$ ,  $K_B$  and  $K_C$  are the adsorption-desorption equilibrium constant for A, B, and C respectively and  $k_s$  is the rate constant for the forward surface reaction.



The ER kinetic model for the reactions of A with B can be written as shown in Eq (2.7), assuming that either A or B could adsorb on the catalyst surface, and that surface reaction is the rate-determining step. The total surface coverage of the catalyst sites using equilibrium state approximation (at equilibrium adsorption-desorption) is given by the balance of the active site in Eq (2.8), where  $\emptyset_j$  is the fraction of the catalytic sites that remain unoccupied. Therefore, the surface coverages of A, B and C are shown in Eq (2.9–2.11), and the surface reaction for the ER model could be re-written as Eq (2.12). The rate equation for the surface reaction in Eq (2.16) was obtained by replacing  $\emptyset_j$  using the Langmuir adsorption isotherms in Eq (2.13–2.15), for the heterogeneous catalysis of the reactions of A with B.

$$r_A = k_s[B][A\emptyset] + k_s[B\emptyset][A] \quad (2.7)$$

$$\emptyset_j = 1 - A\emptyset - B\emptyset - C\emptyset \quad (2.8)$$

$$[A\emptyset] = K_A[A]\emptyset_j \quad (2.9)$$

$$[B\emptyset] = K_B[B]\emptyset_j \quad (2.10)$$

$$[C\emptyset] = K_C[C]\emptyset_j \quad (2.11)$$

$$r_A = k_s K_A [B][A]\emptyset_j + k_s K_B [A][B]\emptyset_j \quad (2.12)$$

$$\theta_i = \frac{K_i[i]}{1 + \sum K_i[i]} \quad (\text{Langmuir adsorption isotherm})$$

(Where i = A, B and C)

$$[A\theta] = \frac{K_A[A]}{(1 + K_A[A] + K_B[B] + K_C[C])} \quad (2.13)$$

$$[B\theta] = \frac{K_B[B]}{(1 + K_A[A] + K_B[B] + K_C[C])} \quad (2.14)$$

$$[C\theta] = \frac{K_C[C]}{(1 + K_A[A] + K_B[B] + K_C[C])} \quad (2.15)$$

$$r_A = \frac{k_s K_A [A][B]}{(1 + K_A[A] + K_B[B] + K_C[C])} + \frac{k_s K_B [A][B]}{(1 + K_A[A] + K_B[B] + K_C[C])} \quad (2.16)$$

Therefore,

$$r_A = \frac{k_s [A][B]}{(1 + K_A[A] + K_B[B] + K_C[C])} (K_A + K_B) \quad (2.17)$$

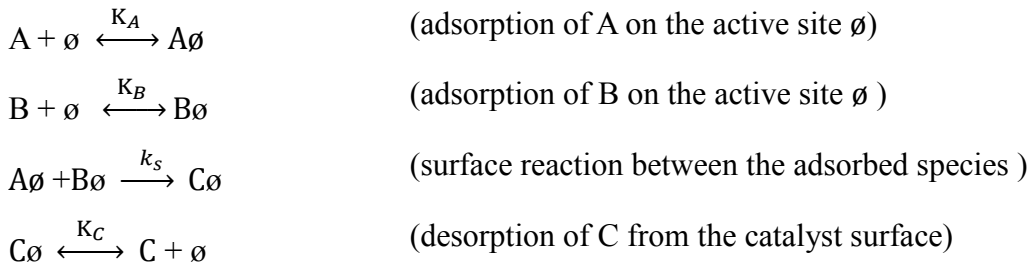
The ER kinetic model in Eq (2.17) can be simplified to Eq (2.18) if there is only selective adsorption of A on the catalyst surface and to Eq (2.19) when only B adsorbs on the catalytic surface.

$$r_A = \frac{k_s [A][B]}{(1 + K_A[A] + K_C[C])} (K_A) \quad (2.18)$$

$$r_A = \frac{k_s [A][B]}{(1 + K_B[B] + K_C[C])} (K_B) \quad (2.19)$$

### 2.13.2 Langmuir-Hinshelwood (LH) mechanism

LH mechanism for heterogeneous catalysis is based on the assumption that all the reactants adsorb over the surface of the catalyst and the reaction takes place between the adsorbed reactants to form an activated complex. Subsequently, the activated complex decomposed to form products which are also adsorbed on the catalytic surface. Finally, the products diffuse from the catalyst surface to the bulk reaction medium. LH mechanism is commonly useful for gas-liquid reactions in the presence of a heterogeneous catalyst. The elementary steps involved in the LH mechanism can be given as follows:



For the LH model, the rate expression for the reaction of A with B is shown in Eq (2.20), when mass transport and diffusion are very fast compared to the surface reaction of the chemisorbed species (surface reaction as the rate-determining step). Using the Langmuir adsorption isotherms, the LH model was simplified to Eq (2.21):

$$r_A = k_s[A\emptyset][B\emptyset] \quad (2.20)$$

$$r_{so} = \frac{k_s K_A K_B [A][B]}{(1 + K_A[A] + K_B[B] + K_C[C])^2} \quad (2.21)$$

### 2.13.3 Diffusion limitations in heterogeneous catalysis

For heterogeneous catalysis, the overall rate of the reaction is not only influenced by the reaction kinetics but also by the internal diffusion and adsorption/desorption of the reactants and products. For a reaction with good mixing, the mass transfer limitations are expected to be negligible. The effect of external mass transfer limitation can be investigated by studying the effect of mixing on the reaction rate. However, the effect of internal diffusion on reaction rate can be determined from theoretical analysis based on Thiele's modulus ( $M_T$ ) and effectiveness factor (Eq 2.22).

$$M_T = \frac{r_s}{3} \sqrt{\frac{k}{De}} \quad (2.22)$$

Where  $r_s$ ,  $k$  and  $De$  represent the radius of a spherical particle, pseudo-first-order rate constant, and effective diffusion constant, respectively. The effective diffusion constant ( $De$ ) can be determined from (Eq 2.23)

$$De = \frac{D_A \cdot \epsilon_p}{\tau_p} \quad (2.23)$$

Where  $D_A$ ,  $\epsilon_p$  and  $\tau_p$  represent the molecular diffusion coefficient, porosity, and tortuosity of the catalyst particles, respectively. From theoretical analysis, the value of  $M_T < 0.4$  gives an

effectiveness factor close to unity, suggesting that the reaction is not internally mass transfer limited and the reactant can enter the solid particles and its entire surface is accessible for reactant (Levenspiel, 1999).

Synthesis of cyclic carbonate from epoxides and CO<sub>2</sub> is a typical gas-liquid multiphase catalytic process involving a gas-liquid mass transfer in a reactor and the catalytic cycloaddition reaction in the liquid phase. Therefore reaction carried out an efficient reactor design in terms of the high rate of heat/mass transfer and continuous flow approach could mitigate many of the shortcomings observed in conventional catalyst systems. Therefore, it may be beneficial to investigate the use of more novel reactor technologies for the synthesis of these carbonates.

#### **2.14 Flow chemistry**

Flow chemistry has many advantages over conventional batch reactors, typically including enhanced rates of heat and mass transfer due to higher surface area to volume ratios and efficient mixing, improved safety due to less use of inventories, easy and highly reproducible screening of reaction parameters, which may improve the reliability of easily scale-up and process optimisation (Pastre *et al.*, 2013). Moreover, the ability to easy scale-up using multiple flow devices is an attractive approach for organic synthesis. The high surface area to volume ratio in flow reactors compared to batch reactors also helps to remove the heat generated through an exothermic reaction to avoid thermal runaway. Therefore, reactions can be performed using solvent-free high concentrations of reactants under continuous flow conditions (Löwe *et al.*, 2006).

The use of flow technologies for gas phase reactions has gained much attention due to improved safety considerations than traditional batch reactors. The use of highly reactive and toxic gases in batch reactors at elevated pressure has also raised many potential safety concerns, which can be avoided by using small volumes of the gases under continuous flow conditions. These advantages of flow chemistry enable to achieve the goals of green chemistry and sustainability in the chemical process industry (Newman and Jensen, 2013).

Flow reactors provide high interfacial surface areas which are essential for high rates of mass transfer in the case of gas-liquid reactions. The use of microchannel gas-liquid reactors has shown a significantly higher interfacial area among other types of gas-liquid contactors (Yue *et al.*, 2007). These reactors result in a significant enhancement in the rate of mass transfer for

reactions which are generally considered as non-feasible in batch reactors. Moreover, the supply of gases under continuous flow conditions can be easily controlled by regulating the volume and by increasing the internal pressure to help the gas dissolution. The use of flow technology by connecting multiple reactors in series also has the advantage to reduce the chemical storage and transportation cost. Similarly, the scale-up of flow technology enables a significant reduction in transition time by replicating the pilot plant flow reactors by the numbering-up method or by simply extending the running time of the same reactor without much changes in the existing design. The ability to easily scale-up using multiple flow devices is an attractive approach for organic synthesis (Mallia and Baxendale, 2015).

Generally, gas-liquid flow in microchannel results in different flow patterns such as slug flow, annular flow, bubble flow and churn flow, depending on the operating conditions and reactor geometry (Kawahara *et al.*, 2011). The method of interfacial contact between liquid and gas phases is an important consideration in biphasic reactions. The majority of biphasic flow chemistry studies are based on segmented (or plug) flow in which mass transfer from gas to liquid phase largely is a function of the degree of interfacial contact (Yao *et al.*, 2015). Among these segmented flow was the most commonly used approach which provides intense mixing due to toroidal currents between gas and liquid segments. Similarly, the injection of gases at high velocity compared to liquids in case of concurrent flow streams results in the annular flow regime. The large volume of the gas bubble in the annular flow regime causes a decrease in a layer thickness of liquid segments which is pushed against the walls of the reactor. This results in the enhancement of mass transfer due to the increase in the interfacial area and the reduction in diffusion length. The use of falling film reactors of gas-liquid reactions was also reported following the same approach, where the liquid falling under gravity forms thin layers of the liquids resulting in enhancement of gas diffusion flowing co or counter-current direction (Jähnisch *et al.*, 2000). Mesh-microreactors are also reported as an alternative design for gas-liquid reactions. The liquid stream splits into multiple narrow channels after passing through a fine pore size mesh (75  $\mu\text{m}$ ), enabling a high gas-liquid contact area (Wenn *et al.*, 2003).

## **2.15 Cyclic carbonate synthesis under continuous flow conditions**

Most productions of cyclic carbonates have been carried out in batch reactors, which were designed to meet the requirements of reaction conditions (e.g. high temperature, pressure and extended reaction time) under traditional catalytic systems. Despite the advantages of flow

chemistry and development of highly efficient catalytic systems, only a few studies of cyclic carbonate synthesis in continuous flow conditions have been reported.

North (2012) reported a continuous method of EC synthesis from EO and waste CO<sub>2</sub> in the presence of their highly active one component SiO<sub>2</sub>-supported bifunctional Al (III) (salen) complex as a heterogeneous catalyst. The activity of the catalyst was evaluated through experiments performed in a batch reactor for SC synthesis from SO and CO<sub>2</sub> at ambient temperature (25 °C) and 1 bar *p* (CO<sub>2</sub>). The recyclability of the catalyst was also tested up to 32 cycles. The results have shown the decrease in catalytic activity due to dequaternisation of a quaternary ammonium salt, which can be reactivated by treating with benzyl bromide. However, the bimetallic Al (III) (salen) complex has shown high stability and catalytic activity of the complex was not affected even operating at high temperature (170 °C), which shows its long life and suitability for cyclic carbonate synthesis from high-temperature flue gases. These properties of the heterogeneous catalyst make it a highly desirable catalyst for cyclic carbonate synthesis under continuous flow condition.

Continuous flow reactor with a mixture of three gases (21% CO<sub>2</sub>, 25% EO and 54 % N<sub>2</sub>) passed through an immobilized catalyst packed column held in a thermostatically controlled oven was applied to achieve almost quantitative conversion of EO to EC after 7 h at 60 °C (North *et al.*, 2009b). In a separate study, the catalyst was also exposed to flue-gas from the combustion of coal for cyclic carbonate synthesis in the gas-phase flow reactor and shown to be compatible with waste CO<sub>2</sub> present in the unpurified flue gas (Meléndez *et al.*, 2011).

Zhao *et al.* (2013) studied the use of a microreactor for the formation of cyclic carbonates, resulting in appreciable enhancement in production rate than a conventional stirred tank reactor. Among the various reactions studied at the microscale, the gas/liquid biphasic reaction is an important category (Su *et al.*, 2009; Bourne *et al.*, 2011). The method of interfacial contact between liquid and gas phases is an important consideration in biphasic reactions. Here, synthesis of PC from PO and CO<sub>2</sub> was carried out in a microreactor using 2-hydroxyethyl-tributylammonium bromide (HETBAB) as OH-functionalized ionic liquid catalyst. The reaction was performed over the range of (140–190) °C and 35 bar *p* (CO<sub>2</sub>). The high surface-to-volume ratio of microreactor resulted in significant enhancement in heat and mass transfer. The synthesis of cyclic carbonates in microreactor resulted in appreciable decrease in the reaction to 14 seconds with > 99% yield with a dramatic increase in TOF from (3000–14000) h<sup>-1</sup> compared to 60 h<sup>-1</sup> in a batch reactor (Zhao *et al.*, 2013). These results

also suggested that the reaction performed in a microreactor can be intensified by increasing temperature. The increase in reaction temperature has a significant effect on the activity of the catalyst by increasing the activation of OH and subsequently nucleophilic attack of Br<sup>-</sup> to open the ring of epoxide. Secondly, with the increase of temperature, the gas-liquid mass transfer coefficient increased significantly as a result of an increase in gas diffusivity in the liquid ( $D_L$ ) and the decrease of liquid viscosity ( $\mu_L$ ) (Ferreira *et al.*, 2010).

Kozak *et al.* (2013) reported CO<sub>2</sub> cycloaddition to epoxides in a gas-liquid continuous flow reactor catalyzed by N-bromosuccinimide (NBS) in conjunction with benzoyl peroxide (BPO) using DMF as the reaction solvent. Here, the simultaneous activation of epoxide by bromine cation and CO<sub>2</sub> activation by the amide provided by DMF has exhibited a high cyclic carbonate yield at mild reaction conditions. A solution of epoxide and catalyst in DMF and CO<sub>2</sub> gas stream was introduced simultaneously under continuous flow conditions in a tubular reactor, resulting in complete conversion of 1,2-epoxyoctane into cyclic carbonate at 120 °C and 6.8 bar *p* (CO<sub>2</sub>) after 45 min reaction time. Furthermore, a series of experiments were performed to study the kinetics to investigate the mechanism involved and to determine the rate of reaction under continuous flow conditions.

Xu *et al.* (2015) reported EC synthesis from EO and CO<sub>2</sub> using ILs as catalysts using a bubbling column. To enhance the phase contact, CO<sub>2</sub> gas was continuously injected to the bottom of the column and bubbling up through the mixture of EO and ILs, resulting in an efficient conversion (99.5%) of EO into EC. The EC obtained from the first column was further conveyed to the next column, in which EC was hydrolyzed to get ethyl glycol (EG). For a heterogeneously catalyzed process, they employed a fixed bed reactor involving liquid-gas phases to contact and react at the surface of the immobilized ILs catalyst.

Microreactor technology is being increasingly used in flow chemistry due to its wide range of applications in chemical synthesis (Yao *et al.*, 2017). Among the various reactions studied at the microscale, the gas/liquid biphasic reaction is an important category (Su *et al.*, 2009). The method of interfacial contact between liquid and gas phases is an important consideration in biphasic reactions. In order to increase the effective (interfacial) surface area, and thus to increase the gas availability in the solution, synthesis of cyclic carbonates have been carried out in a 'tube-in-tube' gas-liquid microreactor (Rehman *et al.*, 2018b).

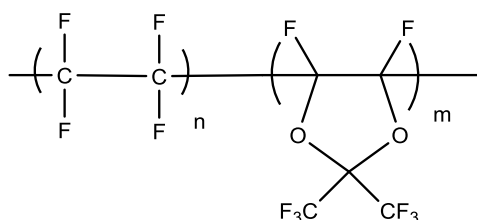
## 2.16 Teflon<sup>®</sup> AF-2400-based ‘tube-in-tube’ gas-liquid reactor

Teflon<sup>®</sup> AF-2400-based ‘tube-in-tube’ is a novel design of gas-liquid reactors to provide the high interfacial surface area and controlled supply of gases to the liquid stream under continuous flow conditions (Figure 2.1).



Figure 2.1 Teflon<sup>®</sup> AF-2400 based ‘tube-in-tube’ gas-liquid reactor.

These reactors have the ability to generate a homogeneous flow stream avoiding some potential issues associated with segmented flow gas-liquid reactors. The inner tube of the reactor is made of an amorphous polymer Teflon<sup>®</sup> AF-2400 based gas-permeable membrane which has the ability to permeate gases only but not the liquids. Teflon<sup>®</sup> AF-2400 is a commercially available amorphous glassy fluoropolymer prepared by copolymerization of perfluorodioxolane ( $m = 87 \text{ mol } \%$ ) and tetrafluoroethylene ( $n = 13 \text{ mol } \%$ ) (Scheme 2.32) (Yampolskii, 2009).



Scheme 2.32 Chemical structure of Teflon<sup>®</sup> AF-2400 membrane.

It has a unique structure characterized by microvoids having high fractional free volume (FFV %) compared to other polymers (Golemme *et al.*, 2003). The origin of these microvoids is the loose chain packing caused by the high energy rotation and reorientation of rigid dioxolane rings in an amorphous structure of the polymer. The size distribution of fractional free volume was determined by various techniques assuming cylindrical and spherical pore geometry and was in the range of 3 to 8 Å (Zhang *et al.*, 2010). These structural properties of AF-2400 along with weak van der Waals forces between fluorocarbon chains makes it useful for its application as an excellent semi-permeable membrane for a wide range of gases. This

concentric tubes reactor design has the ability to form microbubbles of gas on the outer walls of the amorphous fluoropolymer membrane, which are rapidly dissolved into the counterflowing liquid. Diffusion-controlled formation of homogeneous saturated gas solutions is thus obtained under flow-through conditions (Koos *et al.*, 2011). These reactors have higher surface area to volume ratios than conventional batch reactors and very high permeation of CO<sub>2</sub> across the Teflon<sup>®</sup> AF-2400 membrane i.e. (280,000 cB) compared to other gases (Table 2.13) (Biogeneral). This can lead to significantly improved reaction efficiency in terms of increased mass transfer from gas to the liquid phase.

Gas	Gas permeability [cB] <sup>*</sup>
Carbon dioxide (CO <sub>2</sub> )	280,000
Oxygen (O <sub>2</sub> )	99,000
Hydrogen (H <sub>2</sub> )	220,000
Nitrogen (N <sub>2</sub> )	49,000
Ethylene (C <sub>2</sub> H <sub>4</sub> )	35,000
Methane (CH <sub>4</sub> )	34,000
Ethane (C <sub>2</sub> H <sub>6</sub> )	18,000

\* cB = centiBarrer = 10<sup>-8</sup> (cm<sup>2</sup> - cm) / (cm - Hg - sec - cm<sup>2</sup>)

Table 2.13 Gas permeability of different gases through Teflon<sup>®</sup> AF-2400 membrane.

Over the last decade, this novel concept of reactor design has found a wide range of applications in organic chemical synthesis (Brzozowski *et al.*, 2015). The conventional design of the tube-in-tube reactor was only used to provide a gas saturated solution under ambient conditions. However, the new reactor design with an outer tube made of stainless steel has the ability to provide heat during the reaction along with a continuous supply of gas on-demand leading to higher throughput. The use of a tube-in-tube reactor has been reported for various applications of flow chemistry (Table 2.14). The reactor has resulted in a higher yield as compared plug flow and batch reaction.

Application	Reaction conditions	Yield (%)	Reference
Methoxy carbonylation	100 °C, (1–9) bar CO pressure, 0.6 ml/min	62–93	(Koos <i>et al.</i> , 2011)
Alkoxy carbonylation	120 °C, 12.4 bar CO pressure, 0.25 ml/min	91–98	(Mercadante and Leadbeater, 2011)
Homogenous hydrogenation	25 °C, 25 bar H <sub>2</sub> 0.7 ml/min	100	(O'Brien <i>et al.</i> , 2011)
Hydroformylation of Styrene	65 °C 25 bar CO: H <sub>2</sub> (1:1)	69–94	(Baxendale and Ley, 2011)
Carboxylation of Grignard Substrates	65 °C 4 bar CO <sub>2</sub> 0.2 ml/min	75–100	(Polyzos <i>et al.</i> , 2011)
Amino carbonylation	80 °C, 2 h reaction time	81	(Brancour <i>et al.</i> , 2013)
Synthesis of Amitriptyline	25 °C 4 bar CO <sub>2</sub> 0.2 ml/min	76	(Kupracz and Kirschning, 2013)
Oxidation of Alkenes	8 bar O <sub>2</sub> 60 °C	56–80	(Bourne and Ley, 2013)
Heck carbonylation of bromide	120 °C, 10 bar CO 120 ml/min	99	(Akinaga <i>et al.</i> , 2014)

Table 2.14 Applications of the ‘tube-in-tube’ gas-liquid reactor in organic synthesis.

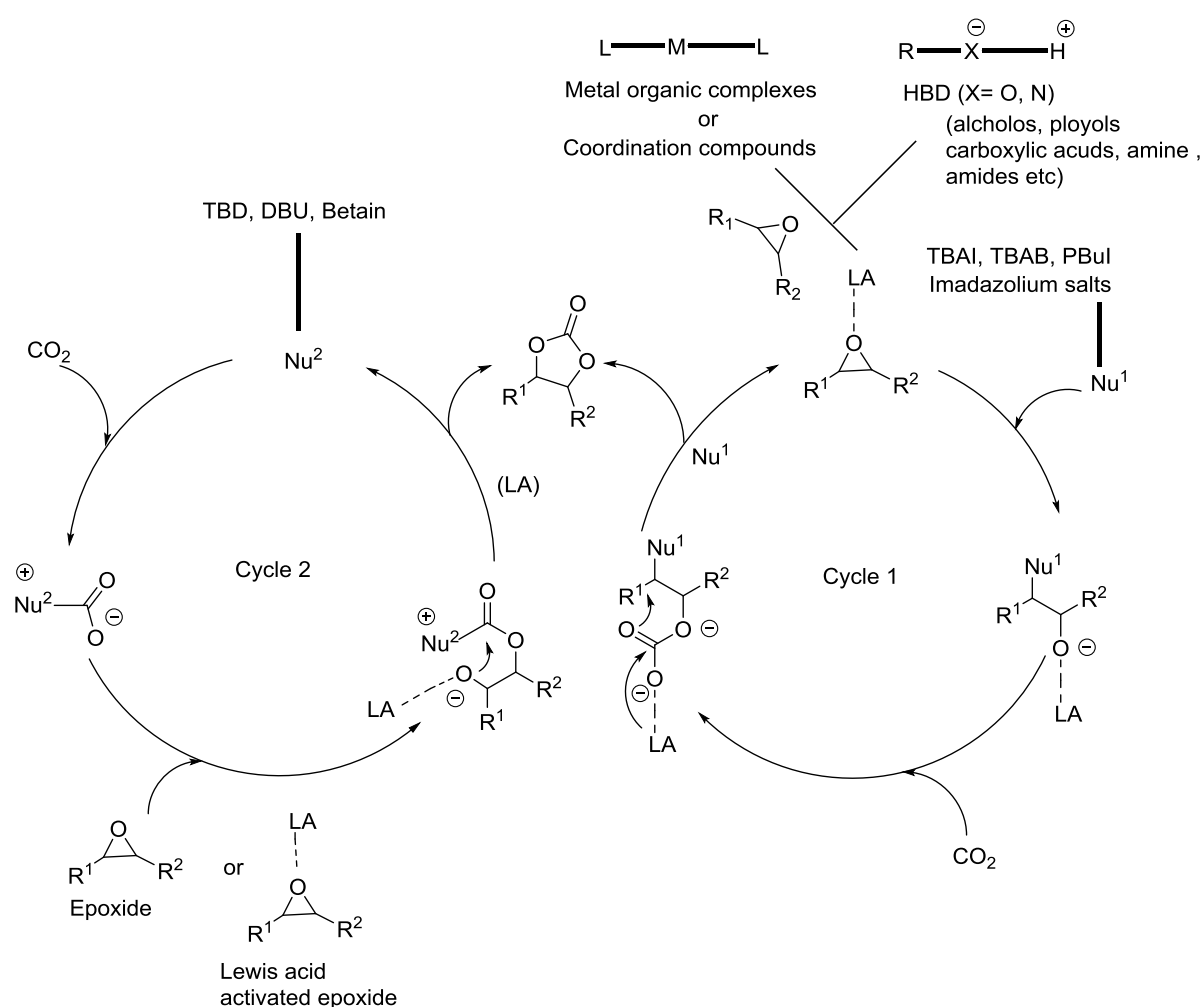
## 2.17 Summary

The use of CO<sub>2</sub> as a C1-building block has attracted the attention of both academia and the chemical process industry. Among the other methods of CO<sub>2</sub> utilization, synthesis of cyclic carbonates from epoxides and CO<sub>2</sub> has been extensively studied using numerous catalyst systems in the last 17 years. The use of organocatalysts such as ammonium, phosphonium and imidazolium salts have the advantage of commercial availability. However, cyclic carbonate synthesis in the presence of most of the organocatalysts still requires harsh reaction conditions due to lack of epoxide activation groups. Therefore, efforts have been made to increase the catalytic activity by combining the organocatalyst with –OH, –COOH groups and zinc salts (Lewis acids) which can activate the epoxide. Overall catalytic performance evaluation of these catalyst systems under variable reaction conditions is a difficult task. Among these catalyst systems, metal-based salen complexes have shown higher catalytic activities under mild reaction conditions such as the use of bimetallic Al (III) salen complexes at ambient conditions i.e. 25 °C and atmospheric pressure. These complexes are employed in combination with nucleophile additives such as TBAX as co-catalysts.

Heterogeneous catalysis for cyclic carbonate synthesis was less extensively studied than their homogeneous counterparts. The use of heterogeneous catalysts still had some potential shortcomings due to the requirement of harsh reaction conditions, use of co-catalysts (nucleophiles) in a homogeneous phase and loss in catalytic activity in consecutive runs. To solve these issues, the immobilizing of active homogeneous catalysts on mesoporous materials e.g. MCM-41, SBA 15 and novel MOFs as high surface area supports are required. Furthermore, immobilizing with more strong covalent grafting methods is highly desirable to avoid leaching of the catalyst under reaction conditions.

Although the synthesis of cyclic carbonates has been extensively studied using various catalyst systems with higher conversion and yield of the product, a detailed study of reaction kinetics is required to investigate the reaction mechanism. From a mechanistic point of view, the CO<sub>2</sub> cycloaddition to epoxides can be carried out using a wide range of catalysts mainly consisting of Lewis acids in combination with nucleophiles as binary catalysts or single-component bifunctional catalysts. The reaction mechanism can be explained by two general pathways including epoxide activation as an initial step or CO<sub>2</sub> activation as an initial step (Scheme 2.33).

Cycle 1 shows the activation of epoxide with Lewis acids provided by metal organic complexes or hydrogen bond donors (HBD), which then undergoes nucleophilic attack by the halide anions ( $\text{Nu}^1$ ) provided by quaternary onium salts to form an alkoxide. Subsequently, the  $\text{CO}_2$  insertion into the alkoxide intermediate takes place. Finally, the corresponding five-membered cyclic carbonate is formed by the intramolecular elimination of the nucleophile. Similarly, Cycle 2 shows activation of  $\text{CO}_2$  by the nucleophilic attack of TBB, DBU, Betaine etc. ( $\text{Nu}^2$ ) on the electrophilic carbon atom of  $\text{CO}_2$ . Subsequently, the activated  $\text{CO}_2$  attacks to open the ring of epoxide or (activated epoxide) to form an intermediate. Finally, the cyclisation of this intermediate leads to form a five-membered ring of the corresponding cyclic carbonate and the nucleophile ( $\text{Nu}^2$ ) is regenerated.



Scheme 2.33 General mechanism of  $\text{CO}_2$  cycloaddition to epoxides by two possible pathways: (Cycle 1) epoxide activation as an initial step, (Cycle 2)  $\text{CO}_2$  activation as an initial step (Shaikh *et al.*, 2017).

Generally, the catalyst systems described in the literature have shown higher catalytic activity for mono-substituted terminal epoxides such as EO, PO and SO. Conversely, the use of internal epoxides (di- and tri-substituted) for cyclic carbonate synthesis under mild reaction conditions is still challenging. The advancement in catalytic systems is highly desirable for cycloaddition of CO<sub>2</sub> to internal epoxides at mild reaction conditions. The use of bio-based epoxides such as limonene oxides,  $\alpha$ -pinene oxide, carvone, linalool oxide and menthene oxide as a potential replacement of petroleum-based epoxides is highly desirable for the sustainable future of cyclic carbonate synthesis. Therefore, the attention of future research needs to be focused on the development of active catalyst systems for CO<sub>2</sub> cycloaddition to renewable bio-based epoxides to make the process 100% sustainable. The optimization of reaction conditions also needs to be a focus to overcome heat and mass transfer limitations to improve the overall performance of this reaction.

Synthesis of cyclic carbonates from epoxides and CO<sub>2</sub> is a typical gas-liquid multiphase catalytic process involving a gas-liquid mass transfer in a reactor and the catalytic cycloaddition reaction in the liquid phase. Therefore reactions carried out in an “efficient” reactor design (in terms of the high rate of heat/mass transfer and continuous flow approach) could mitigate many of the short-comings observed in conventional batch reactors. Therefore, it may be beneficial to investigate the use of more novel reactor technologies for the synthesis of these carbonates.

## Chapter 3 Materials and methods

### 3.1 Introduction

The chemicals, type of the reactors, experimental procedures and analytical techniques used in this study are discussed in this chapter. The main experimental work has been divided into four parts:

Synthesis of cyclic carbonate via CO<sub>2</sub> cycloaddition to bio-based limonene oxide (LO) was carried out using tetrabutylammonium halides (TBAX) as homogeneous catalysts. The reaction was carried out in a high-pressure semi-batch reactor. Initially, the cycloaddition reaction was carried out using commercial LO which is a mixture of *cis*- and *trans*-isomer (40:60). Due to low reactivity of *cis*-isomer in cycloaddition reaction, a stereoselective method of (*R*)-(+)-limonene epoxidation was carried out to get a high yield of *trans*-isomer, which was subsequently used as a substrate. A detailed study of reaction kinetics was carried out to investigate the effect of kinetic parameters on reaction rate and to understand the reaction mechanism involved.

A continuous method of styrene carbonate (SC) synthesis from styrene oxide (SO) and carbon dioxide (CO<sub>2</sub>) is reported, using a semipermeable Teflon<sup>®</sup> AF-2400-based tube-in-tube gas-liquid reactor. The reaction was performed in the presence of TBAB and ZnBr<sub>2</sub>, acting as a highly efficient and economical binary homogeneous catalyst system. The performance of the flow reactor was evaluated by studying the effect of various operating conditions such as reaction temperature, CO<sub>2</sub> pressure, and residence time. Moreover, a detailed kinetic study of SC synthesis was carried out to determine the corresponding kinetic values and thermodynamic activation parameters.

Formation of SC by the cycloaddition of CO<sub>2</sub> to SO was further investigated using pyrrolidinopyridinium iodide (PPI) in combination with zinc halides (ZnX<sub>2</sub> where X= I<sup>-</sup>, Br<sup>-</sup>, Cl<sup>-</sup>) as an acid-base binary homogeneous catalytic system. The effect of reaction parameters such as temperature, pressure, and catalyst ratio and residence time, and the reaction kinetics for the SC synthesis were investigated.

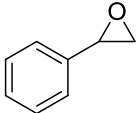
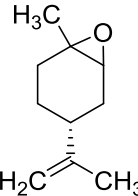
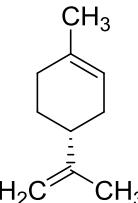
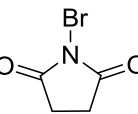
The reaction kinetics for SC synthesis from SO and CO<sub>2</sub> were also investigated using a heterogeneous silica-supported pyrrolidinopyridinium iodide (SiO<sub>2</sub>-PPI) catalyst. The

characterization of SiO<sub>2</sub>-PPI was performed by solid-state <sup>13</sup>C NMR, BET and XRD analysis. The detailed study of heterogeneous kinetics was carried using Pseudo homogeneous, Langmuir-Hinshelwood (LH) and Eley-Rideal (ER) heterogeneous kinetic models. Moreover, the temperature dependence of the reaction was studied to determine the activation energy and thermodynamic activation parameters. Based on the kinetic analysis, the reaction mechanism was proposed.

Qualitative and quantitative analysis of the product samples in this study were carried out using Fourier-transform infrared (FTIR) spectroscopy, gas chromatography (GC) and nuclear magnetic resonance (NMR) spectroscopy.

### 3.2 Materials

The chemicals required in this study are shown in Table 3.1. These are mainly classified as epoxides, catalysts and solvents used to investigate the cyclic carbonate synthesis by CO<sub>2</sub> cycloaddition to epoxides. All chemicals were purchased from Sigma Aldrich and used without further purification. The CO<sub>2</sub> gas (99.9%) was supplied by BOC Gases.

Chemicals/ Reagents	Chemical Formula	Purity (%)	Mol. weight (g/mol)	Description
Styrene oxide		97	120.15	Epoxide
(+)-Limonene oxide (a mixture of <i>cis</i> and <i>trans</i> )		≥97	152.23	Epoxide
Carbon dioxide	CO <sub>2</sub>	99.9	44.01	Substrate
( <i>R</i> )-(+)-limonene		97	120.15	Substrate for epoxidation
N-bromosuccinimide		99	177.98	Source of bromine

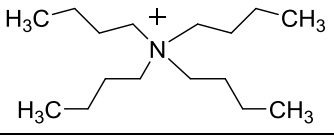
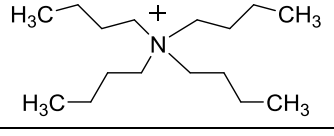
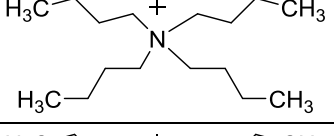
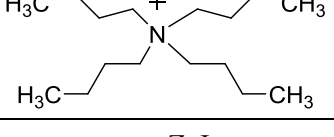
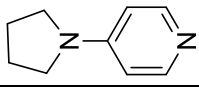
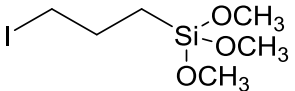
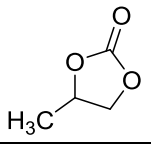
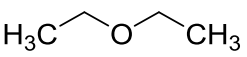
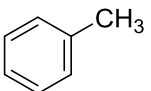
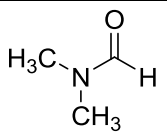
Sodium hydroxide	NaOH	98	40	Epoxidation
Tetrabutylammonium iodide		98	369.37	Catalyst/ Nucleophile additive
Tetrabutylammonium bromide		≥98	322.37	Catalyst/ Nucleophile additive
Tetrabutylammonium chloride		≥97	277.92	Catalyst/ Nucleophile additive
Tetrabutylammonium fluoride		98	261.46	Catalyst/ Nucleophile additive
Zinc iodide	ZnI <sub>2</sub>	98	319.20	Co-catalyst
Zinc bromide	ZnBr <sub>2</sub>	99.99	225.20	Co-catalyst
Zinc chloride	ZnCl <sub>2</sub>	99.99	136.20	Co-catalyst
4-Pyrrolidinopyridine		98	148.20	Catalyst preparation
3-(iodopropyl) trimethoxysilane		95	290.17	Catalyst preparation
Propylene carbonate		99.7	102.09	Solvent for kinetic study
diethyl ether anhydrous		≥97.0	74.12	Solvent for epoxidation
Toluene		99.8	92.14	Solvent for catalyst preparation
N,N-dimethylformamide (anhydrous)		99.8	7.09	Solvent
dichloromethane (anhydrous)	CH <sub>2</sub> Cl <sub>2</sub>	99.8	84.93	Solvent for catalyst preparation
Chloroform (anhydrous)	CHCl <sub>3</sub>	>99	119.38	Solvent
Naphthalene	C <sub>8</sub> H <sub>10</sub>	>99.7%	128.17	Internal standard

Table 3.1 List of the chemicals used in this study.

### 3.3 Experimental setup

#### 3.3.1 Semi-batch reactor

Cyclic carbonate synthesis by CO<sub>2</sub> cycloaddition to epoxides was carried out in a 100 ml high-pressure stainless steel reactor (Parr Model 4793) in semi-batch operation (Figure 3.1). This reactor had the capacity to operate up to a maximum of 200 bar pressure and 350 °C. The reactor was equipped with a band heater to provide uniform heat during the reaction. The temperature of the reaction mixture was measured by a thermocouple and controlled by a PID temperature control system (Elmatic heating controller). The reactor was connected to high pressure (50 bar) CO<sub>2</sub> gas cylinder to provide CO<sub>2</sub> during the reaction. The pressure inside the reactor was measured by a pressure gauge (1–200) bar installed on the top of the reactor. The pressure was controlled by high pressure (70 bar) CO<sub>2</sub> gas regulator connected to the outlet of the CO<sub>2</sub> gas cylinder. The reactor was also equipped with a pressure safety valve (24–51.5) bar and a condensation coil to release the pressure above the set point. The reaction mixture was agitated by a magnetic stirrer (1250 rpm). The schematic diagram of the semi-batch reactor for cyclic carbonate synthesis is shown in Figure 3.2.

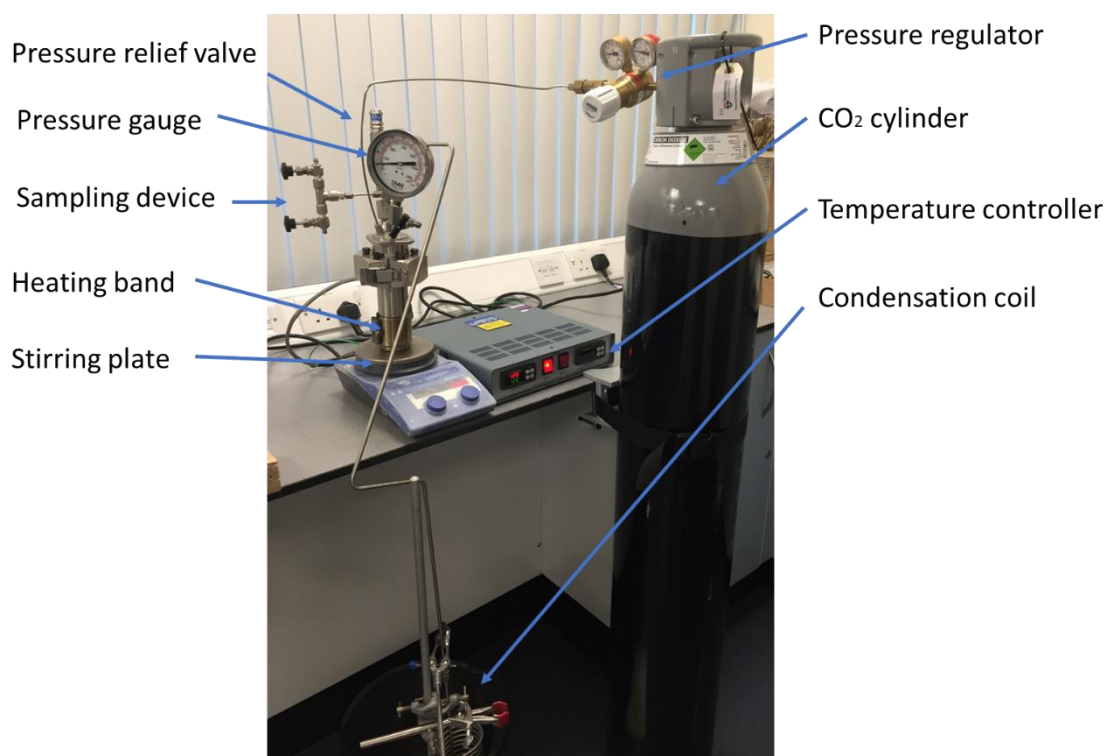


Figure 3.1 Experimental setup for cyclic carbonate synthesis in a semi-batch reactor.

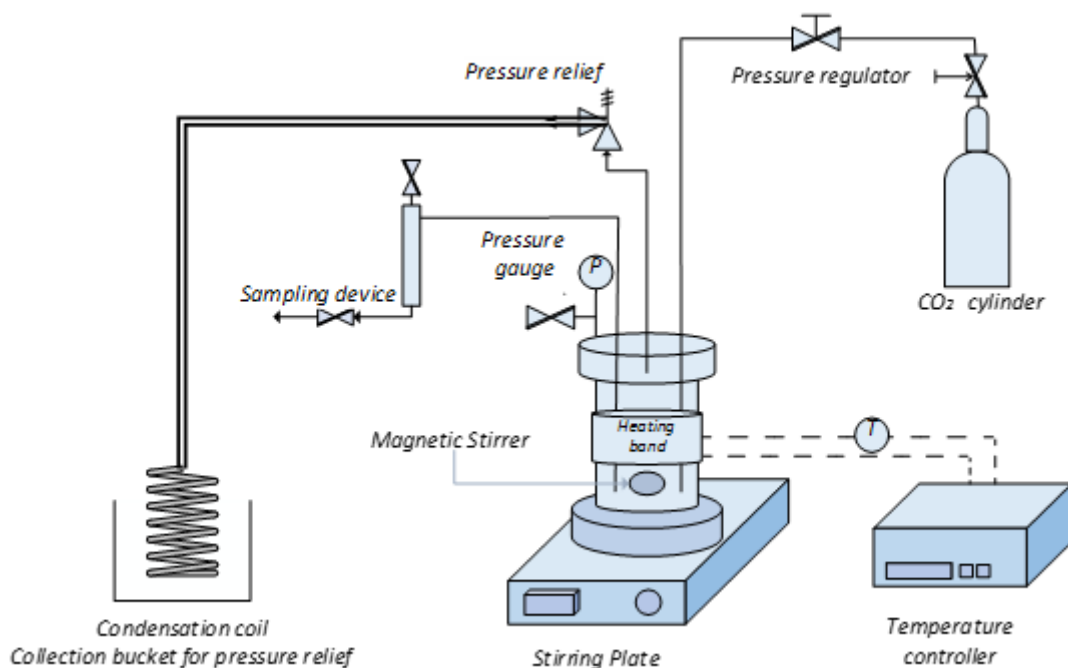


Figure 3.2 Schematic diagram of the semi-batch reactor for cyclic carbonate synthesis.

### 3.3.2 Tube-in-tube gas-liquid reactor

Synthesis of styrene carbonate (SC) from styrene oxide and CO<sub>2</sub> was also carried out in a ‘tube-in-tube’ gas-liquid continuous flow reactor. The tube-in-tube gas/liquid flow reactor was first designed by the Ley group at Cambridge University, UK (O'Brien *et al.*, 2011). It consists of a pair of concentric tubes as shown in Figure 3.3. The inner tube of the reactor is made of Teflon<sup>®</sup> AF-2400 semi-permeable membrane having dimensions (4 m × 1.0 mm OD × 0.8 mm ID) which permits only gases to pass through tubing walls. This inner tube was surrounded by an outer stainless steel tubing having dimensions (4 m × 3.23 cm OD × 2.61 mm ID). The reactor coil was fitted over a Uniqsis Flowsyn operating unit (Figure 3.4). The solution of epoxide and the homogeneous catalyst was introduced by high-pressure pumps through the inner tube. The CO<sub>2</sub> gas was charged into the shell side of the reactor by connecting the outer tube with the CO<sub>2</sub> gas cylinder through a pressure regulator. The CO<sub>2</sub> gas permeates through the inner wall and dissolves into the bulk of the reaction mixture along with the tube length, and the saturated gas solution is obtained under flow-through conditions.

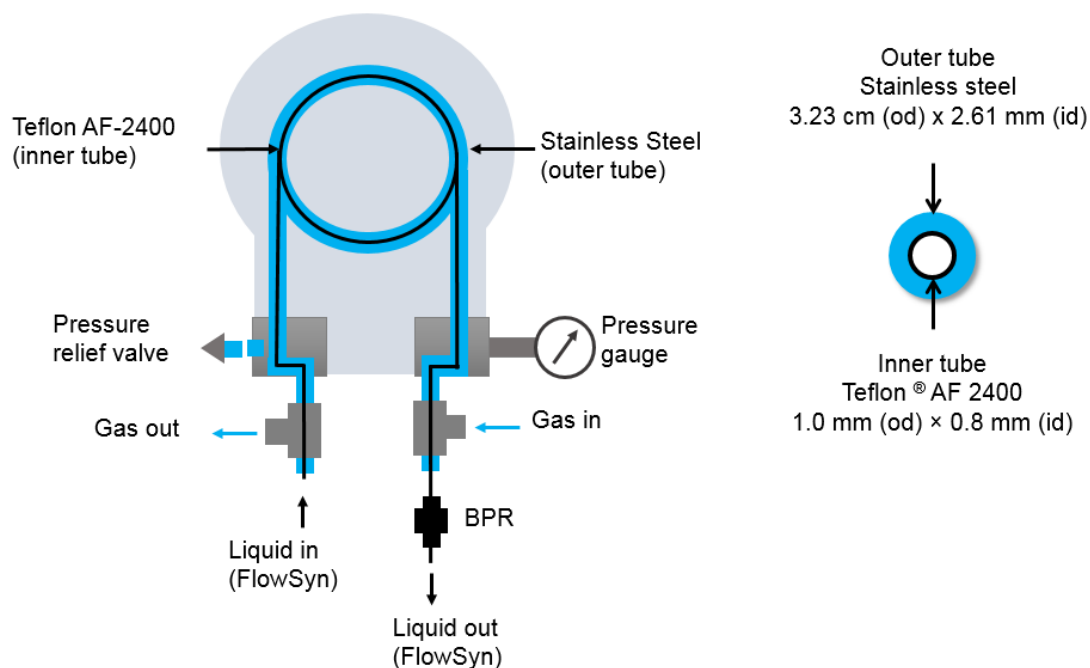


Figure 3.3 Flow configuration in a ‘tube-in-tube’ gas-liquid reactor.

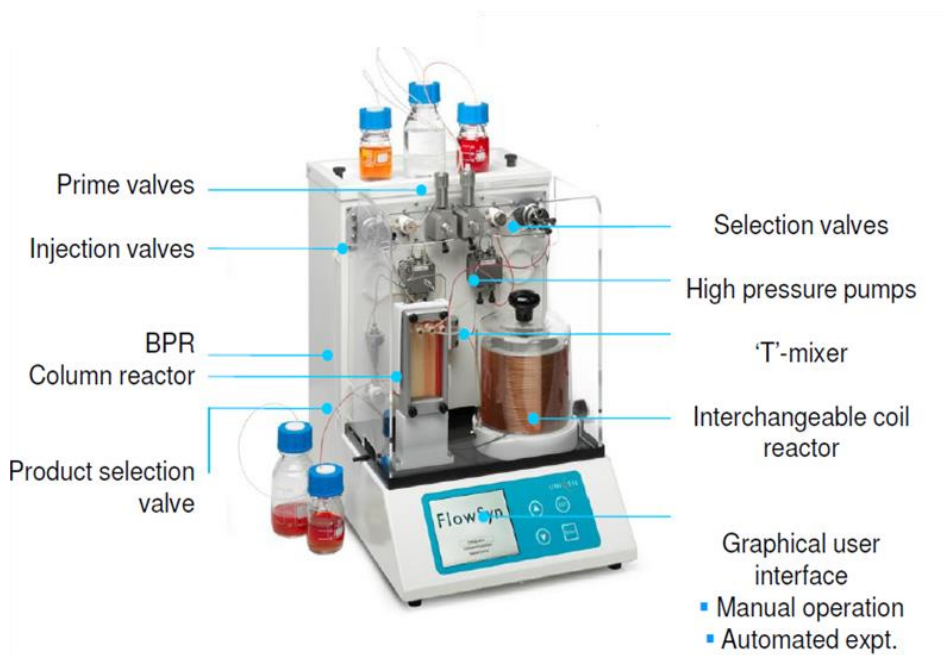


Figure 3.4 Uniqsis Flowsyn system used to operate the ‘tube-in-tube’ gas-liquid reactor.

The Flowsyn unit contains a heated reactor station to provide heat (ambient to 260 °C) and high-pressure pumps which can pump liquid from 0.01 to 10 ml/min at pressures up to 200 bar. The temperature of the reactor was controlled by an automatic temperature control system, and the pressure on the shell side of the reactor by a pressure regulator installed to the outlet of the CO<sub>2</sub> gas cylinder. To keep the pressure constant on the shell side and to prevent

outgassing of the CO<sub>2</sub>, a back pressure regulator (6.9 bar) was installed at the end of the flow stream. A relief valve was also connected at the outlet of the reactor to release the pressure above set-point. The independent control of liquid and gas flow has the advantage that gas can be drawn through the membrane on demand during the reaction leading to higher throughput. A schematic of the continuous flow tube-in-tube gas-liquid coil reactor is shown in Figure 3.5.

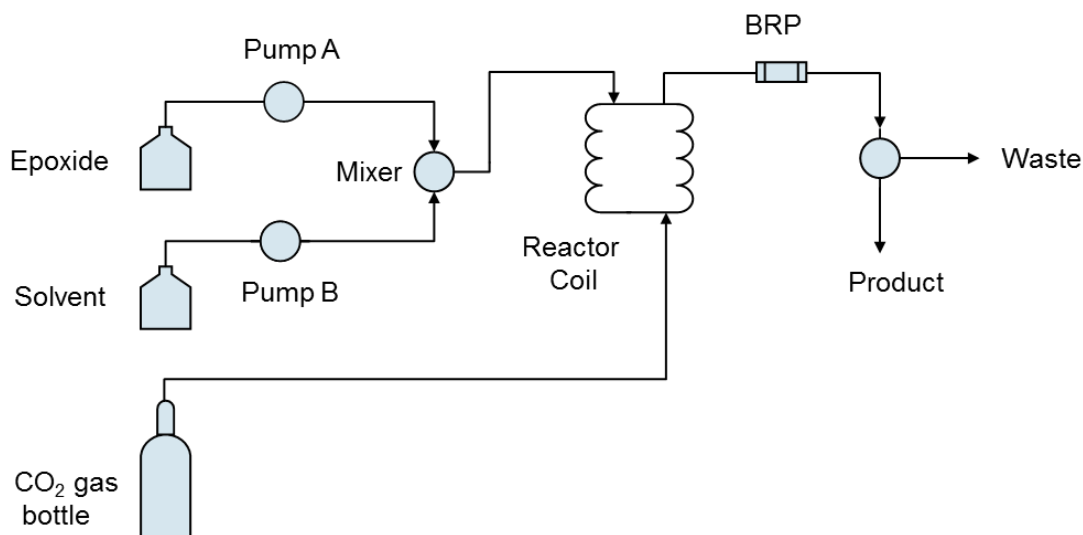


Figure 3.5 Schematic diagram of the continuous flow reactor for cyclic carbonate synthesis.

### 3.4 Experimental procedures

#### 3.4.1 Cyclic carbonate synthesis in a semi-batch reactor

In a typical experiment, the desired amounts of epoxide and catalyst were charged into the batch reactor, and the reactor was heated to the required temperature by setting the value on the temperature controller. After achieving the desired temperature, the reactor was pressurised with CO<sub>2</sub> from a gas cylinder to the required pressure. The CO<sub>2</sub> was continuously supplied to the reactor during the reaction. After completion of the reaction, the reactor was allowed to cool down to room temperature and slowly depressurized to atmospheric pressure. The product samples were analysed by FTIR, GC and NMR spectroscopy. The summary of reaction conditions for CO<sub>2</sub> cycloaddition to SO and LO in the presence of homogeneous and heterogeneous catalyst systems are given below in Table 3.2.

Reaction conditions	Styrene oxide (SO)			Limonene oxide (LO)
Type of catalyst	TBAB	PPI	SiO <sub>2</sub> -PPI	TBAC
Co-catalyst	ZnBr <sub>2</sub>	ZnI <sub>2</sub>	–	–
Epoxide (M)	1.5–5.5	1.5–5.5	1.5–5.5	1.5–5.5
Temperature (°C)	80–120	100–140	100–180	90–140
Pressure (bar)	1–10	1–10	1–10	1–40
Catalyst loading	0.025–0.1 M	38–152 mM	38–152 mM	1.5–7.5 mol%
Co-catalyst loading	3.25–26 mM	19–152 mM	–	–
Mixing speed (rpm)	1250	1250	1250	1250

Table 3.2 Summary of reaction conditions for cyclic carbonates synthesis by CO<sub>2</sub> cycloaddition to styrene oxide (SO) and limonene oxide (LO) in a semi-batch reactor.

### 3.4.2 *Cyclic carbonate synthesis in a ‘tube-in-tube’ gas/liquid reactor*

Synthesis of SC by CO<sub>2</sub> cycloaddition to SO was also carried out in a ‘tube-in-tube’ gas/liquid flow reactor. The reaction was carried out in the presence of TBAB and ZnBr<sub>2</sub> as an acid-base binary homogeneous catalyst. Before the start of the reaction, the catalyst was dissolved in the liquid epoxide and pumped through the inner tube of the reactor. The desired values of reaction conditions such as temperature, pressure and residence time were adjusted on the Uniqsis Flowsyn control panel. After achieving the steady-state conditions, the CO<sub>2</sub> gas was supplied to the shell side of the reactor by connecting the outer tube with the CO<sub>2</sub> gas cylinder through a pressure regulator. The shell side of the reactor was held at a constant pressure during a particular experiment using a back pressure regulator. The reaction takes place inside the spiral ‘tube-in-tube’ reactor. The product was collected at the outlet of the reactor and analysed by FTIR and GC to determine the conversion and yield of the product.

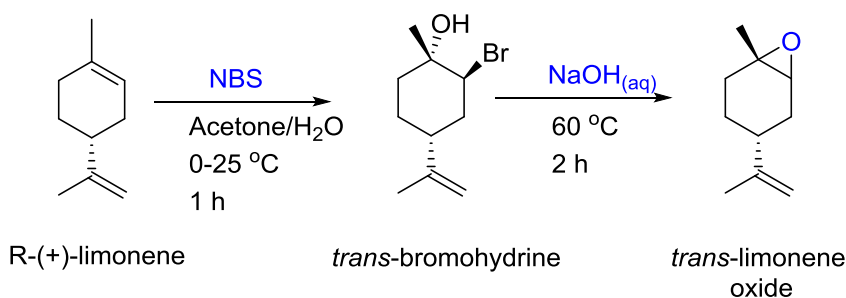
### 3.4.3 *Kinetic experiments for CO<sub>2</sub> cycloaddition to epoxides*

The study of the kinetics of CO<sub>2</sub> cycloaddition to epoxides was carried out in a high-pressure stainless steel reactor, as reported previously (North and Pasquale, 2009). For an exemplary experiment, the desired amounts of epoxide and catalyst were added into the reactor and

heated to the required temperature by setting the value on the temperature controller. When the desired temperature set point was achieved, a continuous supply of CO<sub>2</sub> was provided to the reactor to maintain the constant pressure during the reaction. The reaction started immediately after introducing CO<sub>2</sub> in the reactor. The CO<sub>2</sub> was present in large excess due to continuous supply during a semi-batch operation. Moreover, the kinetics experiments were carried out using PC as the reaction solvent. The rate at which CO<sub>2</sub> dissolves in PC is much faster than the rate of cyclic carbonate formation (Pohorecki and Možeński, 1998a). Therefore, the concentration of CO<sub>2</sub> in the liquid phase remains constant throughout the reaction. The progress of the reaction was monitored by taking aliquots from the reaction mixture at regular intervals (15–60) min through a sampling device installed on the top of the reactor.

#### 3.4.4 General procedure for epoxidation of (*R*)-(+)-limonene

A stereoselective method of (*R*)-(+)-limonene epoxidation was carried out to get a higher yield of *trans*-isomer (Scheme 3.1). Initially, the (*R*)-(+)-limonene was brominated using *N*-bromosuccinimide (NBS) as a source of bromine in an aqueous solution of acetone at low temperature (0–25) °C. The bromination of (+)-limonene results in the formation of endocyclic *trans*-bromohydrin. In the second step, the *trans*-bromohydrin was readily epoxidised using aqueous sodium hydroxide (NaOH) solution at 60 °C for 2 h to get a higher yield of *trans*-limonene oxide.



Scheme 3.1 Stereoselective epoxidation of (*R*)-(+)-limonene using *N*-bromosuccinimide (NBS).

The detailed procedure for stereoselective epoxidation of limonene can be described as follows: In the first step, (*R*)-(+)-limonene (88 mmol, 11.98 ml), water (10 ml), acetone (45 ml) were mixed together in a round bottom flask and allowed to cool down using a jacket of ice under continuous stirring by a magnetic stirrer. At very low temperature (< 5 °C), 16.374 g (92 mmol) of NBS was added and the reaction mixture was stirred for 1 hr to ensure complete

reaction. After the bromination step, the solvent (acetone) was removed from the reaction mixture using a rotary evaporator at 50 °C and 600 mbar. The resulting solution was further diluted with diethyl ether (30 ml) followed by separation of the organic phase using a separation funnel. The organic phase obtained after separation was washed with water (30 ml) followed by evaporation of the solvent (diethyl ether) using rotary evaporator at 50 °C and 600 mbar. The resulting *trans*-bromohydrin was further epoxidised using 20 ml of 6 M sodium hydroxide (NaOH) at 60 °C. The epoxidation of *trans*-bromohydrin was performed in a round bottom flask under continuous stirring. The reaction was carried out for 2 h to ensure complete conversion. After epoxidation, the alkaline phase was separated using a separating funnel and the resulting organic phase was extracted with diethyl ether (30 ml). The resulting extract solution was washed with a saturated solution of sodium bicarbonate (NaHCO<sub>3</sub>) (15 ml) followed by washing with water (15 ml). Finally, the diethyl ether solvent was evaporated and the analysis of the product was performed by GC using naphthalene as an internal standard.

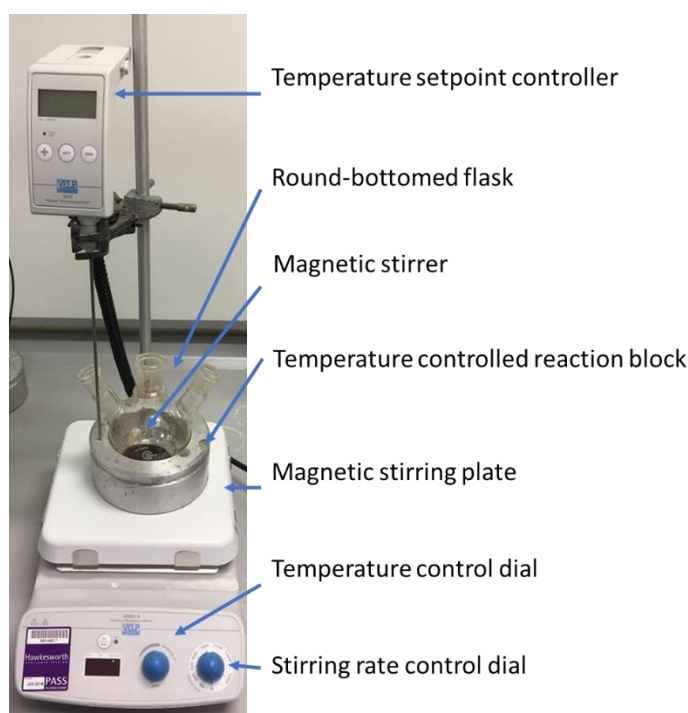
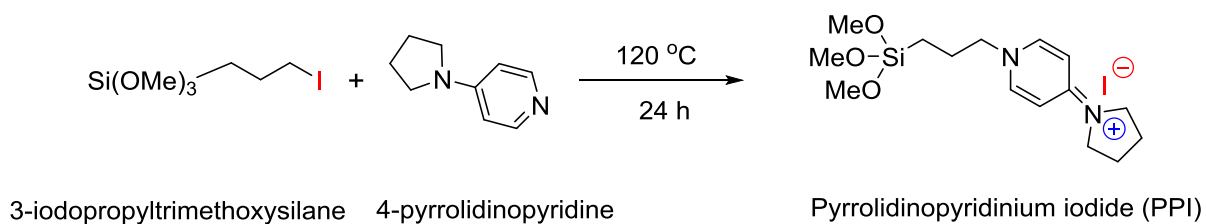


Figure 3.6 Experimental setup for stereoselective epoxidation of (*R*)-(+)-limonene.

### 3.4.5 Preparation of homogeneous pyrrolidinopyridinium iodide catalyst

The pyrrolidinopyridinium iodide (PPI) catalyst was synthesised according to the reported procedure (Motokura *et al.*, 2014). In this study, 2.5 mmol of 4-pyrrolidinopyridine and 2.5 mmol of 3-iodopropyltrimethoxysilane were mixed in a round bottom flask, and the mixture was heated at 120 °C for 24 h (Scheme 3.2). A quantitative yield of PPI was obtained. The structure of the catalyst was confirmed by a <sup>13</sup>C-NMR spectrum of the catalyst sample (Figure 3.7).



Scheme 3.2 Preparation of homogeneous pyrrolidinopyridinium iodide (PPI) catalyst.

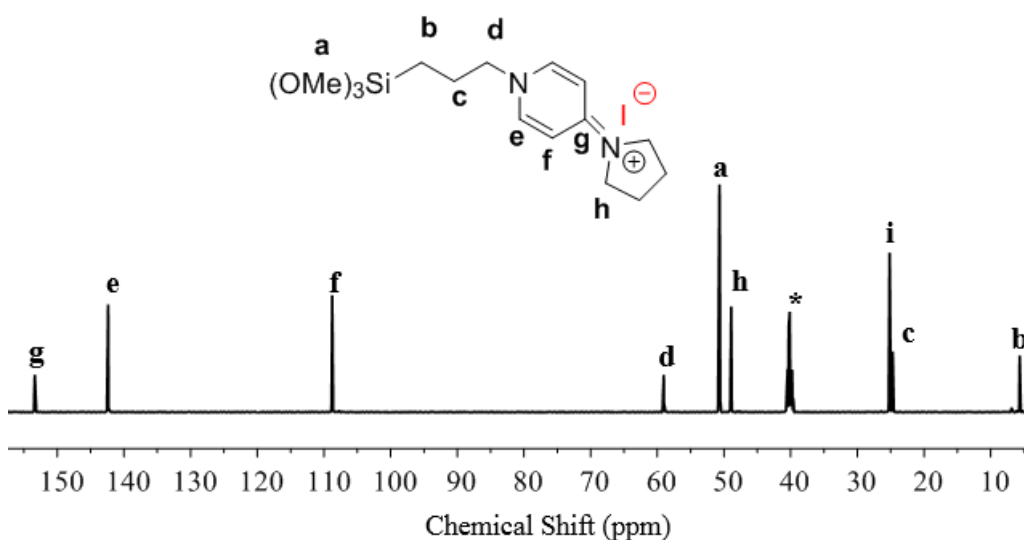
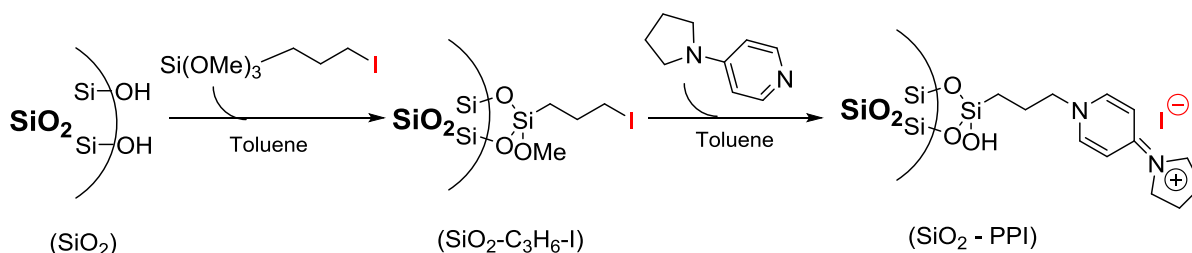


Figure 3.7 <sup>13</sup>C NMR spectrum of pyrrolidinopyridinium iodide (PPI) in DMSO (\*) 500 MHz at 298K.

### 3.4.6 Preparation of silica-supported pyrrolidinopyridinium iodide catalyst

The immobilization of 4-pyrrolidinopyridinium iodide over the SiO<sub>2</sub> was carried out in two steps as in Scheme 3.3.



Scheme 3.3 Preparation of silica-supported pyrrolidinopyridinium iodide (SiO<sub>2</sub>-PPI) catalyst.

Initially, the silica (SiO<sub>2</sub>) was treated in a vacuum oven at 105 °C and 200 mbar for 3 h to remove any moisture and volatile contents. After pre-treatment, treated SiO<sub>2</sub> (2 g) was mixed with a 32 ml solution of anhydrous toluene and 3-iodopropyltrimethoxysilane (8 mmol, 1.56 ml). The resulting solution was kept under reflux for 6 h and filtered to separate the silica-supported methyl iodide (SiO<sub>2</sub>-C<sub>3</sub>H<sub>6</sub>-I) also known as functional silica. SiO<sub>2</sub>-C<sub>3</sub>H<sub>6</sub>-I was dried in a vacuum oven at 105 °C and 200 mbar. After being dried, 1 g of SiO<sub>2</sub>-C<sub>3</sub>H<sub>6</sub>-I was added in 20 ml solution of toluene and 8.4 mmol (1.25 g) 4-pyrrolidinopyridine and again refluxed for 16 h. After that, the solvent (toluene) was separated by filtration. The resulting solid was washed with anhydrous toluene and dichloromethane. Lastly, the SiO<sub>2</sub>-PPI catalyst was dried up in the vacuum oven (200 mbar) at 120 °C and stored in the vacuum desiccator.

### 3.5 Characterization of silica-supported pyrrolidinopyridinium iodide (SiO<sub>2</sub>-PPI)

The characterization of SiO<sub>2</sub>-PPI was carried out using solid-state cross-polarization magic angle spinning (CP MAS) <sup>13</sup>C NMR to confirm the immobilization of active homogeneous analogue (PPI) over silica. The Brunauer-Emmett-Teller (BET) isotherm was used to determine the specific surface area and the porous nature of the catalyst. Elemental analysis (CN) was used to determine the loading of active catalytic species over the solid support. Moreover, Powder X-ray diffraction (PXRD) was carried out to determine the uniform distribution of the catalyst over the solid support.

### 3.5.1 Solid-state $^{13}\text{C}$ CP MAS NMR

The immobilization of the pyrrolidinopyridinium iodide (PPI) over the  $\text{SiO}_2$  surface was confirmed by solid-state  $^{13}\text{C}$  CP MAS NMR. The spectra of the catalyst samples were collected using a Varian infinity plus NMR spectrometer operating at 300 MHz. The catalyst samples were packed into 4 mm zirconia rotors and spun at a rate of 12.5 kHz. A  $^{13}\text{C}$  CP MAS spin echo experiment was conducted at a contact pulse of 0.5 ms, recycle delay of 10 sec and the spin echo delay time of 35  $\mu\text{sec}$ . Total scans were fixed at about 20,000. There were no spinning sidebands observed in the spectra. To calibrate the chemical shifts, the spectra were referenced to adamantane, used as an external standard. The  $^{13}\text{C}$  NMR spectra of 3-iodopropyletrimethoxysilane and pyrrolidinopyridinium iodide (PPI) were collected using Bruker Advance series III spectrometer operating at 500 MHz. The  $^{13}\text{C}$  NMR spectrum of 3-iodopropyletrimethoxysilane and solid-state  $^{13}\text{C}$  CP MAS NMR spectrum of silica-supported propyl iodide ( $\text{SiO}_2\text{-C}_3\text{H}_6\text{-I}$ ) obtained after the first step of catalyst preparation have shown the same positions of signals at  $a = 50$ ,  $b = 12.3$ ,  $c = 26.7$  and  $d = 5.7$  ppm approving the immobilization of organic phase over silica (Figure 3.8 a,b). Similarly, the grafting of 4-pyrrolidinopyridine over the functionalised silica ( $\text{SiO}_2\text{-C}_3\text{H}_6\text{-I}$ ) was confirmed from the  $^{13}\text{C}$  NMR spectra of homogeneous analogue (i.e. PPI) and  $^{13}\text{C}$  CP MAS NMR of finally prepared heterogeneous catalyst (Figure 3.8 c,d), showing the same positions of signals at  $b = 7.8$ ,  $(c, i) = (14\text{--}30)$ ,  $h = 49$ ,  $d = 57.5$ ,  $f = 108$ ,  $e = 142$  and  $g = 152.5$  ppm given as  $(b) = \text{C atom beside Si}$ ,  $(c) = \text{C atom in the centre of C3 chain}$ ,  $(h) = \text{C atom beside N in the pyrrolidine ring}$ ,  $(i) = \text{C atom next to h in the pyrrolidine ring}$ , and  $(e)$ ,  $(f)$ , and  $(g) = \text{C atom at } ortho, meta \text{ and } para \text{ positions of pyridine ring}$ , respectively (Motokura *et al.*, 2009).

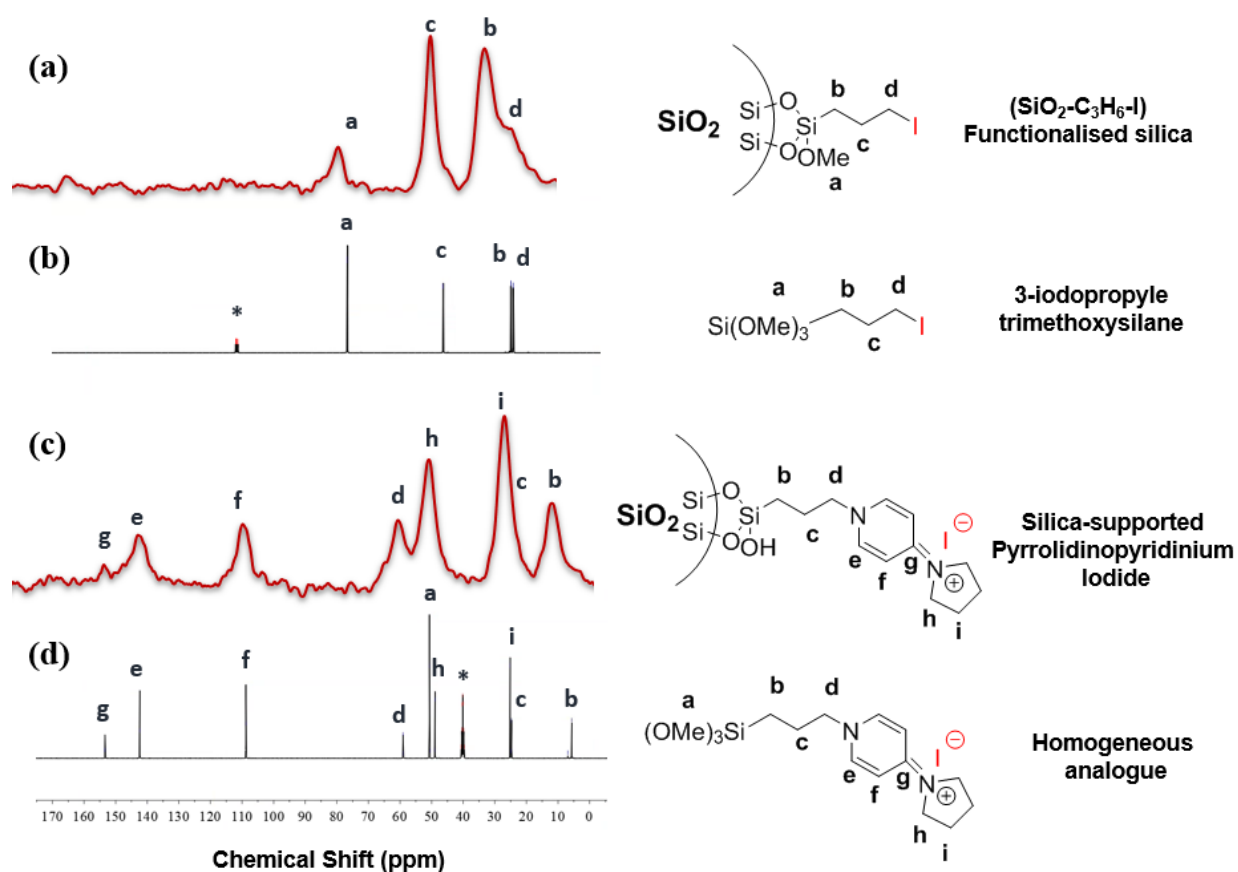


Figure 3.8 (a) Solid-state  $^{13}\text{C}$  CP MAS NMR spectrum of functionalised silica ( $\text{SiO}_2\text{-C}_3\text{H}_6\text{-I}$ ) (b)  $^{13}\text{C}$  NMR spectrum of 3-iodopropyltrimethoxysilane (c) Solid-state  $^{13}\text{C}$  CP MAS NMR spectrum of silica-supported pyrrolidinopyridinium iodide ( $\text{SiO}_2\text{-PPI}$ ) (d)  $^{13}\text{C}$  NMR spectrum of the homogeneous analogue (PPI) (\* solvent peaks).

### 3.5.2 BET analysis

BET specific surface areas and the pore size of the catalyst samples were determined through nitrogen adsorption at 77K using Thermo Fisher Scientific surfer gas adsorption porosimeter. Initially, the burette used for BET analysis was cleaned, dried and evacuated at 120 °C for 1 h to remove any impurities and moisture present in the burette. After determining the weight of the empty degassed burette, the sample was charged into the burette and evacuated at 200 °C for 12 h to ensure complete removal of any moisture or volatile content present in the solid samples. After degassing the weight of the sample was determined by subtracting the weight of empty burette. Nitrogen ( $\text{N}_2$ ) gas adsorption and desorption isotherms of the samples were collected at a relative pressure of (0–1). The analyses were performed using “Surfer” software to determine the specific surface area and pore size of the catalyst. The BET surface areas of the base material ( $\text{SiO}_2$ ) and catalyst ( $\text{SiO}_2\text{-PPI}$ ) were determined to be 330  $\text{m}^2/\text{g}$  and 280

m<sup>2</sup>/g, respectively (Table 3.3). The decrease in the surface area of SiO<sub>2</sub>-PPI was caused by a reduction in the surface sites as a result of immobilisation of the organic phase over the parent silica. The average pore volumes and average pore diameters were also determined.

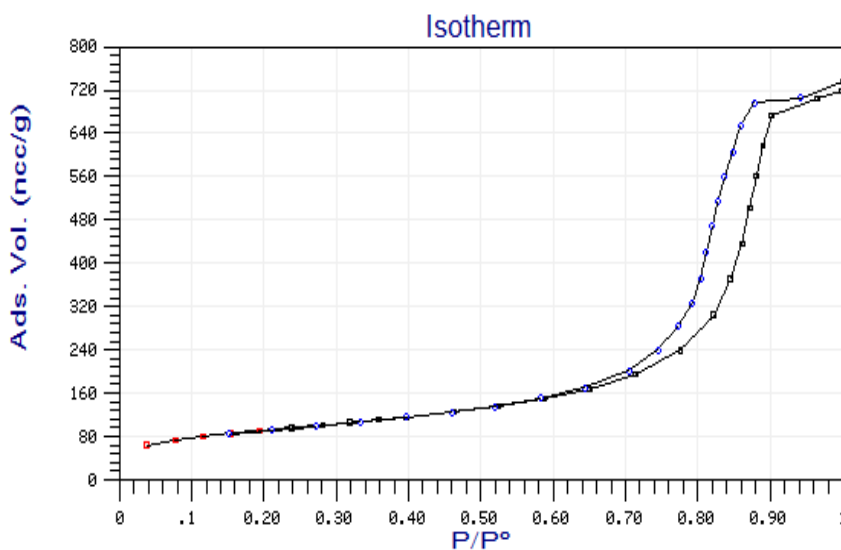


Figure 3.9 Nitrogen (N<sub>2</sub>) gas adsorption and desorption isotherms of silica-supported pyrrolidinopyridinium iodide (SiO<sub>2</sub>-PPI)

Sample	Specific surface area (m <sup>2</sup> /g)	Average pore volume (cm <sup>3</sup> /g)	Average pore diameter (nm)
Parent SiO <sub>2</sub>	330	1.04	11.8
SiO <sub>2</sub> -PPI	280	0.90	13.66

Table 3.3 Summary of BET analysis of the parent SiO<sub>2</sub> and SiO<sub>2</sub>-PPI catalyst.

### 3.5.3 Elemental analysis

The elemental analysis of solid catalyst was performed to determine the loading of active catalytic species over silica supporting material based on the nitrogen content for both fresh and recovered SiO<sub>2</sub>-PPI (Table 3.4). The decrease in the catalyst loading over recovered SiO<sub>2</sub>-PPI was probably as a result of leaching of the catalyst during the reaction and recycling steps.

Catalyst	N %	C %	mmol/g
Fresh SiO <sub>2</sub> -PPI	2.14	12.78	0.76
Recovered SiO <sub>2</sub> -PPI	1.90	11.23	0.67

Table 3.4 Elemental analysis (CN) of fresh and recovered SiO<sub>2</sub>-PPI samples showing catalyst loading over SiO<sub>2</sub>.

### 3.5.4 XRD analysis

Powder XRD patterns of catalyst were obtained for phase identification using a PANalytical diffractometer equipped with CuK<sub>α1</sub> X-ray radiation source. The XRD data were collected between scanning range  $2\theta = (2-70)^\circ$  (5.1.0 silicon plates) operated at 40 kV and 40 mA using a pixel detector. The powder X-ray diffraction patterns of both SiO<sub>2</sub>-C<sub>3</sub>H<sub>6</sub>-I and SiO<sub>2</sub>-PPI catalyst are shown in Figure 3.10. XRD patterns of both samples clearly indicate the uniform dispersion of the organic phase over the silica surface. Both patterns indicate the characteristic peak of the silica gel at 10-30° and no other diffraction peaks appeared (Song *et al.*, 2014).

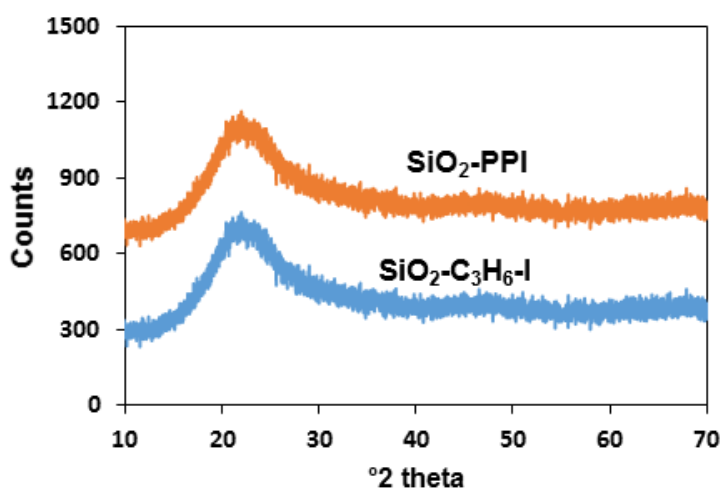


Figure 3.10 XRD patterns of the functionalised silica (SiO<sub>2</sub>-C<sub>3</sub>H<sub>6</sub>-I) and silica-supported pyrrolidinopyridinium iodide (SiO<sub>2</sub>-PPI) catalyst.

### 3.6 Homogeneous kinetics for CO<sub>2</sub> cycloaddition to epoxide

Series of experiments were carried out to determine the rate law to understand the kinetic parameters and ultimately to investigate the reaction mechanism involved in cyclic carbonate synthesis. The general rate equation of cyclic carbonate synthesis in the presence of homogeneous catalysts can be written as Eq (1), where [Epoxide], [CO<sub>2</sub>], [Catalyst] are the concentrations of epoxide, carbon dioxide and catalyst, respectively, and the superscripts a, b, c are the orders of reaction with respect to epoxide, CO<sub>2</sub> and catalyst. Literature precedent shows that cyclic carbonate formation via CO<sub>2</sub> cycloaddition to epoxides has a high negative heat of formation, therefore it can be assumed that there is no back reaction (North et al., 2011). Moreover, the concentration of CO<sub>2</sub> in the liquid phase remains constant throughout the reaction due to a continuous supply of CO<sub>2</sub>. Similarly, the concentration of the catalytic species also remains constant. Therefore, Eq (3.1) can be simplified to Eq (3.2), where  $k_{obs}$  is the observed pseudo-first-order rate constant and can be given as Eq (3.3). Taking the natural logarithm of both sides of Eq (3.3) gives Eq (3.4), which can be used to determine the orders of reaction by changing the concentration of catalyst and CO<sub>2</sub>. By assuming the pseudo-first-order dependence of the reaction rate on epoxide concentration (a=1), the differential rate law gives Eq (3.5). Integrating both sides of Eq (3.5) gives Eq (3.6), which can be used to determine the observed pseudo-first-order rate constant for epoxide conversion.

$$\text{Rate} = k [\text{Epoxide}]^a [\text{CO}_2]^b [\text{Catalyst}]^c \quad (3.1)$$

$$\text{Rate} = k_{obs} [\text{epoxide}]^a \quad (3.2)$$

Where

$$k_{obs} = k [\text{CO}_2]^b [\text{catalyst}]^c \quad (3.3)$$

$$\ln k_{obs} = \ln k + b \ln[\text{CO}_2] + c \ln[\text{Catalyst}] \quad (3.4)$$

$$\text{Rate} = -\frac{d[\text{epoxide}]}{dt} = k_{obs} [\text{epoxide}]^1 \quad (3.5)$$

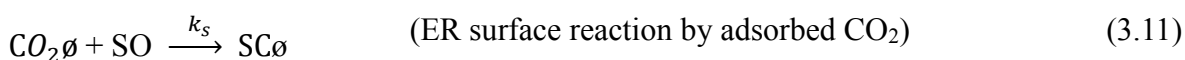
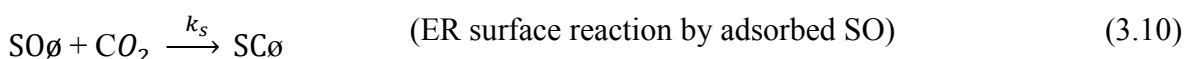
$$-\ln [\text{epoxide}] = k_{obs} \cdot t \quad (3.6)$$

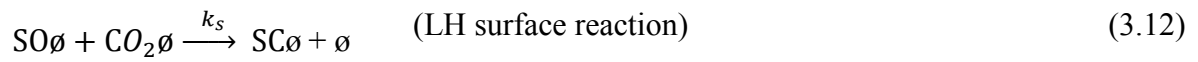
### 3.7 Heterogeneous kinetics for CO<sub>2</sub> cycloaddition to epoxides

Kinetic experiments for SC formation by CO<sub>2</sub> cycloaddition to SO in the presence of SiO<sub>2</sub>-PPI as heterogeneous catalyst were carried out in the high-pressure semi-batch reactor by following the same procedure as described above for homogeneous catalysis. The experimental data were correlated with Pseudo-homogeneous (PH), Eley-Rideal (ER) and Langmuir-Hinshelwood (LH) heterogeneous kinetic models. The PH model assumes that no diffusion, adsorptions and desorption of the reactants and products occur, such that the mechanism is determined only by the chemical reactions in the bulk fluid as shown in Eq (3.7), where  $k_s$  is the rate constant for the surface reaction.

$$r_{SO} = k_s[SO][CO_2] \quad (3.7)$$

However, in heterogeneous catalysis, the observed reaction rate is usually also a function of diffusion, adsorptions and desorption of the reacting species and products (Yadav and Mehta, 1994; Belfiore, 2003). Therefore, heterogeneously catalysed reactions generally proceed by either ER or LH mechanisms. The ER mechanism assumes that the reactions proceed via chemisorption of one of the reactants and subsequent reaction of the adsorbed species with another reactant in the bulk fluid phase. Whereas, the LH kinetic mechanism assumes that all the reacting species are adsorbed onto vacant active sites of the catalysts, therefore, the reaction rate depends upon adsorption-desorption equilibria of the reactants, followed by surface reactions of the adsorbed reactant species (Endalew *et al.*, 2011). The surface reactions between chemisorbed reactant molecules result in chemisorbed products that diffuse from the catalyst sites into the bulk liquid phase. For the conversion of SO to SC, the SO and CO<sub>2</sub> could be the adsorbed species on the catalyst surface. The reaction scheme for the heterogeneous catalysis for cycloaddition reaction of SO and CO<sub>2</sub> to form SC is given in Eq (3.8–3.13), where  $\emptyset$  is the vacant catalyst site,  $K_{SO}$ ,  $K_{CO_2}$  and  $K_{SC}$  are the adsorption-desorption equilibrium constants for SO, CO<sub>2</sub>, and SC respectively.





The ER kinetic model for the reactions of SO with CO<sub>2</sub> can be written as shown in Eq (3.14), assuming that either SO or CO<sub>2</sub> could adsorb on the catalyst surface, and that surface reaction is the rate-determining step. The total surface coverage of the catalyst sites using equilibrium state approximation (at equilibrium adsorption-desorption) is given by the balance of the active sites in Eq (3.15), where  $\theta_j$  is the fraction of the catalytic sites that remain unoccupied. Therefore, the surface coverages of SO, CO<sub>2</sub> and SC are shown in Eq (3.16–3.18), and the surface reaction for the ER model could be re-written as Eq (3.19). The rate equation for the surface reaction in Eq (3.23) was obtained by replacing  $\theta_j$  using the Langmuir adsorption isotherms in Eq (3.20–3.22), for the heterogeneous catalysis of the reactions of SO with CO<sub>2</sub>.

$$r_{SO} = k_s[CO_2][SO\theta] + k_s[CO_2\theta][SO] \quad (3.14)$$

$$\theta_j = 1 - SO\theta - CO_2\theta - SC\theta \quad (3.15)$$

$$[SO\theta] = K_{SO}[SO]\theta_j \quad (3.16)$$

$$[CO_2\theta] = K_{CO_2}[CO_2]\theta_j \quad (3.17)$$

$$[SC\theta] = K_{SC}[SC]\theta_j \quad (3.18)$$

$$r_{SO} = k_s K_{SO}[CO_2][SO]\theta_j + k_s K_{CO_2}[SO][CO_2]\theta_j \quad (3.19)$$

$$[SO\theta] = \frac{K_{SO}[SO]}{(1 + K_{SO}[SO] + K_{CO_2}[CO_2] + K_{SC}[SC])} \quad (3.20)$$

$$[CO_2\theta] = \frac{K_{CO_2}[CO_2]}{(1 + K_{SO}[SO] + K_{CO_2}[CO_2] + K_{SC}[SC])} \quad (3.21)$$

$$[SC\theta] = \frac{K_{SC}[SC]}{(1 + K_{SO}[SO] + K_{CO_2}[CO_2] + K_{SC}[SC])} \quad (3.22)$$

$$r_{SO} = \frac{k_s K_{SO}[SO][CO_2]}{(1 + K_{SO}[SO] + K_{CO_2}[CO_2] + K_{SC}[SC])} + \frac{k_s K_{CO_2}[SO][CO_2]}{(1 + K_{SO}[SO] + K_{CO_2}[CO_2] + K_{SC}[SC])} \quad (3.23)$$

Therefore,

$$r_{SO} = \frac{k_s[SO][CO_2]}{(1 + K_{SO}[SO] + K_{CO_2}[CO_2] + K_{SC}[SC])} (K_{SO} + K_{CO_2}) \quad (3.24)$$

The ER kinetic model in Eq (3.24) can be simplified to Eq (3.25) if there is only selective adsorption of SO on the catalyst surface and to Eq (3.26) when only CO<sub>2</sub> adsorbs on the catalytic surface.

$$r_{SO} = \frac{k_s[SO][CO_2]}{(1 + K_{SO}[SO] + K_{SC}[SC])} (K_{SO}) \quad (3.25)$$

$$r_{SO} = \frac{k_s[SO][CO_2]}{(1 + K_{CO_2}[CO_2] + K_{SC}[SC])} (K_{CO_2}) \quad (3.26)$$

For the LH model, the rate expression for the reactions of SO with CO<sub>2</sub> is shown in Eq (3.27), when mass transport and diffusion are very fast compared to the surface reaction of the chemisorbed species (surface reaction as the rate-determining step). Using the Langmuir adsorption isotherms, the LH model was simplified to Eq (3.28):

$$r_{SO} = k_s[SO\emptyset][CO_2\emptyset] \quad (3.27)$$

$$r_{SO} = \frac{k_s K_{SO} K_{CO_2} [SO][CO_2]}{(1 + K_{SO}[SO] + K_{CO_2}[CO_2] + K_{SC}[SC])^2} \quad (3.28)$$

The reaction kinetic models developed based on a pseudo-homogeneous Eq (3.27), ER Eq (3.24–3.26), and LH Eq (3.28) were fitted to the experimental data with MATLAB using ODE45 solver (Runge-Kutta method). The concentrations of CO<sub>2</sub> were calculated from  $[CO_2] = P/ZRT$ , where P is pressure (kPa), R is universal gas constant (8.3145 L.kPa.mol<sup>-1</sup>.K<sup>-1</sup>), T is temperature (K), and Z is the compressibility of CO<sub>2</sub> at the set T and P (Z ~ 0.98). The reaction rate constants that minimised the sum of squared errors (SSE) between the model prediction and the experimental data were obtained.

### 3.8 Determination of kinetic and thermodynamic activation parameters

The temperature dependence of the reaction was studied to determine the activation and thermodynamic parameters of cyclic carbonate synthesis by CO<sub>2</sub> cycloaddition to epoxide. The E<sub>a</sub> for cyclic carbonate formation was determined based on the Arrhenius equation Eq (3.29). The E<sub>a</sub> was calculated from the gradient of the graph between ln (k<sub>obs</sub>) and reciprocal

of absolute temperature ( $1/T$ ) Eq (3.30), where  $k_{obs}$  is the observed pseudo first-order rate constant ( $\text{min}^{-1}$ ),  $A$  is the pre-exponential factor ( $\text{min}^{-1}$ ),  $R$  is the ideal gas law constant ( $8.314 \text{ J mol}^{-1} \text{ K}^{-1}$ ),  $T$  is absolute temperature (K). Similarly, the thermodynamic activation parameters such as enthalpy of activation ( $\Delta H^\ddagger$ ), the entropy of activation ( $\Delta S^\ddagger$ ) and Gibbs free energy of activation ( $\Delta G^\ddagger$ ) were determined from Eyring equation (Eq 3.31), and the  $\Delta H^\ddagger$  and  $\Delta S^\ddagger$  were determined from gradient ( $-\frac{\Delta H^\ddagger}{RT}$ ) and y-intercept ( $\frac{\Delta S^\ddagger}{R} + \ln \frac{k_B}{h}$ ), respectively Eq (3.32). Moreover,  $\Delta G^\ddagger$  was determined from the fundamental thermodynamic equation Eq (3.33) for all temperatures.

$$k_{obs} = A \cdot \exp\left(-\frac{E_a}{R.T}\right) \quad (3.29)$$

$$\ln k_{obs} = \ln A - \left(\frac{E_a}{R.T}\right) \quad (3.30)$$

$$k = \frac{k_B T}{h} \exp\left(-\frac{\Delta G^\ddagger}{RT}\right) = \frac{k_B T}{h} \exp\left(-\frac{\Delta H^\ddagger}{RT} + \frac{\Delta S^\ddagger}{R}\right) \quad (3.31)$$

$$\ln\left(\frac{k}{T}\right) = -\frac{\Delta H^\ddagger}{RT} + \frac{\Delta S^\ddagger}{R} + \ln\left(\frac{k_B}{h}\right) \quad (3.32)$$

$$\Delta G^\ddagger = \Delta H^\ddagger - T\Delta S^\ddagger \quad (3.33)$$

Where

$R$  = Universal gas constant ( $8.314 \text{ J mol}^{-1} \text{ K}^{-1}$ )

$h$  = Planck's constant ( $6.62608 \times 10^{-34} \text{ J s}$ )

$k_B$  = Boltzmann constant ( $1.38065 \times 10^{-23} \text{ J K}^{-1}$ )

## 3.9 Analytical techniques

### 3.9.1 FTIR spectroscopy

For kinetic study experiments, the progress of the reaction was monitored using ATR-FTIR spectroscopy, using a Mettler Toledo React IR 4000 equipped with a DiComp diamond probe (K6 conduit 16 mm probe). The spectra of the product samples were collected over the range of 4000 to 650  $\text{cm}^{-1}$ . The instrument was initialized by collecting 256-scans background spectra for air and water vapours before collecting the spectra of the product samples. The analysis was performed using iC IR<sup>TM</sup> 4.2.26 software. For SC synthesis, a new peak appears at 1800  $\text{cm}^{-1}$  due to stretching vibration of C=O corresponds to carbonyl stretch of SC and the intensity of epoxide (SO) peak (C–O) at 876  $\text{cm}^{-1}$  starts decreasing (Figure 3.12). Similarly, the increase in the intensities of peaks at 1065 and 1159  $\text{cm}^{-1}$  correspond to asymmetric  $\nu$  (C–O) stretching vibrations of cyclic carbonate (Jutz *et al.*, 2008). There were no other new peaks in the spectra that would indicate side reactions, and the rate of the epoxy group disappearance was directly proportional to the rate of cyclic carbonate formation (Clegg *et al.*, 2010b). Therefore, the progress of the reaction was monitored by following the decrease in the intensity of epoxide peaks (C–O) at 876  $\text{cm}^{-1}$  for SO. To determine the conversion of epoxide to cyclic carbonate, the calibration curves were obtained by collecting the areas of epoxide peak for different concentrations of SO (Table 3.5, Figure 3.14 a). Similarly, the progress of the limonene carbonate (LC) synthesis from limonene oxide (LO) and  $\text{CO}_2$  was monitored by following the decrease in the intensity of epoxide peak at 841  $\text{cm}^{-1}$  (Figure 3.13). A calibration curve has been drawn by collecting the area of epoxide peak at 841  $\text{cm}^{-1}$  (Table 3.6, Figure 3.14 b).

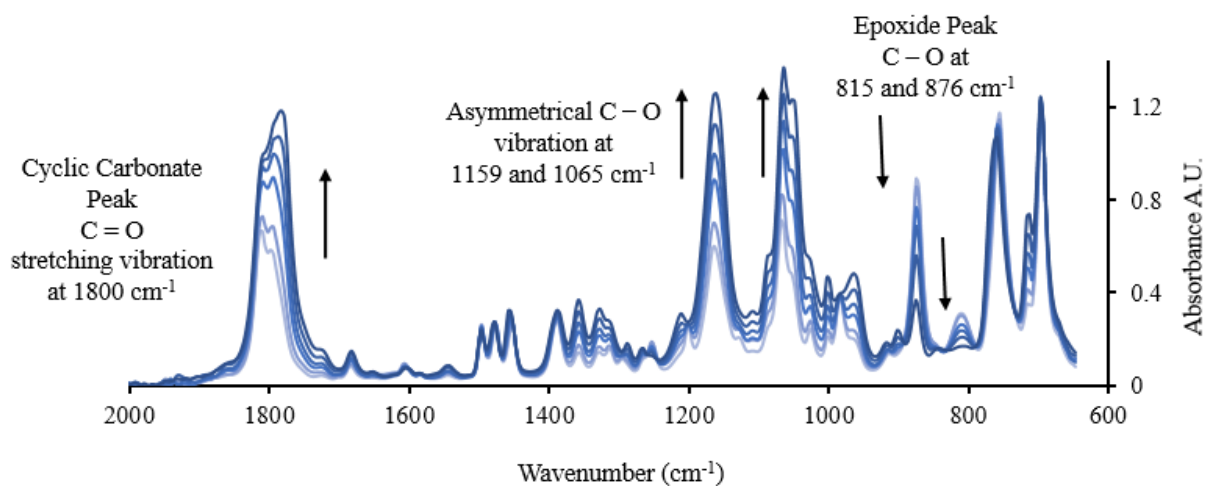


Figure 3.11 FTIR spectra of styrene carbonate (SC) synthesis by CO<sub>2</sub> cycloaddition to styrene oxide (SO).

[SO] M	FTIR epoxide peak area at 876 cm <sup>-1</sup>
0	0
0.5	0.78
1	1.97
1.5	2.82
2	3.75
2.5	4.60
3	5.52
3.5	6.12
4	6.85
4.5	7.65
5	8.41

Table 3.5 Summary of FTIR epoxide peak intensity data for calibration curve using different concentrations of SO (0.5–5) M in PC as a solvent.

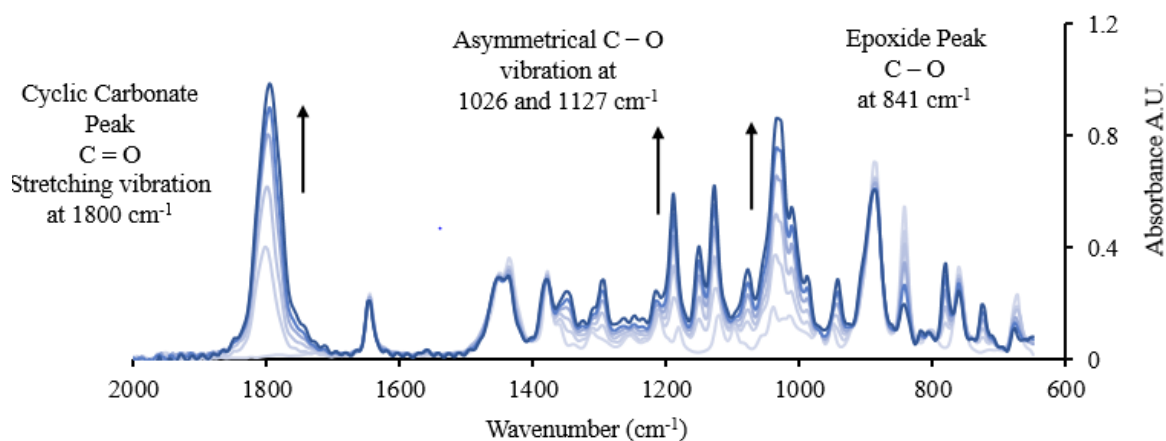


Figure 3.12 FTIR spectra of limonene carbonate (LC) synthesis by CO<sub>2</sub> cycloaddition to limonene oxide (LO).

[LO] M	FTIR epoxide peak area at 841 cm <sup>-1</sup>
0.5	0
0.5	0.58
1	0.93
1.5	1.51
2	2.13
2.5	2.62
3	3.34
3.5	3.75
4	4.17

Table 3.6 Summary of FTIR epoxide peak intensity data for the calibration curve using different concentrations of LO (0.5–4.5) M in PC as a solvent.

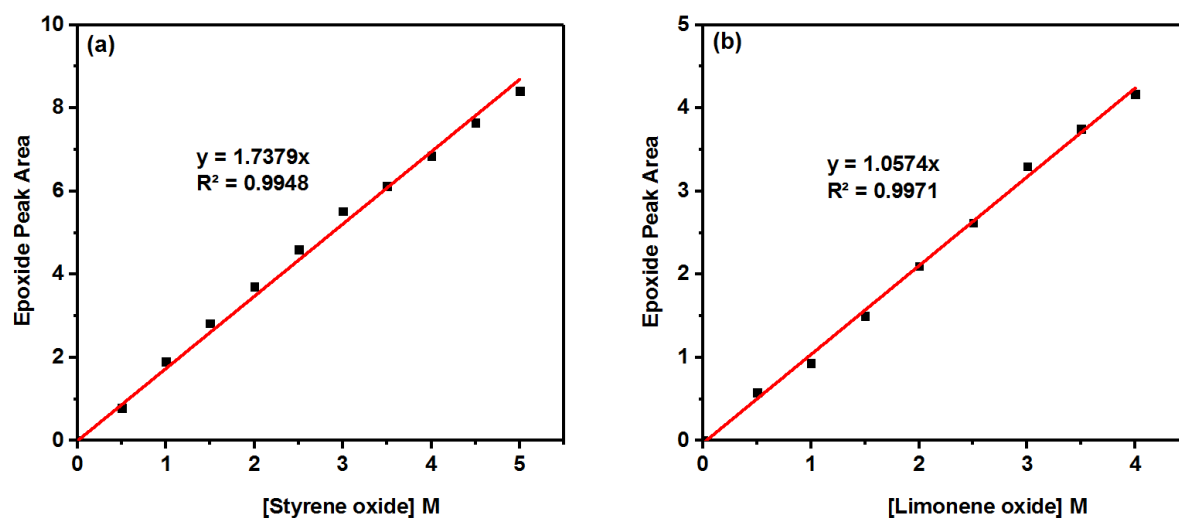


Figure 3.13 FTIR calibration curves for (a) Styrene oxide (SO) peak area at  $876\text{ cm}^{-1}$  against [SO] M (b) Limonene oxide (LO) peak area at  $841\text{ cm}^{-1}$  against [LO] M.

### 3.9.2 Gas chromatography (GC)

Quantitative analysis of cyclic carbonate synthesis by  $\text{CO}_2$  cycloaddition to epoxides was performed using gas chromatography (GC) with naphthalene as an internal standard. The equipment used was an Agilent HP 6890 gas chromatography equipped with a flame ionization detector (FID) and helium as carrier gas. The injection temperature for the GC was  $250\text{ }^\circ\text{C}$ , while the FID temperature was set at  $260\text{ }^\circ\text{C}$ . The appearance of the peak at residence time of 5.80 min is probably due to the sample decomposition of SO having boiling point (known to be thermally unstable)  $194\text{ }^\circ\text{C}$ . To analyse the samples of  $\text{CO}_2$  cycloaddition to SO, the temperature programme was: initial temperature  $60\text{ }^\circ\text{C}$  held for 2 min, then ramped at heating rates of  $15\text{ }^\circ\text{C}/\text{min}$  to  $260\text{ }^\circ\text{C}$  final temperature and held for 5 min. The peaks of SO and naphthalene (internal standard) appeared at residence time 6.08 and 7.80 min (Figure 3.15). The peaks at residence time 1.59 and 1.86 min correspond to the solvent (chloroform) used to prepare the samples. The GC peak of the SC product appeared at 11.30 min.

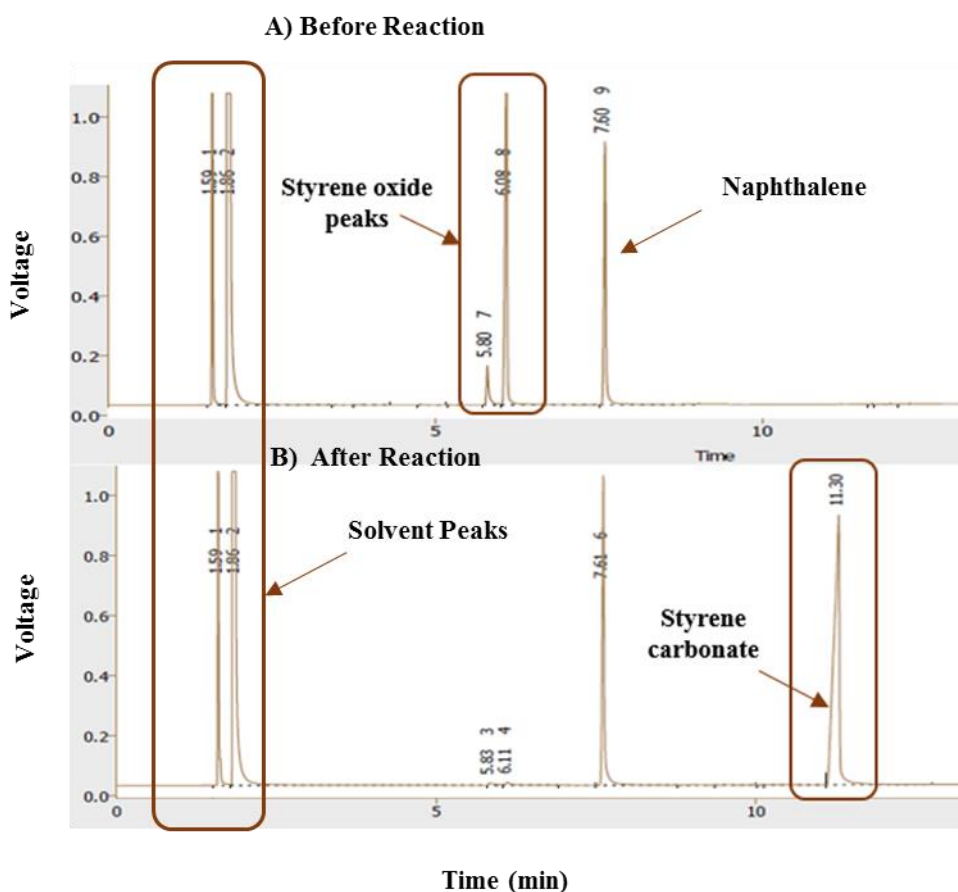


Figure 3.14 Example GC spectra of SO and SC using naphthalene (internal standard) before and after the reaction.

Similarly, to quantify the conversion and yield of the LO prepared by the stereoselective epoxidation of limonene, a different GC method was used by setting the conditions such as initial temperature 80 °C held, 4 min, followed by ramped heating at the rate of 15 °C/min to 260 °C final temperature and held for 2 min. The peaks of LO appeared at residence time 6.94 and 7.12 min, corresponding to *cis* and *trans*-isomers, respectively, and the unreacted limonene peak appeared at 5.17 min (Figure 3.16). The calibration curves for the determination of the conversion and the yield of the epoxides were prepared by collecting the areas of epoxide and naphthalene peaks for different concentrations (Tables 3.7 and 3.8, Figure 3.17).

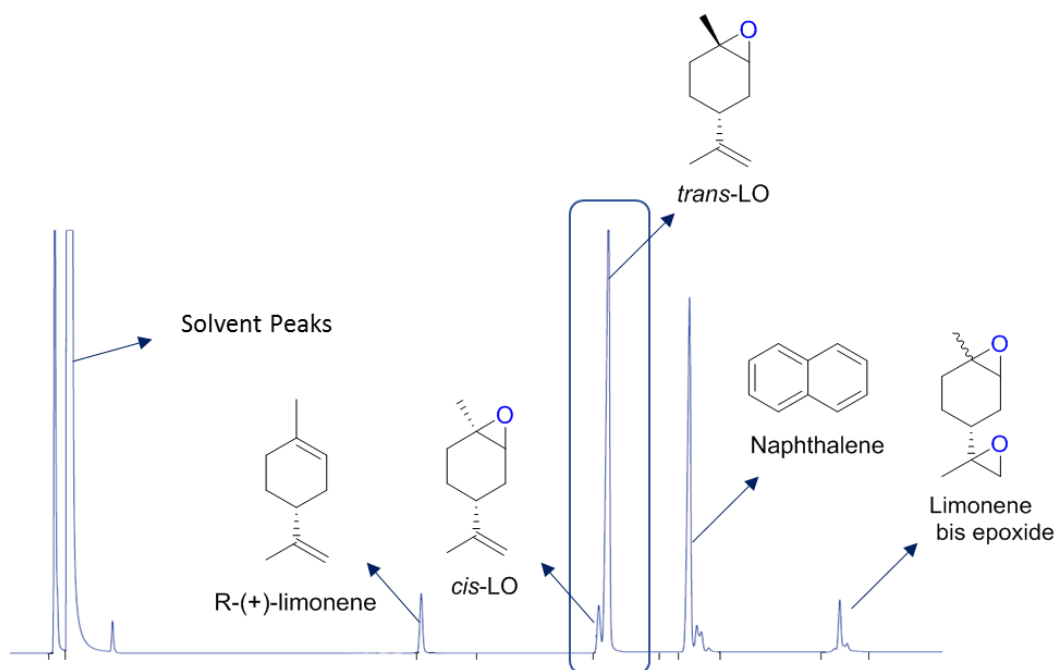


Figure 3.15 GC spectra of LO obtained as a result of stereoselective epoxidation of (*R*)-(+)-limonene.

Run	[SO] (C <sub>x</sub> ) mg/ml	Internal standard Conc. (C <sub>is</sub> ) mg/ml	C <sub>x</sub> /C <sub>is</sub>	SO Peak area (A <sub>x</sub> )	Internal standard peak area (A <sub>is</sub> )	A <sub>x</sub> /A <sub>is</sub>
1	2.5	5	0.5	886.5	2558.6	0.35
2	5	5	1	1896.8	2552.8	0.74
3	7.5	5	1.5	3313.8	2886.8	1.15
4	10	5	2	3953.9	2550.1	1.55

Table 3.7 Summary of GC peak areas against different concentrations of SO using chloroform as a solvent.

Run	LO Conc. (C <sub>x</sub> ) mg/ml	Internal standard Conc. (C <sub>is</sub> ) mg/ml	C <sub>x</sub> /C <sub>is</sub>	LO Peak area (A <sub>x</sub> )	Internal standard Peak area (A <sub>is</sub> )	A <sub>x</sub> /A <sub>is</sub>
1	2.5	5	0.50	494.6	1438.3	0.34
2	5	5	1.00	682.6	1382.7	0.49
3	10	5	2	868.6	1231.9	0.71
4	20	5	4	1252.1	1017.1	1.23
5	40	5	8	1657.8	753.8	2.13

Table 3.8 Summary of GC peak areas against different concentrations of limonene oxide (LO) using chloroform as a solvent.

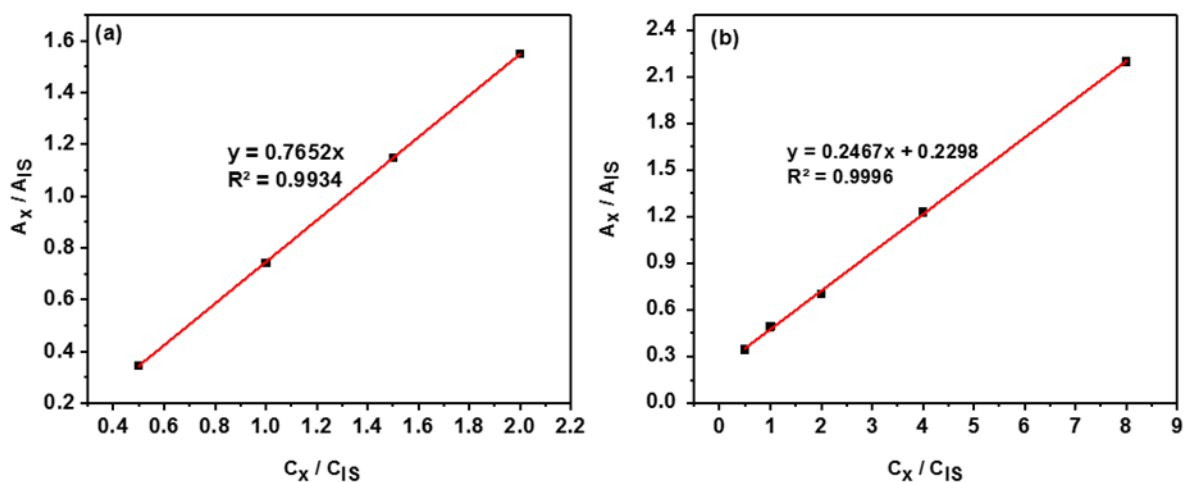


Figure 3.16 GC calibration curves for different concentrations of (a) Styrene oxide (SO) (b) Limonene oxide (LO).

### 3.9.3 $^1\text{H}$ NMR spectroscopy

The progress of the reaction for LC synthesis from LO and  $\text{CO}_2$  was also measured using  $^1\text{H}$ -NMR spectroscopy. Nuclear magnetic resonance spectra ( $^1\text{H}$ -NMR) were recorded on a Bruker Avance spectrometer using chloroform-d ( $\text{CDCl}_3$ ) as a solvent operating at 500 MHz. Here, the appearance of new signals at 4.4 ppm corresponds to cyclic carbonates as a result of the decrease in intensity of signals at 3 ppm corresponds to the epoxide group. The signals between 1 and 2.5 ppm correspond to methyl and methylene protons of LO and LC. The triplet at 3.4 ppm is because of the methylene protons of quaternary alkylammonium halides used as a catalyst. The conversion of epoxide (LO) to cyclic carbonate (LC) and yield of the product can be determined by recording the integrated intensities of epoxide peaks using naphthalene as an internal standard (Figure 3.18). The data was analysed using MestReNova software.

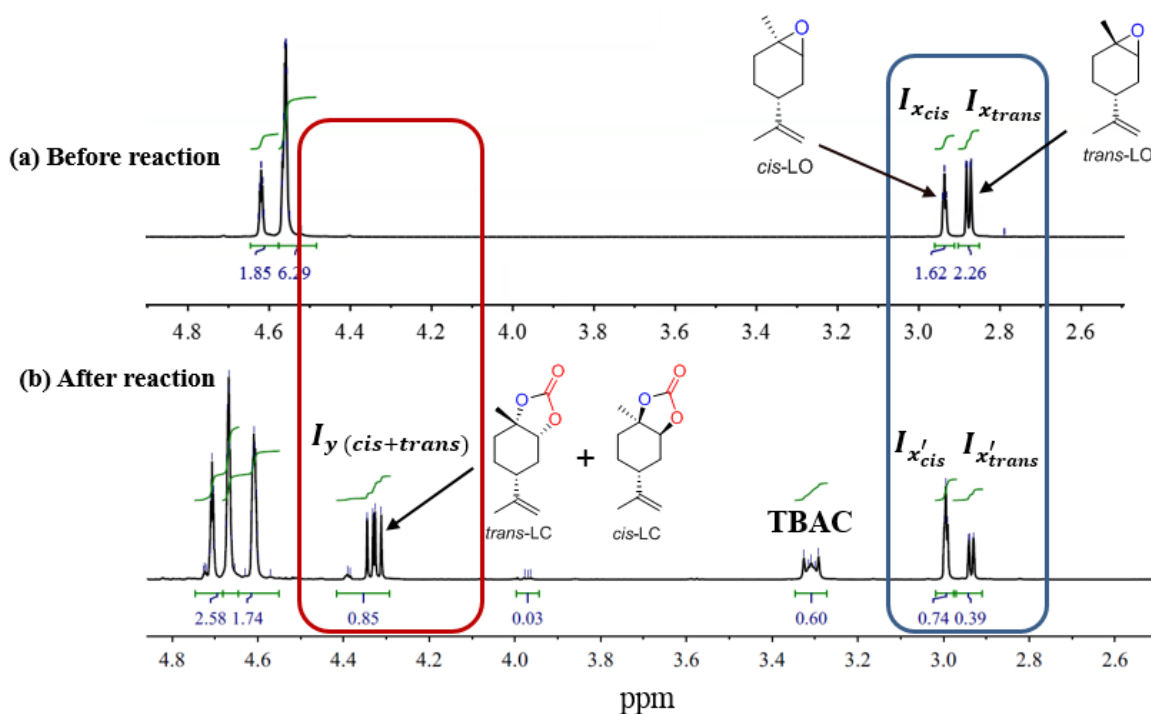


Figure 3.17  $^1\text{H}$ -NMR spectra to determine the conversion and yield of limonene carbonate (LC).

The conversion and yield of LC were determined from the intensities (I) of *cis* and *trans*-isomers before and after reaction using TBAC as a catalyst.

$$\text{Conversion of cis LO (\%)} = \frac{(I_{x \text{ cis}} - I_{x' \text{ cis}})}{(I_{x \text{ cis}})} \times 100$$

$$\text{Conversion of trans LO (\%)} = \frac{(I_{x \text{ trans}} - I_{x' \text{ trans}})}{(I_{x \text{ trans}})} \times 100$$

$$\text{Conversion of cis + trans LO (\%)} = \frac{(I_{x \text{ cis}} + I_{x \text{ trans}}) - (I_{x' \text{ cis}} + I_{x' \text{ trans}})}{(I_{x \text{ cis}} + I_{x \text{ trans}})} \times 100$$

$$\text{Yield of LC (cis + trans) (\%)} = \frac{(I_{y \text{ (cis+trans)}})}{(I_{x \text{ cis}} + I_{x \text{ trans}})} \times 100$$

Where:

$I_{x \text{ cis}}, I_{x \text{ trans}}$  = Intensities of *cis* and *trans*-LO before the reaction.

$I_{x' \text{ cis}}, I_{x' \text{ trans}}$  = Intensities of *cis* and *trans*-LO after the reaction.

$I_{y \text{ (cis+trans)}}$  = Intensity of *cis* and *trans*-LO after the reaction.

## Chapter 4 Bio-based cyclic carbonates synthesis from limonene oxide (LO) and CO<sub>2</sub> catalysed by tetrabutylammonium chloride (TBAC).

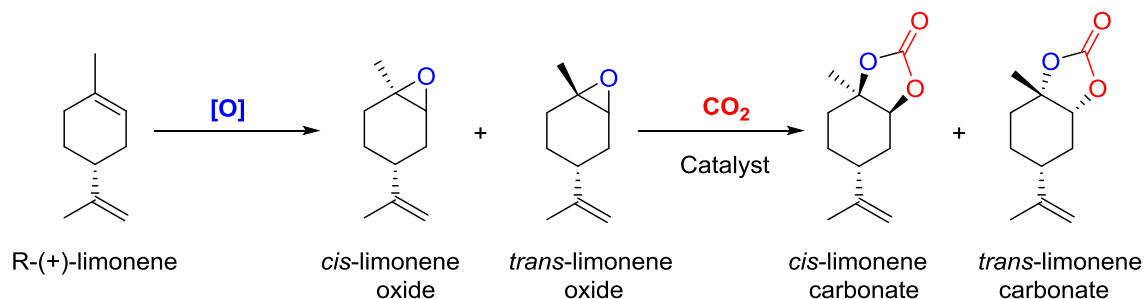
### 4.1 Introduction

This chapter discusses the results for the synthesis of cyclic carbonates from bio-based limonene oxide (LO) and CO<sub>2</sub> in the presence of tetrabutylammonium chloride (TBAC) as a homogeneous catalyst. The experiments were carried out in a high-pressure stainless-steel semi-batch reactor. The effect of reaction parameters, such as temperature, CO<sub>2</sub> pressure, catalyst loading and residence time are also discussed. Moreover, a detailed study of reaction kinetics was carried out to determine the corresponding kinetic values ( $k$  and  $E_a$ ) and thermodynamic activation parameters ( $\Delta H^\ddagger$ ,  $\Delta S^\ddagger$  and  $\Delta G^\ddagger$ ). As a result of the kinetic analysis, a reaction mechanism was proposed which is in agreement with the generally accepted mechanism for cyclic carbonate synthesis and highlights the importance of small nucleophiles when such reactions are performed with highly substituted epoxides.

### 4.2 Effect of halide anion on CO<sub>2</sub> cycloaddition to LO

Preliminary studies of cyclic carbonate synthesis were carried out using commercial LO (a mixture of *cis*- and *trans*-isomers 40:60). To study the effect of halide anions activity, the experiments were carried out using different tetrabutylammonium halides (TBAX). The reaction carried out using TBAC has exhibited the highest conversion among the other catalysts i.e. 71% conversion at 120 °C, 40 bar  $p$  (CO<sub>2</sub>) after 20 h (Table 4.1). The order of halide anions activities was found to be TBAC > TBAB > TBAI > TBAF. Generally, the catalytic activity of halide anions for CO<sub>2</sub> cycloaddition to terminal epoxides was determined by the balance of their nucleophilicity ( $F^- > Cl^- > Br^- > I^-$ ) and leaving group ability ( $I^- > Br^- > Cl^- > F^-$ ) (Clegg *et al.*, 2010a; Langanke *et al.*, 2013). However, in the case of CO<sub>2</sub> cycloaddition to internal epoxides, the steric hindrance seems to be an important factor. Therefore,  $Cl^-$ , having a smaller size than  $Br^-$  and  $I^-$  and a better leaving group ability than  $F^-$  exhibits greater catalytic activity. Recently, a similar order of halide anion activity for CO<sub>2</sub> cycloaddition to di-substituted epoxides catalysed by TBAX was also reported (Hirose *et al.*, 2018). In all cases, the reactivity of *cis*-LO was found to be lower than *trans*-LO due to its higher energy transition state when reacted with nucleophilic amines (Steiner *et al.*, 2002).

Moreover, the reaction was also carried out using metallic salts e.g. (LiBr, LiCl, ZnBr<sub>2</sub>, and ZnCl<sub>2</sub>) in combination with TBAX, with the aim to enhance the catalytic activity. However, no enhancement in reaction rate was observed, presumably due to poor solubility of the metallic salts in the reaction mixture.



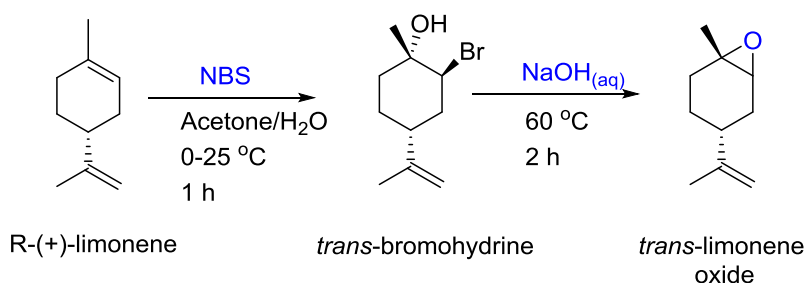
Scheme 4.1 Epoxidation of (*R*)-(+)-limonene and subsequent limonene carbonate (LC) synthesis via CO<sub>2</sub> cycloaddition to limonene oxide (LO).

Entry	Catalyst	Conversion (%)			Yield (%)
		LO ( <i>cis</i> + <i>trans</i> )	<i>trans</i> -LO	<i>cis</i> -LO	LC ( <i>cis</i> + <i>trans</i> )
1	TBAC	71	55	16	70
2	TBAB	55	40	15	52
3	TBAI	18	14	4	12
4	TBAF	12	9	3	8

Table 4.1 Catalytic activities of TBAX for LC synthesis by CO<sub>2</sub> cycloaddition to commercial LO, (reaction conditions: 120 °C, *p* (CO<sub>2</sub>) = 40 bar, 3 mol% TBAX, 20 h).

### 4.3 Stereoselective epoxidation of (*R*)-(+)-limonene

Due to the low reactivity of *cis*-LO, the use of commercial LO as a substrate is not economically feasible, as it contains approximately 40% less reactive isomer. Therefore, a stereoselective method of (*R*)-(+)-limonene epoxidation was performed with the aim to achieve a high yield of *trans*-LO (Hauenstein *et al.*, 2016). Briefly, the method involves bromination of (*R*)-(+)-limonene with *N*-bromosuccinimide (NBS) (Scheme 4.2). The reaction was performed in an aqueous solution of acetone at (0–25) °C for 1 h. This results in the formation of *trans*-bromohydrin which was readily epoxidised into subsequent *trans*-LO using aqueous sodium hydroxide (NaOH) solution at 60 °C for 2 h. The conversion and (*R*)-(+)-limonene and yield of *cis* and *trans*-LO were determined by gas chromatography (GC) using naphthalene as an internal standard. As a result, 87% yield of *trans*-LO was achieved.



Scheme 4.2 Stereoselective epoxidation of (*R*)-(+)-limonene using *N*-bromosuccinimide.

### 4.4 Effect of reaction parameters on CO<sub>2</sub> cycloaddition to LO

At ambient conditions, i.e. 25 °C and 1 bar *p* (CO<sub>2</sub>), using 3 mol% TBAC, the extent of reaction was negligible due to the steric hindrance of tri-substituted LO. Literature precedent shows that cycloaddition of CO<sub>2</sub> to internal epoxides generally requires more extreme reaction conditions (higher temperatures, pressures and catalyst loadings) than for terminal epoxides (Castro-Osma *et al.*, 2016). Moreover, the use of TBAX alone also requires more extreme reaction conditions, due to the lack of an acidic group in the catalyst system (Sun *et al.*, 2009). Therefore, the effect of temperature on CO<sub>2</sub> cycloaddition to LO was studied over the range of 100–140 °C at 40 bar *p* (CO<sub>2</sub>) using 6 mol% TBAC catalyst. As expected, the rate of the reaction increased with increasing temperature. The highest yield was 77%, obtained at 140 °C (Figure 4.1 a). Similarly, the effect of CO<sub>2</sub> pressure was studied over the range of (5–40) bar (Figure 4.1 b). The increase in pressure from (5–20) bar has a considerable effect on the product yield (18–38) %, due to increased CO<sub>2</sub> concentration in the

reaction mixture. However, on a further increase in pressure from (20–40) bar, the increase in the product yield did not increase significantly, and a 45% yield of the product was achieved at 40 bar  $p$  ( $\text{CO}_2$ ). Similar results have been reported for  $\text{CO}_2$  cycloaddition to epoxide, where the increase in  $\text{CO}_2$  pressure from (1–10) bar has a increasing effect on reaction kinetics as compared to (10–30) bar (Bähr and Mülhaupt, 2012). Clearly the rate is more dependent on mass transfer at lower pressures, and limited by some other phenomenon at higher pressures probably the inherent reaction rate. Moreover, the viscosity of cyclic carbonates is also higher than epoxide due to saturation of double bond with steric chemical groups, which causes a decrease in gas-liquid mass transfer (Campanella *et al.*, 2010).  $\text{CO}_2$  cycloaddition to epoxides reduces the gas-liquid mass-transfer coefficient as the product's viscosity is higher, whereas the solubility of  $\text{CO}_2$  was found to be independent of epoxide conversion (Zheng *et al.*, 2015; Cai *et al.*, 2017). Moreover, the decrease in the solubility of TBAX in the reaction mixture under supercritical  $\text{CO}_2$  conditions and hence the decrease in the reaction rate was also reported (Langanke *et al.*, 2013).

The effect of catalyst loading was also studied over the range of (1.5–7.5) mol% TBAC (Figure 4.1 c). From the results obtained, the yield of limonene carbonate (LC) increased linearly with the increase in TBAC concentration. The literature precedent shows that synthesis of cyclic carbonates by  $\text{CO}_2$  cycloaddition to terminal epoxides catalysed by metal-complexes in combination with TBAX generally requires a low concentration of TBAX (1.5–2.5) mol%. However, a higher concentration of TBAX up to 5 mol% was reported for  $\text{CO}_2$  cycloaddition to internal epoxides due to their challenging nature (Castro-Osma *et al.*, 2016). The effect of reaction time was also studied over (0–20) h (Figure 4.1 d). From the results obtained, the product yield increases with reaction time. Initially, the rate of reaction was higher and almost 80% yield of the product was achieved in the first 10 h of the reaction. However, a further increase in reaction time did not show a significant increase i.e. 86% yield of LC was achieved after 20 h, which is presumably due to the low reactivity of *cis*-isomers.

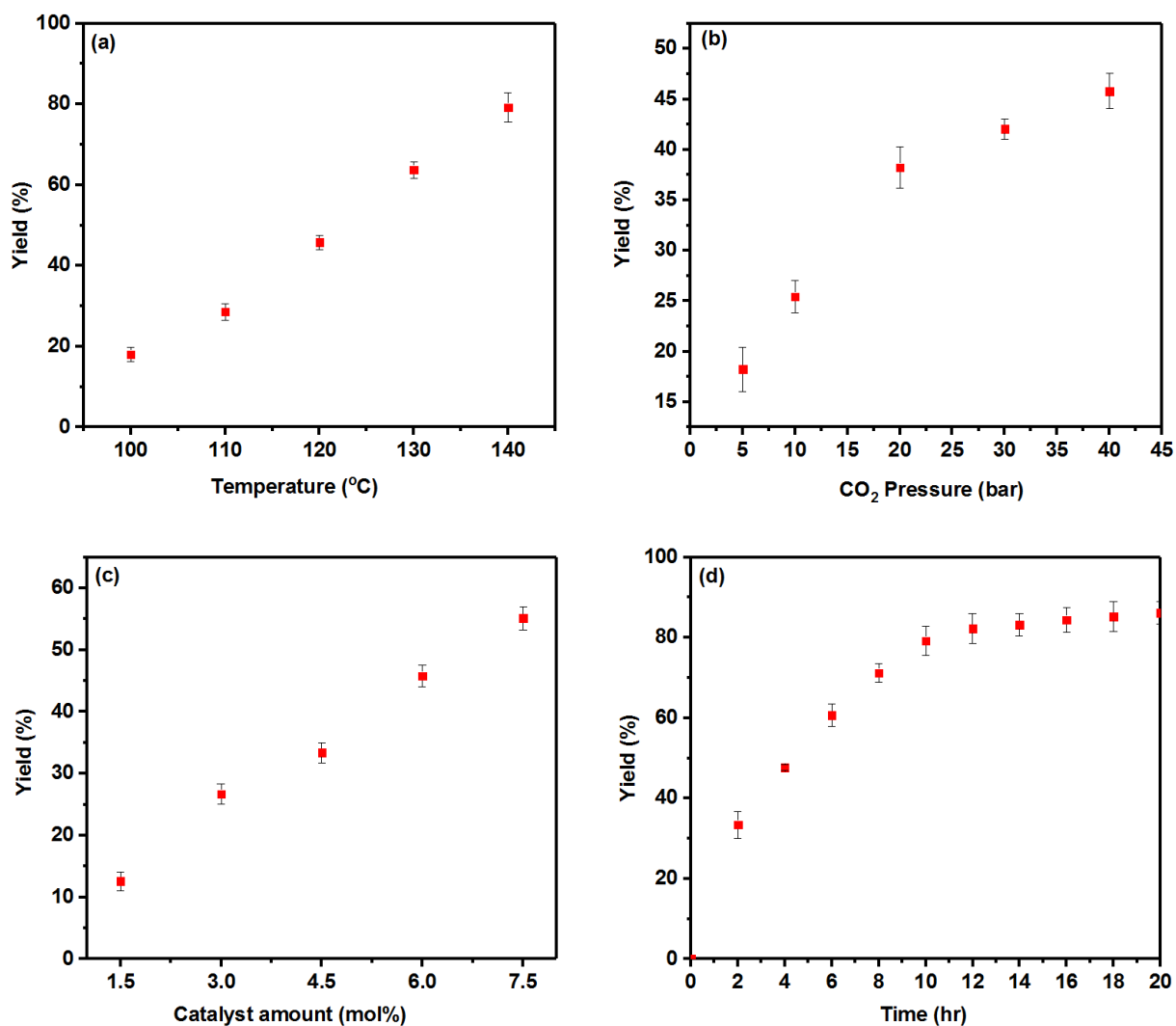


Figure 4.1 (a) Effect of temperature over the range of (100–140) °C at 40 bar  $p$  (CO<sub>2</sub>), 6 mol% TBAC and 10 h reaction time (b) Effect of  $p$  (CO<sub>2</sub>) over the range of (5–40) bar at 120 °C, 6 mol% TBAC and 10 h reaction time (c) Effect of catalyst loading over the range of (1.5–7.5) mol% at 120 °C, 40 bar  $p$  (CO<sub>2</sub>) and 10 h reaction time (d) Effect of reaction time over the range of (0–20) hr at 140 °C, 40 bar  $p$  (CO<sub>2</sub>) and 6 mol% TBAC.

#### 4.5 Selection of solvent

Initial experiments of catalyst screening and parametric study for CO<sub>2</sub> cycloaddition to LO were performed under solvent-free conditions. However, the use of a solvent was required to perform the kinetic experiments for the determination of reaction order with respect to epoxide. To find a suitable solvent, the reactions were performed in the presence of toluene, N,N-dimethylformamide (DMF), acetonitrile (CH<sub>3</sub>CN) and propylene carbonate (PC) (Figure 4.2). The results indicate a higher rate of reaction in the presence of polar aprotic solvents

such as DMF, PC, and CH<sub>3</sub>CN than toluene, a non-polar solvent (Table 4.2). Due to their high dielectric constants (>20) and large dipole moments, polar aprotic solvents have a high affinity for dissolution of charged species such as nucleophiles than non-polar solvents (Pazuki and Pahlavanzadeh, 2005). The use of polar aprotic solvents such as DMF and DMSO was also reported to enhance the activity of nucleophiles (Ritchie, 1972). The enhanced rate of reaction using DMF as solvent compared to other polar aprotic solvents was presumably due to nucleophilic activation of the CO<sub>2</sub> by an amide. This catalytic role of DMF in CO<sub>2</sub> cycloaddition to epoxides was also reported previously (Kozak *et al.*, 2013; Wang *et al.*, 2014b). However, PC is being increasingly used as a ‘greener’ alternative to traditionally used toxic, polar aprotic solvents such as DMF which is likely to be banned according to REACH regulations due to its impacts on human health (e.g. acute toxicity and reproductively toxicity) (Comerford *et al.*, 2015). Therefore, PC was chosen as the most advantageous ‘green’ reaction solvent to study the reaction kinetics.

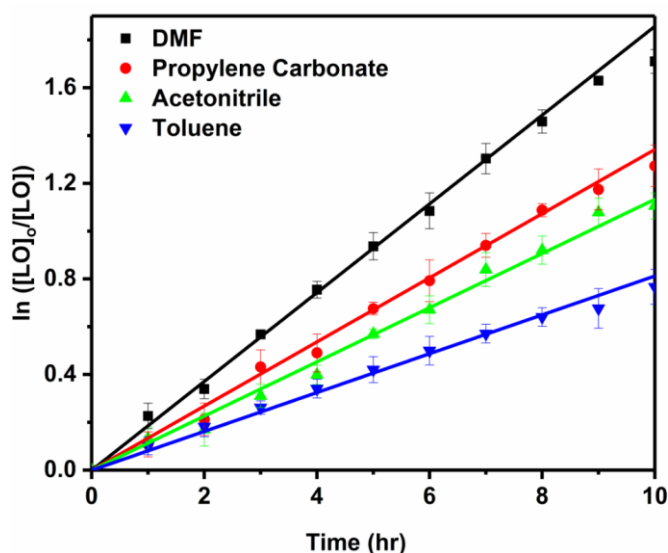


Figure 4.2 Plot of  $\ln ([LO]_0/[LO])$  against reaction time (hr) showing the change in the reaction rate using different solvents, (reaction conditions: 4.5 M LO, 120 °C, 40 bar  $p$  (CO<sub>2</sub>) and 6 mol% TBAC).

Solvent	Rate constant (sec <sup>-1</sup> ) × 10 <sup>-5</sup>
DMF	4.91 ± 0.28
Propylene carbonate	3.64 ± 0.17
Acetonitrile	3.26 ± 0.14
Toluene	2.09 ± 0.15

Table 4.2 Rate constants of limonene carbonate (LC) synthesis using different reaction solvents.

#### 4.6 Kinetics study of CO<sub>2</sub> cycloaddition to LO catalysed by TBAC

To investigate the reaction mechanism involved in CO<sub>2</sub> cycloaddition to LO and to determine the general rate law, a detailed study of reaction kinetics was carried out. A series of experiments were performed to determine the order of the reaction with respect to LO, CO<sub>2</sub> and TBAC by varying the concentration of the substance of interest and keeping all other reaction parameters at constant. The general form of the rate equation for CO<sub>2</sub> cycloaddition to LO catalysed by TBAC can be written as:

$$\text{rate} = \frac{-d[\text{LO}]}{dt} = k [\text{LO}]^a [\text{CO}_2]^b [\text{TBAC}]^c \quad (4.1)$$

Where a, b and c are the unknown orders of the reaction with respect to limonene oxide, carbon dioxide, and tetrabutylammonium chloride concentrations, respectively. All kinetic studies were performed in a semi-batch operation using a continuous supply of CO<sub>2</sub> during the reaction. Since CO<sub>2</sub> was present in large excess during the reaction, it can be assumed that the concentration of CO<sub>2</sub> remains unchanged throughout the reaction. Similarly, TBAC acts as a catalyst, therefore it can be assumed that catalyst concentration remains constant.

Therefore Eq (4.1) can be simplified as Eq (4.2):

$$\text{rate} = \frac{-d[\text{LO}]}{dt} = k_{\text{obs}} [\text{LO}]^a \quad (4.2)$$

Where

$$k_{\text{obs}} = k [\text{CO}_2]^b [\text{TBAC}]^c$$

Assuming the pseudo-first-order reaction and by integration of both sides, Eq (4.2) can be written as Eq (4.3):

$$-\ln [\text{LO}] = k_{\text{obs}} \cdot t \quad (4.3)$$

Here,  $k_{\text{obs}}$  is the pseudo-first-order observed rate constant.

Prior to detailed kinetic study, the experiments were also performed using both commercial and *trans*-enriched LO to compare the observed rate ( $k_{\text{obs}}$ ) for cyclic carbonate synthesis at two different reaction temperatures (i.e. 120 and 140 °C), whilst keeping the other reaction parameters constant i.e. 40 bar  $p$  ( $\text{CO}_2$ ) and 6 mol% TBAC (Figure 4.3 a, b). From the results obtained, the rate of reaction was found to be significantly higher (more than 3-fold) using *trans*-enriched LO than commercial LO mixture of *cis*- and *trans*-isomers. This increase in reaction rate was due to higher reactivity of *trans*-isomer in cycloaddition reaction compared to *cis*-isomer.

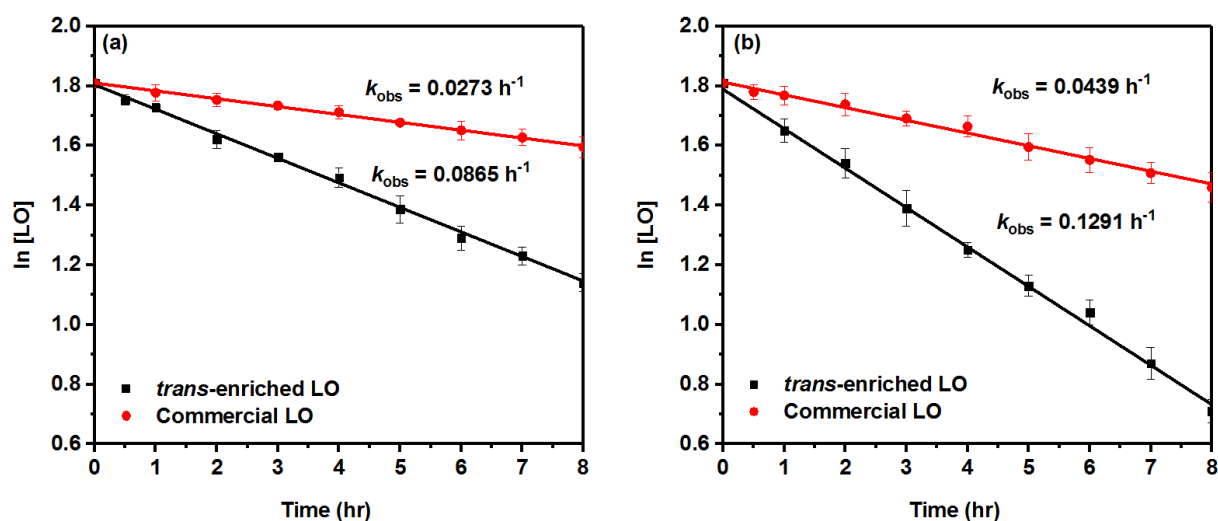


Figure 4.3 Comparison of the rate constants for limonene carbonate (LC) formation using commercial and *trans*-enriched limonene oxide (LO) as substrates at (a) 120 °C (b) 140 °C, (reaction conditions: LO (solvent-free), 6 mol % TBAC and 40 bar  $p$  ( $\text{CO}_2$ )).

#### 4.6.1 Reaction order with respect to [LO]

To find the reaction order with respect to epoxide (LO), experiments were performed by changing the initial concentration of LO from (1.5–5.5) M using PC as solvent at 120 °C and 40 bar  $\text{CO}_2$  pressure in the presence of 6 mol% TBAC catalyst (Figure 4.4 a). The decrease in  $[\text{LO}]$  was monitored by following the decrease in the intensity of epoxide peak area ( $\text{C}-\text{O}$  stretch i.e.  $841 \text{ cm}^{-1}$ ) using FTIR spectroscopy. The graph of experimentally determined values of  $\ln [\text{LO}]$  against time (hr) shows a linear-correlation as all the data points were found to be a good fit into first-order kinetics (Figure 4.4 b). Moreover, the order of the reaction was

determined from the slope of the double logarithmic plot of observed reaction rates ( $k_{\text{obs}}$ ) against [LO] i.e.  $0.82 \approx 1$ , suggesting a first-order reaction in epoxide concentration ( $a = 1$ ), (Figure 4.4 c). This was further confirmed from the plot of  $k_{\text{obs}}$  against the initial concentration of epoxide [LO] showing a good fit to the straight line almost passing through the origin ( $R^2 = 0.99$ ), (Figure 4.4 d). Conversely, the values of  $R^2$  for zero and 2<sup>nd</sup> order dependence on epoxide concentration exhibited a significantly poorer fit (Appendix A Table 9.3). The summary of the kinetic experiments to determine the order of the reaction w.r.t epoxide (LO) is given in Appendix A Table 9.2.

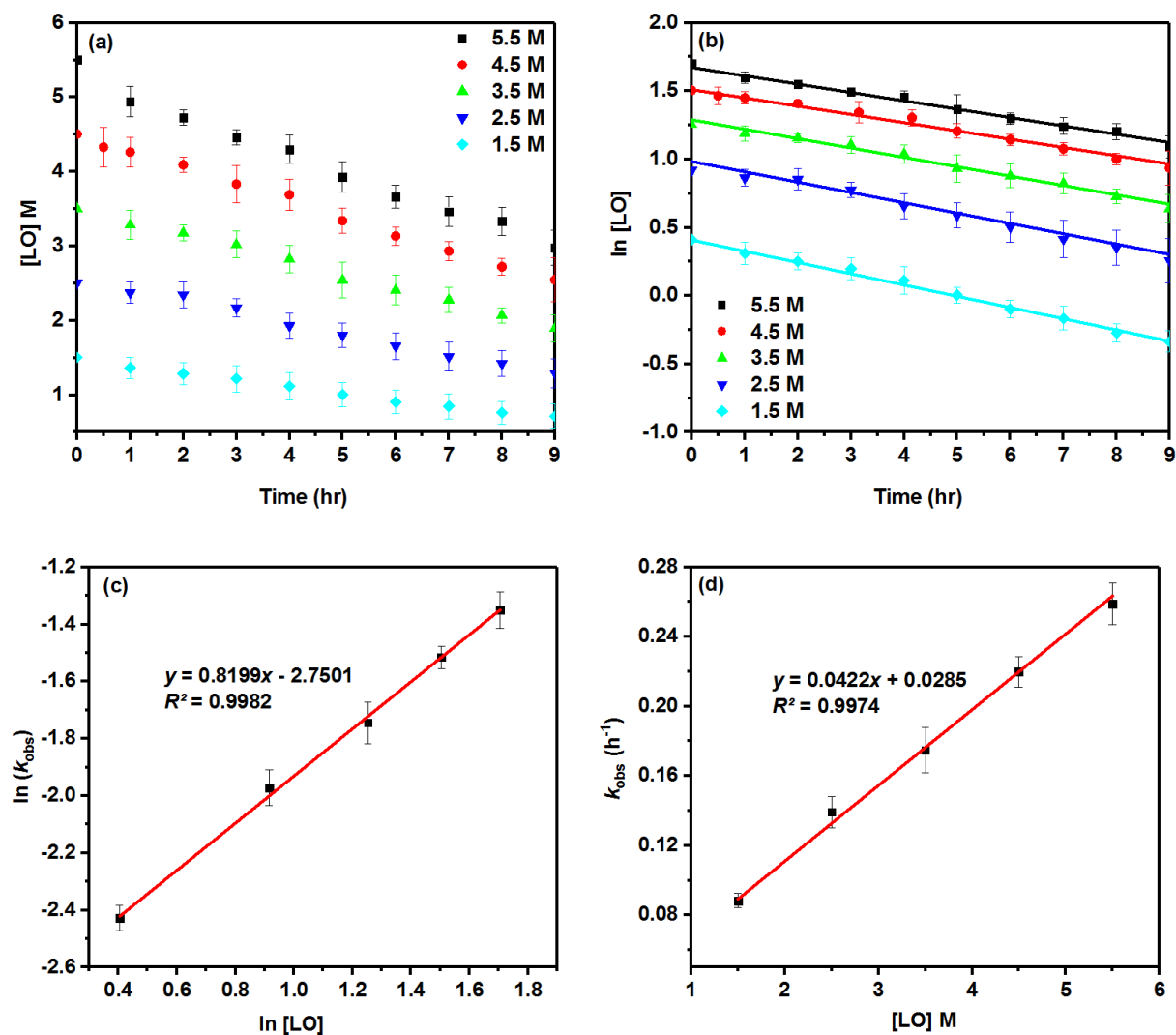


Figure 4.4 (a) Decrease in [LO] M as a function of reaction time (hr) for five different concentrations of LO (1.5–5.5) M (b) First-order kinetics plot i.e. ln [LO] against the reaction time (hr) showing the conversion of LO to LC (c) Plot of ln ( $k_{\text{obs}}$ ) against ln [LO] showing the first-order dependence of the reaction w.r.t [LO] (d) Plot of ( $k_{\text{obs}}$ ) against [LO] showing a linear-correlation, (reaction conditions: 120 °C,  $p$  ( $\text{CO}_2$ ) = 40 bar and 6 mol% TBAC).

#### 4.6.2 Reaction order with respect to [TBAC]

The order of the reaction with respect to catalyst (TBAC) was determined using five different concentrations of TBAC from (1.5–7.5) mol%, whilst keeping other reaction parameters constant. The results indicate that the rate of the reaction increases with the catalyst concentration, and a linear relation between  $\ln [\text{LO}]$  and time (hr) was obtained (Figure 4.5 a). The double logarithmic graph between  $k_{\text{obs}}$  and [TBAC] had a slope of 1.07 clearly indicating first-order dependence with respect to catalyst concentration ( $c=1$ ), (Figure 4.5 b). This was further confirmed by the plot of  $k_{\text{obs}}$  against [TBAC] showing a good fit to the straight line ( $R^2 = 0.99$ ), almost passing through the origin (Figure 4.6). The role of the halide anion (X) in the catalytic cycle of cyclic carbonate formation has been well-established (North and Pasquale, 2009). Here, the chloride anion ( $\text{Cl}^-$ ) of the TBAC catalyst opens the ring of epoxide by the nucleophilic attack on the least substituted C atom of epoxide to form a chloro-alkoxide intermediate. This chloro-alkoxide further incorporates  $\text{CO}_2$  to form carbonate anion, which then undergoes intramolecular formation of the five-membered cyclic carbonate by the elimination of  $\text{Cl}^-$  ion acting as a leaving group. The summary of the kinetic experiments to determine the order of the reaction w.r.t TBAC is given in Appendix A, Table 9.5.

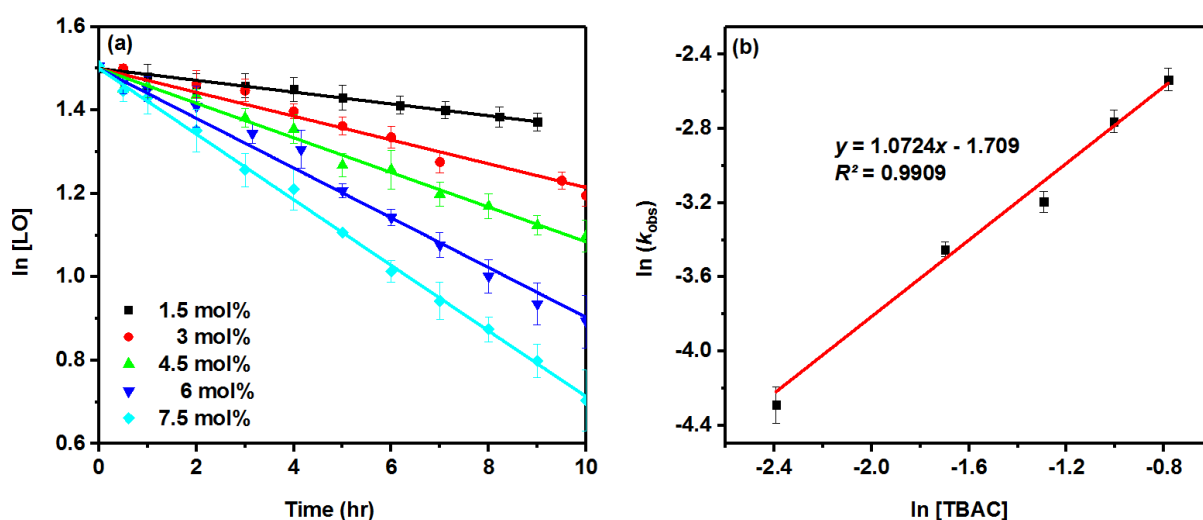


Figure 4.5 (a) First-order kinetics plot of  $\ln [\text{LO}]$  against reaction time (hr) for five different concentrations of TBAC (1.5–7.5) mol % (b) Plot of  $\ln (k_{\text{obs}})$  against  $\ln [\text{TBAC}]$  showing the first-order dependence of the reaction w.r.t [TBAC], (reaction condition: 4.5 M LO, 120 °C and  $p(\text{CO}_2) = 40$  bar).

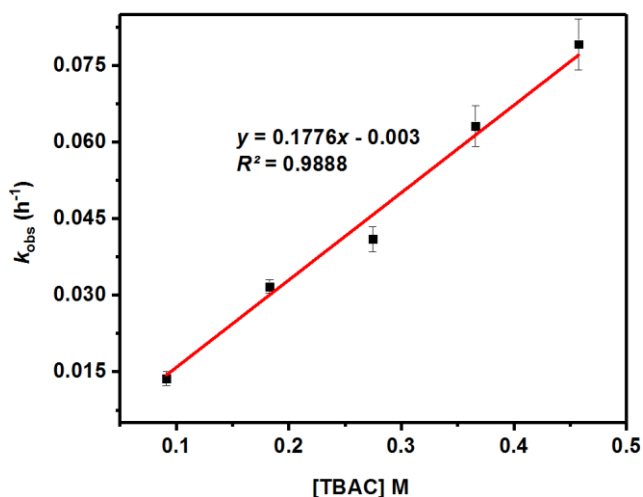


Figure 4.6 Plot showing a linear-correlation between ( $k_{\text{obs}}$ ) and [TBAC], (reaction conditions: 4.5 M LO, (1.5–7.5) mol% TBAC, 120 °C, 40 bar  $p$  ( $\text{CO}_2$ )).

#### 4.6.3 Reaction order with respect to $[\text{CO}_2]$

The order of the reaction with respect to  $\text{CO}_2$  concentration was investigated by changing the  $\text{CO}_2$  pressure from (10–40) bar whilst keeping all other reaction parameters constant (i.e. 4.5 M LO, 120 °C and 6 mol% TBAC). The rate of  $\text{CO}_2$  dissolution in PC is well known and is considerably higher than the rate of the cycloaddition reaction (Pohorecki and Možeński, 1998a). Therefore, the equilibrium between the concentration of  $\text{CO}_2$  in the liquid phase and above the reaction mixture will be rapidly achieved. The increased reaction rate was observed by increasing the pressure due to the increase in  $\text{CO}_2$  concentration in the reaction mixture at higher pressure. The data obtained from these experiments were found to fit in first-order kinetics (Figure 4.7 a). Furthermore, the order of the reaction was determined from the slope of the double logarithmic graph of  $k_{\text{obs}}$  vs.  $p$  ( $\text{CO}_2$ ) i.e.  $0.87 \approx 1$  (Figure 4.7 b), suggesting a first-order dependence of reaction in  $\text{CO}_2$  concentration ( $b=1$ ) over the range of (10–40) bar  $p$  ( $\text{CO}_2$ ). This was further confirmed by the plot of  $k_{\text{obs}}$  against  $p$  ( $\text{CO}_2$ ) showing a good fit to the straight line ( $R^2 = 0.99$ ), almost passing through the origin (Figure 4.7 c). The summary of the kinetic experiments to determine the order of the reaction w.r.t  $\text{CO}_2$  is given in Appendix A, Table 9.6.

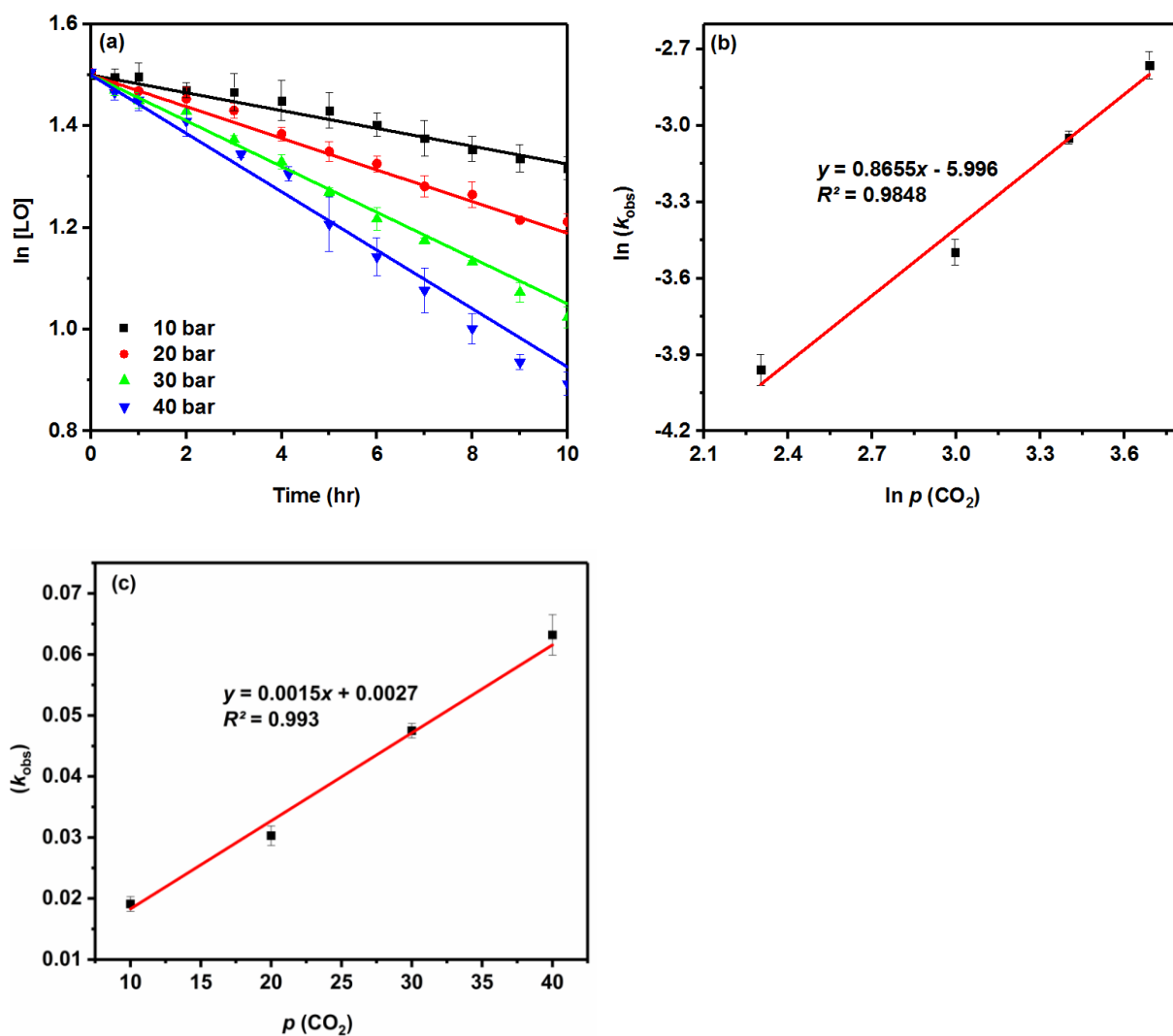


Figure 4.7 (a) First-order kinetics plot of  $\ln [LO]$  against reaction time (hr) for four different  $p(CO_2)$  ranging from (10–40) bar (b) Plot of  $\ln(k_{obs})$  against the  $\ln p(CO_2)$  showing a linear correlation (c) Plot showing a linear-correlation between  $(k_{obs})$  and  $p(CO_2)$ , (reaction condition: 4.5 M LO, 120 °C and  $p(CO_2) = (10\text{--}40)$  bar).

#### 4.6.4 Temperature dependence and determination of activation parameters

To calculate the activation energy ( $E_a$ ) for LC formation, the dependence of the reaction rate was studied over the range of (100–140) °C at 40 bar  $p(CO_2)$  using 6 mol% of TBAC catalyst. As expected, the reaction rate increased with the increase in temperature due to increased catalytic activity at higher temperatures. All the data points obtained were found to fit into first-order kinetics (Figure 4.8 a). The activation energy ( $E_a$ ) was determined from the plot of  $(\ln k_{obs})$  against the reciprocal of the absolute reaction temperature ( $1/T$ ) using the Arrhenius equation i.e.  $k_{obs} = A \cdot \exp(-E_a/RT)$ , (Figure 4.8 b). As a result, the  $E_a$  for LC

formation was found to be  $64 \text{ kJ mol}^{-1}$  over the range of (100–140) °C. Synthesis of cyclic carbonates from internal epoxides generally has high values of activation energies compared to terminal epoxides. For instance, the activation energies required for cyclohexane carbonate (CHC) synthesis from cyclohexene oxide (CHO) and  $\text{CO}_2$  catalysed by di-zinc and tri-zinc complexes were determined as  $137.5$  and  $83.1 \text{ kJ mol}^{-1}$ , respectively (Jutz *et al.*, 2011; Xu *et al.*, 2017). These high values of kinetic energies for cyclic carbonate synthesis from internal epoxides show the challenging nature of internal epoxides. The summary of the kinetic experiments to determine the activation energy for limonene carbonate (LC) formation is given in Appendix A, Table 9.7.

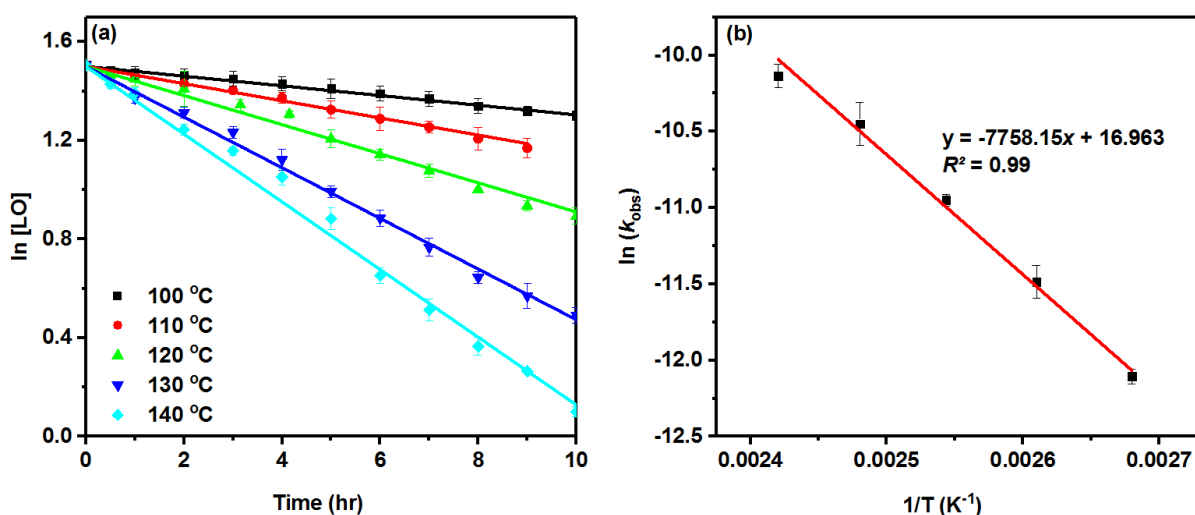


Figure 4.8 (a) First-order kinetics plot of  $\ln [LO]$  against reaction time (hr) over the range of (100–140) °C (b) Curve fitting of  $\ln (k_{obs})$  against the reciprocal absolute temperature ( $1/T$ ) to determine the activation energy ( $E_a$ ), (reaction conditions: 4.5 M LO at  $p(\text{CO}_2) = 40$  bar and 6 mol% TBAC).

The thermodynamic activation parameters were also determined using the Eyring equation (Lente *et al.*, 2005). A graph between  $\ln (k/T)$  vs.  $1/T$  was plotted to determine the enthalpy of activation ( $\Delta H^\ddagger$ ) and entropy of activation ( $\Delta S^\ddagger$ ) from the slope and y-intercept, respectively (Figure 4.9, Table 4.3). Gibbs free energy of activation ( $\Delta G^\ddagger$ ) was determined from the equation ( $\Delta G^\ddagger = \Delta H^\ddagger - T \cdot \Delta S^\ddagger$ ). From the results obtained, the high positive values of  $\Delta H^\ddagger$  and  $\Delta G^\ddagger$  show the endergonic and chemically controlled nature of the cycloaddition reaction. Moreover, the activation energy for LC formation determined from the Eyring plot (i.e.  $64.3 \text{ kJ mol}^{-1}$ ) was found to be in close agreement with the value determined from the Arrhenius equation.

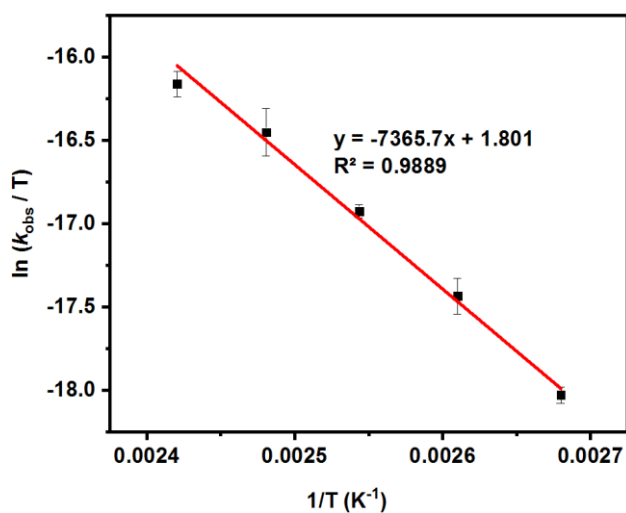


Figure 4.9 Eyring plot of  $\ln(k_{\text{obs}}) / T$  against the reciprocal of absolute temperature ( $1/T$ ) over the range of (100–140) °C to determine the activation parameters.

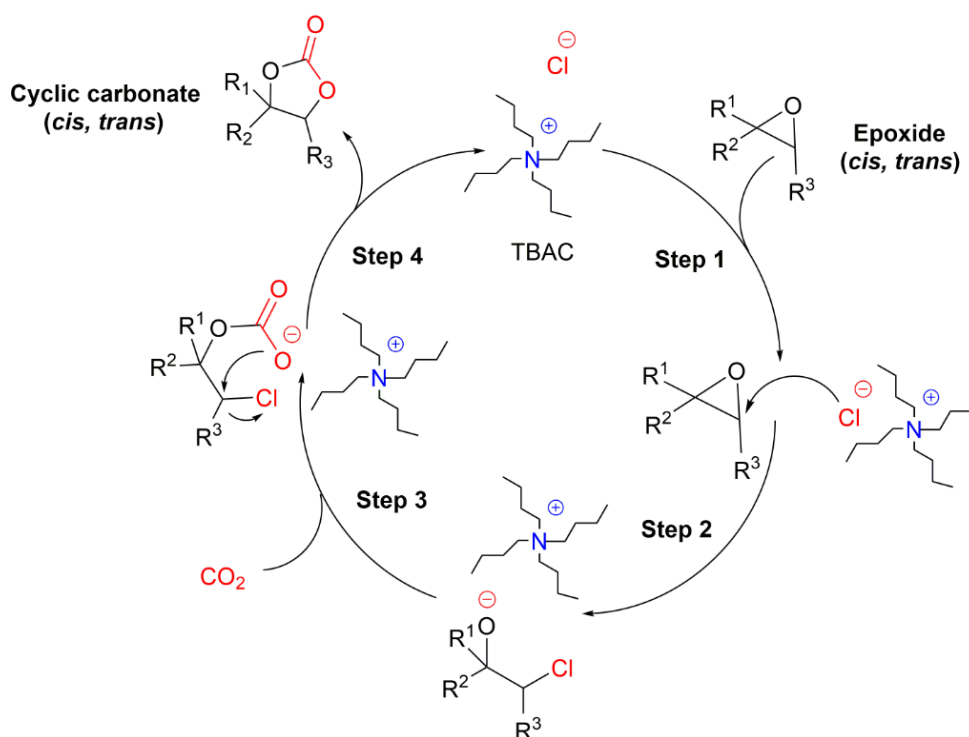
Activation enthalpy $\Delta H^\ddagger$ (kJ mol <sup>-1</sup> )	Activation entropy $\Delta S^\ddagger$ (J mol <sup>-1</sup> K <sup>-1</sup> )	Gibbs free energy $\Delta G^\ddagger$ (kJ mol <sup>-1</sup> )	Activation energy $E_a$ (kJ mol <sup>-1</sup> )
$61.84 \pm 1.2$	$-99.80 \pm 3.57$	$97.88 \pm 2.82^a$	$64.34 \pm 1.2^d$

<sup>a</sup>  $\Delta G^\ddagger = \Delta H^\ddagger - T.\Delta S^\ddagger$  at 373 K, <sup>b</sup>  $E_a = \Delta H^\ddagger + RT$

Table 4.3 Summary of activation parameters of limonene carbonate (LC) synthesis determined from Eyring equation.

## 4.7 Proposed reaction mechanism

On the basis of the detailed kinetic study, a reaction mechanism was proposed (Scheme 4.3). In the absence of Lewis acid catalyst, there was no partial positive charge on any carbon atom and the 2 carbon atoms in the epoxide ring have the same electrophilicity. Therefore, the epoxide ring opening took place by nucleophilic attack of the halide anion ( $\text{Cl}^-$ ) on the least hindered carbon atom of the epoxide due to its higher accessibility (Step 1). This results in the formation of a reactive chloro-alkoxide intermediate which is stabilized by the counter cations ( $\text{TBA}^+$ ) to enable  $\text{CO}_2$  insertion into the ring opened epoxide (Step 2). This alkoxide intermediate further undergoes nucleophilic attack on the electrophilic carbon atom of  $\text{CO}_2$  to form carbonate anion (Step 3). Finally, the carbonate anion goes through the intramolecular elimination of the halide anion to form a five-membered cyclic carbonate and the catalyst is regenerated (Step 4). Moreover, the overall stereochemical information was retained as result of double inversion reaction mechanisms during epoxide ring opening and ring closure steps.



Scheme 4.3 Proposed reaction mechanism of cyclic carbonate synthesis from tri-substituted epoxide and  $\text{CO}_2$ .

## 4.8 Summary

Synthesis of cyclic carbonates from bio-based LO and CO<sub>2</sub> was carried out with high stereoselectivity using commercially available, inexpensive TBAC as an effective homogeneous catalyst. The initial studies of cycloaddition from a commercially available LO (a mixture of *cis* and *trans*-LO 40:60) revealed high reactivity of *trans*-isomer under the given reaction conditions. Therefore, a stereoselective method of (*R*)-(+)-limonene epoxidation was carried out to achieve a high yield of the more reactive *trans*-isomer (up to 87%). Moreover, a detailed study of reaction kinetics was carried out in the presence of a PC as a greener polar aprotic solvent. The results indicate first-order dependence of the reaction with respect to LO, TBAC and CO<sub>2</sub> concentrations. The temperature dependence of the reaction rate was also studied over a range of (100–140) °C to determine the activation parameters. The activation energy ( $E_a$ ) for LC synthesis was determined to be 64 kJ mol<sup>-1</sup>. The high positive value of free energy ( $\Delta G^\ddagger = 97.8$  kJ mol<sup>-1</sup>) and negative value of activation entropy ( $\Delta S^\ddagger = -99.8$  J mol<sup>-1</sup> K<sup>-1</sup>), indicate endergonic and chemically controlled nature of the cycloaddition reaction. Furthermore, a general reaction mechanism of cyclic carbonate synthesis from tri-substituted epoxides and CO<sub>2</sub> in the presence of TBAC catalyst was proposed.

## **Chapter 5 Continuous styrene carbonate (SC) synthesis from styrene oxide (SO) and CO<sub>2</sub> in a ‘tube-in-tube’ gas-liquid flow reactor.**

### **5.1 Introduction**

Synthesis of cyclic carbonates from epoxides and CO<sub>2</sub> is a typical gas-liquid multiphase catalytic process involving a gas-liquid mass transfer in a reactor and the catalytic cycloaddition reaction in the liquid phase. Thus, it was anticipated that an efficient reactor design in terms of the high rate of heat/mass transfer and continuous flow approach could mitigate many of the limitations observed in the conventional batch reactor. This chapter discusses the results of continuous styrene carbonate (SC) synthesis from styrene oxide (SO) and CO<sub>2</sub> using a semipermeable membrane (Teflon<sup>®</sup> AF-2400) based ‘tube-in-tube’ gas-liquid flow reactor. The experiments were performed using TBAB and ZnBr<sub>2</sub>, acting as a highly efficient binary homogeneous catalyst system. The performance of the flow reactor was evaluated by studying the effect of various operating conditions such as reaction temperature, CO<sub>2</sub> pressure, and residence time. Moreover, a detailed kinetic study of SC synthesis was carried out to study the effect of reaction parameters and to investigate the reaction mechanism.

### **5.2 Effect of halide anion activity and catalyst loading**

Synthesis of styrene carbonate (SC) from styrene oxide (SO) and CO<sub>2</sub> was carried out in the presence of various TBAX (X = I<sup>-</sup>, Br<sup>-</sup>, Cl<sup>-</sup>, F<sup>-</sup>) in combination with zinc halides (ZnX<sub>2</sub> where X = Br<sup>-</sup>, Cl<sup>-</sup>) as acid-base binary homogeneous catalysts. Initial experiments of catalyst screening were carried out in a 100 ml stainless steel high-pressure semi-batch reactor (Table 5.1). The cycloaddition reaction carried out using TBAB (0.1 mmol) as a catalyst alone exhibited only 7% yield of SC at 100 °C and 1 bar *p* (CO<sub>2</sub>) after 3 h (run 1). Similarly, the reaction performed using ZnBr<sub>2</sub> as a catalyst only exhibited no catalytic activity (run 2). However, when the reaction was carried out using an equimolar combination of TBAB and ZnBr<sub>2</sub>, the synergistic effect resulted in a 46% yield under the same reaction conditions (run 3). The significant enhancement in catalytic activity of TBAB in conjunction with ZnBr<sub>2</sub> was due to epoxide activation by the interaction of Lewis acidic zinc site with the oxygen atom of epoxide, thereby promoting epoxide ring-opening by the nucleophilic attack of halide anion.

Similarly, to investigate the catalytic activity of counter halide anion (X), the reactions were also performed using TBAI, TBAC and TBAF in combination with ZnBr<sub>2</sub> (runs 3–6). The order of reactivity was found to be TBAB > TBAI > TBAC > TBAF, which is in agreement with the order of leaving group abilities of halide anions, except Br<sup>-</sup> exhibiting higher catalytic activity than I<sup>-</sup>. Generally, the catalytic activity of halide anions is determined by the balance between nucleophilicity and leaving-group ability, which may vary depending upon the reaction conditions and type of second catalyst (e.g. Lewis acid), if used (Langanke *et al.*, 2013). A similar order of halide anions catalytic activity for the CO<sub>2</sub> cycloaddition to terminal epoxides using TBAX in combination with bimetallic Al-salen complex was reported previously (Clegg *et al.*, 2010). It is well-established that the role of the halide anion in the catalytic cycle is to open the ring of the epoxide to form a halo-alkoxide intermediate, which then reacts with CO<sub>2</sub> to form carbonate, with the halide then becoming the leaving group (Jutz *et al.*, 2008; Sun *et al.*, 2009).

The catalytic activity of ZnCl<sub>2</sub> was also tested in a combination of TBAB, resulting in lower catalytic activity compared to ZnBr<sub>2</sub> i.e. 26% yield (run 7), which is presumably due to higher leaving group ability i.e. Br<sup>-</sup> > Cl<sup>-</sup> (Song *et al.*, 2014). Therefore, further experiments were carried out using ZnBr<sub>2</sub> in combination with TBAB. It was observed that ZnBr<sub>2</sub> and TBAB molar ratios have a substantial effect on SC synthesis. Therefore, more experiments were performed using different molar ratios to find the optimum catalyst ratio. The results in Table 5.1 showed that the yield of SC increases with the amount of TBAB from 1 to 4 equivalent of ZnBr<sub>2</sub> i.e. 46 to 74% (runs 3, 8 and 9). However, an increase in ZnBr<sub>2</sub>/TBAB to 1:6 molar ratio did not result in any substantial increase in the SC yield, i.e. 76% (run 10). Therefore, ZnBr<sub>2</sub>/TBAB with an optimum molar ratio (1:4) was chosen for further experiments in a tube-in-tube flow reactor.

Run	Metallic salt	Tetrabutylammonium halides	Molar ratio (ZnX <sub>2</sub> /TBAX)	Yield (%)
1	--	TBAB (0.1 mmol)	--	7
2	ZnBr <sub>2</sub> (0.1 mmol)	--	--	0
3	ZnBr <sub>2</sub>	TBAB	1:1	46
4	ZnBr <sub>2</sub>	TBAI	1:1	37
5	ZnBr <sub>2</sub>	TBAC	1:1	29
6	ZnBr <sub>2</sub>	TBAF	1:1	12
7	ZnCl <sub>2</sub>	TBAB	1:1	26
8	ZnBr <sub>2</sub>	TBAB	1:2	62
9	ZnBr <sub>2</sub>	TBAB	1:4	74
10	ZnBr <sub>2</sub>	TBAB	1:6	76

Table 5.1 Catalyst screening for styrene carbonate (SC) synthesis in a semi-batch reactor, (reaction conditions: SO (35 mmol), 100 °C, 1bar  $p$  (CO<sub>2</sub>) and 3 h).

### 5.3 Effect of reaction parameters in a continuous flow reactor

The effect of the reaction parameters on the SC synthesis for CO<sub>2</sub> cycloaddition to SO was investigated in a ‘tube-in-tube’ reactor under continuous flow conditions, using the determined optimum catalyst molar ratio i.e. (ZnBr<sub>2</sub>/TBAB 1:4). Table 5.2 shows the results for the performance of the reactor under various temperature, CO<sub>2</sub> pressure and residence time conditions. The effect of a change in  $p$  (CO<sub>2</sub>) from (2–6) bar (runs 1–3) at fixed temperature (100 °C), and 30 (min) reaction time showed that the yield (%) of SC increased with the increase in  $p$  (CO<sub>2</sub>) on the shell side of the tube-in-tube reactor. The inner tube of the reactor is made of a Teflon<sup>®</sup> AF-2400 based semi-permeable membrane through which only gas can permeate. The exceptionally high permeation of CO<sub>2</sub> i.e. 280,000 cB (Biogeneral) through the membrane and the significantly increased surface area to volume ratio results in higher rate of mass transfer and 80% yield was obtained in a considerably reduced reaction time i.e. 30 min (run 3). Previous studies of mass transfer coefficient measurement in a gas-liquid microreactor also suggest a substantial enhancement in the rate of mass transfer due to increase in gas bubbles dissolution in the liquid phase at higher pressure (Yao *et al.*, 2015).

As expected, increasing the temperature results in an increase in reaction rate and complete conversion of SO to SC was achieved in a significantly reduced reaction time of 45 (min) at 120 °C and 6 bar of  $p$  (CO<sub>2</sub>) under flow conditions (run 5). The mass transfer coefficient in a

gas-liquid reaction is greatly influenced by the gas diffusivity in the liquid ( $D_L$ ) and the liquid viscosity ( $\mu_L$ ) (Ferreira *et al.*, 2010). Increasing the temperature increases  $D_L$  and decreases  $\mu_L$ , both of which act to increase the gas-liquid mass transfer coefficient. Note that complete selectivity of SC formation (100%) was observed in all experiments by using  $ZnBr_2/TBAB$  catalyst under these reaction conditions.

Run	$ZnBr_2/TBAB$ (molar ratio)	Temperature (°C)	$CO_2$ Pressure (bar)	Time (min)	Yield (%)
1	1:4	100	2	30	52
2	1:4	100	4	30	71
3	1:4	100	6	30	80
4	1:4	120	6	30	91
5	1:4	120	6	45	100

Table 5.2 Study of reaction parameters for styrene carbonate (SC) formation in a continuous flow reactor.

#### 5.4 Kinetics study of $CO_2$ cycloaddition to SO catalysed by $TBAB/ZnBr_2$

Reactor design can affect the rate of gas-liquid catalytic reaction (Klaewkla *et al.*, 2011; Lokhat *et al.*, 2016). Previous studies of reaction kinetics for cyclic carbonate synthesis performed in a batch reactor suggested that rate of reaction is controlled by the rate of  $CO_2$  mass transfer from the gaseous phase to the reaction mixture (Metcalf *et al.*, 2013). Kinetic data obtained from experiments carried out in mass transfer limited reactors cannot be used to formulate meaningful kinetic expressions. Here, the initial study of reaction kinetics carried out in a batch reactor also indicated that the reaction is mixing/mass transfer limited, as the observed rate constants ( $k_{obs}$ ) for SO conversion at temperature range (90–120) °C, were significantly lower than the experiments carried out in a continuous flow reactor at the same reaction conditions (Table 5. 3). Higher reaction rates in flow reactor were achieved as a result of the enhanced rate of mass transfer and rapid diffusion of  $CO_2$  through membrane tubing containing high surface area to volume ratio compared to the conventional magnetically stirred batch reactor.

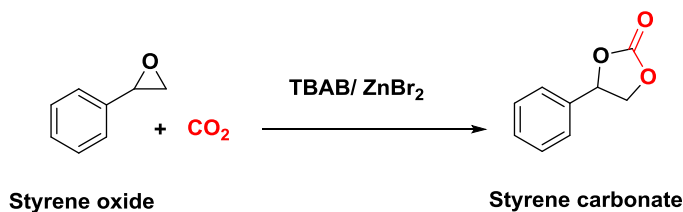
Temperature (°C)	Observed rate constant ( $k_{\text{obs}}$ )	
	Batch ( $\times 10^{-2}$ )	Flow ( $\times 10^{-2}$ )
90	1.23	3.07
100	1.54	4.01
110	1.86	5.33
120	2.37	6.88

Table 5.3 Rate constants for the conversion of SO to SC as a function of reaction temperature in both batch and continuous flow reactor, (reaction conditions: 4.5 M SO, 1:4 ZnBr<sub>2</sub>/TBAB, 6 bar  $p$  (CO<sub>2</sub>)).

In order to investigate the mechanism of SC synthesis using ZnBr<sub>2</sub>/TBAB as a binary homogeneous catalyst and to determine the equation of rate law, a detailed study of reaction kinetics has been carried out using FTIR spectroscopy. The experiments of the kinetic study were performed using PC as a reaction solvent. The rate at which CO<sub>2</sub> dissolves in PC is known and is much faster than the rate of cyclic carbonate formation (Pohorecki and Možeński, 1998a). PC as a carbonyl group-containing solvent has a greater ability to solubilise CO<sub>2</sub> than other solvents (Pazuki and Pahlavanzadeh, 2005). Moreover, the catalytic activity of TBAB and ZnBr<sub>2</sub> is not inhibited as the formation of PC from PO and CO<sub>2</sub> can also be carried out using the same catalyst system. The literature precedent shows that cyclic carbonate formation via CO<sub>2</sub> cycloaddition to epoxides has a highly negative heat of formation, therefore it can be assumed that there is no back reaction which is in agreement with experimental observations (North and Pasquale, 2009; North *et al.*, 2011).

The overall rate equation of SC synthesis from SO and CO<sub>2</sub> in the presence of TBAB and ZnBr<sub>2</sub> as a binary catalyst system (Scheme 5.1) can be written as Eq (5.1), where [SO], [CO<sub>2</sub>], [TBAB], and [ZnBr<sub>2</sub>] are the concentrations of styrene oxide, carbon dioxide, tetrabutylammonium bromide and zinc bromide, respectively, and (a–d) are the orders of reaction with respect to SO, CO<sub>2</sub>, TBAB, and ZnBr<sub>2</sub>. The shell-side of the reactor was held at a constant CO<sub>2</sub> pressure during a particular reaction. Therefore, a rapid equilibrium will be established between the concentration of CO<sub>2</sub> in the shell-side of the ‘tube-in-tube’ reactor and the concentration of CO<sub>2</sub> dissolved in the reaction mixture. Since CO<sub>2</sub> was present in the shell side of the reactor in large excess, it can be assumed that the concentration of CO<sub>2</sub> in the liquid phase remains constant during the reaction. Similarly, the concentration of TBAB and

ZnBr<sub>2</sub> acting as a catalyst also remains constant during the reaction. Therefore, Eq (5.1) can be simplified to Eq (5.2) where  $k_{obs}$  is the observed rate constant and can be given as Eq (5.3). By taking the natural logarithm of both sides of Eq (5.3), it gives Eq (5.4), which can be used to determine the values of orders of reaction (b-d). By assuming the system to be first order (a=1) and integrating Eq (5.5), it gives Eq (5.6).



Scheme 5.1 Chemical reaction for styrene carbonate (SC) synthesis from styrene oxide (SO) and CO<sub>2</sub>.

$$\text{Rate} = k [\text{SO}]^a [\text{CO}_2]^b [\text{TBAB}]^c [\text{ZnBr}_2]^d \quad (5.1)$$

$$\text{Rate} = k_{obs} [\text{SO}]^a \quad (5.2)$$

$$k_{obs} = k [\text{CO}_2]^b [\text{TBAB}]^c [\text{ZnBr}_2]^d \quad (5.3)$$

$$\ln k_{obs} = \ln k + b \ln[\text{CO}_2] + c \ln[\text{TBAB}] + d \ln[\text{ZnBr}_2] \quad (5.4)$$

$$\text{Rate} = -\frac{d[\text{SO}]}{dt} = k_{obs} [\text{SO}]^1 \quad (5.5)$$

$$-\ln [\text{SO}] = k_{obs} \cdot t \quad (5.6)$$

$$k_{obs} = A \cdot \exp\left(-\frac{E_a}{R.T}\right) \quad (5.7)$$

$$\ln k_{obs} = \ln A - \left(\frac{E_a}{R.T}\right) \quad (5.8)$$

#### 5.4.1 Reaction order with respect to [TBAB]

The order of the reaction with respect to TBAB was determined by varying the concentration of TBAB over (0.025–0.1) M and keeping all other reaction parameters constant. The decrease in the concentration of SO as a result of SC formation was monitored as a function of reaction time (Figure 5.1 a). The data obtained from these experiments exhibited a close fit to first-order kinetics (Figure 5.1 b). Moreover, the order of reaction with respect to TBAB concentrations was determined from the gradient of a double logarithmic plot slope i.e. 1.05 (Figure 5.1 c). This indicates that reaction is first-order ( $c = 1$ ) with respect to TBAB concentrations. This was further confirmed by a plot of ( $k_{\text{obs}}$ ) values against [TBAB], exhibiting a linear dependence of reaction rate on TBAB concentrations (Figure 5.1 d). Previously, North and Pasquale (2009) reported a second order dependence of cycloaddition reaction between SO and CO<sub>2</sub> with respect to TBAB used in combination with bimetallic Al (III)-salen complex, suggesting an additional role of TBAB to activate CO<sub>2</sub> by *in-situ* tri-butylamine formation. However, the experimental results obtained in this study strongly suggest a first-order dependence of reaction in TBAB concentration. The role of tetrabutylammonium halide anion in CO<sub>2</sub>/epoxide cycloaddition is already well established (Calo et al., 2002). The halide anion (X) attacks nucleophilically on the least hindered carbon atom to form a halo-alkoxide by opening the ring of epoxide, which then reacts with CO<sub>2</sub> to form carbonate, with the halide anion acting as a leaving group in a cyclic carbonate formation. The summary of kinetic experiments to determine the order of the reaction w.r.t TBAB is given in Appendix B, Table 9.8.

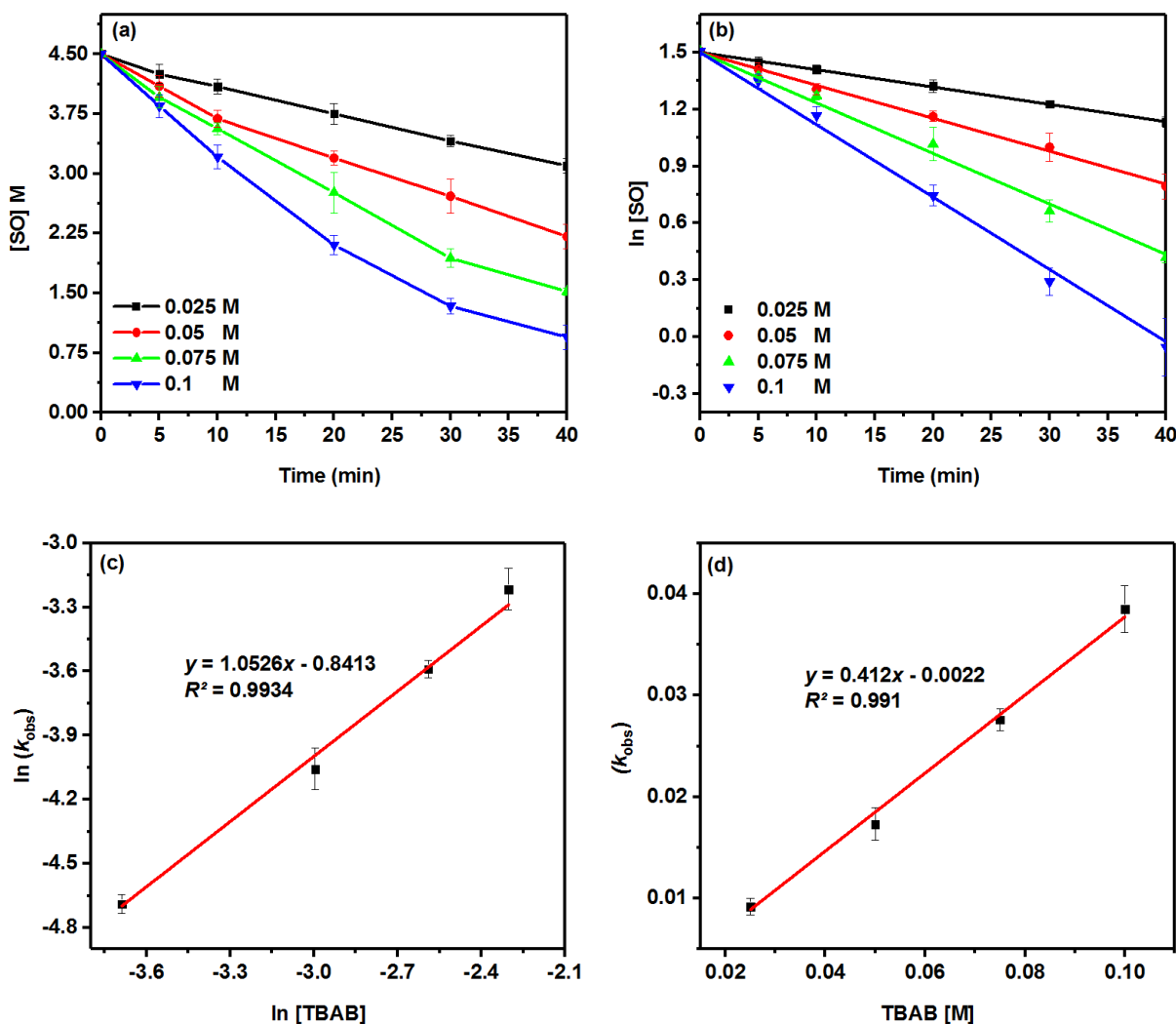


Figure 5.1 (a) Decrease in [SO] M as a function of reaction time (min) using four different concentrations of TBAB (0.025–0.1) M and  $ZnBr_2$  (6.5 mM) at 100 °C and 6 bar  $p$  ( $CO_2$ ) (b) First-order kinetic plots i.e. ln [SO] against reaction time (min) (c) Curve fitting of ln ( $k_{obs}$ ) against ln [TBAB] to determine the order of the reaction (d) Plot of the observed rate constant ( $k_{obs}$ ) against [TBAB] showing a linear correlation.

#### 5.4.2 Reaction order with respect to $[CO_2]$

To determine the order of reaction with respect to  $CO_2$ , the experiments were performed by varying the  $CO_2$  pressures over the range of (2–8) bar, while keeping otherwise constant reaction conditions. The shell side of the reactor held at a constant value of pressure during a particular reaction. The reaction rate increased with  $CO_2$  pressure due to increased  $CO_2$  concentration in the reaction mixture. All the data points obtained from the experiments were found to be a good fit in first-order kinetics (Figure 5.2 a). A plot of experimentally

determined values of  $\ln(k_{\text{obs}})$  against the  $\ln p [\text{CO}_2]$  also shows a linear relation (i.e. gradient of line  $0.80 \sim 1$ , Figure 5.2 b) suggesting that reaction is first-order in  $\text{CO}_2$  concentration ( $b = 1$ ). This was further confirmed by a plot of  $(k_{\text{obs}})$  values against  $p (\text{CO}_2)$ , exhibiting a linear dependence of reaction rate on  $\text{CO}_2$  pressure (i.e.  $R^2 = 0.99$ ), almost passing through the origin (Figure 5.2 c). This apparent first-order reaction with respect to  $\text{CO}_2$  suggests that only one molecule of  $\text{CO}_2$  is involved in the rate-determining step of the catalytic cycle (Cuesta-Aluja *et al.*, 2016). The summary of the kinetic experiments to determine the order of the reaction w.r.t  $\text{CO}_2$  is given in Appendix B, Table 9.9.

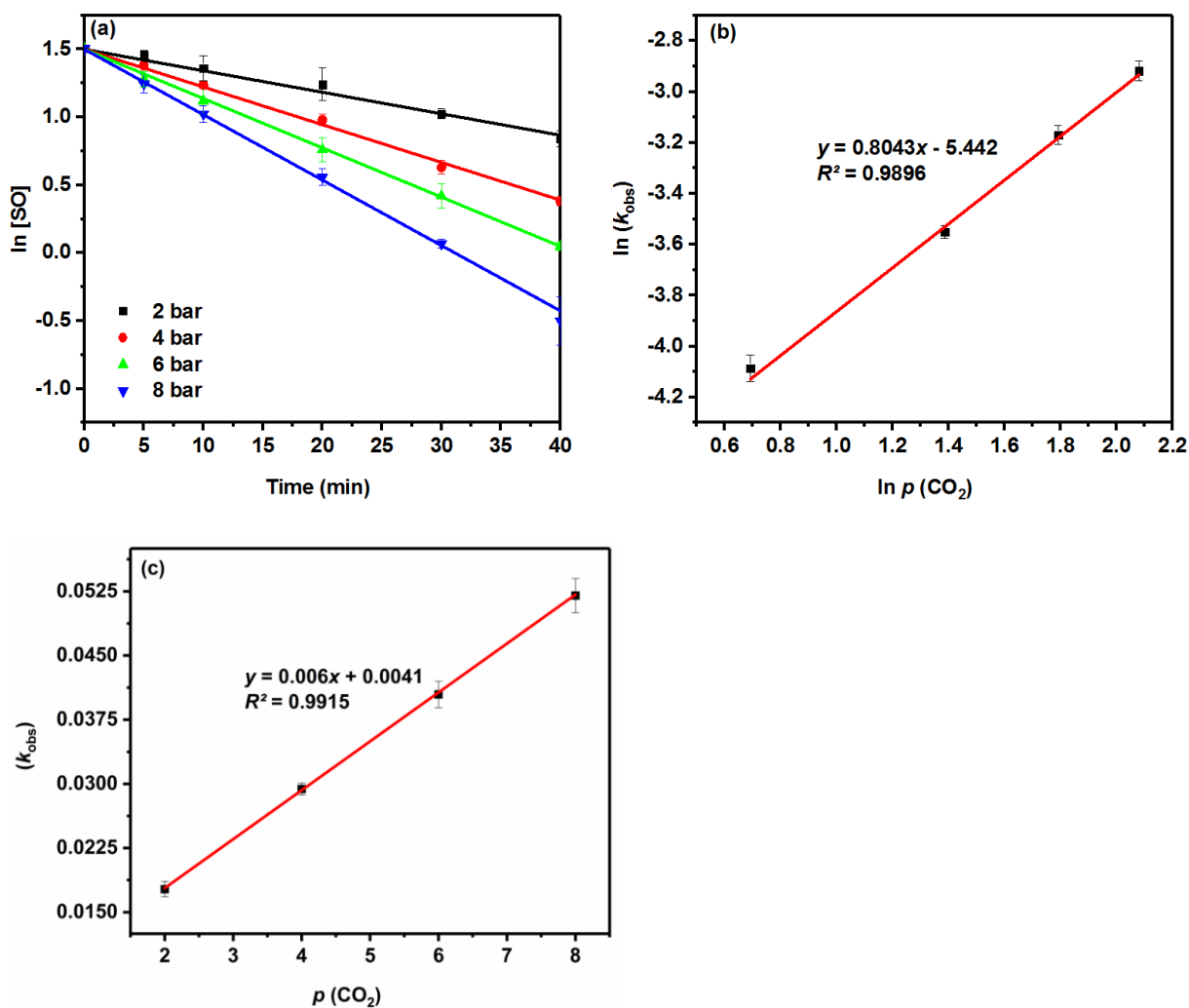


Figure 5.2 (a) First-order kinetic plots i.e.  $\ln [\text{SO}]$  against reaction time (min) for four different  $p (\text{CO}_2)$  (2-8 bar) at  $100^\circ\text{C}$ ,  $[\text{TBAB}]$  (0.1M) and  $[\text{ZnBr}_2]$  (6.5 mM) (b) Curve fitting of  $\ln(k_{\text{obs}})$  against  $\ln p [\text{CO}_2]$  to determine the order of the reaction w.r.t.  $\text{CO}_2$  (c) Plot of the observed rate constant ( $k_{\text{obs}}$ ) against  $p (\text{CO}_2)$  showing a linear correlation.

### 5.4.3 Reaction order with respect to $[ZnBr_2]$

The order of the reaction with respect to  $ZnBr_2$  was also investigated by performing experiments using four different concentrations of  $ZnBr_2$  (3.25–26) mM in the presence of a fixed concentration of TBAB (0.1 M). All other reaction parameters were kept constant. The data showed a good fit to first-order kinetics (Figure 5.3 a). The double logarithmic plot had a slope of 0.50 (Figure 5.3 b), suggesting a non-integer ( $d= 0.5$ ) value of reaction order (non-first-order kinetics) in  $ZnBr_2$  concentrations. A fractional order is normally an indication of the complex reaction (Lehenmeier *et al.*, 2011). This was probably due to a complex formation by the coordination of one molecule of  $ZnBr_2$  with two molecules of SO. The literature precedent shows that an optimum molar ratio between catalyst and co-catalyst has a significant effect on the catalytic activity of binary catalytic systems rather than simply changing the concentration of one-component relative to other (Martín and Kleij, 2014). The role of zinc halides in catalyst cycle is to activate the epoxide by Lewis acidic  $Zn^{+2}$  site through the formation of the zinc-epoxide adduct, which facilitates epoxide ring opening by the nucleophilic attack of halide anion ( $Br^-$ ) on the least hindered C atom of epoxide. The summary of the kinetic experiments to determine the order of the reaction w.r.t  $ZnBr_2$  is given in Appendix B, Table 9.10.

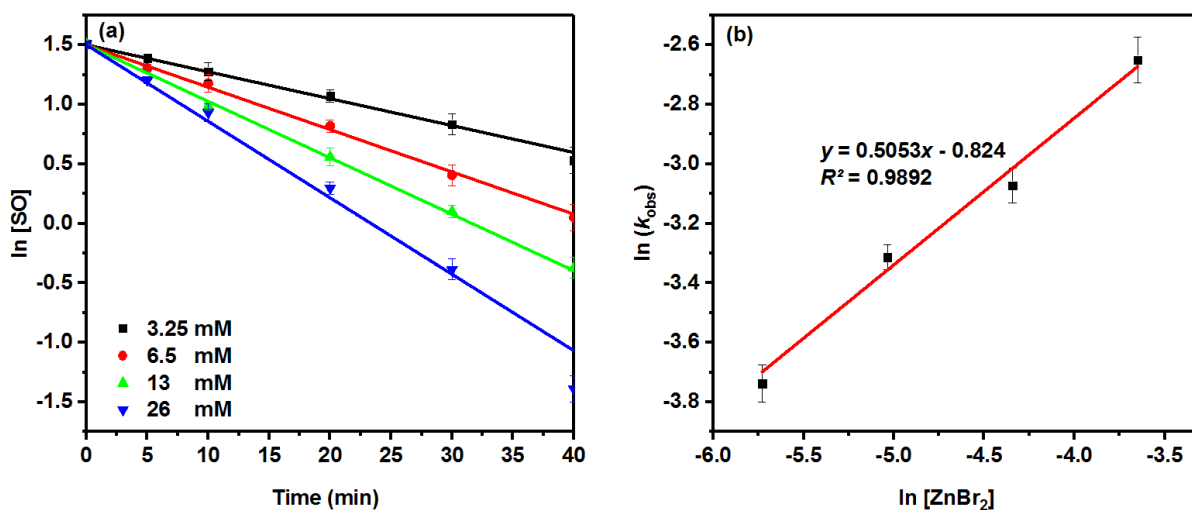


Figure 5.3 (a) First-order kinetics plot i.e.  $\ln [SO]$  against reaction time (min) for four different concentrations of  $ZnBr_2$  (3.25–26) mM and [TBAB] (0.1M) at 100 °C and 6 bar  $p$  ( $CO_2$ ) (b) Curve fitting of  $\ln k_{obs}$  against  $\ln [ZnBr_2]$  to determine the order of the reaction w.r.t  $ZnBr_2$ .

#### 5.4.4 Temperature dependence and determination of activation parameters

To study the temperature dependence on the reaction rate, experiments were carried out over the range of (90–120) °C while keeping all other parameters constant. The decrease in the concentration of SO was monitored as a function of reaction time (min) (Figure 5.4 a). As expected, the rate of the reaction increases with the reaction temperature. The data points obtained as result of these experiments showed a good fit to first-order kinetics i.e. ( $\ln [\text{SO}]$  vs time (Figure 5.4 b), suggesting first-order dependence in epoxide concentration ( $a = 1$ ). Moreover, the activation energy ( $E_a$ ) of SC synthesis was determined from Arrhenius plot i.e.  $\ln (k_{\text{obs}})$  against the reciprocal of absolute temperature ( $1/T$ ) (Eq 5.7, 5.8). The activation energy ( $E_a$ ) for SC synthesis in the presence of TBAB as catalyst alone was determined to be  $53 \text{ kJ mol}^{-1}$ . However, it was reduced to  $34 \text{ kJ mol}^{-1}$  when using TBAB in combination with  $\text{ZnBr}_2$  as a binary homogeneous catalyst, clearly demonstrating the appreciable enhancement in catalytic activity due to a synergistic effect (Figure 5.4 c). A similar value of activation energy ( $E_a$ ) for SC synthesis catalysed by Al-complex in conjunction with TBAB was reported previously (Cuesta-Aluja *et al.*, 2016). The summary of the kinetic experiments to determine the activation energy ( $E_a$ ) for styrene carbonate (SC) formation is given in Appendix B, Table 9.11. Moreover, the thermodynamic activation parameters such as  $\Delta H^\ddagger$ ,  $\Delta S^\ddagger$  and  $\Delta G^\ddagger$  were also studied using the Eyring equation (Table 5.4). The values of  $\Delta H^\ddagger$  and  $\Delta S^\ddagger$  were determined from the gradient and y-intercept, respectively (Figure 5.4 d). From the results obtained, the positive values of  $\Delta H^\ddagger$  and  $\Delta G^\ddagger$  indicate the endergonic and chemically controlled nature of the reaction. Moreover, the value of  $E_a$  obtained from the Eyring equation was found in close agreement with the value obtained from the Arrhenius equation.

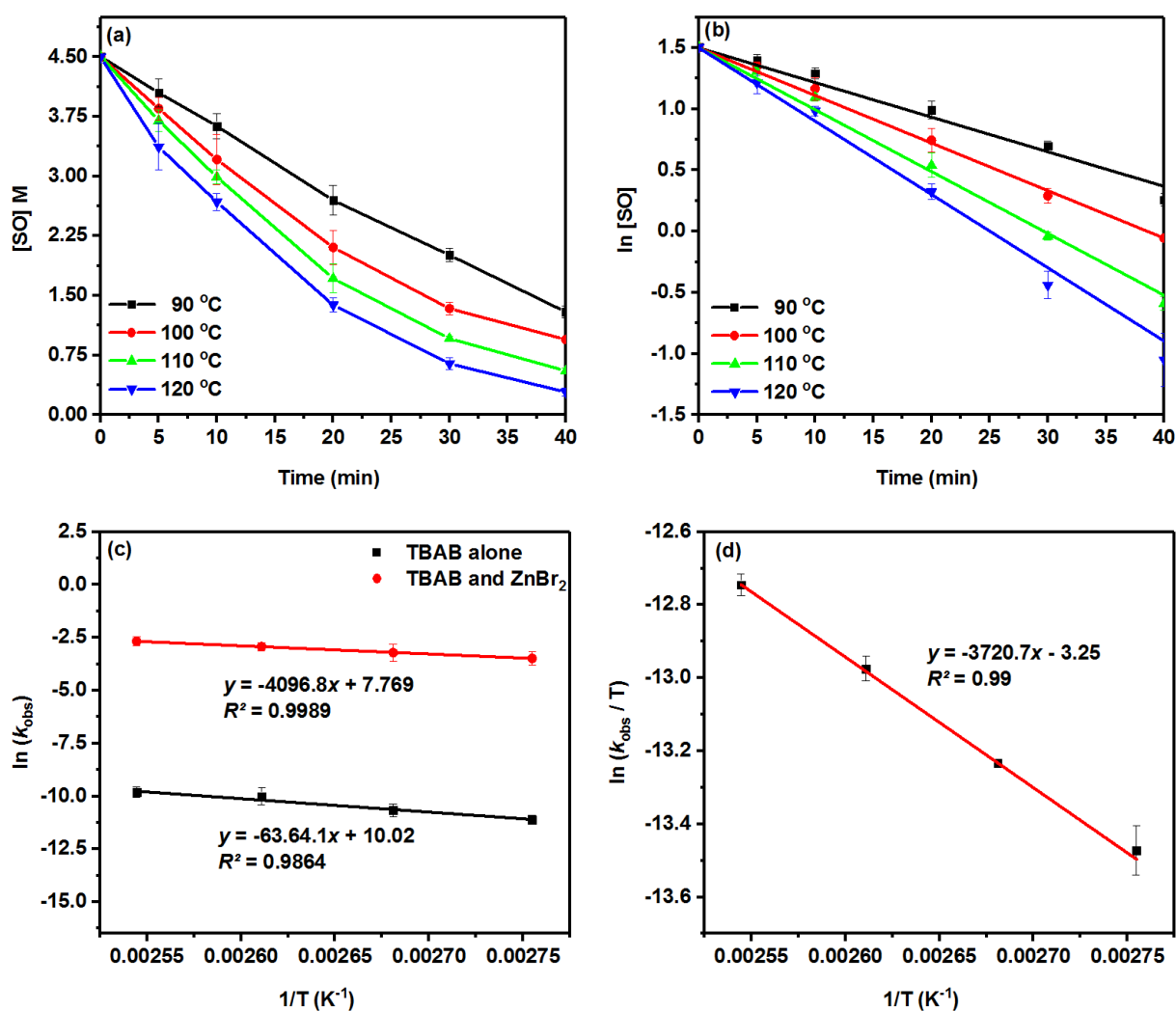


Figure 5.4 (a) Decrease in [SO] M as a function of reaction time (min) over the range of (90–120) °C using [TBAB] (0.1 M) and [ZnBr<sub>2</sub>] (6.5 mM) at 6 bar *p* (CO<sub>2</sub>) (b) First-order kinetic plots i.e. ln [SO] against reaction time (min) (c) Arrhenius plot for SC formation over the range of (90–120) °C using TBAB (alone) and TBAB/ZnBr<sub>2</sub> as a binary catalyst (d) Eyring plot for SC formation using TBAB/ZnBr<sub>2</sub> over the range of (90–120) °C.

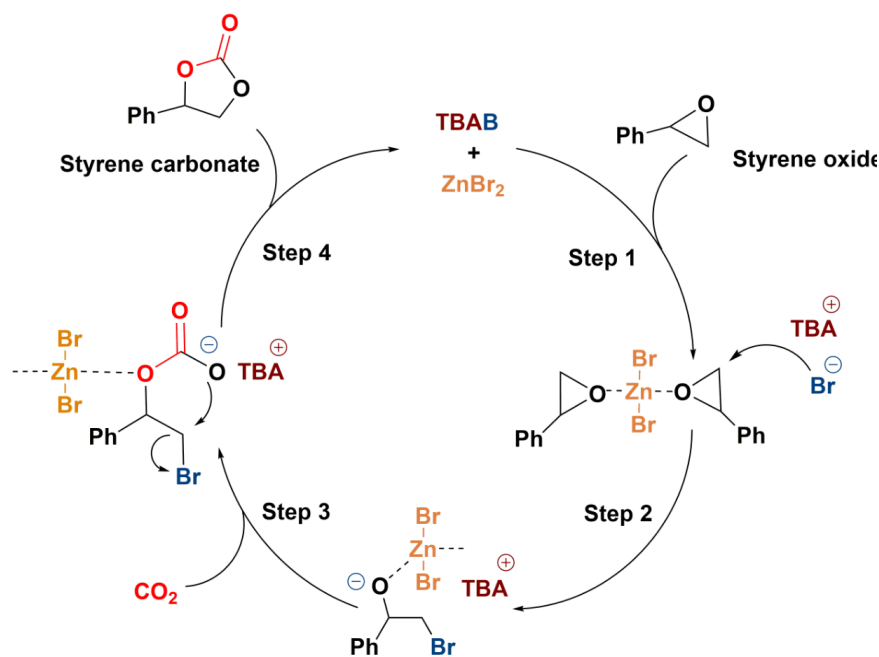
Activation enthalpy $\Delta H^\ddagger$ (kJ mol <sup>-1</sup> )	Activation entropy $\Delta S^\ddagger$ (J mol <sup>-1</sup> K <sup>-1</sup> )	Gibbs free energy $\Delta G^\ddagger$ (kJ mol <sup>-1</sup> )	Activation energy $E_a$ (kJ mol <sup>-1</sup> )
30.92 ± 3.96	-197.32 ± 1.08	104.35 ± 2.19 <sup>a</sup>	34.06 ± 2 <sup>b</sup>

<sup>a</sup>  $\Delta G^\ddagger$  at 373.15 K, <sup>b</sup> ( $E_a = \Delta H^\ddagger + RT$ )

Table 5.4 Summary of activation parameters of SC formation from SO and CO<sub>2</sub> catalysed by TBAB/ZnBr<sub>2</sub> determined from Eyring equation.

## 5.5 Proposed reaction mechanism

Based on the detailed kinetics analysis and previous literature, a possible reaction mechanism for SC synthesis using  $\text{ZnBr}_2$  and TBAB as a binary homogeneous catalyst system can be proposed (Scheme 5.2). Here the reaction is initiated by the coordination of SO with Lewis acid  $\text{Zn}^{+2}$  site of  $\text{ZnBr}_2$  to activate the epoxide by the formation of the zinc-epoxide adduct (Step 1). Simultaneously, the halide anion ( $\text{Br}^-$ ) (basic site) provided by TBAB undergoes a nucleophilic attack on the least hindered ( $\beta$ -carbon) atom of the activated epoxide to open the ring and producing a bromo-alkoxide intermediate (Step 2). The stability to this ring-opened intermediate was provided by the counter cation ( $\text{TBA}^+$ ) of TBAB to facilitate  $\text{CO}_2$  insertion. Subsequently,  $\text{CO}_2$  insertion takes place by nucleophilic attack of negatively charged oxygen atom of alkoxide intermediate on the electrophilic carbon atom of  $\text{CO}_2$  to form an oxyanion carbonate species (Step 3). Finally, the ring-closure of open-chain carbonate takes place by the intramolecular displacement of nucleophile provided by the TBAB to form SC and the catalyst is regenerated (Step 4).



Scheme 5.2 Proposed reaction mechanism of styrene carbonate (SC) formation from styrene oxide (SO) and  $\text{CO}_2$  catalysed by TBAB/ $\text{ZnBr}_2$  as an acid-base binary homogeneous catalyst.

## 5.6 Summary

For the first time, highly efficient styrene carbonate (SC) synthesis from styrene oxide (SO) and CO<sub>2</sub> was demonstrated in a ‘tube-in-tube’ gas-liquid continuous flow reactor. The high permeation rate of CO<sub>2</sub> through the inner Teflon<sup>®</sup> AF-2400 semipermeable tube combined with the high surface area to volume ratio resulted in complete conversion (100%) of SO to SC in a significantly reduced reaction time of 45 min. The continuous flow reactor generates homogeneous solutions of gas in the liquid in a reliable and controlled manner, thereby facilitating rapid optimization of the reaction, which can greatly enhance the efficiency (rate) of the reaction as compared to the conventional batch reactor. A detailed kinetic study of SC synthesis catalysed by acid-base binary homogeneous catalyst system (ZnBr<sub>2</sub>/TBAB) was carried out to find the initial rate law equation. The kinetic study suggests a first-order dependence of the reaction rate on the epoxide (SO), catalyst (TBAB) and CO<sub>2</sub> concentrations and a fractional-order (i.e. 0.5) dependence on ZnBr<sub>2</sub> when used in conjunction with TBAB. The activation energy (E<sub>a</sub>) of the reaction in the presence of TBAB alone was calculated to be 53 kJ mol<sup>-1</sup>, which was reduced to 34 kJ mol<sup>-1</sup> when using ZnBr<sub>2</sub> in combination with TBAB. Based on the kinetic analysis, a synergistic reaction mechanism for SC synthesis using TBAB and ZnBr<sub>2</sub> was proposed.

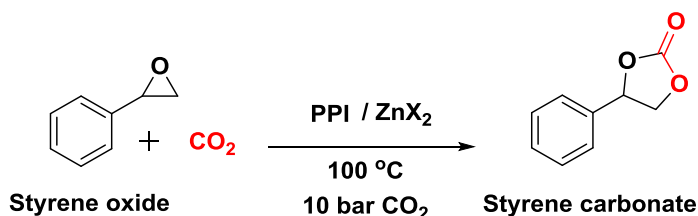
## Chapter 6 Styrene carbonate (SC) synthesis by CO<sub>2</sub> cycloaddition to styrene oxide (SO) using pyrrolidinopyridinium iodide (PPI) and zinc halides (ZnX<sub>2</sub>).

### 6.1 Introduction

In this chapter, results of styrene carbonate (SC) synthesis by the cycloaddition of CO<sub>2</sub> to styrene oxide (SO) catalysed by pyrrolidinopyridinium iodide (PPI) in combination with zinc halides (ZnX<sub>2</sub> where X = Cl<sup>-</sup>, Br<sup>-</sup> and I<sup>-</sup>), are discussed. A detailed study of reaction kinetics was carried out to understand the effect of reaction parameters and to investigate the reaction mechanism. The orders of the reaction with respect to SO, CO<sub>2</sub> and (PPI/ZnI<sub>2</sub>) catalyst concentrations, were determined. The temperature dependence of the reaction was studied to determine the activation energy and thermodynamic activation parameters. Based on the kinetic analysis, a reaction mechanism was proposed.

### 6.2 Effect of zinc halide anions activity on CO<sub>2</sub> cycloaddition to SO

Figure 6.1 shows the relative catalytic activity of PPI with and without Zn halides (i.e. ZnCl<sub>2</sub>, ZnBr<sub>2</sub> and ZnI<sub>2</sub>) for SC formation via CO<sub>2</sub> cycloaddition to SO (Scheme 6.1).



Scheme 6.1 Styrene carbonate (SC) synthesis by CO<sub>2</sub> cycloaddition to styrene oxide (SO) in the presence of PPI/ZnX<sub>2</sub> as a binary homogeneous catalyst.

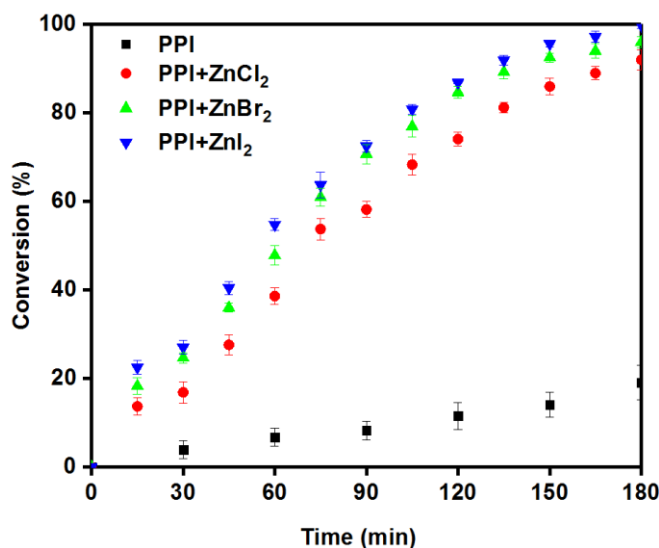


Figure 6.1 Relative catalytic activity of PPI catalyst for SC formation with and without  $ZnX_2$ , (reaction conditions SO, [PPI] 76 mM,  $[ZnX_2]$  38 mM, 100 °C and 10 bar  $p$  ( $CO_2$ )).

The reaction carried out in the presence of PPI as homogeneous catalyst alone exhibited only 19% conversion of SO to SC at 100 °C and 10 bar  $p$  ( $CO_2$ ) after 3 h and the rate of the reaction ( $k_{obs}$ ) was determined to be  $1.5 \times 10^{-3} \text{ min}^{-1}$  (Table 6.1, entry 1). However, when PPI was used in combination with  $ZnI_2$  as an acid-base binary homogeneous catalyst, the rate of the reaction increased by 10-fold compared to PPI alone and almost complete conversion of SO to SC was achieved at 100 °C, 10 bar  $p$  ( $CO_2$ ) using 1:0.5 molar ratio (PPI/ $ZnI_2$ ) after 3 h (Table 6.1, entry 2). The significant enhancement in reaction rate was attributed to epoxide activation by the interaction of the Lewis acidic site (Zn) with the oxygen atom of epoxide. The rate of reaction was also studied using PPI in conjunction with  $ZnBr_2$  and  $ZnCl_2$  (entry 3-4). The order of catalytic activity of Zn halides in combination with PPI was found to be  $ZnI_2 > ZnBr_2 > ZnCl_2$  which is consistent with the order of nucleophilicity of halide anions. A similar order of halide anions activity in combination with ionic liquids for epoxide/ $CO_2$  cycloaddition was reported previously (Liu *et al.*, 2015a). The difference in the activity of zinc halides was presumably due to different activation ability of epoxide which can be explained due to the difference in the electronegativity of halide anions that varies in the order  $Cl^- > Br^- > I^-$ . The greater the electronegativity, the greater would be the strength of interaction between the Lewis-acidic zinc site and the oxygen atom of epoxide. This will make the regeneration of the Lewis-acidic zinc site more difficult during the intramolecular ring-closure step to form cyclic carbonate due to a slower rate of cleavage of Zn–O bond. Therefore, Zn Lewis acidic site in  $ZnI_2$  has a less strong interaction with the oxygen atom of

the epoxide, resulting in higher co-catalytic activity than ZnBr<sub>2</sub> and ZnCl<sub>2</sub>. Based on the relative co-catalytic activities of these zinc halides, the ZnI<sub>2</sub> was selected in combination with PPI for the further study of reaction kinetics. Moreover, the effects of the catalyst molar ratio (PPI: ZnI<sub>2</sub>) on the reaction rate was also studied (entry 5–7). The results exhibited a significant enhancement in reaction rate and the rate of reaction was almost doubled by increasing PPI/ZnI<sub>2</sub> molar ratio from 1:0.25 to 1:0.5 (entry 2 and 5). However, a further increase in molar ratios i.e. 1: 0.75 and 1:1 has not shown an obvious increase in the reaction rate (entry 6 and 7).

Entry	Catalyst	Molar ratio (PPI:ZnX <sub>2</sub> )	Rate constant <sup>a</sup> 10 <sup>-3</sup> (min) <sup>-1</sup>
1	PPI	1:0	1.5
2	PPI:ZnI <sub>2</sub>	1:0.5	15.2
3	PPI:ZnBr <sub>2</sub>	1:0.5	13.9
4	PPI:ZnCl <sub>2</sub>	1:0.5	10.8
5	PPI:ZnI <sub>2</sub>	1.0.25	7.4
6	PPI:ZnI <sub>2</sub>	1:0.75	17.3
7	PPI:ZnI <sub>2</sub>	1:1	19.1

Reaction conditions: SO, [PPI] 76 mM, [ZnX<sub>2</sub>] (0–152) mM, 100 °C and 10 bar CO<sub>2</sub>.

<sup>a</sup> Determined from the gradient of plot between ln [SO] vs time (min).

Table 6.1 Relative catalytic activity for SC formation from SO and CO<sub>2</sub> in terms of the initial reaction rate.

### 6.3 Kinetics study of CO<sub>2</sub> cycloaddition to SO catalysed by PPI/ZnI<sub>2</sub> catalyst

A detailed study of reaction kinetics was carried out to understand the effect of reaction parameters and to investigate the reaction mechanism. The general rate equation for SC formation by CO<sub>2</sub> cycloaddition to SO in the presence of PPI/ZnI<sub>2</sub> can be written as Eq (6.1), where *k* is the rate constant and [SO], [CO<sub>2</sub>], [CAT] are the concentrations of SO, CO<sub>2</sub> and PPI/ZnI<sub>2</sub> respectively; *a*, *b* and *c* are the orders of reaction with respect to epoxide, CO<sub>2</sub> and catalyst. A series of experiments were performed to determine the orders of the reaction with respect to SO, CO<sub>2</sub> and catalyst concentrations. The CO<sub>2</sub> was supplied continuously during the reaction due to a semi-batch operation. Hence, it can be assumed that the concentration of

CO<sub>2</sub> remained constant throughout the reaction. Similarly, the concentration of the catalyst (PPI/ZnI<sub>2</sub>) also remained constant. Therefore, Eq (6.1) can be simplified as Eq (6.2). Taking natural logarithm of both sides of Eq (6.3) gives Eq (6.4), which can be used to determine the order of reaction with respect to CO<sub>2</sub> and the catalyst. Assuming pseudo-first-order dependence of the reaction i.e. a=1 and by combining Eq (6.2) and (6.5), the rate of reaction can be given as Eq (6.6). The integrating of Eq (6.6) gives Eq (6.7) which can be used to determine the order of reaction with respect to [SO].

$$\text{rate} = k [\text{SO}]^a [\text{CO}_2]^b + [\text{PP}^+\text{ZnI}_3]^c \quad (6.1)$$

$$\text{rate} = k_{\text{obs}} [\text{SO}]^a \quad (6.2)$$

Where:

$$k_{\text{obs}} = k [\text{CO}_2]^b [\text{PP}^+\text{ZnI}_3]^c \quad (6.3)$$

$$\ln k_{\text{obs}} = \ln k + b \ln [\text{CO}_2] + c \ln [\text{PP}^+\text{ZnI}_3] \quad (6.4)$$

$$\text{rate} = -\frac{d[\text{SO}]}{dt} \quad (6.5)$$

$$-\frac{d[\text{SO}]}{dt} = k_{\text{obs}} [\text{SO}] \quad (6.6)$$

$$-\ln[\text{SO}] = k_{\text{obs}}.t \quad (6.7)$$

### 6.3.1 Reaction order with respect to epoxide

To determine the order of reaction w.r.t epoxide [SO], experiments were performed using four different concentrations of SO i.e. (2.5–5.5) M and keeping all other reaction parameters constant i.e. 76 mM [PPI], 38 mM [ZnI<sub>2</sub>] at 100 °C and 10 bar *p* (CO<sub>2</sub>). PC has been increasingly used as a green solvent and a potential replacement of traditional polar aprotic solvents due to its high boiling point and higher CO<sub>2</sub> solubility (Parker *et al.*, 2014). Moreover, the density of the PC (1.2 g/cm<sup>3</sup>) has also a close similarity to that of SO (1.05 g/cm<sup>3</sup>). Therefore, a reaction medium could be established that did not vary considerably from solvent-free reaction conditions in terms of mass transfer properties and miscibility. The progress of the reaction was monitored as a function of time (min). The results indicate an increase in reaction rate with the increase in [SO] (Figure 6.2 a). The graph between initial reaction rate (mol. L<sup>-1</sup>. min<sup>-1</sup>) and initial epoxide concentration [SO] has exhibited a linear correlation with R<sup>2</sup>=0.99 (Figure 6.2 b), suggesting a first-order dependence of the reaction.

The order of the reaction in [SO] was further confirmed by the integrated law method. Thus, an experiment was performed using 2.5 M [SO] in the presence of 76 mM [PPI], 38 mM [ZnI<sub>2</sub>] at 100 °C and 10 bar *p* (CO<sub>2</sub>). The decrease in [SO] as a result of cyclic carbonate formation was monitored as a function of time (min) (Figure 6.3). All the data points were found to be in a good fit with first-order kinetics i.e. ln [SO] vs time, validating a first-order dependence of the reaction as determined by the initial rate law method. These results suggest the involvement of one molecule of epoxide per molecule of the catalyst in the reaction mechanism (Luo *et al.*, 2015).

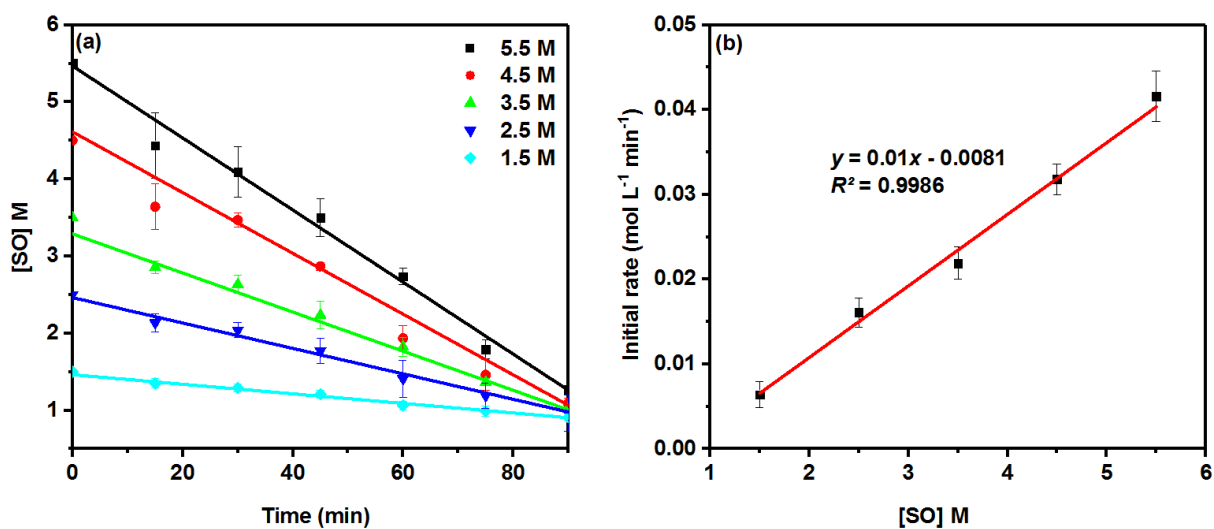


Figure 6.2 (a) Decrease in [SO] M as a function of reaction time (min) for five different concentrations of SO (1.5–5.5 M) (b) Plot of initial reaction rate (mol L<sup>-1</sup> min<sup>-1</sup>) against initial [SO] M showing a linear correlation, (reaction conditions: (2.5–5.5) M SO, 76 mM [PPI], 38 mM [ZnI<sub>2</sub>], 100 °C and 10 bar CO<sub>2</sub>).

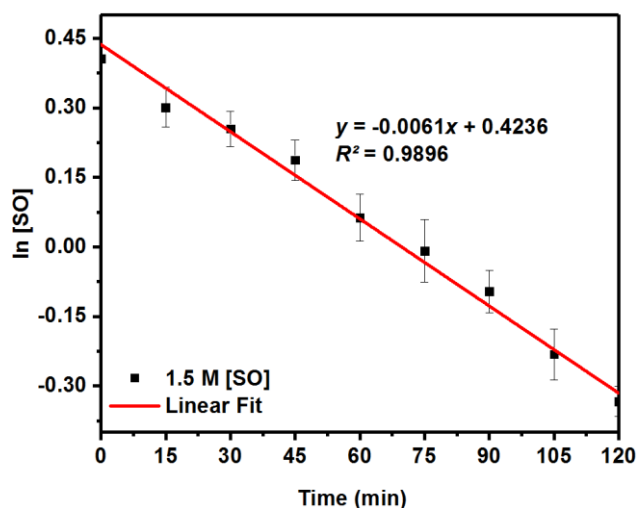


Figure 6.3 First-order kinetics plot showing a linear fit of all the data points (reaction conditions: 1.5 M SO, 76 mM [PPI], 38 mM [ZnI<sub>2</sub>], 100 °C and 10 bar *p* (CO<sub>2</sub>)).

### 6.3.2 Reaction order with respect to catalyst

Initially, the order of the reaction was studied using PPI as a catalyst alone by varying the concentration from (76–304) mM while keeping other reaction parameters constant. As a result, the order of the reaction was determined to be 0.93 ~ 1, suggesting the involvement of one PPI molecule in the catalytic cycle (Figure 6.4 a) (Cuesta-Aluja *et al.*, 2016). Similarly, to determine the order of reaction with respect to PPI in conjunction with ZnI<sub>2</sub>, the second series of experiments were performed using a fixed concentration of PPI (76 mM) in combination with the variable concentration of ZnI<sub>2</sub> (38–152) mM (Figure 6.4 b). The order of the reaction was found to be 0.55 (a fractional order), indicating a ‘complex reaction network’ (Lehenmeier *et al.*, 2011). Therefore, another series of experiments were performed using a fixed molar ratio i.e. PPI/ZnI<sub>2</sub> (1:1 molar ratio) and varying the concentration of binary catalyst from (19–76) mM. The rate of the reaction was increased with the increase in catalyst concentration and all the data points exhibit good fit to first-order kinetics and the order of the reaction was found to be unity i.e. 1.09 (Figure 6.4 c,d). These results suggest the formation of acid-base zinc-pyrrolidinopyridinium iodide complex (PP<sup>+</sup> ZnI<sub>3</sub><sup>-</sup>) by the interaction of equimolar PPI and ZnI<sub>2</sub>. PP<sup>+</sup> ZnI<sub>3</sub><sup>-</sup> activates the epoxide by its Lewis acidic Zn site and the activated epoxide undergoes a nucleophilic attack by the iodide anion (I<sup>-</sup>) to ring-open the epoxides. The stability to the ring-opened intermediate was provided by the large delocalized pyrrolidinopyridinium cations (PP<sup>+</sup>), a key factor to rapid CO<sub>2</sub> insertion.

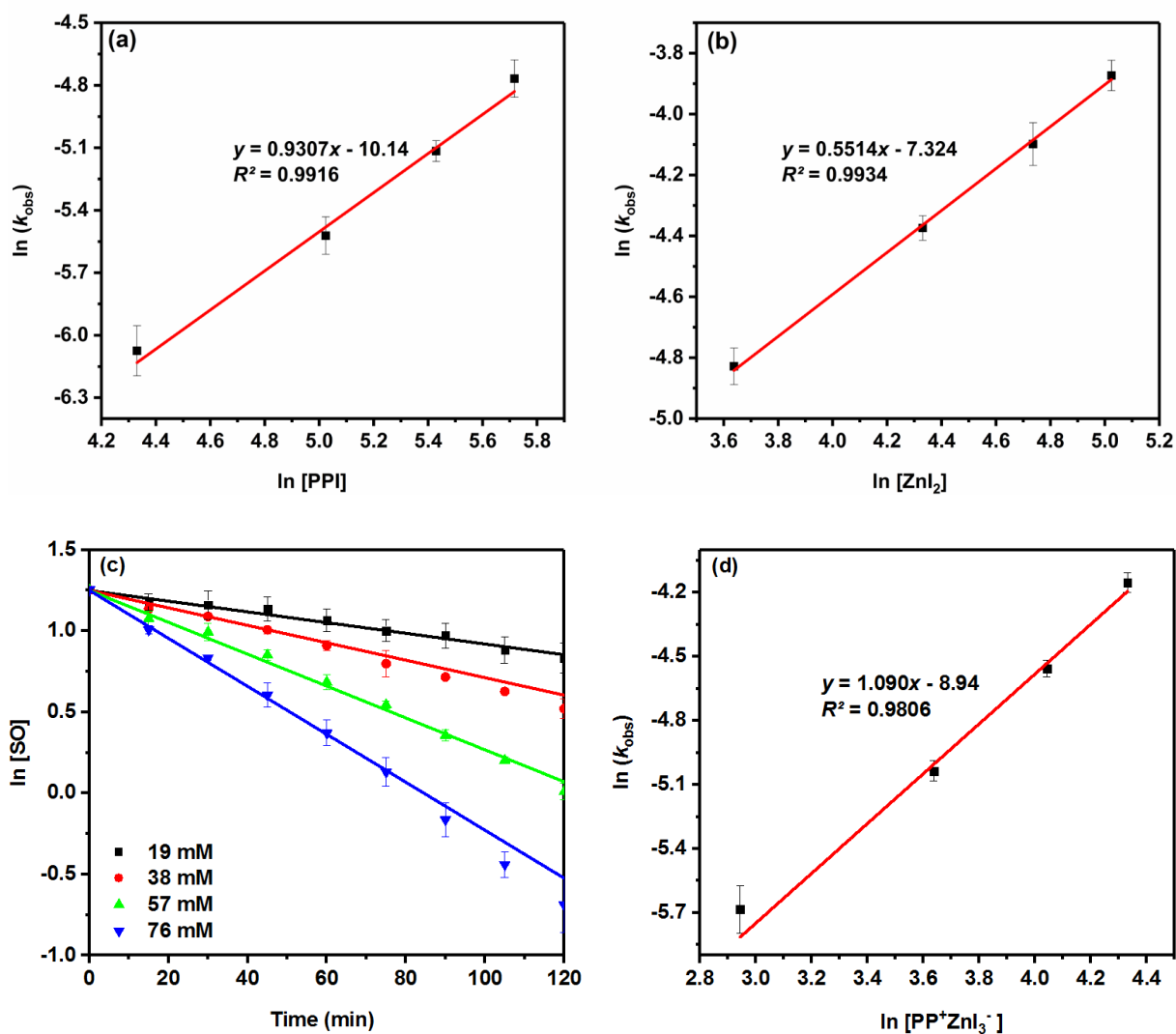


Figure 6.4 (a) Double logarithmic plot between ( $k_{\text{obs}}$ ) and PPI concentrations (76–304) mM to determine the order w.r.t [PPI] (b) Double logarithmic plot between ( $k_{\text{obs}}$ ) and  $\text{ZnI}_2$  concentrations (38–152) mM to determine the order of the reaction w.r.t  $[\text{ZnI}_2]$  (c) First-order kinetics Plot showing a linear fit of all data points into first-order kinetics plot (19–76) mM (d) Double logarithmic plot between ( $k_{\text{obs}}$ ) and  $\text{PP}^+ \text{ZnI}_3^-$  concentrations to determine the order w.r.t catalyst, (reaction conditions: 3.5 M SO,  $\text{PPI}/\text{ZnI}_2$  (1:1), 100 °C and 10 bar  $p$  ( $\text{CO}_2$ )).

### 6.3.3 Reaction order with respect to CO<sub>2</sub>

To study the effect of CO<sub>2</sub> pressure on the reaction rate, the experiments were performed by changing the  $p$  (CO<sub>2</sub>) over two pressure regimes i.e. (2–10) and (10–40) bar while keeping other reaction parameters constant. The experiments were performed using PC as a solvent. The rate at which CO<sub>2</sub> dissolves in PC is much faster than the rate of cyclic carbonate formation (Pohorecki and Možeński, 1998b). Therefore, a rapid equilibrium was established between CO<sub>2</sub> dissolved and CO<sub>2</sub> above the reaction mixture (Clegg *et al.*, 2010c). A linear increase in reaction rate was obtained over the range of (2–10) bar  $p$  (CO<sub>2</sub>). Moreover, the order of reaction was determined to be unity from the gradient of the double logarithmic plot i.e. 1.02 (Figure 6.5 a). This was further confirmed by the plot of  $k_{\text{obs}}$  against  $p$  (CO<sub>2</sub>) showing a good fit to the straight line ( $R^2 = 0.99$ ), almost passing through the origin (Figure 4.7 c). However, the experiments performed over the pressure range of (10–40) bar exhibited no significant increase in reaction rate and the order of reaction tends to decrease from 1 to 0.36 (Figure 6.5 b), presumably due to saturation of CO<sub>2</sub> in the reaction mixture at higher pressure. The decrease in reaction rate at higher CO<sub>2</sub> pressure due to a dilution effect (i.e. CO<sub>2</sub> induced expansion of reaction mixture), causing a decrease in epoxide and catalyst concentrations was also reported previously (Guadagno and Kazarian, 2004; Darensbourg *et al.*, 2005).

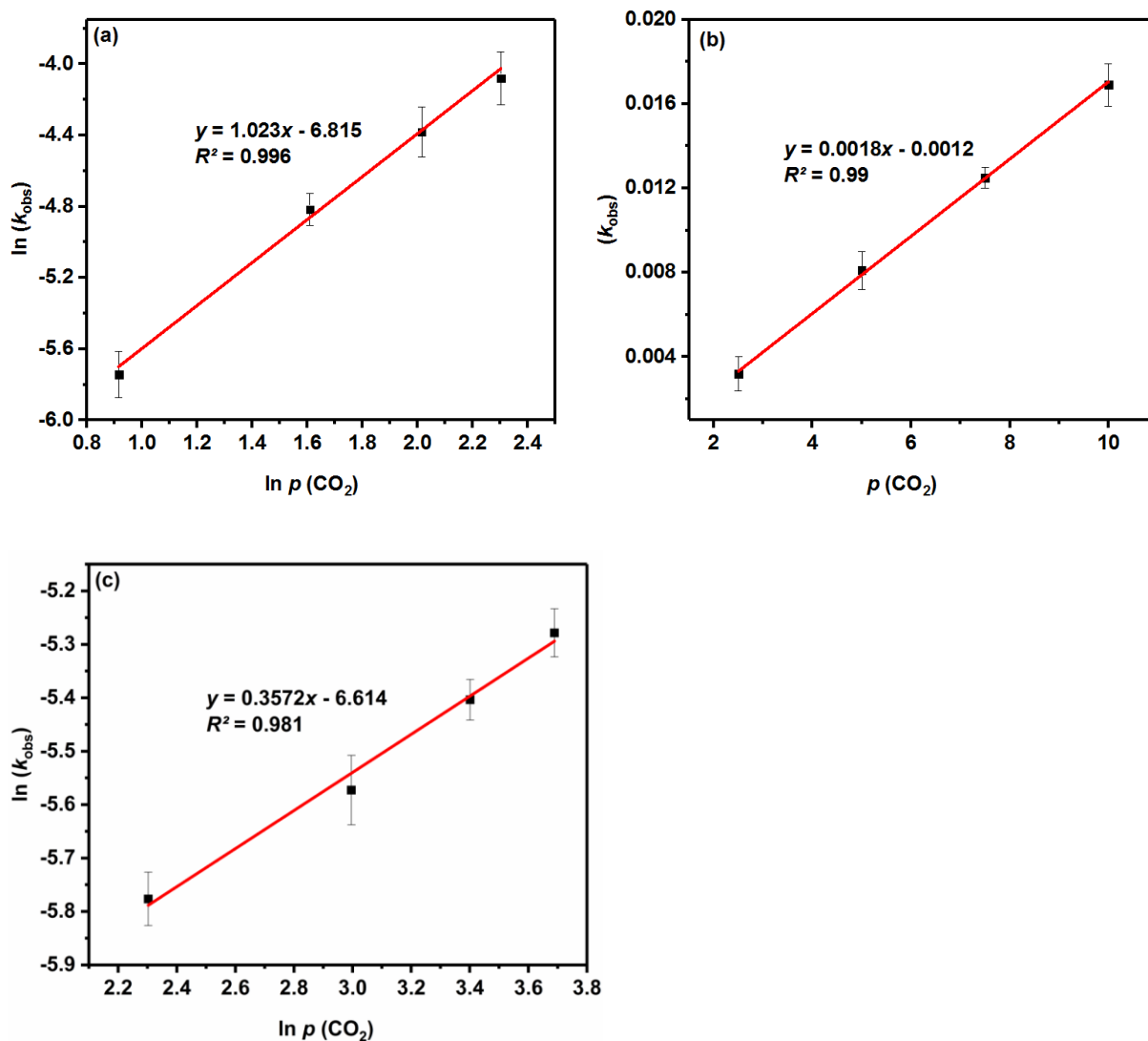


Figure 6.5 (a) Double logarithmic plot between ( $k_{\text{obs}}$ ) and  $p(\text{CO}_2)$  over the range of (2–10) bar (b) Plot showing a linear correlation between ( $k_{\text{obs}}$ ) and  $p(\text{CO}_2)$ , (c) Double logarithmic plot between ( $k_{\text{obs}}$ ) and  $p(\text{CO}_2)$  over the range of (10–40) bar (reaction conditions: 3.5 M SO, 76 mM [PPI], 38 mM [ $\text{ZnI}_2$ ], and 100 °C).

### 6.3.4 Temperature dependence and determination of activation parameters

The effect of temperature on the reaction rate was investigated by performing experiments at the range of (100–140) °C using both PPI as catalyst alone and PPI in combination with ZnI<sub>2</sub>. As expected, the rate of reaction increased with the increase in temperature and data points obtained exhibited a good fit to first order kinetics. The  $E_a$  for SC formation in the presence of PPI as catalyst alone was determined to be 78.47 kJ mol<sup>-1</sup> (Figure 6.6 a). However, when the temperature dependence of the reaction was studied using PPI in combination with ZnI<sub>2</sub>, the synergistic effect resulted in a significant decrease in  $E_a$  from 78.47 to 46.75 kJ mol<sup>-1</sup>. The  $E_a$  for SC formation was also determined using PPI in combination with ZnBr<sub>2</sub> and ZnCl<sub>2</sub> (Table 6.2). The difference amongst the activation energies for SC formation determined using different zinc halides as co-catalysts was not significant. Furthermore, the values of thermodynamic parameters such as  $\Delta H^\ddagger$ ,  $\Delta S^\ddagger$  and  $\Delta G^\ddagger$  were also determined by the Eyring equation (Figure 6.6 b) (Urry, 1982). The summary of the corresponding results is given in Table 6.2. The high positive values of  $\Delta H^\ddagger$  and  $\Delta G^\ddagger$  shows endergonic and chemically controlled nature of the cycloaddition reaction. Whereas, the large negative values of  $\Delta S^\ddagger$  indicate a highly ordered activated complex at the transition state.

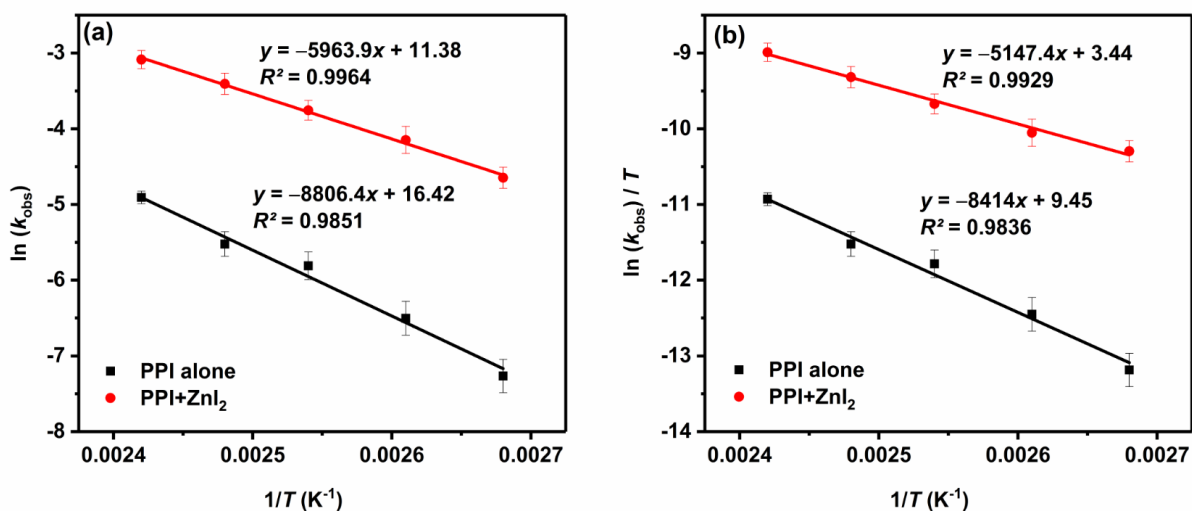


Figure 6.6 (a) Arrhenius plot for SC formation using PPI catalyst with and without ZnI<sub>2</sub> (b) Eyring plot for SC formation using PPI catalyst with and without ZnI<sub>2</sub>, (reaction conditions 3.5 M [SO], 76 mM [PPI], 38 mM [ZnI<sub>2</sub>], (100–140) °C and 10 bar  $p$  (CO<sub>2</sub>)).

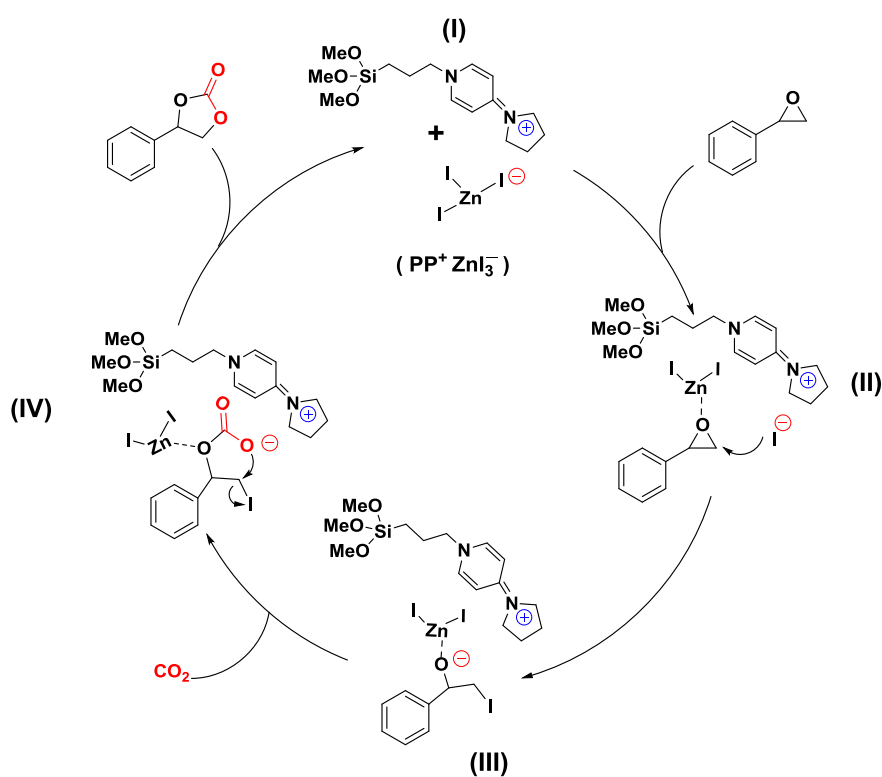
Catalyst type	Activation energy ( $E_a$ )	Enthalpy of activation ( $\Delta H^\ddagger$ )	Entropy of activation ( $\Delta S^\ddagger$ )	Gibbs free energy $\Delta G^\ddagger$ (a)
	(kJ mol <sup>-1</sup> )	(kJ mol <sup>-1</sup> )	(J mol <sup>-1</sup> K <sup>-1</sup> )	(kJ mol <sup>-1</sup> )
<b>PPI</b>	78.47±2.03	69.96±1.42	-77.86±1.41	99.01± 2.41
<b>PPI+ZnI<sub>2</sub></b>	45.27± 1.48	42.01± 1.80	-154.39± 2.52	99.62± 1.34

$$\Delta G^\ddagger \text{ (a)} = \Delta H^\ddagger - T \cdot \Delta S^\ddagger \text{ at } 373 \text{ K}$$

Table 6.2 Summary of activation parameters for SC formation using PPI catalyst with and without zinc halides as co-catalysts determined from Eyring equation.

## 6.4 Proposed reaction mechanism

Based on the detailed kinetics analysis, the reaction mechanism for SC formation in the presence of PPI/ $\text{ZnI}_2$  as a binary homogenous acid-based catalyst was proposed (Scheme 6.2). The combination of  $\text{ZnI}_2$  with PPI resulted in  $(\text{PP}^+ \text{ZnI}_3^-)$  as an active catalyst species **(I)**. The Lewis acidic Zn site activates the epoxide (SO) by the interaction with the oxygen atom of epoxide to form Zn-adduct **(II)**, which undergoes a nucleophilic attack by the iodo-anion (I) on the least sterically hindered carbon atom to form an iodo-alkoxide intermediate **(III)**. This further undergoes  $\text{CO}_2$ -insertion into the ring-opened epoxide to form a carbonate species **(IV)** which eventually leads to a five-membered ring of cyclic carbonate (SC) by the intramolecular elimination of the iodo-anion ( $\text{I}^-$ ), and the catalyst is regenerated.



Scheme 6.2 Proposed reaction mechanism for styrene carbonate (SC) formation catalysed by PPI and  $\text{ZnI}_2$ .

## 6.5 Summary

The reaction kinetics of SC formation from SO and CO<sub>2</sub> were investigated in the presence of PPI in combination with Zn halides (ZnCl<sub>2</sub>, ZnBr<sub>2</sub> and ZnI<sub>2</sub>). The synergistic effect of ZnI<sub>2</sub> and PPI resulted in a more than 10-fold increase in the reaction rate than PPI alone. The detailed study of reaction kinetics was carried out to give mechanistic insight and to determine the rate law for SC formation. As a result, the reaction has shown first-order dependence on SO and the catalyst concentrations. The reaction was also determined to be first-order with respect CO<sub>2</sub> over the pressure range of (2–10) bar, and clearly less than first-order (0.36) at higher *p* (CO<sub>2</sub>) (10–40) bar. The results of the kinetic analysis revealed that the formation of active species consists of a PP<sup>+</sup> ZnI<sub>3</sub><sup>-</sup> as an acid-base complex in the catalytic cycle leading to cyclic carbonate formation. The E<sub>a</sub> for SC formation catalysed by PPI alone was determined to be 77.3 kJ mol<sup>-1</sup>, which was reduced to 46.1 kJ mol<sup>-1</sup> using ZnI<sub>2</sub> in combination with PPI. The catalytic activity of zinc halides in combination with PPI was determined to be ZnI<sub>2</sub> > ZnBr<sub>2</sub> > ZnCl<sub>2</sub>. The positive values of ΔH<sup>‡</sup> and ΔG<sup>‡</sup> revealed an endergonic and chemically controlled nature of the reaction. Based on the kinetic study, a synergistic acid-based reaction mechanism was proposed.

## **Chapter 7 Styrene carbonate (SC) synthesis from styrene oxide (SO) and CO<sub>2</sub> using silica-supported pyrrolidinopyridinium iodide (SiO<sub>2</sub>-PPI).**

### **7.1 Introduction**

In this chapter, synthesis of styrene carbonate (SC) by CO<sub>2</sub> cycloaddition to styrene oxide (SO) was investigated in the presence of silica-supported pyrrolidinopyridinium iodide (SiO<sub>2</sub>-PPI) as an acid-base bifunctional heterogeneous catalyst. The catalyst was prepared by immobilizing pyrrolidinopyridinium iodide (PPI) on a silica support. A detailed study of heterogeneous kinetics was performed to understand the effect of reaction parameters and to investigate the reaction mechanism involved. The experimental results were correlated with pseudo-homogeneous (PH), Langmuir-Hinshelwood (LH) and Eley-Rideal (ER) heterogeneous kinetic models. The temperature dependence of the reaction was also studied to determine the kinetic and thermodynamic activation parameters.

### **7.2 Mixing dependence**

For heterogeneous catalysis, the overall rate of the reaction is not only influenced by the intrinsic kinetics but also depends on the external and internal mass transfer limitations (Yadav and Mehta, 1994). To investigate the effect of external mass transfer limitations on the reaction rate, experiments were performed under solvent-free conditions by varying the stirring speed from (200–800) rpm (Figure 7.1). The results showed that an increase in mixing rate had no substantial effect on the reaction rate, suggesting that the external mass transfer was not the limiting step.

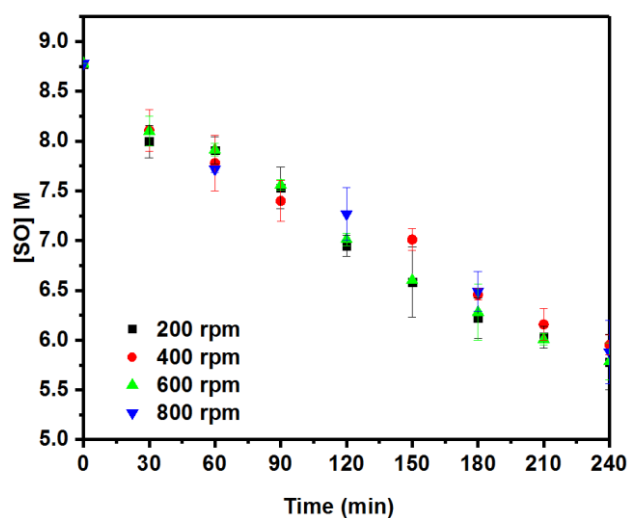


Figure 7.1 Effect of stirring speed on reaction rate (SO (Solvent-free), 76 mM [SiO<sub>2</sub>-PPI], 140 °C and 10 bar *p* (CO<sub>2</sub>)).

### 7.3 Reusability of SiO<sub>2</sub>-PPI

The reusability of SiO<sub>2</sub>-PPI catalyst for CO<sub>2</sub> cycloaddition to SO was also investigated. The results exhibited reasonably high maintenance of catalytic activity and selectivity towards SC formation, even after 5 runs (Figure 7.2). The nitrogen contents of the fresh and the spent SiO<sub>2</sub>-PPI catalysts were determined by elemental analysis. There was a slight decrease in the nitrogen content, from 2.14 wt % (0.76 mmol/g) in the fresh SiO<sub>2</sub>-PPI catalyst to 1.90 wt % (0.67 mmol/g) in the recovered catalyst, whereas the carbon content reduced from 12.78 wt % in the fresh catalyst to 11.23 wt % in the recovered catalyst. This was probably a result of leaching during the reaction and recycling steps.

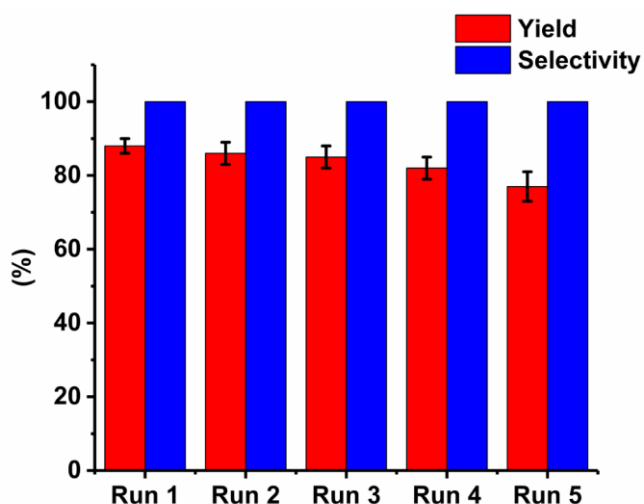


Figure 7.2 Reusability of the SiO<sub>2</sub>-PPI catalyst at 120 °C, 1 bar  $p$  (CO<sub>2</sub>), 76 mM [SiO<sub>2</sub>-PPI], 20 h.

#### 7.4 Effect of internal mass transfer limitations

The effect of internal mass transfer limitations on the reaction rate was determined from theoretical analysis based on Thiele's modulus ( $M_T$ ) and effectiveness factor (Eq 7.1). Where  $k$  is the pseudo-first-order rate constant for SC formation,  $r_s$  is the radius of catalyst particles assuming spherical (cm),  $De$  is the effective diffusion constant for the limiting reactant (cm<sup>2</sup>/sec). The effective diffusion constant ( $De$ ) was determined from (Eq 7.2), where  $D_A$  is the diffusion coefficient of the limiting reactant (cm<sup>2</sup>/sec),  $\epsilon_p$  is the porosity of the catalyst particles, and  $\tau_p$  is the tortuosity of the catalyst particles. The porosity and tortuosity of different materials are usually given in the range of (0.3–0.8) and (1.2–12), respectively (Veljković *et al.*, 2009). For silica particles, the values of  $\epsilon_p$  and  $\tau_p$  were determined from the literature i.e. 0.73 and 1.22 respectively (Barrande *et al.*, 2007).  $D_A$  can be calculated from the Wilke-Chang equation (Wilke and Chang, 1955) (Eq 7.3). The molar volume of the SO at its boiling point ( $V_{bA}$ ) was determined from the correlation between critical and molar volumes (Eq 7.4) (Sastri *et al.*, 1997). The value of  $M_T$  was determined to be  $4.81 \times 10^{-5}$ , which was less than the critical value ( $< 0.4$ ) required to obtain an effectiveness factor close to unity, suggesting that the reaction was not internally mass transfer limited (Levenspiel, 1999). The calculations of  $M_T$  are shown in Appendix D.

$$M_T = \frac{r_s}{3} \sqrt{\frac{k}{De}} \quad (7.1)$$

$$De = \frac{D_A \cdot \epsilon_p}{\tau_p} \quad (7.2)$$

$$D_A = 7.4 \times 10^{-8} \frac{T \cdot (MW)^{0.5}}{\eta \cdot (V_{bA})^{0.6}} \quad (7.3)$$

$$V_{bA} = \frac{V_c}{2.68} \quad (7.4)$$

## 7.5 Kinetics study of CO<sub>2</sub> cycloaddition to SO using SiO<sub>2</sub>-PPI catalyst

From the results of mixing study and calculation of the Thiele's modulus ( $M_T$ ), no internal or external mass transfer limitations were found during the reaction, indicating that both adsorption and desorption steps involved in this heterogeneous catalysis kinetics are instantaneous and the surface reaction is the rate-determining step. The experimental results of kinetic experiments were correlated with pseudo-homogeneous, Eley-Rideal (ER) and Langmuir-Hinshelwood (LH) heterogeneous kinetic models. The effect of temperature on cycloaddition of CO<sub>2</sub> to SO was studied over the range of (100–180) °C and keeping otherwise reaction parameters constant i.e. 76 mM SiO<sub>2</sub>-PPI catalyst and 10 bar of  $p$  (CO<sub>2</sub>). The rate of reaction increased with the temperature due to higher catalytic activity at a higher temperature. Figure 7.3 (a, b) clearly shows that the experimental data was not found to be fit with pseudo-homogeneous and LH heterogeneous kinetic models. This indicates that the reaction does not take place between SO and CO<sub>2</sub> in the bulk fluid phase (Pseudo-homogeneous model), nor between both SO and CO<sub>2</sub> adsorbed on the catalytic active sites (LH heterogeneous model). However, the experimental data was found to be a good fit to the combined ER mechanism (Figure 7.3 c), assuming SO adsorbed over the catalyst surface reacting with CO<sub>2</sub> present in the bulk reaction mixture or adsorbed CO<sub>2</sub> reacting with the SO present in the bulk, suggesting two possible reaction mechanisms occurring at the same time. Based on the combined ER kinetic model, the activation energy ( $E_a$ ) for SC formation was determined from the Arrhenius plot (Figure 7.3 d). The  $E_a$  for SC formation was determined to be 64.93 kJ mol<sup>-1</sup> which was less than  $E_a$  determined for the SC formation in the presence of homogeneous analogue (PPI alone) i.e. 78.47 kJ mol<sup>-1</sup> (Rehman *et al.*, 2018a). The increase in catalytic activity of SiO<sub>2</sub>-PPI was observed due to the synergistic effect of the halide anion ( $I^-$ ) combined with the acidic surface (Si–OH group) provided by the silica. The Si–OH acts as weak acidic sites to activate the epoxide by the interaction with the oxygen atom of the epoxide and favours the epoxide ring-opening by the nucleophilic attack of iodide anion ( $I^-$ ). The increase in catalytic activity by immobilization of basic homogeneous catalyst

over the acidic catalytic support was also reported previously (Takahashi *et al.*, 2006; Hajipour *et al.*, 2015).

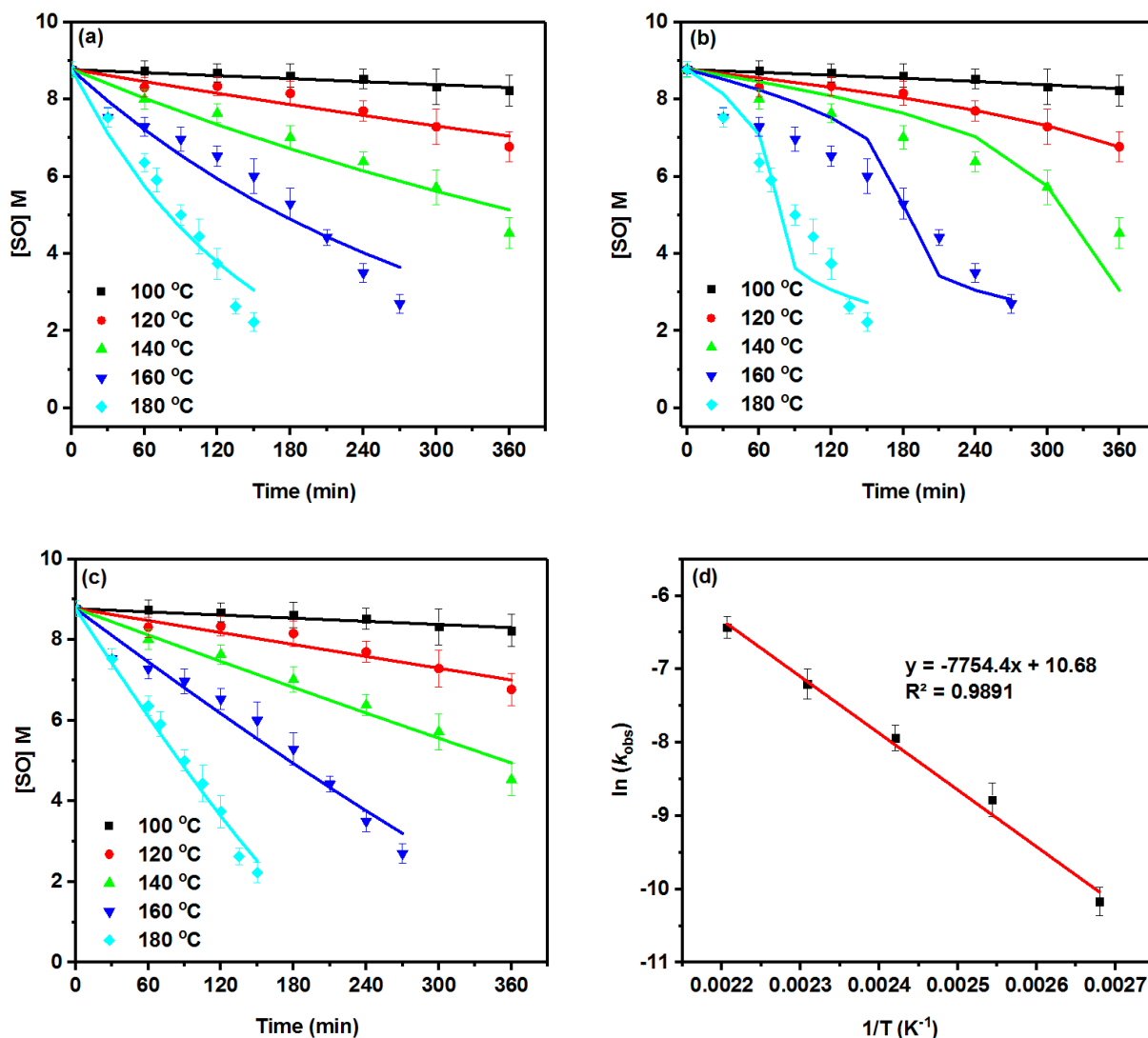


Figure 7.3 Kinetic models and experimental data for the conversion of SO to SC (a) Pseudo-homogeneous model (b) LH model (c) ER model with combined SO and CO<sub>2</sub> adsorption (d) Arrhenius plot to determine the activation energy for SC formation (dots: experimental data, lines: model), (reaction conditions: solvent-free SO, 76 mM [SiO<sub>2</sub>-PPI], (100–180) °C, 10 bar of  $p$  (CO<sub>2</sub>) for (0–360) min reaction time).

The thermodynamic activation parameters were also determined based on the ER mechanism, using the Eyring equation (Figure 7.4). A summary of the results is shown in Table 7.1. The positive values of  $\Delta H^\ddagger$  and  $\Delta G^\ddagger$  indicate the endergonic and chemically controlled nature of the reaction. Similarly, the negative value of  $\Delta S^\ddagger$  shows that the adsorption of the epoxide led to the formation of an activated complex between epoxide and catalyst grafted over the silica surface, suggesting that the adsorption process involves an associative mechanism (Doğan *et al.*, 2009; Saha and Chowdhury, 2011).

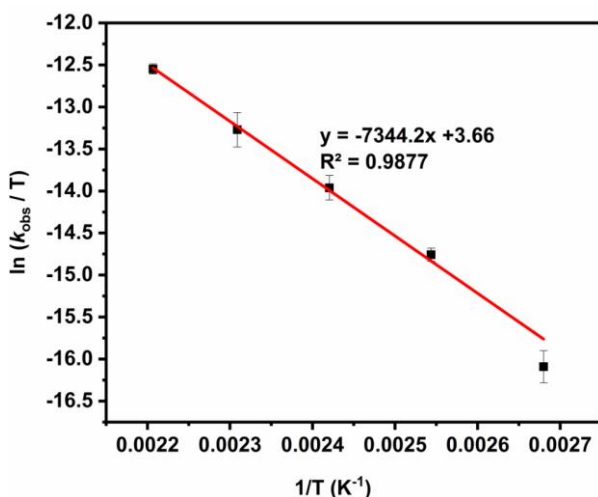


Figure 7.4 Eyring plot for SC formation over the range of (100–180) °C using SiO<sub>2</sub>-PPI catalyst.

Enthalpy of activation ( $\Delta H^\ddagger$ )	Entropy of activation ( $\Delta S^\ddagger$ )	Gibbs free energy				
		$\Delta G^\ddagger = \Delta H^\ddagger - T \cdot \Delta S^\ddagger$ (kJ mol <sup>-1</sup> )				
(kJ mol <sup>-1</sup> )	(J mol <sup>-1</sup> K <sup>-1</sup> )	373 K	393 K	413 K	433 K	453 K
61.53	-149.03	117.14	119.19	122.17	125.15	128.13
±0.94	± 0.75	±1.21	± 0.29	± 0.31	± 0.37	± 0.33

Table 7.1 Summary of activation parameters for SC formation from SO and CO<sub>2</sub> using SiO<sub>2</sub>-PPI catalyst determined from the Eyring equation.

## 7.6 Determination of the reaction orders with respect to SO, CO<sub>2</sub> and SiO<sub>2</sub>-PPI

The order of reaction with respect to the SO was determined using five different concentrations (1.5–5.5) M SO in PC at 140 °C and 10 bar  $p$  (CO<sub>2</sub>) using 76 mM SiO<sub>2</sub>-PPI. The decrease in the SO concentration was monitored as a function of time by taking aliquots from the reaction mixture after a regular time interval. The graph between the reaction rate (mol L<sup>-1</sup> min<sup>-1</sup>) and initial [SO] was linear, suggesting a first-order reaction in epoxide concentration (Figure 7.5 a). The order of the reaction was also confirmed by an integrated law method (Hinde, 1997). From the results obtained, all the data points were found to be fit with first-order kinetics i.e. ln [SO] vs time (Figure 7.5 b). The first-order dependence of the reaction w.r.t epoxide suggests the involvement of one molecule of epoxide in the catalytic cycle (Cuesta-Aluja *et al.*, 2016).

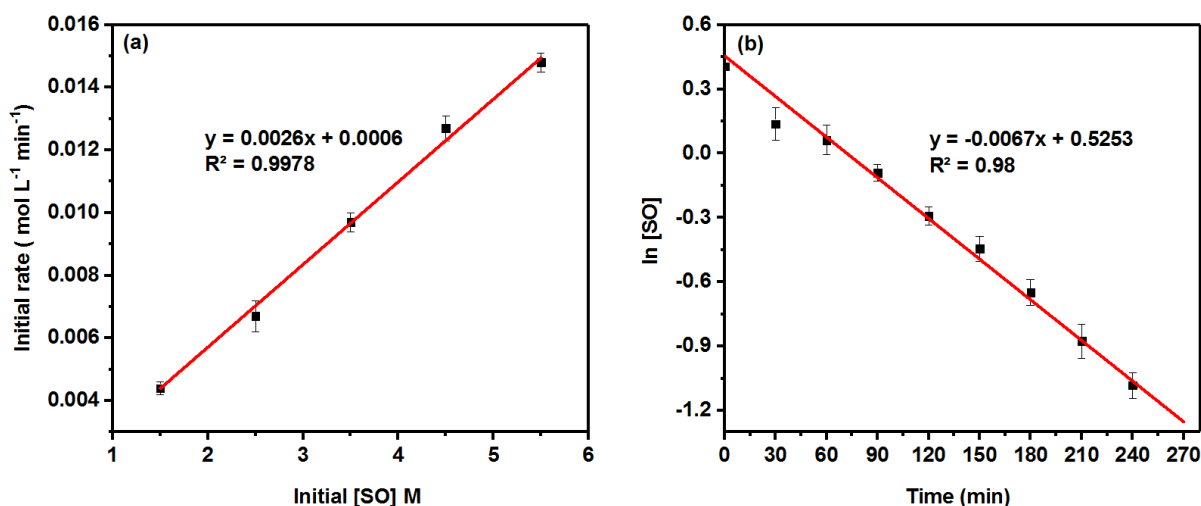


Figure 7.5 (a) Plot showing the linear correlation between initial reaction rate (mol L<sup>-1</sup> min<sup>-1</sup>) and initial [SO] over the range of (1.5–5.5) M SO (b) Plot showing a linear fit of all the data points to first-order kinetics for 1.5 M SO, (reaction conditions: 76 mM [SiO<sub>2</sub>-PPI], 140 °C and 10 bar  $p$  (CO<sub>2</sub>)).

To determine the order of the reaction with respect to the CO<sub>2</sub>, the experiments were performed by varying the CO<sub>2</sub> pressure over the range of (2.5–10) bar while keeping other reaction parameters constant i.e. 140 °C and 76 mM SiO<sub>2</sub>-PPI. The rate of CO<sub>2</sub> dissolution in SO is much faster than the rate of cycloaddition reaction (Pohorecki and Možeński, 1998b). Therefore, a rapid equilibrium will be established between the CO<sub>2</sub> dissolved and CO<sub>2</sub> above the reaction mixture. The results indicate that the rate of reaction increased linearly with the increase in CO<sub>2</sub> concentration in the reaction mixture. All the data points were found to be fit in first-order kinetics (Figure 7.6 a). Moreover, the order of the reaction was determined from

the double logarithmic plot between  $k_{\text{obs}}$  versus  $p(\text{CO}_2)$  with a gradient of 1.12 which clearly indicates the first-order dependence of the reaction (Figure 7.6 b). This was further confirmed by the plot of  $k_{\text{obs}}$  against  $p(\text{CO}_2)$  showing a good fit to the straight line ( $R^2 = 0.99$ ), almost passing through the origin (Figure 7.6 c). A similar order of cycloaddition reaction w.r.t  $\text{CO}_2$  was reported previously (North and Pasquale, 2009; Dengler *et al.*, 2011). These results suggest the involvement of one molecule of  $\text{CO}_2$  in the catalytic cycle (North and Pasquale, 2009).

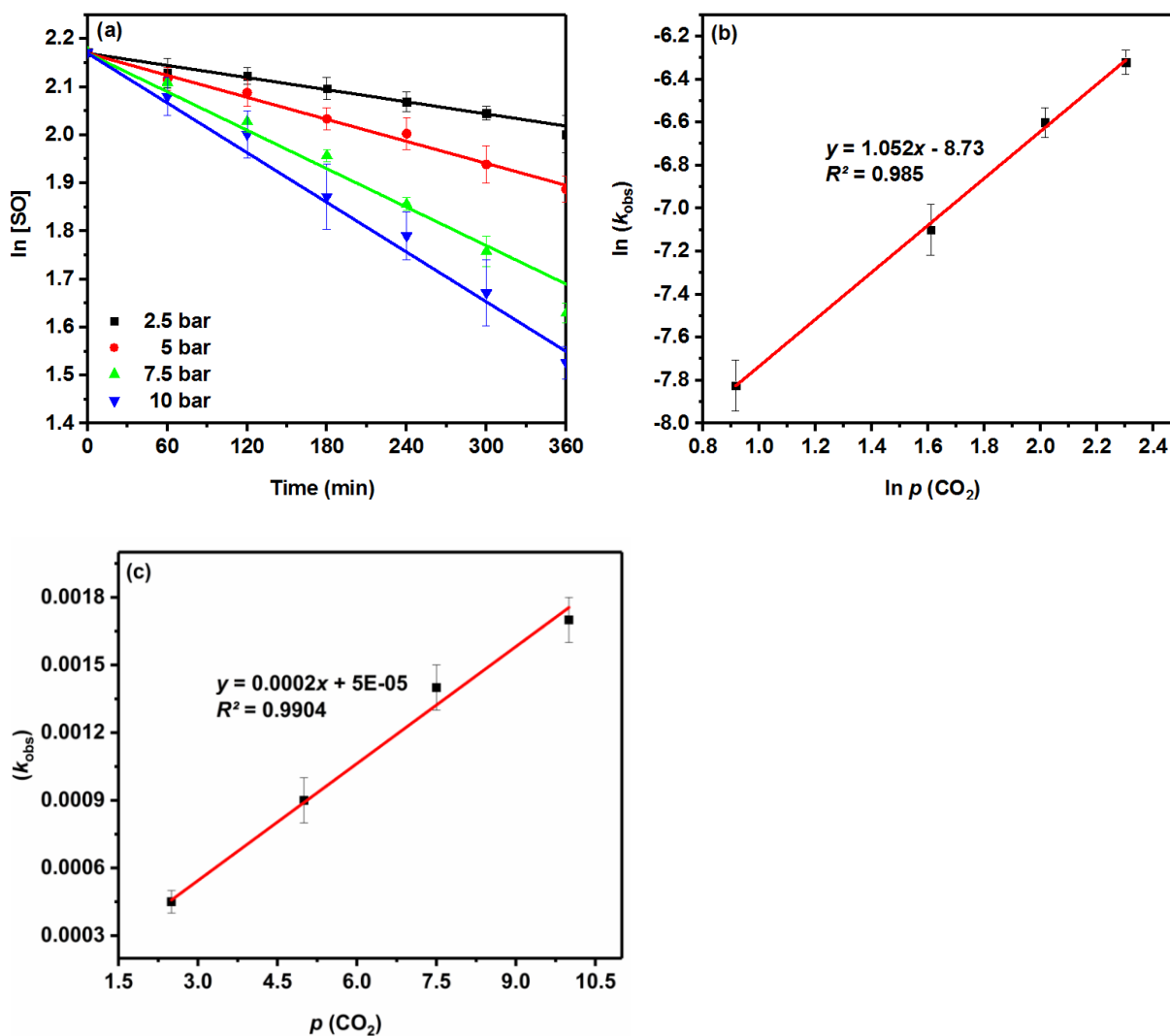


Figure 7.6 (a) First-order kinetic plots i.e.  $\ln[\text{SO}]$  against reaction time (min) over the pressure range of (2.5–10) bar  $p(\text{CO}_2)$  (b) Double logarithmic plot between  $(k_{\text{obs}})$  and  $p(\text{CO}_2)$  to determine the order of reaction w.r.t  $\text{CO}_2$  (c) Plot of the observed rate constant  $(k_{\text{obs}})$  against  $p(\text{CO}_2)$  showing a linear correlation, (reaction conditions: SO, 76 mM  $[\text{SiO}_2\text{-PPI}]$ , 140 °C).

The order of reaction with respect to the SiO<sub>2</sub>-PPI catalyst was determined over the range of (38–152) mM. The rate of the reaction increased with the catalyst concentration and all data points exhibit a good fit to first-order kinetics (Figure 7.7 a). The double logarithmic graph between  $k_{\text{obs}}$  and [SiO<sub>2</sub>-PPI] shows a linear dependence with a slope of 0.93~1, suggesting first-order dependence with respect to [SiO<sub>2</sub>-PPI] (Figure 7.7 b). These results were found in contrast to some of the previous studies for epoxide/CO<sub>2</sub> cycloaddition reactions catalysed by bifunctional catalyst systems, suggesting a binuclear reaction pathway with the involvement of two catalyst molecules to form an active catalyst (Dengler *et al.*, 2011; Martín and Kleij, 2014). However, the order of the reaction w.r.t catalyst obtained in this study seems reasonable, since the role of the SiO<sub>2</sub>-PPI catalyst is to provide weak acidic Si–OH sites for epoxide activation and subsequent ring-opening of the activated epoxide by the nucleophilic attack of halide anion ( $\text{I}^-$ ) to form a halo-alkoxide intermediate. This intermediate further undergoes CO<sub>2</sub> insertion and ring-closure steps to form the corresponding cyclic carbonate. Therefore, it is expected that only one mole of SiO<sub>2</sub>-PPI would be required for the ring-opening of a mole of the epoxide.

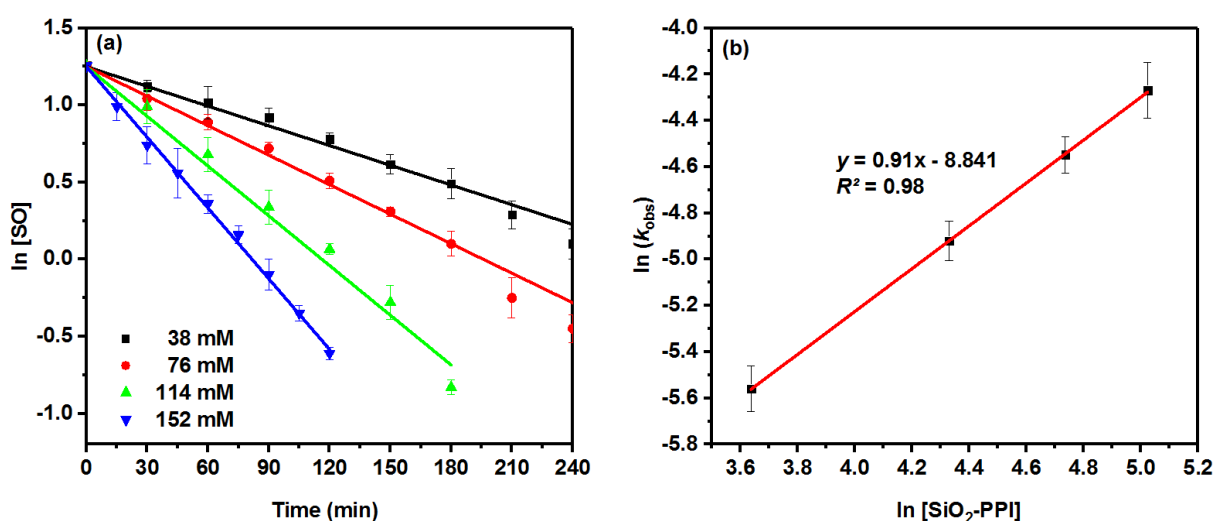
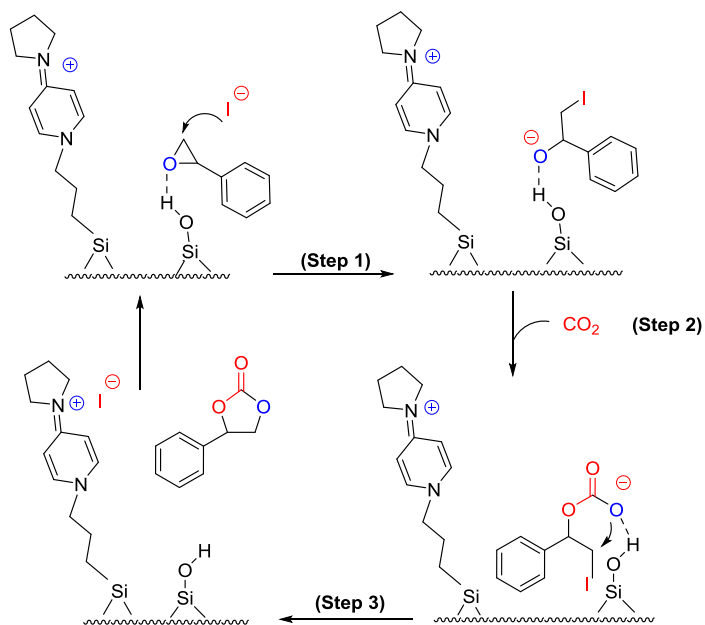


Figure 7.7 (a) First-order kinetic plots i.e.  $\ln [\text{SO}]$  against reaction time (min) over the range of (38–152) mM [SiO<sub>2</sub>-PPI], (b) Double logarithmic plot between ( $k_{\text{obs}}$ ) and [SiO<sub>2</sub>-PPI] to determine the order of reaction w.r.t SiO<sub>2</sub>-PPI, (reaction conditions: 3.5 M SO, 140 °C and 10 bar  $p$  (CO<sub>2</sub>)).

## 7.7 Proposed reaction mechanisms

Based on the detailed kinetic study above, the ER reaction mechanisms were proposed for SC formation from SO and CO<sub>2</sub> in the presence of SiO<sub>2</sub>-PPI catalyst. The most commonly accepted reaction mechanism for CO<sub>2</sub> cycloaddition to SO in the presence of an acid-base catalyst can be given as Scheme 7.1. The reaction initiates by the adsorption of SO on the silica surface whereas CO<sub>2</sub> was present in the bulk of the reaction mixture. The silanol groups (Si–OH) present over the silica surface act as acidic sites to activate the SO by the interaction with the oxygen atom of the epoxide. Subsequently, the activated SO experiences a nucleophilic attack by the I<sup>−</sup> provided by the immobilized PPI acting as the basic site of the catalyst. This results in the formation of an iodo-alkoxide intermediate by the ring-opening of the activated epoxide (Step 1). The stability to this ring-opened intermediate was provided by the large delocalised pyrrolidinopyridinium (PP<sup>+</sup>) cations to facilitate rapid CO<sub>2</sub> insertion. This intermediate further coordinates with the CO<sub>2</sub> present in the bulk of reaction medium by the nucleophilic attack of the iodo-alkoxide intermediate on the electrophilic C atom of CO<sub>2</sub> to form a carbonate intermediate (Step 2). Finally, this open-chain carbonate intermediate undergoes ring-closure by the intramolecular elimination of iodide anion to form a five-membered ring of SC and the catalyst is regenerated in the catalytic cycle (Step 3).



Scheme 7.1 Proposed mechanism of SC formation based on the reaction of adsorbed SO with CO<sub>2</sub> in the bulk stream.

## 7.8 Summary

Synthesis of SC from SO and CO<sub>2</sub> was successfully carried out in the presence of SiO<sub>2</sub>-PPI as an acid-based heterogeneous catalyst. The catalyst has exhibited reasonably high maintenance of catalytic activity and selectivity towards SC formation, even after 5 runs. The reaction kinetics for cycloaddition of CO<sub>2</sub> and SO using SiO<sub>2</sub>-PPI catalyst revealed that the reaction follows a combined ER model. The cycloaddition reaction exhibited first-order dependence on epoxide, CO<sub>2</sub> and SiO<sub>2</sub>-PPI concentrations. Moreover, the E<sub>a</sub> obtained for SC formation in the presence of SiO<sub>2</sub>-PPI was found to 64.93 kJ mol<sup>-1</sup>, which was lower than using the homogeneous analogue (PPI) due to the synergistic effect of Si-OH in combination with halide anion. The thermodynamic parameters of the reaction determined from the Eyring equation showed that the reaction was endergonic and chemically controlled in at conditions used. Based on the kinetic study, two possible ER reaction mechanisms for SC formation from cycloadditions of CO<sub>2</sub> to SO have been proposed.

## Chapter 8 Conclusions and Further Work

### 8.1 Conclusions

The aim of this study was to demonstrate process development and improvement in the synthesis of terpene carbonates, with a view to their future use as renewable monomers. To this end, limonene carbonate (LC) was successfully produced, and the catalytic role of tetrabutylammonium halides was evaluated. Reactor engineering was investigated in the shape of a novel 'tube-in-tube' gas/liquid reactor with exceptionally high permeation of CO<sub>2</sub> through the semi-permeable AF-2400 membrane. This necessitated the use of terminal epoxide such as styrene oxide (SO) rather than challenging limonene oxide (LO) for the proof-of-concept. The use of a continuous flow reactor significantly enhances the efficiency of epoxide/CO<sub>2</sub> cycloaddition reaction than in a convention batch reactor. The potential for the carbonation of SO to be further intensified was investigated via a study of the synergistic effects of pyrrolidinopyridinium iodide (PPI) and zinc halides (ZnX<sub>2</sub>) acting as a binary homogeneous catalyst system. This system was developed further by heterogenising the PPI onto silica. In all cases, a detailed kinetic study of cyclic carbonate synthesis was carried out to determine the corresponding kinetic values ( $k$  and  $E_a$ ) and activation parameters ( $\Delta H^\ddagger$ ,  $\Delta S^\ddagger$  and  $\Delta G^\ddagger$ ).

The synthesis of cyclic carbonates from limonene, in particular, is of significant interest as it is bio-renewable monomer for the production of fully bio-based polymers such as non-isocyanate polyurethanes (NIPUs), which have potential applications as thermoset materials, elastomers, or thermoplastics. Bio-based limonene oxide (LO) is a tri-substituted epoxide containing an internal epoxide attached to the highly substituted, bulky structure of limonene. Due to the high steric hindrance on the internal epoxide, LO is a challenging substrate for CO<sub>2</sub> cycloaddition. Recently, amino triphenolate based aluminium complexes were used as catalysts in combination with nucleophilic additives showing activity towards di- and tri-substituted epoxides. However, preparation of these catalysts involves several steps. Alternatively, tetrabutylammonium halides have been extensively studied as nucleophile additives for the cycloaddition of CO<sub>2</sub> to epoxides due to their strong nucleophilicity and commercial availability. Particularly, for internal epoxides where the steric hindrance plays an important to decide the activity of the catalyst, the use of small nucleophiles is highly

advantageous compared to bulky catalyst system. In this study, a 100% selective synthesis of sustainable cyclic carbonates from bio-based LO and CO<sub>2</sub> was carried out using a commercially available, inexpensive TBAC as an effective homogeneous catalyst. The initial studies of cycloaddition from a commercially available LO (a mixture of *cis* and *trans*-LO) revealed that the reaction was stereoselective and the *trans*-isomer was found to be more reactive than the *cis*-isomer. To overcome the low reactivity of commercially available limonene oxide, stereoselective epoxidation of limonene has been carried out to achieve a significantly higher yield of the reactive *trans*-isomer (87%), leading to high conversions to limonene cyclic carbonate. The rate of reaction was found to be more than 3-fold higher using *trans*-enriched LO compared to commercial LO mixture under the same reaction conditions. Moreover, the catalytic activity of halide anions for the cycloaddition reaction was studied using different tetrabutylammonium halides and the order of reactivity was found to be  $\text{Cl}^- > \text{Br}^- > \text{I}^- > \text{F}^-$  which is consistent with nucleophilicity of halide anions except  $\text{F}^-$  showing low reactivity due to its poor leaving group ability. Moreover, a detailed study of reaction kinetics was carried out in the presence of PC as a greener polar aprotic solvent. The results indicate the reaction was first-order with respect to LO, TBAC and CO<sub>2</sub> concentrations. The activation energy ( $E_a$ ) calculated for LC synthesis was found to be 64 kJ mol<sup>-1</sup>. This high value of a kinetic barrier for cyclic carbonate synthesis from internal epoxides show the challenging nature of internal epoxides. The high positive value of free energy and negative value of activation entropy obtained from Eyring plot, indicate that the reaction was endergonic and kinetically controlled. Moreover, a reaction mechanism was also proposed which is in agreement with the generally accepted mechanism for cyclic carbonate synthesis and highlight the importance of small nucleophiles when such reactions are performed with highly substituted epoxides. The use of bio-based resources will not only help to make processes more sustainable but also should generate new products such as bio-based polymers and green solvents.

Despite the advantages of flow chemistry and development of highly efficient catalytic systems, only a few studies of cyclic carbonate synthesis in continuous flow conditions have been reported. In this study, reactor engineering was investigated in the shape of a novel 'tube-in-tube' gas/liquid reactor with exceptionally high permeation of CO<sub>2</sub> through the semi-permeable AF-2400 membrane. This necessitated the use of terminal epoxide such as styrene oxide (SO) rather than challenging limonene oxide (LO) for the proof-of-concept. The use of a continuous flow reactor significantly enhances the efficiency of epoxide/CO<sub>2</sub> cycloaddition

reaction than in a conventional batch reactor. In order to increase the effective (interfacial) surface area, and thus to increase the gas availability in the solution, styrene carbonate (SC) synthesis from styrene oxide (SO) and CO<sub>2</sub> was carried out in 'tube-in-tube' gas-liquid continuous flow reactor. The reaction was performed in the presence of commercially available, inexpensive TBAB and ZnBr<sub>2</sub> as a highly active combined catalyst system. The performance of the flow reactor was evaluated by studying the effect of various operating conditions such as reaction temperature, CO<sub>2</sub> pressure, and residence time. The exceptionally high permeation of CO<sub>2</sub> through the semi-permeable AF-2400 membrane combined with the high surface area to volume ratio resulted in quantitative conversion to SC in 45 min at 120 °C and 6 bar *p* (CO<sub>2</sub>) using ZnBr<sub>2</sub>/TBAB 1:4 molar ratio. The continuous reactor generates homogeneous solutions of gas in the liquid in a reliable and controlled manner, thereby facilitating rapid optimization of the reaction, which can greatly enhance the efficiency (rate) of the reaction as compared to the conventional batch reactor. The reaction rates were approximately twice as high in the flow reactor as in a conventional batch reactor, due to the enhanced rate of mass transfer due to rapid diffusion of CO<sub>2</sub> through the membrane. The synergistic catalytic effect between TBAB and ZnBr<sub>2</sub> enhanced the reaction rate by more than 6-fold compared to TBAB alone. A detailed kinetic study of reaction kinetics was carried out to find the initial rate law equation. The detailed study of reaction kinetics suggests a first-order dependence of the reaction with respect to SO, CO<sub>2</sub> and TBAB and a non-first-order dependence on ZnBr<sub>2</sub> when used in conjunction with TBAB. The activation energy of the reaction in the presence of TBAB alone was calculated to be 53 kJ mol<sup>-1</sup>, which was reduced to 34 kJ mol<sup>-1</sup> when using ZnBr<sub>2</sub> in combination with TBAB. Based on the detailed kinetic study, a reaction mechanism was proposed explaining the synergistic role of the acid-base binary homogeneous catalyst. Based on the detailed kinetic study, a reaction mechanism was proposed explaining the synergistic role of the acid-base binary homogeneous catalyst. This study has demonstrated the novel concept of process intensification by speeding the kinetics of the reaction and significantly reducing the reaction time of cyclic carbonate synthesis.

The potential for the carbonation of SO to be further intensified was investigated via a study of the synergistic effects of pyrrolidinopyridinium iodide (PPI) and zinc halides (ZnX<sub>2</sub>) acting as a binary homogeneous catalyst system. The synergistic effect of ZnI<sub>2</sub> and PPI resulted in a ~10-fold increase in the reaction rate compared to PPI alone. Almost complete conversion of the SO to SC was achieved in 3 h with 100% selectivity using 1:0.5 molar ratio PPI/ZnI<sub>2</sub> at 100 °C and 10 bar *p* (CO<sub>2</sub>). Although synthesis of cyclic carbonates has been broadly

investigated using various catalyst systems with higher conversion and yield of the product, a comprehensive kinetics study is required to investigate the reaction mechanism. In this study, a series of experiments were performed to determine the rate law in order to examine the kinetic parameters and ultimately to enable the synergistic mechanism hypothesis to be tested. Studies of the reaction kinetics revealed that the formation of active species consists of  $PP^+ZnI_3^-$  as an acid-base complex in the catalytic cycle leading to cyclic carbonate formation. The role of zinc halides in catalyst cycle is to activate the epoxide by Lewis acidic  $Zn^{+2}$  site through the formation of the zinc-epoxide adduct, which facilitates epoxide ring opening by the nucleophilic attack of halide anion ( $X^-$ ) on the least hindered C atom of epoxide. The reaction exhibited first-order dependence with respect to SO,  $CO_2$  and PPI/ $ZnI_2$  concentrations. The activation energy ( $E_a$ ) for SC formation catalysed by PPI alone was determined to be  $78\text{ kJ mol}^{-1}$ , which was reduced to  $47\text{ kJ mol}^{-1}$  due to the synergistic effect of using  $ZnI_2$  in combination with PPI. Moreover, the positive values of  $\Delta H^\ddagger$  and  $\Delta G^\ddagger$  determined from the Eyring equation suggesting endergonic and chemically controlled nature of the reaction. Based on the detailed kinetic study, a reaction mechanism was suggested, explaining the *modus operandi* of the binary homogeneous catalyst.

Heterogeneous catalysis for cyclic carbonate synthesis was less extensively studied than their homogeneous counterparts. The use of heterogeneous catalysts still had some potential shortcomings due to the requirement of harsh reaction conditions, use of co-catalysts (nucleophiles) in a homogeneous phase and loss in catalytic activity in consecutive runs. To solve these issues, the immobilizing of active homogeneous catalysts on high surface area supports are required. In this study, the system was developed further by heterogenising the PPI onto silica. From the past few years, heterogeneous catalysts for cyclic carbonate synthesis have gained much attention due to ease of separation and recyclability, thereby avoiding extensive use of solvents in downstream processes. To facilitate catalyst separation and to reuse the catalyst for consecutive runs, the immobilizing of active homogeneous catalysts on high surface area inorganic support such as high surface silica was considered as a promising approach. In this study, the potential for the carbonation of SO to be further intensified was investigated by heterogenising the PPI onto silica.  $SiO_2$ -supported aminopyridinium halides also have several advantages over other alkylammonium halide based catalysts, such as the presence of a long chain of delocalized cations in resonance form, facile methods of preparation and high stability in the air. Almost quantitative conversion of the SO to SC was achieved with 100% selectivity using 76 mM  $SiO_2$ -PPI catalyst at  $180\text{ }^\circ\text{C}$

and 10 bar  $p$  ( $\text{CO}_2$ ) after 3 h. The catalyst exhibited reasonably high maintenance of catalytic activity and selectivity towards SC formation even after 5 runs. Synthesis of cyclic carbonates by  $\text{CO}_2$  cycloaddition to epoxides has been carried out in the presence of various heterogeneous catalyst systems. However, to the best of our knowledge, no kinetic study for cycloaddition reaction using a heterogeneous catalyst has been reported. The experimental results and theoretical analysis based on Thiele modulus and the effectiveness factor revealed the absence of external and internal mass transfer limitations. The experimental results were found to be a better fit with Eley-Rideal (ER) model than the Langmuir Hinshelwood (LH) or pseudo-homogeneous models. The reaction exhibited first-order dependence with respect to SO,  $\text{CO}_2$  and  $\text{SiO}_2$ -PPI concentrations. The activation energy ( $E_a$ ) for SC formation in the presence of  $\text{SiO}_2$ -PPI was found to be  $64.14 \text{ kJ mol}^{-1}$  over the range of (100–180) °C, which was lower than when the reaction was catalysed by the homogeneous analogue (PPI) due to the synergistic effect of the halide anions in combination with acidic Si–OH (silanol) surface. Based on the kinetic analysis, a reaction mechanisms for SC formation were proposed.

## 8.2 Further work

### 8.2.1 New substrate

In this study, the synthesis of cyclic carbonates was carried out using bio-based limonene oxide (LO) as a renewable substrate for cycloaddition reaction. However, further studies should also be performed using other bio-based epoxides such as epoxides derived from pinene, menthene, carvone oxide, linalool and vegetable oils to minimize the dependence on petroleum-derived raw materials. The use of bio-based resources will not only help to make processes more sustainable but also should generate new products such as bio-based polymers and green solvents. Bio-derived polymers frequently have desirable properties such as biodegradability, hydrophobicity, bioactivity and liquid crystallinity.

Epoxidation of terpenes is of particular interest as these products have many commercial applications. For instance, pinene (C<sub>10</sub>H<sub>16</sub>) is a bicyclic monoterpene, having two isomeric chemical structures:  $\alpha$ -pinene and  $\beta$ -pinene. These are the main constituents of turpentine oil obtained by distillation of pine gum.  $\alpha$ -pinene is also obtained as a by-product of the paper industry from the Kraft process. Due to its abundance as a waste by-product and suitability for organic synthesis in the presence of two double bonds, it can be used as a sustainable replacement for petrol-based epoxides without competing with food crops. This approach will not only help to overcome the threat of an increasing shortage of fossil resources but also eliminate the production of toxic intermediates in the polymer industry.

### 8.2.2 CO<sub>2</sub> cycloaddition to limonene oxide (LO) under mild reaction conditions

In this study, the synthesis of cyclic carbonate from CO<sub>2</sub> cycloaddition to LO be carried out in the presence of TBAC as a homogeneous catalyst at relatively extreme reaction conditions i.e. (100–140) °C, (10–40) bar and 6 mol% catalyst loading. The challenge from a sustainability standpoint is to carry out the reaction selectively and efficiently under milder conditions (P = 5–10 bar, T < 100 °C, 1–2 mol% catalyst loading). Recently, Castro-Osma *et al.* (2016) reported chromium salphen complexes in combination with TBAB exhibiting high catalytic activity towards challenging internal epoxides. However, the cycloaddition reaction takes place at elevated temperature and pressure i.e. 50 °C and 10 bar *p* (CO<sub>2</sub>) using 1.5 mol% catalyst loading. Therefore, more catalyst systems for CO<sub>2</sub> cycloaddition to bio-based epoxides must be developed in the future to carry out the reaction under milder conditions.

This will allow further intensification of the process by performing the reaction in continuous flow reactors having a high surface area to volume ratio.

### **8.2.3 Cyclic carbonate synthesis by oxidative carboxylation of d-limonene**

Future research also needs to focus on the development of direct cyclic carbonates synthesis by oxidative carboxylation of d-limonene. This could be achieved by the development of multifunctional catalyst having the ability to catalyse both oxidation and cycloaddition reactions with high selectivity. For instance, Chen *et al.* (2011) reported oxidative carboxylation of cyclohexene in the presence of TBHP as an oxidant. Here, molybdenyl acetylacetonate  $\text{MoO}_2(\text{acac})_2$  was used as a catalyst for the epoxidation step to produce CHO. Subsequently, the cycloaddition of  $\text{CO}_2$  to CHO was performed using TBAB catalyst resulting 84% yield at 140 °C and 30 bar  $p$  ( $\text{CO}_2$ ) after 6 h, which is the highest reported yield by oxidative carboxylation of cyclohexene. Therefore, this catalyst system is likely to be used for oxidative carboxylation of d-limonene. Synthesis of cyclic carbonates via this route will help to make the process more economical by decreasing the cost involved in epoxidation, purification, handling of epoxide and thus increase the sustainability of the process.

### **8.2.4 Cyclic carbonate synthesis from industrial flue gases**

The tube-in-tube gas/liquid continuous flow reactor has an exceptionally high permeability for  $\text{CO}_2$  compared to other gases, therefore, it can be potentially used for cyclic carbonate synthesis from flue gases as an indirect source of  $\text{CO}_2$ . For instance, a nearly pure  $\text{CO}_2$  is generated by the industries containing oxy-fuel combustion technology. Metcalfe *et al.* (2010) reported cyclic carbonates synthesis from  $\text{CO}_2$  emitted from the oxy-fuel combustion reactor using bimetallic Al (III) salen complex in combination with TBAB as a catalyst. This catalyst has the ability to work at very low  $p$  ( $\text{CO}_2$ ) (i.e. 300–400 ppm) with high tolerance against the impurities present in waste flue gas (e.g.  $\text{SO}_x$ ,  $\text{NO}_x$ , and CO etc). Almost quantitative conversion of epoxide to cyclic carbonate was achieved at 26 °C after 5000 min using a semi-batch reactor. Therefore, in the future, Al(III) salen complex/TBAB can be used as a homogeneous catalyst for continuous cyclic carbonate synthesis from waste  $\text{CO}_2$  using a tube-in-tube gas/liquid reactor. High permeation of  $\text{CO}_2$  through the semi-permeable AF-2400 membrane combined with the high surface area to volume ratio in such continuous flow reactors may help to intensify the process at mild reaction conditions such as reduced pressure, less reaction time and improved yield of the product. This approach will not only

help to reduce the emission of greenhouse gases into the atmosphere but also has the benefit of making useful products from the industrial flue gases.

#### ***8.2.5 Heterogeneous catalysts for CO<sub>2</sub> cycloaddition to internal epoxides***

Until now, the catalyst systems developed for CO<sub>2</sub> cycloaddition to internal epoxides are in the homogeneous phase. However, in the future, heterogeneous catalyst systems should be investigated. Based upon this study, one likely route is via heterogenising of alkylammonium halides in combination with –OH, –COOH groups or other active catalyst systems such as chromium salen complexes with higher catalytic activity towards internal epoxides. Moreover, the development of the robust active heterogeneous catalyst with the ability to tolerate the impurities present in flue gases is desirable to start the industrial application of cyclic carbonate synthesis from waste CO<sub>2</sub> as a feedstock.

#### ***8.2.6 Sustainable and green epoxidation method***

In this study, a stereoselective method of (*R*)-limonene epoxidation was carried out using a relatively large amount of N-bromosuccinimide (NBS) which is not very ‘green’. The recycling of the NBS was also challenging. Therefore, future research needs to focus on recycling of NBS and finding more green epoxidation routes with the aim to achieve a high yield of *trans*-isomer.

## References

- Aida, T., Ishikawa, M. and Inoue, S. (1986) 'Alternating copolymerization of carbon dioxide and epoxide catalyzed by the aluminum porphyrin-quaternary organic salt or-triphenylphosphine system. Synthesis of polycarbonate with well-controlled molecular weight', *Macromolecules*, 19(1), pp. 8-13.
- Akinaga, H., Masaoka, N., Takagi, K., Ryu, I. and Fukuyama, T. (2014) 'Flow Carbonylation Using Near-stoichiometric Carbon Monoxide. Application to Heck Carbonylation', *Chemistry Letters*, 43(9), pp. 1456-1458.
- Amaral, A.J.R., Coelho, J.F.J. and Serra, A.C. (2013) 'Synthesis of bifunctional cyclic carbonates from CO<sub>2</sub> catalysed by choline-based systems', *Tetrahedron Letters*, 54(40), pp. 5518-5522.
- Ampelli, C., Perathoner, S. and Centi, G. (2015) 'CO<sub>2</sub> utilization: an enabling element to move to a resource-and energy-efficient chemical and fuel production', *Phil. Trans. R. Soc. A*, 373(2037), p. 20140177.
- Anthofer, M.H., Wilhelm, M.E., Cokoja, M., Markovits, I.I.E., Pöthig, A., Mink, J., Herrmann, W.A. and Kühn, F.E. (2014) 'Cycloaddition of CO<sub>2</sub> and epoxides catalyzed by imidazolium bromides under mild conditions: influence of the cation on catalyst activity', *Catalysis Science & Technology*, 4(6), pp. 1749-1758.
- Aravindan, V., Gnanaraj, J., Madhavi, S. and Liu, H.K. (2011) 'Lithium-ion conducting electrolyte salts for lithium batteries', *Chemistry—A European Journal*, 17(51), pp. 14326-14346.
- Arayachukiat, S., Kongtes, C., Barthel, A., Vummaleti, S.V.C., Poater, A., Wannakao, S., Cavallo, L. and D'Elia, V. (2017) 'Ascorbic acid as a bifunctional hydrogen bond donor for the synthesis of cyclic carbonates from CO<sub>2</sub> under ambient conditions', *ACS Sustainable Chemistry & Engineering*, 5(8), pp. 6392-6397.
- Archelas, A. and Furstoss (1997) 'Synthesis of enantiopure epoxides through biocatalytic approaches', *Annual Reviews in Microbiology*, 51(1), pp. 491-525.

Aresta, M. and Dibenedetto, A. (2004) 'The contribution of the utilization option to reducing the CO<sub>2</sub> atmospheric loading: research needed to overcome existing barriers for a full exploitation of the potential of the CO<sub>2</sub> use'. Elsevier.

Aresta, M. and Dibenedetto, A. (2007) 'Utilisation of CO<sub>2</sub> as a chemical feedstock: opportunities and challenges', *Dalton Transactions*, (28), pp. 2975-2992.

Aresta, M., Dibenedetto, A. and Angelini, A. (2013) 'Catalysis for the valorization of exhaust carbon: from CO<sub>2</sub> to chemicals, materials, and fuels. Technological use of CO<sub>2</sub>', *Chemical reviews*, 114(3), pp. 1709-1742.

Aresta, M., Dibenedetto, A., Nocito, F. and Pastore, C. (2006) 'A study on the carboxylation of glycerol to glycerol carbonate with carbon dioxide: the role of the catalyst, solvent and reaction conditions', *Journal of Molecular Catalysis A: Chemical*, 257(1-2), pp. 149-153.

Aresta, M., Dibenedetto, A. and Tommasi, I. (2000) 'Direct synthesis of organic carbonates by oxidative carboxylation of olefins catalyzed by metal oxides: developing green chemistry based on carbon dioxide', *Applied organometallic chemistry*, 14(12), pp. 799-802.

Aresta, M. and Quaranta, E. (1997) 'Carbon dioxide: a substitute for phosgene', *Chemtech*, 27(3).

Aresta, M., Quaranta, E. and Ciccarese, A. (1987) 'Direct synthesis of 1, 3-benzodioxol-2-one from styrene, dioxygen and carbon dioxide promoted by Rh (I)', *Journal of molecular catalysis*, 41(3), pp. 355-359.

Astruc, D. (2007) *Organometallic chemistry and catalysis*. Springer.

Bähr, M., Bitto, A. and Mülhaupt, R. (2012) 'Cyclic limonene dicarbonate as a new monomer for non-isocyanate oligo- and polyurethanes (NIPU) based upon terpenes', *Green Chemistry*, 14(5), pp. 1447-1454.

Bähr, M. and Mülhaupt, R. (2012) 'Linseed and soybean oil-based polyurethanes prepared via the non-isocyanate route and catalytic carbon dioxide conversion', *Green Chemistry*, 14(2), pp. 483-489.

- Barbarini, A., Maggi, R., Mazzacani, A., Mori, G., Sartori, G. and Sartorio, R. (2003) 'Cycloaddition of CO<sub>2</sub> to epoxides over both homogeneous and silica-supported guanidine catalysts', *Tetrahedron letters*, 44(14), pp. 2931-2934.
- Barrande, M., Bouchet, R. and Denoyel, R. (2007) 'Tortuosity of porous particles', *Analytical Chemistry*, 79(23), pp. 9115-9121.
- Barzagli, F., Mani, F. and Peruzzini, M. (2011) 'From greenhouse gas to feedstock: formation of ammonium carbamate from CO<sub>2</sub> and NH<sub>3</sub> in organic solvents and its catalytic conversion into urea under mild conditions', *Green Chemistry*, 13(5), pp. 1267-1274.
- Baxendale, I.R. and Ley, S.V. (2011) 'Syngas-mediated C–C bond formation in flow: Selective rhodium-catalysed hydroformylation of styrenes', *Synlett*, 2011(18), pp. 2648-2651.
- Beattie, C., North, M., Villuendas, P. and Young, C. (2013) 'Influence of temperature and pressure on cyclic carbonate synthesis catalyzed by bimetallic aluminum complexes and application to overall syn-bis-hydroxylation of alkenes', *The Journal of organic chemistry*, 78(2), pp. 419-426.
- Belfiore, L.A. (2003) *Transport Phenomena for Chemical Reactor Design*. John Wiley & Sons: New York, USA.
- Biogeneral <http://www.biogeneral.com/teflon-af/> (Accessed on 06-03-2019).
- Bourne, S.L., Koos, P., O'Brien, M., Martin, B., Schenkel, B., Baxendale, I.R. and Ley, S.V. (2011) 'The continuous-flow synthesis of styrenes using ethylene in a palladium-catalysed Heck cross-coupling reaction', *Synlett*, 2011(18), pp. 2643-2647.
- Bourne, S.L. and Ley, S.V. (2013) 'A Continuous Flow Solution to Achieving Efficient Aerobic Anti-Markovnikov Wacker Oxidation', *Advanced Synthesis & Catalysis*, 355(10), pp. 1905-1910.
- Brancour, C., Fukuyama, T., Mukai, Y., Skrydstrup, T. and Ryu, I. (2013) 'Modernized low pressure carbonylation methods in batch and flow employing common acids as a CO source', *Organic letters*, 15(11), pp. 2794-2797.

- Brzozowski, M., O'Brien, M., Ley, S.V. and Polyzos, A. (2015) 'Flow Chemistry: Intelligent processing of gas-liquid transformations using a tube-in-tube reactor', *Accounts of chemical research*, 48(2), pp. 349-362.
- Buchard, A., Kember, M.R., Sandeman, K.G. and Williams, C.K. (2011) 'A bimetallic iron (III) catalyst for CO<sub>2</sub>/epoxide coupling', *Chemical Communications*, 47(1), pp. 212-214.
- Buettner, H., Longwitz, L., Steinbauer, J., Wulf, C. and Werner, T. (2017) 'Recent developments in the synthesis of cyclic carbonates from epoxides and CO<sub>2</sub>', *Topics in Current Chemistry*, 375(3), p. 50.
- Büttner, H., Lau, K., Spannenberg, A. and Werner, T. (2015) 'Bifunctional one-component catalysts for the addition of carbon dioxide to epoxides', *ChemCatChem*, 7(3), pp. 459-467.
- Byrne, C.M., Allen, S.D., Lobkovsky, E.B. and Coates, G.W. (2004) 'Alternating copolymerization of limonene oxide and carbon dioxide', *Journal of the American Chemical Society*, 126(37), pp. 11404-11405.
- Cai, X., Zheng, J.L., Wärnå, J., Salmi, T., Taouk, B. and Leveneur, S. (2017) 'Influence of gas-liquid mass transfer on kinetic modeling: Carbonation of epoxidized vegetable oils', *Chemical Engineering Journal*, 313, pp. 1168-1183.
- Calo, V., Nacci, A., Monopoli, A. and Fanizzi, A. (2002) 'Cyclic carbonate formation from carbon dioxide and oxiranes in tetrabutylammonium halides as solvents and catalysts', *Organic letters*, 4(15), pp. 2561-2563.
- Campanella, A., Rustoy, E., Baldessari, A. and Baltanás, M.A. (2010) 'Lubricants from chemically modified vegetable oils', *Bioresource Technology*, 101(1), pp. 245-254.
- Canali, L. and Sherrington, D.C. (1999) 'Utilisation of homogeneous and supported chiral metal (salen) complexes in asymmetric catalysis', *Chemical Society Reviews*, 28(2), pp. 85-93.
- Castro-Osma, J.A., Lamb, K.J. and North, M. (2016) 'Cr (salophen) complex catalyzed cyclic carbonate synthesis at ambient temperature and pressure', *ACS Catalysis*, 6(8), pp. 5012-5025.

- Castro-Gómez, F., Salassa, G., Kleij, A.W. and Bo, C. (2013) 'A DFT study on the mechanism of the cycloaddition reaction of CO<sub>2</sub> to epoxides catalyzed by Zn (Salphen) complexes', *Chemistry–A European Journal*, 19(20), pp. 6289-6298.
- Castro-Osma, J.A., North, M. and Wu, X. (2016) 'Synthesis of cyclic carbonates catalysed by chromium and aluminium salphen complexes', *Chemistry–A European Journal*, 22(6), pp. 2100-2107.
- Cavani, F. and Teles, J.H. (2009) 'Sustainability in catalytic oxidation: an alternative approach or a structural evolution?', *ChemSusChem: Chemistry & Sustainability Energy & Materials*, 2(6), pp. 508-534.
- Chen, F., Dong, T., Xu, T., Li, X. and Hu, C. (2011) 'Direct synthesis of cyclic carbonates from olefins and CO<sub>2</sub> catalyzed by a MoO<sub>2</sub> (acac) 2-quaternary ammonium salt system', *Green Chemistry*, 13(9), pp. 2518-2524.
- Chen, X., Sun, J., Wang, J. and Cheng, W. (2012) 'Polystyrene-bound diethanolamine based ionic liquids for chemical fixation of CO<sub>2</sub>', *Tetrahedron letters*, 53(22), pp. 2684-2688.
- Chisholm, M.H. and Zhou, Z. (2004) 'Concerning the mechanism of the ring opening of propylene oxide in the copolymerization of propylene oxide and carbon dioxide to give poly (propylene carbonate)', *Journal of the American Chemical Society*, 126(35), pp. 11030-11039.
- Choi, J.-C., Kohno, K., Ohshima, Y., Yasuda, H. and Sakakura, T. (2008) 'Tin- or titanium-catalyzed dimethyl carbonate synthesis from carbon dioxide and methanol: Large promotion by a small amount of triflate salts', *Catalysis Communications*, 9(7), pp. 1630-1633.
- Ciriminna, R., Lomeli-Rodriguez, M., Carà, P.D., Lopez-Sanchez, J.A. and Pagliaro, M. (2014) 'Limonene: a versatile chemical of the bioeconomy', *Chemical Communications*, 50(97), pp. 15288-15296.
- Clegg, W., Harrington, R.W., North, M. and Pasquale, R. (2010a) 'Cyclic carbonate synthesis catalysed by bimetallic aluminium–salen complexes', *Chemistry–A European Journal*, 16(23), pp. 6828-6843.

Clegg, W., Harrington, R.W., North, M. and Pasquale, R. (2010b) 'Cyclic carbonate synthesis catalysed by bimetallic aluminium–salen complexes', *Chemistry-A European Journal*, 16(23), pp. 6828-6843.

Clegg, W., Harrington, R.W., North, M., Pizzato, F. and Villuendas, P. (2010c) 'Cyclic carbonates as sustainable solvents for proline-catalysed aldol reactions', *Tetrahedron: Asymmetry*, 21(9), pp. 1262-1271.

Clements, J.H. (2003) 'Reactive applications of cyclic alkylene carbonates', *Industrial & Engineering Chemistry Research*, 42(4), pp. 663-674.

Coates, G.W. and Moore, D.R. (2004) 'Discrete metal-based catalysts for the copolymerization of CO<sub>2</sub> and epoxides: discovery, reactivity, optimization, and mechanism', *Angewandte Chemie International Edition*, 43(48), pp. 6618-6639.

Cokoja, M., Wilhelm, M.E., Anthofer, M.H., Herrmann, W.A. and Kuehn, F.E. (2015) 'Synthesis of cyclic carbonates from epoxides and carbon dioxide by using organocatalysts', *ChemSusChem*, 8(15), pp. 2436-2454.

Comerford, J.W., Ingram, I.D.V., North, M. and Wu, X. (2015) 'Sustainable metal-based catalysts for the synthesis of cyclic carbonates containing five-membered rings', *Green Chemistry*, 17(4), pp. 1966-1987.

Cuesta-Aluja, L., Castilla, J. and Masdeu-Bultó, A.M. (2016) 'Aluminium salabza complexes for fixation of CO<sub>2</sub> to organic carbonates', *Dalton Transactions*, 45(37), pp. 14658-14667.

Da Silva, E., Dayoub, W., Mignani, G., Raoul, Y. and Lemaire, M. (2012) 'Propylene carbonate synthesis from propylene glycol, carbon dioxide and benzonitrile by alkali carbonate catalysts', *Catalysis Communications*, 29, pp. 58-62.

Darensbourg, D.J. (2007) 'Making plastics from carbon dioxide: salen metal complexes as catalysts for the production of polycarbonates from epoxides and CO<sub>2</sub>', *Chemical reviews*, 107(6), pp. 2388-2410.

Darensbourg, D.J., Mackiewicz, R.M. and Billodeaux, D.R. (2005) 'Pressure dependence of the carbon dioxide/cyclohexene oxide coupling reaction catalyzed by chromium salen

- complexes. Optimization of the comonomer-alternating enchainment pathway', *Organometallics*, 24(1), pp. 144-148.
- Darensbourg, D.J. and Phelps, A.L. (2005) 'Effective, selective coupling of propylene oxide and carbon dioxide to poly (propylene carbonate) using (salen) CrN<sub>3</sub> catalysts', *Inorganic chemistry*, 44(13), pp. 4622-4629.
- Darensbourg, D.J. and Yarbrough, J.C. (2002) 'Mechanistic aspects of the copolymerization reaction of carbon dioxide and epoxides, using a chiral salen chromium chloride catalyst', *Journal of the American Chemical Society*, 124(22), pp. 6335-6342.
- Darensbourg, D.J., Yarbrough, J.C., Ortiz, C. and Fang, C.C. (2003) 'Comparative kinetic studies of the copolymerization of cyclohexene oxide and propylene oxide with carbon dioxide in the presence of chromium salen derivatives. In situ FTIR measurements of copolymer vs cyclic carbonate production', *Journal of the American Chemical Society*, 125(25), pp. 7586-7591.
- de Jong, E., Higson, A., Walsh, P. and Wellisch, M. (2012) 'Bio-based chemicals value added products from biorefineries', *IEA Bioenergy, Task42 Biorefinery*.
- Decortes, A., Belmonte, M.M., Benet-Buchholz, J. and Kleij, A.W. (2010) 'Efficient carbonate synthesis under mild conditions through cycloaddition of carbon dioxide to oxiranes using a Zn (salphen) catalyst', *Chemical Communications*, 46(25), pp. 4580-4582.
- Decortes, A. and Kleij, A.W. (2011) 'Ambient fixation of carbon dioxide using a ZnII salphen catalyst', *ChemCatChem*, 3(5), pp. 831-834.
- Del Sesto, R.E., Corley, C., Robertson, A. and Wilkes, J.S. (2005) 'Tetraalkylphosphonium-based ionic liquids', *Journal of Organometallic Chemistry*, 690(10), pp. 2536-2542.
- Dengler, J.E., Lehenmeier, M.W., Klaus, S., Anderson, C.E., Herdtweck, E. and Rieger, B. (2011) 'A One-Component Iron Catalyst for Cyclic Propylene Carbonate Synthesis', *European Journal of Inorganic Chemistry*, 2011(3), pp. 336-343.
- Doğan, M., Abak, H. and Alkan, M. (2009) 'Adsorption of methylene blue onto hazelnut shell: kinetics, mechanism and activation parameters', *Journal of Hazardous Materials*, 164(1), pp. 172-181.

Du, Y., Kong, D.-L., Wang, H.-Y., Cai, F., Tian, J.-S., Wang, J.-Q. and He, L.-N. (2005) 'Sn-catalyzed synthesis of propylene carbonate from propylene glycol and CO<sub>2</sub> under supercritical conditions', *Journal of Molecular Catalysis A: Chemical*, 241(1-2), pp. 233-237.

Du, Y., Wang, J.-Q., Chen, J.-Y., Cai, F., Tian, J.-S., Kong, D.-L. and He, L.-N. (2006) 'A poly (ethylene glycol)-supported quaternary ammonium salt for highly efficient and environmentally friendly chemical fixation of CO<sub>2</sub> with epoxides under supercritical conditions', *Tetrahedron Letters*, 47(8), pp. 1271-1275.

Duranleau, R.G., Nieh, E.C.Y. and Knifton, J.F. (1987) 'Process for production of ethylene glycol and dimethyl carbonate'. Google Patents.

Eghbali, N. and Li, C.-J. (2007) 'Conversion of carbon dioxide and olefins into cyclic carbonates in water', *Green Chemistry*, 9(3), pp. 213-215.

Ema, T., Fukuhara, K., Sakai, T., Ohbo, M., Bai, F.-Q. and Hasegawa, J.-y. (2015) 'Quaternary ammonium hydroxide as a metal-free and halogen-free catalyst for the synthesis of cyclic carbonates from epoxides and carbon dioxide', *Catalysis Science & Technology*, 5(4), pp. 2314-2321.

Endalew, A.K., Kiros, Y. and Zanzi, R. (2011) 'Inorganic heterogeneous catalysts for biodiesel production from vegetable oils', *Biomass and Bioenergy*, In Press, Corrected Proof.

Etacheri, V., Marom, R., Elazari, R., Salitra, G. and Aurbach, D. (2011) 'Challenges in the development of advanced Li-ion batteries: a review', *Energy & Environmental Science*, 4(9), pp. 3243-3262.

Federsel, C., Jackstell, R. and Beller, M. (2010) 'Moderne Katalysatoren zur Hydrierung von Kohlendioxid', *Angewandte Chemie*, 122(36), pp. 6392-6395.

Ferreira, A., Ferreira, C., Teixeira, J.A. and Rocha, F. (2010) 'Temperature and solid properties effects on gas-liquid mass transfer', *Chemical Engineering Journal*, 162(2), pp. 743-752.

Fiorani, G., Stuck, M., Martín, C., Belmonte, M.M., Martín, E., Escudero-Adán, E.C. and Kleij, A.W. (2016) 'Catalytic Coupling of Carbon Dioxide with Terpene Scaffolds: Access to Challenging Bio-Based Organic Carbonates', *ChemSusChem*, 9(11), pp. 1304-1311.

- Firdaus, M., Montero de Espinosa, L. and Meier, M.A.R. (2011) 'Terpene-based renewable monomers and polymers via thiol–ene additions', *Macromolecules*, 44(18), pp. 7253-7262.
- Fuchs, M.A., Staudt, S., Altesleben, C., Walter, O., Zevaco, T.A. and Dinjus, E. (2014) 'A new air-stable zinc complex based on a 1, 2-phenylene-diimino-2-cyanoacrylate ligand as an efficient catalyst of the epoxide–CO<sub>2</sub> coupling', *Dalton Transactions*, 43(6), pp. 2344-2347.
- Fukuoka, S., Kawamura, M., Komiya, K., Tojo, M., Hachiya, H., Hasegawa, K., Aminaka, M., Okamoto, H., Fukawa, I. and Konno, S. (2003) 'A novel non-phosgene polycarbonate production process using by-product CO<sub>2</sub> as starting material', *Green Chemistry*, 5(5), pp. 497-507.
- Gabriele, B., Mancuso, R., Salerno, G., Veltri, L., Costa, M. and Dibenedetto, A. (2011) 'A General and Expedient Synthesis of 5- and 6-Membered Cyclic Carbonates by Palladium-Catalyzed Oxidative Carbonylation of 1, 2- and 1, 3-Diols', *ChemSusChem*, 4(12), pp. 1778-1786.
- George, J., Patel, Y., Pillai, S.M. and Munshi, P. (2009) 'Methanol assisted selective formation of 1, 2-glycerol carbonate from glycerol and carbon dioxide using nBu<sub>2</sub>SnO as a catalyst', *Journal of Molecular Catalysis A: Chemical*, 304(1-2), pp. 1-7.
- Geueke, B., Wagner, C.C. and Muncke, J. (2014) 'Food contact substances and chemicals of concern: a comparison of inventories', *Food Additives & Contaminants: Part A*, 31(8), pp. 1438-1450.
- Gillis, H.R., Stanssens, D., De Vos, R., Postema, A.R. and Randall, D. (1997) 'Polymeric foams'. Google Patents.
- Girard, A.-L., Simon, N., Zanatta, M., Marmitt, S., Gonçalves, P. and Dupont, J. (2014) 'Insights on recyclable catalytic system composed of task-specific ionic liquids for the chemical fixation of carbon dioxide', *Green Chemistry*, 16(5), pp. 2815-2825.
- Golemme, G., Nagy, J.B., Fonseca, A., Algieri, C. and Yampolskii, Y. (2003) '<sup>129</sup>Xe-NMR study of free volume in amorphous perfluorinated polymers: comparison with other methods', *Polymer*, 44(17), pp. 5039-5045.

- Guadagno, T. and Kazarian, S.G. (2004) 'High-pressure CO<sub>2</sub>-expanded solvents: simultaneous measurement of CO<sub>2</sub> sorption and swelling of liquid polymers with in-situ near-IR spectroscopy', *The Journal of Physical Chemistry B*, 108(37), pp. 13995-13999.
- Hajipour, A.R., Heidari, Y. and Kozehgary, G. (2015) 'Silica grafted ammonium salts based on DABCO as heterogeneous catalysts for cyclic carbonate synthesis from carbon dioxide and epoxides', *RSC Advances*, 5(29), pp. 22373-22379.
- Han, L., Choi, H.-J., Choi, S.-J., Liu, B. and Park, D.-W. (2011) 'Ionic liquids containing carboxyl acid moieties grafted onto silica: Synthesis and application as heterogeneous catalysts for cycloaddition reactions of epoxide and carbon dioxide', *Green Chemistry*, 13(4), pp. 1023-1028.
- Han, Z., Rong, L., Wu, J., Zhang, L., Wang, Z. and Ding, K. (2012) 'Catalytic hydrogenation of cyclic carbonates: a practical approach from CO<sub>2</sub> and epoxides to methanol and diols', *Angewandte Chemie*, 124(52), pp. 13218-13222.
- Hardman-Baldwin, A.M. and Mattson, A.E. (2014) 'Silanediol-Catalyzed Carbon Dioxide Fixation', *ChemSusChem*, 7(12), pp. 3275-3278.
- Hauenstein, O., Reiter, M., Agarwal, S., Rieger, B. and Greiner, A. (2016) 'Bio-based polycarbonate from limonene oxide and CO<sub>2</sub> with high molecular weight, excellent thermal resistance, hardness and transparency', *Green Chemistry*, 18(3), pp. 760-770.
- Hinde, R.J. (1997) 'Reaction Kinetics (Pilling, Michael J.; Seakins, Paul W.)'. ACS Publications.
- Hirose, T., Qu, S., Kodama, K. and Wang, X. (2018) 'Organocatalyst system for disubstituted carbonates from cycloaddition between CO<sub>2</sub> and internal epoxides', *Journal of CO<sub>2</sub> Utilization*, 24, pp. 261-265.
- Huang, S.-y., Liu, S.-g., Li, J.-p., Ning, Z., Wei, W.E.I. and Sun, Y.-h. (2007) 'Synthesis of cyclic carbonate from carbon dioxide and diols over metal acetates', *Journal of Fuel Chemistry and Technology*, 35(6), pp. 701-705.

Huang, S., Ma, J., Li, J., Zhao, N., Wei, W. and Sun, Y. (2008) 'Efficient propylene carbonate synthesis from propylene glycol and carbon dioxide via organic bases', *Catalysis Communications*, 9(2), pp. 276-280.

Hudgin, D.E. and Bendler, T. (2000) 'Handbook of polycarbonate science and technology'. Marcel Dekker, New York.

Inoue, S., Koinuma, H. and Tsuruta, T. (1969) 'Copolymerization of carbon dioxide and epoxide', *Journal of Polymer Science Part B: Polymer Letters*, 7(4), pp. 287-292.

IPCC ((2018)) '<https://www.co2.earth/global-co2-emissions>' (Accessed on 06-03-2019).

Jähnisch, K., Baerns, M., Hessel, V., Ehrfeld, W., Haverkamp, V., Löwe, H., Wille, C. and Guber, A. (2000) 'Direct fluorination of toluene using elemental fluorine in gas/liquid microreactors', *Journal of Fluorine Chemistry*, 105(1), pp. 117-128.

Jutz, F., Andanson, J.-M. and Baiker, A. (2010) 'Ionic liquids and dense carbon dioxide: a beneficial biphasic system for catalysis', *Chemical reviews*, 111(2), pp. 322-353.

Jutz, F., Buchard, A., Kember, M.R., Fredriksen, S.B. and Williams, C.K. (2011) 'Mechanistic investigation and reaction kinetics of the low-pressure copolymerization of cyclohexene oxide and carbon dioxide catalyzed by a dizinc complex', *Journal of the American Chemical Society*, 133(43), pp. 17395-17405.

Jutz, F., Grunwaldt, J.-D. and Baiker, A. (2008) 'Mn (III)(salen)-catalyzed synthesis of cyclic organic carbonates from propylene and styrene oxide in "supercritical" CO<sub>2</sub>', *Journal of Molecular Catalysis A: Chemical*, 279(1), pp. 94-103.

Kawahara, A., Sadatomi, M., Nei, K. and Matsuo, H. (2011) 'Characteristics of two-phase flows in a rectangular microchannel with a T-junction type gas-liquid mixer', *Heat Transfer Engineering*, 32(7-8), pp. 585-594.

Kawanami, H., Sasaki, A., Matsui, K. and Ikushima, Y. (2003) 'A rapid and effective synthesis of propylene carbonate using a supercritical CO<sub>2</sub>-ionic liquid system', *Chemical Communications*, (7), pp. 896-897.

- Kember, M.R., Buchard, A. and Williams, C.K. (2011) 'Catalysts for CO<sub>2</sub>/epoxide copolymerisation', *Chemical Communications*, 47(1), pp. 141-163.
- Kim, H.S., Kim, J.J., Kim, H. and Jang, H.G. (2003) 'Imidazolium zinc tetrahalide-catalyzed coupling reaction of CO<sub>2</sub> and ethylene oxide or propylene oxide', *Journal of Catalysis*, 220(1), pp. 44-46.
- Klaewkla, R., Arend, M. and Hoelderich, W.F. (2011) *A review of mass transfer controlling the reaction rate in heterogeneous catalytic systems*. INTECH Open Access Publisher.
- Kleij, A.W., North, M. and Urakawa, A. (2017) 'CO<sub>2</sub> catalysis', *ChemSusChem*, 10(6), pp. 1036-1038.
- Koos, P., Gross, U., Polyzos, A., O'Brien, M., Baxendale, I. and Ley, S.V. (2011) 'Teflon AF-2400 mediated gas-liquid contact in continuous flow methoxycarbonylations and in-line FTIR measurement of CO concentration', *Organic & biomolecular chemistry*, 9(20), pp. 6903-6908.
- Kozak, J.A., Wu, J., Su, X., Simeon, F., Hatton, T.A. and Jamison, T.F. (2013) 'Bromine-catalyzed conversion of CO<sub>2</sub> and epoxides to cyclic carbonates under continuous flow conditions', *Journal of the American Chemical Society*, 135(49), pp. 18497-18501.
- Kristufek, S.L., Wacker, K.T., Tsao, Y.-Y.T., Su, L. and Wooley, K.L. (2017) 'Monomer design strategies to create natural product-based polymer materials', *Natural product reports*, 34(4), pp. 433-459.
- Kupracz, L. and Kirschning, A. (2013) 'Multiple organolithium generation in the continuous flow synthesis of amitriptyline', *Advanced Synthesis & Catalysis*, 355(17), pp. 3375-3380.
- Kuznetsov, V.A., Pervova, M.G. and Pestov, A.V. (2013) 'Synthesis of alkylene carbonates in ionic liquid', *Russian Journal of Organic Chemistry*, 12(49), pp. 1859-1860.
- Langanke, J., Greiner, L. and Leitner, W. (2013) 'Substrate dependent synergetic and antagonistic interaction of ammonium halide and polyoxometalate catalysts in the synthesis of cyclic carbonates from oleochemical epoxides and CO<sub>2</sub>', *Green Chemistry*, 15(5), pp. 1173-1182.

- Laugel, G., Rocha, C.C., Massiani, P., Onfroy, T. and Launay, F. (2013) 'Homogeneous and Heterogeneous Catalysis for the Synthesis of Cyclic and Polymeric Carbonates from CO<sub>2</sub> and Epoxides: A Mechanistic Overview', *Advanced Chemistry Letters*, 1(3), pp. 195-214.
- Lehenmeier, M.W., Bruckmeier, C., Klaus, S., Dengler, J.E., Deglmann, P., Ott, A.K. and Rieger, B. (2011) 'Differences in Reactivity of Epoxides in the Copolymerisation with Carbon Dioxide by Zinc-Based Catalysts: Propylene Oxide versus Cyclohexene Oxide', *Chemistry—A European Journal*, 17(32), pp. 8858-8869.
- Lente, G., Fábíán, I. and Poë, A.J. (2005) 'A common misconception about the Eyring equation', *New journal of chemistry*, 29(6), pp. 759-760.
- Levenspiel, O. (1999) 'Chemical reaction engineering', *Industrial & engineering chemistry research*, 38(11), pp. 4140-4143.
- Li, F., Xiao, L., Xia, C. and Hu, B. (2004) 'Chemical fixation of CO<sub>2</sub> with highly efficient ZnCl<sub>2</sub>/[BMIm] Br catalyst system', *Tetrahedron letters*, 45(45), pp. 8307-8310.
- Liu, M., Liang, L., Liang, T., Lin, X., Shi, L., Wang, F. and Sun, J. (2015a) 'Cycloaddition of CO<sub>2</sub> and epoxides catalyzed by dicationic ionic liquids mediated metal halide: Influence of the dication on catalytic activity', *Journal of Molecular Catalysis A: Chemical*, 408, pp. 242-249.
- Liu, M., Liu, B., Zhong, S., Shi, L., Liang, L. and Sun, J. (2015b) 'Kinetics and mechanistic insight into efficient fixation of CO<sub>2</sub> to epoxides over N-heterocyclic compound/ZnBr<sub>2</sub> catalysts', *Industrial & Engineering Chemistry Research*, 54(2), pp. 633-640.
- Liu, S., Suematsu, N., Maruoka, K. and Shirakawa, S. (2016a) 'Design of bifunctional quaternary phosphonium salt catalysts for CO<sub>2</sub> fixation reaction with epoxides under mild conditions', *Green Chemistry*, 18(17), pp. 4611-4615.
- Liu, X.-F., Song, Q.-W., Zhang, S. and He, L.-N. (2016b) 'Hydrogen bonding-inspired organocatalysts for CO<sub>2</sub> fixation with epoxides to cyclic carbonates', *Catalysis Today*, 263, pp. 69-74.

- Lokhat, D., Domah, A.K., Padayachee, K., Baboolal, A. and Ramjugernath, D. (2016) 'Gas-liquid mass transfer in a falling film microreactor: Effect of reactor orientation on liquid-side mass transfer coefficient', *Chemical Engineering Science*, 155, pp. 38-44.
- Löwe, H., Hessel, V., Löb, P. and Hubbard, S. (2006) 'Addition of secondary amines to  $\alpha$ ,  $\beta$ -unsaturated carbonyl compounds and nitriles by using microstructured reactors', *Organic process research & development*, 10(6), pp. 1144-1152.
- Lu, X.-B., Shi, L., Wang, Y.-M., Zhang, R., Zhang, Y.-J., Peng, X.-J., Zhang, Z.-C. and Li, B. (2006) 'Design of highly active binary catalyst systems for CO<sub>2</sub>/epoxide copolymerization: Polymer selectivity, enantioselectivity, and stereochemistry control', *Journal of the American Chemical Society*, 128(5), pp. 1664-1674.
- Lu, X.-B., Zhang, Y.-J., Liang, B., Li, X. and Wang, H. (2004) 'Chemical fixation of carbon dioxide to cyclic carbonates under extremely mild conditions with highly active bifunctional catalysts', *Journal of Molecular Catalysis A: Chemical*, 210(1-2), pp. 31-34.
- Lu, X.B. and Wang, Y. (2004) 'Highly active, binary catalyst systems for the alternating copolymerization of CO<sub>2</sub> and epoxides under mild conditions', *Angewandte Chemie International Edition*, 43(27), pp. 3574-3577.
- Luo, R., Zhou, X., Fang, Y. and Ji, H. (2015) 'Metal- and solvent-free synthesis of cyclic carbonates from epoxides and CO<sub>2</sub> in the presence of graphite oxide and ionic liquid under mild conditions: A kinetic study', *Carbon*, 82, pp. 1-11.
- Mallia, C.J. and Baxendale, I.R. (2015) 'The use of gases in flow synthesis', *Organic Process Research & Development*, 20(2), pp. 327-360.
- Martin, C., Fiorani, G. and Kleij, A.W. (2015) 'Recent advances in the catalytic preparation of cyclic organic carbonates', *Acs Catalysis*, 5(2), pp. 1353-1370.
- Martín, C. and Kleij, A.W. (2014) 'Comparing kinetic profiles between bifunctional and binary type of Zn (salen)-based catalysts for organic carbonate formation', *Beilstein journal of organic chemistry*, 10, p. 1817.

- Martin, C., Whiteoak, C.J., Martin, E., Belmonte, M.M., Escudero-Adán, E.C. and Kleij, A.W. (2014) 'Easily accessible bifunctional Zn (salpyr) catalysts for the formation of organic carbonates', *Catalysis Science & Technology*, 4(6), pp. 1615-1621.
- Martin, R. and Kleij, A.W. (2011) 'Myth or reality? Fixation of carbon dioxide into complex organic matter under mild conditions', *ChemSusChem*, 4(9), pp. 1259-1263.
- Martínez, J., Fernández-Baeza, J., Sánchez-Barba, L.F., Castro-Osma, J.A., Lara-Sánchez, A. and Otero, A. (2017) 'An Efficient and Versatile Lanthanum Heteroscorpionate Catalyst for Carbon Dioxide Fixation into Cyclic Carbonates', *ChemSusChem*, 10(14), pp. 2886-2890.
- Melendez, J., North, M. and Pasquale, R. (2007) 'Synthesis of cyclic carbonates from atmospheric pressure carbon dioxide using exceptionally active aluminium (salen) complexes as catalysts', *European journal of inorganic chemistry*, 2007(21), pp. 3323-3326.
- Melendez, J., North, M. and Villuendas, P. (2009) 'One-component catalysts for cyclic carbonate synthesis', *Chemical Communications*, (18), pp. 2577-2579.
- Meléndez, J., North, M., Villuendas, P. and Young, C. (2011) 'One-component bimetallic aluminium (salen)-based catalysts for cyclic carbonate synthesis and their immobilization', *Dalton Transactions*, 40(15), pp. 3885-3902.
- Mercadante, M.A. and Leadbeater, N.E. (2011) 'Continuous-flow, palladium-catalysed alkoxy carbonylation reactions using a prototype reactor in which it is possible to load gas and heat simultaneously', *Organic & biomolecular chemistry*, 9(19), pp. 6575-6578.
- Metcalfe, I.S., North, M., Pasquale, R. and Thursfield, A. (2010) 'An integrated approach to energy and chemicals production', *Energy & Environmental Science*, 3(2), pp. 212-215.
- Metcalfe, I.S., North, M. and Villuendas, P. (2013) 'Influence of reactor design on cyclic carbonate synthesis catalysed by a bimetallic aluminium (salen) complex', *Journal of CO<sub>2</sub> Utilization*, 2, pp. 24-28.
- Moore, D.R., Cheng, M., Lobkovsky, E.B. and Coates, G.W. (2003) 'Mechanism of the alternating copolymerization of epoxides and CO<sub>2</sub> using  $\beta$ -diiminate zinc catalysts: evidence for a bimetallic epoxide enchainment', *Journal of the American Chemical Society*, 125(39), pp. 11911-11924.

Motokura, K., Itagaki, S., Iwasawa, Y., Miyaji, A. and Baba, T. (2009) 'Silica-supported aminopyridinium halides for catalytic transformations of epoxides to cyclic carbonates under atmospheric pressure of carbon dioxide', *Green Chemistry*, 11(11), pp. 1876-1880.

Motokura, K., Itagaki, S., Iwasawa, Y., Miyaji, A. and Baba, T. (2014) 'Zinc-accelerated cycloaddition of carbon dioxide to styrene oxide catalyzed by pyrrolidinopyridinium iodides', *Topics in Catalysis*, 57(10-13), pp. 953-959.

Newman, S.G. and Jensen, K.F. (2013) 'The role of flow in green chemistry and engineering', *Green Chemistry*, 15(6), pp. 1456-1472.

'NIST database', (2018) *NIST database*: <http://webbook.nist.gov/chemistry/name-ser.html> (Accessed on 06-03-2019).

North, M. (2012) 'Synthesis of cyclic carbonates from epoxides and carbon dioxide using bimetallic aluminium (salen) complexes', *ARKIVOC: Online Journal of Organic Chemistry*.

North, M. and Pasquale, R. (2009) 'Mechanism of cyclic carbonate synthesis from epoxides and CO<sub>2</sub>', *Angewandte Chemie*, 121(16), pp. 2990-2992.

North, M., Pizzato, F. and Villuendas, P. (2009a) 'Organocatalytic, asymmetric aldol reactions with a sustainable catalyst in a green solvent', *ChemSusChem*, 2(9), pp. 862-865.

North, M., Villuendas, P. and Young, C. (2009b) 'A Gas-Phase Flow Reactor for Ethylene Carbonate Synthesis from Waste Carbon Dioxide', *Chemistry—A European Journal*, 15(43), pp. 11454-11457.

North, M., Villuendas, P. and Young, C. (2012) 'Inter- and intramolecular phosphonium salt cocatalysis in cyclic carbonate synthesis catalysed by a bimetallic aluminium (salen) complex', *Tetrahedron letters*, 53(22), pp. 2736-2740.

North, M., Wang, B. and Young, C. (2011) 'Influence of flue gas on the catalytic activity of an immobilized aluminium (salen) complex for cyclic carbonate synthesis', *Energy & Environmental Science*, 4(10), pp. 4163-4170.

North, M. and Young, C. (2011) 'Reducing the cost of production of bimetallic aluminium catalysts for the synthesis of cyclic carbonates', *ChemSusChem*, 4(11), pp. 1685-1693.

O'Brien, M., Taylor, N., Polyzos, A., Baxendale, I.R. and Ley, S.V. (2011) 'Hydrogenation in flow: Homogeneous and heterogeneous catalysis using Teflon AF-2400 to effect gas-liquid contact at elevated pressure', *Chemical Science*, 2(7), pp. 1250-1257.

Omae, I. (2012) 'Recent developments in carbon dioxide utilization for the production of organic chemicals', *Coordination Chemistry Reviews*, 256(13-14), pp. 1384-1405.

Paddock, R.L. and Nguyen, S.T. (2001) 'Chemical CO<sub>2</sub> fixation: Cr (III) salen complexes as highly efficient catalysts for the coupling of CO<sub>2</sub> and epoxides', *Journal of the American Chemical Society*, 123(46), pp. 11498-11499.

Paddock, R.L. and Nguyen, S.T. (2004) 'Chiral (salen) Co III catalyst for the synthesis of cyclic carbonates', *Chemical Communications*, (14), pp. 1622-1623.

Parker, H.L., Sherwood, J., Hunt, A.J. and Clark, J.H. (2014) 'Cyclic carbonates as green alternative solvents for the Heck reaction', *ACS Sustainable Chemistry & Engineering*, 2(7), pp. 1739-1742.

Pastre, J.C., Browne, D.L. and Ley, S.V. (2013) 'Flow chemistry syntheses of natural products', *Chemical Society Reviews*, 42(23), pp. 8849-8869.

Pazuki, G.R. and Pahlavanzadeh, H. (2005) 'Correlation and Prediction of the Solubility of CO<sub>2</sub> in a Mixture of Organic Solution Solvents', *Theoretical Foundations of Chemical Engineering*, 39(3), pp. 240-245.

Peng, J. and Deng, Y. (2001) 'Cycloaddition of carbon dioxide to propylene oxide catalyzed by ionic liquids', *New Journal of Chemistry*, 25(4), pp. 639-641.

Peppel, W.J. (1958) 'Preparation and properties of the alkylene carbonates', *Industrial & Engineering Chemistry*, 50(5), pp. 767-770.

Pescarmona, P.P. and Taherimehr, M. (2012) 'Challenges in the catalytic synthesis of cyclic and polymeric carbonates from epoxides and CO<sub>2</sub>', *Catalysis Science & Technology*, 2(11), pp. 2169-2187.

Pohorecki, R. and Možeński, C. (1998a) 'A new absorbent for carbon dioxide and hydrogen sulphide absorption process', *Chemical Engineering and Processing: Process Intensification*, 37(1), pp. 69-78.

Pohorecki, R. and Možeński, C. (1998b) 'A new absorbent for carbon dioxide and hydrogen sulphide absorption process1', *Chemical Engineering and Processing: Process Intensification*, 37(1), pp. 69-78.

Polyzos, A., O'Brien, M., Petersen, T.P., Baxendale, I.R. and Ley, S.V. (2011) 'The continuous-flow synthesis of carboxylic acids using CO<sub>2</sub> in a tube-in-tube gas permeable membrane reactor', *Angewandte Chemie*, 123(5), pp. 1222-1225.

Qin, J., Wang, P., Li, Q., Zhang, Y., Yuan, D. and Yao, Y. (2014) 'Catalytic production of cyclic carbonates mediated by lanthanide phenolates under mild conditions', *Chemical Communications*, 50(75), pp. 10952-10955.

Ramidi, P., Gerasimchuk, N., Gartia, Y., Felton, C.M. and Ghosh, A. (2013) 'Synthesis and characterization of Co (III) amidoamine complexes: influence of substituents of the ligand on catalytic cyclic carbonate synthesis from epoxide and carbon dioxide', *Dalton Transactions*, 42(36), pp. 13151-13160.

Rehman, A., Eze, V.C., Resul, M.F.M.G. and Harvey, A. (2018a) 'Kinetics and mechanistic investigation of epoxide/CO<sub>2</sub> cycloaddition by a synergistic catalytic effect of pyrrolidinopyridinium iodide and zinc halides', *Journal of Energy Chemistry*.

Rehman, A., Fernandez, A.M.L., Resul, M.F.M.G. and Harvey, A. (2018b) 'Kinetic investigations of styrene carbonate synthesis from styrene oxide and CO<sub>2</sub> using a continuous flow tube-in-tube gas-liquid reactor', *Journal of CO<sub>2</sub> Utilization*, 24, pp. 341-349.

Ritchie, C.D. (1972) 'Nucleophilic reactivities toward cations', *Accounts of Chemical Research*, 5(10), pp. 348-354.

Roshan, K.R., Jose, T., Kim, D., Cherian, K.A. and Park, D.W. (2014) 'Microwave-assisted one pot-synthesis of amino acid ionic liquids in water: simple catalysts for styrene carbonate synthesis under atmospheric pressure of CO<sub>2</sub>', *Catalysis Science & Technology*, 4(4), pp. 963-970.

- Roshan, K.R., Mathai, G., Kim, J., Tharun, J., Park, G.-A. and Park, D.-W. (2012) 'A biopolymer mediated efficient synthesis of cyclic carbonates from epoxides and carbon dioxide', *Green Chemistry*, 14(10), pp. 2933-2940.
- Saha, P. and Chowdhury, S. (2011) 'Insight into adsorption thermodynamics', in *Thermodynamics*. InTech.
- Sakai, T., Tsutsumi, Y. and Ema, T. (2008) 'Highly active and robust organic–inorganic hybrid catalyst for the synthesis of cyclic carbonates from carbon dioxide and epoxides', *Green Chemistry*, 10(3), pp. 337-341.
- Sakakura, T., Choi, J.-C. and Yasuda, H. (2007) 'Transformation of carbon dioxide', *Chemical Reviews*, 107(6), pp. 2365-2387.
- Sakakura, T. and Kohno, K. (2009) 'The synthesis of organic carbonates from carbon dioxide', *Chemical Communications*, (11), pp. 1312-1330.
- Sastri, S.R.S., Mohanty, S. and Rao, K.K. (1997) 'A new method for predicting critical volumes of organic compounds', *Fluid phase equilibria*, 129(1-2), pp. 49-59.
- Satterfield, C.N. (1991) 'Heterogeneous catalysis in industrial practice'.
- Schaffner, B., Schaffner, F., Verevkin, S.P. and Borner, A. (2010) 'Organic carbonates as solvents in synthesis and catalysis', *Chemical reviews*, 110(8), pp. 4554-4581.
- Schimpf, V., Ritter, B.S., Weis, P., Parison, K. and Mülhaupt, R. (2017) 'High purity limonene dicarbonate as versatile building block for sustainable non-isocyanate polyhydroxyurethane thermosets and thermoplastics', *Macromolecules*, 50(3), pp. 944-955.
- Seki, T., Grunwaldt, J.-D. and Baiker, A. (2008) 'In situ attenuated total reflection infrared spectroscopy of imidazolium-based room-temperature ionic liquids under “supercritical” CO<sub>2</sub>', *The Journal of Physical Chemistry B*, 113(1), pp. 114-122.
- Selva, M., Caretto, A., Noè, M. and Perosa, A. (2014) 'Carbonate phosphonium salts as catalysts for the transesterification of dialkyl carbonates with diols. The competition between cyclic carbonates and linear dicarbonate products', *Organic & biomolecular chemistry*, 12(24), pp. 4143-4155.

- Seo, U.R. and Chung, Y.K. (2014) 'Poly (4-vinylimidazolium) s/Diazabicyclo [5.4. 0] undec-7-ene/Zinc (II) Bromide-Catalyzed Cycloaddition of Carbon Dioxide to Epoxides', *Advanced Synthesis & Catalysis*, 356(9), pp. 1955-1961.
- Shaikh, A.-A.G. and Sivaram, S. (1996) 'Organic carbonates', *Chemical reviews*, 96(3), pp. 951-976.
- Shaikh, R.R., Pornpraprom, S. and D'Elia, V. (2017) 'Catalytic strategies for the cycloaddition of pure, diluted, and waste CO<sub>2</sub> to epoxides under ambient conditions', *ACS Catalysis*, 8(1), pp. 419-450.
- Shen, Y.M., Duan, W.L. and Shi, M. (2003) 'Phenol and Organic Bases Co-Catalyzed Chemical Fixation of Carbon Dioxide with Terminal Epoxides to Form Cyclic Carbonates', *Advanced Synthesis & Catalysis*, 345(3), pp. 337-340.
- Shi, T.-Y., Wang, J.-Q., Sun, J., Wang, M.-H., Cheng, W.-G. and Zhang, S.-J. (2013) 'Efficient fixation of CO<sub>2</sub> into cyclic carbonates catalyzed by hydroxyl-functionalized poly (ionic liquids)', *RSC Advances*, 3(11), pp. 3726-3732.
- Sibaouih, A., Ryan, P., Leskelä, M., Rieger, B. and Repo, T. (2009) 'Facile synthesis of cyclic carbonates from CO<sub>2</sub> and epoxides with cobalt (II)/onium salt based catalysts', *Applied Catalysis A: General*, 365(2), pp. 194-198.
- Song, B., Guo, L., Zhang, R., Zhao, X., Gan, H., Chen, C., Chen, J., Zhu, W. and Hou, Z. (2014) 'The polymeric quaternary ammonium salt supported on silica gel as catalyst for the efficient synthesis of cyclic carbonate', *Journal of CO<sub>2</sub> Utilization*, 6, pp. 62-68.
- Srivastava, R., Bennur, T.H. and Srinivas, D. (2005) 'Factors affecting activation and utilization of carbon dioxide in cyclic carbonates synthesis over Cu and Mn peraza macrocyclic complexes', *Journal of Molecular Catalysis A: Chemical*, 226(2), pp. 199-205.
- Steinbauer, J., Kubis, C., Ludwig, R. and Werner, T. (2018) 'Mechanistic Study on the Addition of CO<sub>2</sub> to Epoxides Catalyzed by Ammonium and Phosphonium Salts: A Combined Spectroscopic and Kinetic Approach', *ACS Sustainable Chemistry & Engineering*.

- Steiner, D., Ivison, L., Goralski, C.T., Appell, R.B., Gojkovic, J.R. and Singaram, B. (2002) 'A facile and efficient method for the kinetic separation of commercially available cis- and trans-limonene epoxide', *Tetrahedron: Asymmetry*, 13(21), pp. 2359-2363.
- Su, Y., Chen, G., Zhao, Y. and Yuan, Q. (2009) 'Intensification of liquid–liquid two-phase mass transfer by gas agitation in a microchannel', *AIChE journal*, 55(8), pp. 1948-1958.
- Sun, J., Cheng, W., Yang, Z., Wang, J., Xu, T., Xin, J. and Zhang, S. (2014) 'Superbase/cellulose: an environmentally benign catalyst for chemical fixation of carbon dioxide into cyclic carbonates', *Green Chemistry*, 16(6), pp. 3071-3078.
- Sun, J., Fujita, S.-i., Bhanage, B.M. and Arai, M. (2004a) 'Direct oxidative carboxylation of styrene to styrene carbonate in the presence of ionic liquids', *Catalysis communications*, 5(2), pp. 83-87.
- Sun, J., Fujita, S.-i., Zhao, F. and Arai, M. (2004b) 'Synthesis of styrene carbonate from styrene oxide and carbon dioxide in the presence of zinc bromide and ionic liquid under mild conditions', *Green Chemistry*, 6(12), pp. 613-616.
- Sun, J., Fujita, S.-I., Zhao, F. and Arai, M. (2005a) 'A highly efficient catalyst system of ZnBr<sub>2</sub>/n-Bu<sub>4</sub>NI for the synthesis of styrene carbonate from styrene oxide and supercritical carbon dioxide', *Applied Catalysis A: General*, 287(2), pp. 221-226.
- Sun, J., Fujita, S.-i., Zhao, F., Hasegawa, M. and Arai, M. (2005b) 'A direct synthesis of styrene carbonate from styrene with the Au/SiO<sub>2</sub>–ZnBr<sub>2</sub>/Bu<sub>4</sub>NBr catalyst system', *Journal of Catalysis*, 230(2), pp. 398-405.
- Sun, J., Han, L., Cheng, W., Wang, J., Zhang, X. and Zhang, S. (2011) 'Efficient Acid–Base Bifunctional Catalysts for the Fixation of CO<sub>2</sub> with Epoxides under Metal- and Solvent-Free Conditions', *ChemSusChem*, 4(4), pp. 502-507.
- Sun, J., Ren, J., Zhang, S. and Cheng, W. (2009) 'Water as an efficient medium for the synthesis of cyclic carbonate', *Tetrahedron Letters*, 50(4), pp. 423-426.
- Sun, J., Wang, J., Cheng, W., Zhang, J., Li, X., Zhang, S. and She, Y. (2012) 'Chitosan functionalized ionic liquid as a recyclable biopolymer-supported catalyst for cycloaddition of CO<sub>2</sub>', *Green Chemistry*, 14(3), pp. 654-660.

Sun, J., Zhang, S., Cheng, W. and Ren, J. (2008) 'Hydroxyl-functionalized ionic liquid: a novel efficient catalyst for chemical fixation of CO<sub>2</sub> to cyclic carbonate', *Tetrahedron Letters*, 49(22), pp. 3588-3591.

Sun, X., Lee, H., Lee, S. and Tan, K.L. (2013) 'Catalyst recognition of cis-1, 2-diols enables site-selective functionalization of complex molecules', *Nature Chemistry*, 5(9), pp. 790-795.

Supasitmongkol, S. and Styring, P. (2014) 'A single centre aluminium (III) catalyst and TBAB as an ionic organo-catalyst for the homogeneous catalytic synthesis of styrene carbonate', *Catalysis Science & Technology*, 4(6), pp. 1622-1630.

Taherimehr, M., Al-Amsyar, S.M., Whiteoak, C.J., Kleij, A.W. and Pescarmona, P.P. (2013) 'High activity and switchable selectivity in the synthesis of cyclic and polymeric cyclohexene carbonates with iron amino triphenolate catalysts', *Green chemistry*, 15(11), pp. 3083-3090.

Taherimehr, M., Decortes, A., Al-Amsyar, S.M., Lueangchaichaweng, W., Whiteoak, C.J., Escudero-Adán, E.C., Kleij, A.W. and Pescarmona, P.P. (2012) 'A highly active Zn (salphen) catalyst for production of organic carbonates in a green CO<sub>2</sub> medium', *Catalysis Science & Technology*, 2(11), pp. 2231-2237.

Takahashi, T., Watahiki, T., Kitazume, S., Yasuda, H. and Sakakura, T. (2006) 'Synergistic hybrid catalyst for cyclic carbonate synthesis: Remarkable acceleration caused by immobilization of homogeneous catalyst on silica', *Chemical communications*, (15), pp. 1664-1666.

Tamura, M., Honda, M., Nakagawa, Y. and Tomishige, K. (2014) 'Direct conversion of CO<sub>2</sub> with diols, aminoalcohols and diamines to cyclic carbonates, cyclic carbamates and cyclic ureas using heterogeneous catalysts', *Journal of Chemical Technology & Biotechnology*, 89(1), pp. 19-33.

Tharun, J., Kim, D.W., Roshan, R., Hwang, Y. and Park, D.-W. (2013) 'Microwave assisted preparation of quaternized chitosan catalyst for the cycloaddition of CO<sub>2</sub> and epoxides', *Catalysis Communications*, 31, pp. 62-65.

Toda, Y., Komiyama, Y., Kikuchi, A. and Suga, H. (2016) 'Tetraarylphosphonium salt-catalyzed carbon dioxide fixation at atmospheric pressure for the synthesis of cyclic carbonates', *ACS Catalysis*, 6(10), pp. 6906-6910.

Urry, D.W. (1982) 'Henry Eyring (1901–1981): A 20th century physical chemist and his models', *Mathematical Modelling*, 3(6), pp. 503-522.

Veljković, V.B., Stamenković, O.S., Todorović, Z.B., Lazić, M.L. and Skala, D.U. (2009) 'Kinetics of sunflower oil methanolysis catalyzed by calcium oxide', *Fuel*, 88(9), pp. 1554-1562.

Vignesh, H.B. and Muralidharan, K. (2013) 'Zn (II), Cd (II) and Cu (II) complexes of 2, 5-bis {N-(2, 6-diisopropylphenyl) iminomethyl} pyrrole: synthesis, structures and their high catalytic activity for efficient cyclic carbonate synthesis', *Dalton transactions (Cambridge, England: 2003)*, 42(4), pp. 1238-1248.

Villa de P, A.L., Sels, B.F., De Vos, D.E. and Jacobs, P.A. (1999a) *Am. J. Org. Chem.*, 64(19), pp. 7267-7270.

Villa de P, A.L., Sels, B.F., De Vos, D.E. and Jacobs, P.A. (1999b) 'A heterogeneous tungsten catalyst for epoxidation of terpenes and tungsten-catalyzed synthesis of acid-sensitive terpene epoxides', *The Journal of Organic Chemistry*, 64(19), pp. 7267-7270.

Wang, J.-L., Wang, J.-Q., He, L.-N., Dou, X.-Y. and Wu, F. (2008) 'A CO<sub>2</sub>/H<sub>2</sub>O<sub>2</sub>-tunable reaction: direct conversion of styrene into styrene carbonate catalyzed by sodium phosphotungstate/n-Bu<sub>4</sub>NBr', *Green Chemistry*, 10(11), pp. 1218-1223.

Wang, J.-Q., Cheng, W.-G., Sun, J., Shi, T.-Y., Zhang, X.-P. and Zhang, S.-J. (2014a) 'Efficient fixation of CO<sub>2</sub> into organic carbonates catalyzed by 2-hydroxymethyl-functionalized ionic liquids', *RSC Advances*, 4(5), pp. 2360-2367.

Wang, J.-Q., Dong, K., Cheng, W.-G., Sun, J. and Zhang, S.-J. (2012) 'Insights into quaternary ammonium salts-catalyzed fixation carbon dioxide with epoxides', *Catalysis Science & Technology*, 2(7), pp. 1480-1484.

Wang, J.-Q., Kong, D.-L., Chen, J.-Y., Cai, F. and He, L.-N. (2006) 'Synthesis of cyclic carbonates from epoxides and carbon dioxide over silica-supported quaternary ammonium salts under supercritical conditions', *Journal of Molecular Catalysis A: Chemical*, 249(1-2), pp. 143-148.

- Wang, J.-Q., Yue, X.-D., Cai, F. and He, L.-N. (2007) 'Solventless synthesis of cyclic carbonates from carbon dioxide and epoxides catalyzed by silica-supported ionic liquids under supercritical conditions', *Catalysis Communications*, 8(2), pp. 167-172.
- Wang, J. and Zhang, Y. (2016) 'Boronic acids as hydrogen bond donor catalysts for efficient conversion of CO<sub>2</sub> into organic carbonate in water', *ACS Catalysis*, 6(8), pp. 4871-4876.
- Wang, J.T., Zhu, Q., Lu, X.L. and Meng, Y.Z. (2005) 'ZnGA–MMT catalyzed the copolymerization of carbon dioxide with propylene oxide', *European polymer journal*, 41(5), pp. 1108-1114.
- Wang, L., Lin, L., Zhang, G., Kodama, K., Yasutake, M. and Hirose, T. (2014b) 'Synthesis of cyclic carbonates from CO<sub>2</sub> and epoxides catalyzed by low loadings of benzyl bromide/DMF at ambient pressure', *Chemical Communications*, 50(94), pp. 14813-14816.
- Wang, L., Zhang, G., Kodama, K. and Hirose, T. (2016) 'An efficient metal- and solvent-free organocatalytic system for chemical fixation of CO<sub>2</sub> into cyclic carbonates under mild conditions', *Green Chemistry*, 18(5), pp. 1229-1233.
- Watile, R.A., Deshmukh, K.M., Dhake, K.P. and Bhanage, B.M. (2012) 'Efficient synthesis of cyclic carbonate from carbon dioxide using polymer anchored diol functionalized ionic liquids as a highly active heterogeneous catalyst', *Catalysis Science & Technology*, 2(5), pp. 1051-1055.
- Wenn, D.A., Shaw, J.E.A. and Mackenzie, B. (2003) 'A mesh microcontactor for 2-phase reactions', *Lab on a Chip*, 3(3), pp. 180-186.
- Whiteoak, C.J., Gjoka, B., Martin, E., Belmonte, M.M., Escudero-Adán, E.C., Zonta, C., Licini, G. and Kleij, A.W. (2012a) 'Reactivity control in iron (III) amino triphenolate complexes: comparison of monomeric and dimeric complexes', *Inorganic chemistry*, 51(20), pp. 10639-10649.
- Whiteoak, C.J., Kielland, N., Laserna, V., Escudero-Adán, E.C., Martin, E. and Kleij, A.W. (2013a) 'A powerful aluminum catalyst for the synthesis of highly functional organic carbonates', *Journal of the American Chemical Society*, 135(4), pp. 1228-1231.

- Whiteoak, C.J., Martin, E., Belmonte, M.M., Benet-Buchholz, J. and Kleij, A.W. (2012b) 'An Efficient Iron Catalyst for the Synthesis of Five- and Six-Membered Organic Carbonates under Mild Conditions', *Advanced Synthesis & Catalysis*, 354(2-3), pp. 469-476.
- Whiteoak, C.J., Martin, E., Escudero-Adán, E. and Kleij, A.W. (2013b) 'Stereochemical divergence in the formation of organic carbonates derived from internal epoxides', *Advanced Synthesis & Catalysis*, 355(11-12), pp. 2233-2239.
- Whiteoak, C.J., Nova, A., Maseras, F. and Kleij, A.W. (2012c) 'Merging sustainability with organocatalysis in the formation of organic carbonates by using CO<sub>2</sub> as a feedstock', *ChemSusChem*, 5(10), pp. 2032-2038.
- Wilhelm, M.E., Anthofer, M.H., Cokoja, M., Markovits, I.I.E., Herrmann, W.A. and Kühn, F.E. (2014) 'Cycloaddition of carbon dioxide and epoxides using pentaerythritol and halides as dual catalyst system', *ChemSusChem*, 7(5), pp. 1357-1360.
- Wilke, C.R. and Chang, P. (1955) 'Correlation of diffusion coefficients in dilute solutions', *AIChE Journal*, 1(2), pp. 264-270.
- Wu, G.-P., Wei, S.-H., Lu, X.-B., Ren, W.-M. and Darensbourg, D.J. (2010) 'Highly selective synthesis of CO<sub>2</sub> copolymer from styrene oxide', *Macromolecules*, 43(21), pp. 9202-9204.
- Wu, G.-P., Wei, S.-H., Ren, W.-M., Lu, X.-B., Li, B., Zu, Y.-P. and Darensbourg, D.J. (2011) 'Alternating copolymerization of CO<sub>2</sub> and styrene oxide with Co (iii)-based catalyst systems: differences between styrene oxide and propylene oxide', *Energy & Environmental Science*, 4(12), pp. 5084-5092.
- Wu, S.-S., Zhang, X.-W., Dai, W.-L., Yin, S.-F., Li, W.-S., Ren, Y.-Q. and Au, C.-T. (2008) 'ZnBr<sub>2</sub>-Ph<sub>4</sub>PI as highly efficient catalyst for cyclic carbonates synthesis from terminal epoxides and carbon dioxide', *Applied Catalysis A: General*, 341(1-2), pp. 106-111.
- Wu, X., Castro-Osma, J. and North, M. (2016) 'Synthesis of chiral cyclic carbonates via kinetic resolution of racemic epoxides and carbon dioxide', *Symmetry*, 8(1), p. 4.
- Wu, X. and North, M. (2017) 'A Bimetallic Aluminium (Salphen) Complex for the Synthesis of Cyclic Carbonates from Epoxides and Carbon Dioxide', *ChemSusChem*, 10(1), pp. 74-78.

Xie, H., Duan, H., Li, S. and Zhang, S. (2005) 'The effective synthesis of propylene carbonate catalyzed by silica-supported hexaalkylguanidinium chloride', *New Journal of Chemistry*, 29(9), pp. 1199-1203.

Xie, Y., Wang, T.T., Yang, R.X., Huang, N.Y., Zou, K. and Deng, W.Q. (2014) 'Efficient Fixation of CO<sub>2</sub> by a Zinc-Coordinated Conjugated Microporous Polymer', *ChemSusChem*, 7(8), pp. 2110-2114.

Xie, Y., Zhang, Z., Jiang, T., He, J., Han, B., Wu, T. and Ding, K. (2007) 'CO<sub>2</sub> cycloaddition reactions catalyzed by an ionic liquid grafted onto a highly cross-linked polymer matrix', *Angewandte Chemie International Edition*, 46(38), pp. 7255-7258.

Xiong, Y., Bai, F., Cui, Z., Guo, N. and Wang, R. (2013) 'Cycloaddition reaction of carbon dioxide to epoxides catalyzed by polymer-supported quaternary phosphonium salts', *Journal of Chemistry*, 2013.

Xu, B.-H., Wang, J.-Q., Sun, J., Huang, Y., Zhang, J.-P., Zhang, X.-P. and Zhang, S.-J. (2015) 'Fixation of CO<sub>2</sub> into cyclic carbonates catalyzed by ionic liquids: a multi-scale approach', *Green Chemistry*, 17(1), pp. 108-122.

Xu, Y., Lin, L., He, C.-T., Qin, J., Li, Z., Wang, S., Xiao, M. and Meng, Y. (2017) 'Kinetic and mechanistic investigation for the copolymerization of CO<sub>2</sub> and cyclohexene oxide catalyzed by trizinc complexes', *Polymer Chemistry*, 8(23), pp. 3632-3640.

Yadav, G.D. and Mehta, P.H. (1994) 'Heterogeneous catalysis in esterification reactions: preparation of phenethyl acetate and cyclohexyl acetate by using a variety of solid acidic catalysts', *Industrial & engineering chemistry research*, 33(9), pp. 2198-2208.

Yampolskii, Y.P. (2009) 'Amorphous perfluorinated membrane materials: structure, properties and application', *Russian Journal of General Chemistry*, 79(3), pp. 657-665.

Yao, C., Dong, Z., Zhao, Y. and Chen, G. (2015) 'Gas-liquid flow and mass transfer in a microchannel under elevated pressures', *Chemical Engineering Science*, 123, pp. 137-145.

Yao, C., Zhu, K., Liu, Y., Liu, H., Jiao, F. and Chen, G. (2017) 'Intensified CO<sub>2</sub> absorption in a microchannel reactor under elevated pressures', *Chemical Engineering Journal*, 319, pp. 179-190.

- Yasuda, H., He, L.-N., Takahashi, T. and Sakakura, T. (2006) 'Non-halogen catalysts for propylene carbonate synthesis from CO<sub>2</sub> under supercritical conditions', *Applied Catalysis A: General*, 298, pp. 177-180.
- Yoshida, M. and Ihara, M. (2004) 'Novel methodologies for the synthesis of cyclic carbonates', *Chemistry—A European Journal*, 10(12), pp. 2886-2893.
- Yu, K. and Jones, C.W. (2003) 'Silica-immobilized zinc  $\beta$ -diiminate catalysts for the copolymerization of epoxides and carbon dioxide', *Organometallics*, 22(13), pp. 2571-2580.
- Yue, H., Zhao, Y., Ma, X. and Gong, J. (2012) 'Ethylene glycol: properties, synthesis, and applications', *Chemical Society Reviews*, 41(11), pp. 4218-4244.
- Yue, J., Chen, G., Yuan, Q., Luo, L. and Gonthier, Y. (2007) 'Hydrodynamics and mass transfer characteristics in gas-liquid flow through a rectangular microchannel', *Chemical Engineering Science*, 62(7), pp. 2096-2108.
- Zhang, H., Hussam, A. and Weber, S.G. (2010) 'Properties and transport behavior of perfluorotripropylamine (FC-70)-doped amorphous teflon AF 2400 films', *Journal of the American Chemical Society*, 132(50), pp. 17867-17879.
- Zhang, J., Yueming, L.I.U., Ningning, L.I., Haihong, W.U., Xiaohong, L.I., Wei, X.I.E., Zhonglin, Z., Peng, W.U. and Mingyuan, H.E. (2008) 'Synthesis of Propylene Carbonate on a Bifunctional Titanosilicate Modified with Quaternary Ammonium Halides', *Chinese Journal of Catalysis*, 29(7), pp. 589-591.
- Zhang, X., Zhao, N., Wei, W. and Sun, Y. (2006) 'Chemical fixation of carbon dioxide to propylene carbonate over amine-functionalized silica catalysts', *Catalysis today*, 115(1-4), pp. 102-106.
- Zhao, Y., Tian, J.-S., Qi, X.-H., Han, Z.-N., Zhuang, Y.-Y. and He, L.-N. (2007) 'Quaternary ammonium salt-functionalized chitosan: An easily recyclable catalyst for efficient synthesis of cyclic carbonates from epoxides and carbon dioxide', *Journal of Molecular Catalysis A: Chemical*, 271(1-2), pp. 284-289.

Zhao, Y., Yao, C., Chen, G. and Yuan, Q. (2013) 'Highly efficient synthesis of cyclic carbonate with CO<sub>2</sub> catalyzed by ionic liquid in a microreactor', *Green Chemistry*, 15(2), pp. 446-452.

Zheng, J.L., Burel, F., Salmi, T., Taouk, B. and Leveneur, S.b. (2015) 'Carbonation of vegetable oils: Influence of mass transfer on reaction kinetics', *Industrial & Engineering Chemistry Research*, 54(43), pp. 10935-10944.

Zhou, H., Wang, G.-X., Zhang, W.-Z. and Lu, X.-B. (2015) 'CO<sub>2</sub> adducts of phosphorus ylides: highly active organocatalysts for carbon dioxide transformation', *ACS Catalysis*, 5(11), pp. 6773-6779.

Zhu, Y., Romain, C. and Williams, C.K. (2016) 'Sustainable polymers from renewable resources', *Nature*, 540(7633), p. 354.

## Chapter 9 Appendices

### Appendix A

#### *Solubility of CO<sub>2</sub> in epoxide (Styrene oxide)*

Time (sec)	Solubility (mmol of CO <sub>2</sub> per mol of epoxide)
0	0
180	28.11
280	36.25
380	39.84
480	47.05
580	48.72
680	46.3
780	45.54
980	45.61

Table 9.1 Summary of the solubility data of CO<sub>2</sub> in epoxide at 1 bar and 25 °C.

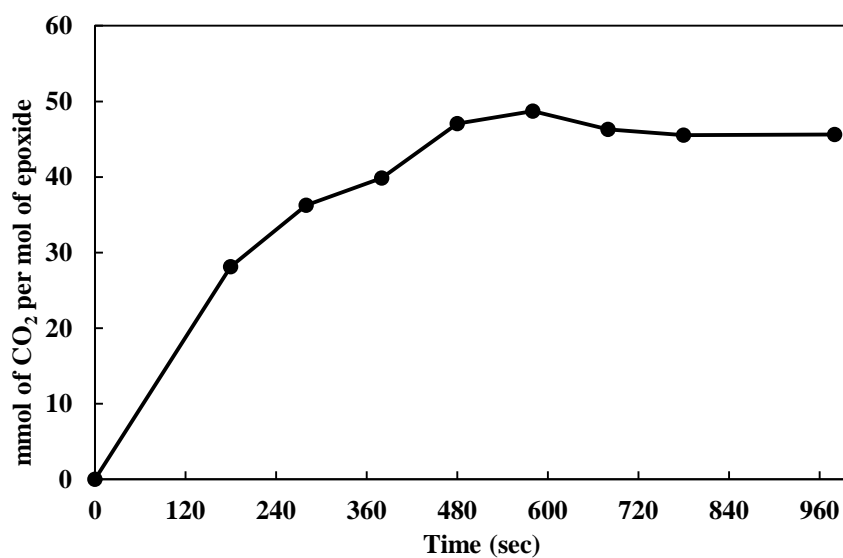


Figure 9.1 Solubility of CO<sub>2</sub> (mmol of CO<sub>2</sub> per mol of epoxide) in styrene oxide.

**Kinetic study of limonene carbonate (LC) synthesis from limonene oxide (LO) and CO<sub>2</sub> using tetrabutylammonium chloride (TBAC) as a homogeneous catalyst.**

***Order of the reaction w.r.t. [LO]***

LO [M]	ln [LO]	Average ( $k_{obs}$ ) (h <sup>-1</sup> )	ln ( $k_{obs}$ )
5.5	1.704	0.259	-1.350
4.5	1.504	0.219	-1.515
3.5	1.252	0.174	-1.744
2.5	0.916	0.139	-1.971
1.5	0.405	0.088	-2.427

Table 9.2 Summary of the kinetic experiments to determine the order of the reaction w.r.t epoxide (LO), (reaction conditions: (5.5–1.5) M LO in PC, 6 mol% TBAC, 120 °C, 40 bar  $p$  (CO<sub>2</sub>)).

Order	R <sup>2</sup>
0	0.9798
1 <sup>st</sup>	0.9909
2 <sup>nd</sup>	0.8359

Table 9.3 Curve fitting of the experimental data points obtained from the experiments by changing the concentration of epoxide (LO) (1.5–5.5) M in zero, first and second order plots.

**Order of the reaction w.r.t. [TBAC]**

TBAC mol%	TBAC [M]	Average ( $k_{obs}$ ) ( $h^{-1}$ )	ln[TBAC]	ln( $k_{obs}$ )
1.5	0.091	0.0137	-4.29	-4.290
3	0.183	0.0317	-3.451	-3.451
4.5	0.274	0.041	-3.194	-3.194
6	0.366	0.0632	-2.761	-2.761
7.5	0.457	0.0792	-2.535	-2.535

Table 9.4 Summary of the kinetic experiments to determine the order of the reaction w.r.t catalyst (TBAC), (reaction conditions: 4.5 M LO in PC, (1.5–7.5) mol% TBAC, 120 °C, 40 bar  $p$  ( $CO_2$ )).

Order	R <sup>2</sup>
0	0.9798
1 <sup>st</sup>	0.9909
2 <sup>nd</sup>	0.8359

Table 9.5 Curve fitting of the experimental data points obtained from the experiments by changing the concentration of epoxide (LO) (1.5–5.5) M in zero, first and second order plots.

### *Order of the reaction w.r.t. [CO<sub>2</sub>]*

<i>p</i> (CO <sub>2</sub> ) (bar)	ln <i>p</i> (CO <sub>2</sub> )	Average ( <i>k<sub>obs</sub></i> ) (h <sup>-1</sup> )	ln ( <i>k<sub>obs</sub></i> )
10	1	0.191	-3.958
20	1.30103	0.0303	-3.496
30	1.477	0.0475	-3.047
40	1.602	0.0632	-2.761

Table 9.6 Summary of the kinetic experiments to determine the order of the reaction w.r.t CO<sub>2</sub>, (reaction conditions: 4.5 M LO in PC, 6 mol% TBAC, 120 °C, 10–40 bar *p* (CO<sub>2</sub>)).

### *Effect of reaction temperature*

Temperature °C	Temperature K	Average ( <i>k<sub>obs</sub></i> ) (sec <sup>-1</sup> )	ln ( <i>k<sub>obs</sub></i> )	1/T (1/K)
100	373.15	6E-06	-12.08	0.00268
110	383.15	1E-05	-11.43	0.00261
120	393.15	2E-05	-10.93	0.00254
130	403.15	3E-05	-10.38	0.00248
140	413.15	4E-05	-10.1	0.00242

Table 9.7 Summary of the kinetic experiments to determine the activation energy for limonene carbonate formation, (reaction conditions: 4.5 M LO in PC, 6 mol% TBAC, (100–140) °C, 40 bar *p* (CO<sub>2</sub>)).

## Appendix B

**Kinetic study of styrene carbonate (SC) synthesis from styrene oxide (SO) and CO<sub>2</sub> in the presence of TBAB/ZnBr<sub>2</sub> as a binary homogeneous catalyst.**

### *Order of reaction w.r.t. [TBAB]*

TBAB [M]	ZnBr <sub>2</sub> [mM]	Average ( $k_{obs}$ ) (min <sup>-1</sup> )	ln [TBAB]	ln ( $k_{obs}$ )
0.025	6.5	0.0092	-3.68	-4.68
0.5	6.5	0.0173	-2.99	-4.06
0.75	6.5	0.0276	-2.59	-3.59
0.1	6.5	0.0401	-2.30	-3.22

Table 9.8 Summary of the kinetic experiments to determine the order of the reaction w.r.t catalyst (TBAB), (reaction conditions: 4.5 M SO [TBAB] (0.025–0.1) M and ZnBr<sub>2</sub> (6.5 mM) at 100 °C and 6 bar CO<sub>2</sub>).

### *Order of reaction w.r.t. [CO<sub>2</sub>]*

$p$ CO <sub>2</sub> (bar)	ln $p$ (CO <sub>2</sub> )	Average ( $k_{obs}$ ) (min <sup>-1</sup> )	ln ( $k_{obs}$ )
2	0.69	0.0091	-4.85
4	1.38	0.0123	-4.39
6	1.79	0.0167	-4.09
8	2.079	0.0212	-3.85

Table 9.9 Summary of the kinetic experiments to determine the order of the reaction w.r.t CO<sub>2</sub>, (reaction conditions: 4.5 M SO in PC, 0.1M TBAB, 100 °C, (2–8) bar  $p$  (CO<sub>2</sub>)).

**Order of reaction w.r.t. [ZnBr<sub>2</sub>]**

ZnBr <sub>2</sub> [M]	ln (ZnBr <sub>2</sub> )	Average ( <i>k<sub>obs</sub></i> ) (min <sup>-1</sup> )	ln ( <i>k<sub>obs</sub></i> )
0.00325	-5.72	0.0238	-3.73
0.0065	-5.03	0.0364	-3.31
0.013	-4.34	0.0463	-3.07
0.026	-3.64	0.0706	-2.65

Table 9.10 Summary of the kinetic experiments to determine the order of the reaction w.r.t ZnBr<sub>2</sub>, (reaction conditions: 4.5 M SO in PC, 0.1M TBAB, (3.25–26) mM ZnBr<sub>2</sub> 100 °C, (2–8) bar *p* (CO<sub>2</sub>)).

**Effect of temperature (using TBAB alone)**

°C	K	Average ( <i>k<sub>obs</sub></i> ) × 10 <sup>-5</sup> (sec <sup>-1</sup> )	ln ( <i>k<sub>obs</sub></i> )	1/T
90	363	1.67	-11	0.00275
100	373	2.25	-10.70	0.00268
110	383	4.42	-10.02	0.00261
120	393	5.58	-9.79	0.00254

Table 9.11 Summary of the kinetic experiments to determine the activation energy for styrene carbonate formation, (reaction conditions: 4.5 M SO in PC, 0.1 M TBAB, (90–120) °C, 6 bar *p* (CO<sub>2</sub>)).

*Effect of temperature (using TBAB in combination with ZnBr<sub>2</sub>)*

°C	K	Average ( $k_{obs}$ ) $10^{-5}(\text{sec}^{-1})$	$\ln(k_{obs})$	1/T
90	363	4.58	-9.99	0.00275
100	373	4.46	-10.02	0.00268
110	383	4.35	-10.04	0.00261
120	393	4.23	-10.07	0.00254

Table 9.12 Summary of the kinetic experiments to determine the activation energy for styrene carbonate formation, (reaction conditions: 4.5 M SO in PC, 0.1 M TBAB, 6.5 mM ZnBr<sub>2</sub>, (90–120) °C, 6 bar  $p$  (CO<sub>2</sub>)).

## Appendix C

**Kinetics study of styrene carbonate (SC) synthesis from styrene oxide (SO) and CO<sub>2</sub> using PPI/ZnI<sub>2</sub> as a binary homogeneous catalyst.**

### *Order of reaction w.r.t ZnI<sub>2</sub>*

PPI [mM]	Average ( $k_{obs}$ ) (min <sup>-1</sup> )	ln [PPI]	ln ( $k_{obs}$ )
76	0.0094	4.33	-4.66
152	0.0129	5.02	-4.35
228	0.0173	5.43	-4.05
304	0.0202	5.72	-3.90

Table 9.13 Summary of the kinetic experiments to determine the order of the reaction w.r.t PPI alone, (reaction conditions: 3.5 M SO, PPI (76–304) mM, at 100 °C and 10 bar  $p$  (CO<sub>2</sub>)).

### *Order of reaction w.r.t ZnI<sub>2</sub>*

ZnI <sub>2</sub> [mM]	PPI [mM]	Average ( $k_{obs}$ ) (min <sup>-1</sup> )	ln [ZnI <sub>2</sub> ]	ln ( $k_{obs}$ )
38	76	0.0069	3.637	-4.97
76	76	0.0125	4.330	-4.38
114	76	0.0152	4.736	-4.18
152	76	0.0171	5.023	-4.06

Table 9.14 Summary of the kinetic experiments to determine the order of the reaction w.r.t ZnI<sub>2</sub> using (38–152) mM ZnI<sub>2</sub> in combination with 76 mM PPI, (reaction conditions: 3.5 M SO at 100 °C and 10 bar  $p$  (CO<sub>2</sub>)).

### *Effect of CO<sub>2</sub> pressure*

Temperature °C	Average ( $k_{obs}$ )			
	PPI $\times 10^{-5}$ (sec <sup>-1</sup> )	PPI+ZnI <sub>2</sub> $\times 10^{-4}$ (sec <sup>-1</sup> )	PPI+ZnBr <sub>2</sub> $\times 10^{-4}$ (sec <sup>-1</sup> )	PPI+ZnCl <sub>2</sub> $\times 10^{-4}$ (sec <sup>-1</sup> )
100	1.2	2.1	1.6	1.16
110	2.5	2.75	2.63	1.66
120	5.0	4.13	3.9	2.33
130	6.6	6.03	5.53	3.33
140	12.3	8.58	7.61	5.83

Table 9.15 Summary of the kinetic experiments to determine the activation energy for styrene carbonate formation, (reaction conditions: 3.5 M SO in PC, 76 mM PPI, 38 mM ZnX<sub>2</sub>, (100–140) °C, 10 bar  $p$  (CO<sub>2</sub>)).

## Appendix D

### Kinetic study of Styrene carbonate (SC) synthesis from styrene oxide (SO) and CO<sub>2</sub> using heterogeneous SiO<sub>2</sub>-PPI catalyst

#### Calculations of Thiele's modulus and effectiveness factor

$$M_T = \frac{r_s}{3} \sqrt{\frac{k}{De}} \quad (1)$$

$$De = \frac{D_A \cdot \epsilon_p}{\tau_p} \quad (2)$$

Where:

$r_s$  = radius of spherical particle (cm)

$k$  = Pseudo-first order rate constant (s<sup>-1</sup>)

$De$  = effective diffusivity of the limiting reactant into the catalyst pores (cm<sup>2</sup>/sec)

$D_A$  = Molecular diffusion coefficient of the limiting reactant (cm<sup>2</sup>/sec)

$\epsilon_p$  = Porosity of the catalyst particles

$\tau_p$  = Tortuosity of the catalyst pores

$D_A$  can be calculated from the Wilke-Chang equation (Eq 3). The molar volume of the limiting reactant at its boiling point ( $V_{bA}$ ) was determined from the correlation between critical and molar volumes (Eq 4).

$$D_A = 7.4 \times 10^{-8} \frac{T \cdot (Mw)^{0.5}}{\eta \cdot (V_{bA})^{0.6}} \quad (3)$$

$$V_{bA} = \frac{V_c}{2.68} \quad (4)$$

Where:

$Mw$  = Molecular weight of the limiting reactant (g/mol)

$T$  = Reaction temperature (K)

$\eta$  = Viscosity of the reaction mixture (cP)

$V_{bA}$  = Molar volume of the limiting reactant at boiling point.

$V_c$  = Critical volume

$$V_{bA} = \frac{108}{2.68} = 40.29$$

$$D_A = 7.4 \times 10^{-8} \frac{413 \times (120.15)^{0.5}}{1.35 \times 10^{-2} (40.29)^{0.6}} = 2.702 \times 10^{-3}$$

$$De = \frac{2.702 \times 10^{-3} \times 0.73}{1.22} = 1.62 \times 10^{-3}$$

$$M_T = \frac{0.375}{3} \sqrt{\frac{0.0024}{1.62 \times 10^{-4}}}$$

$$M_T = 4.81 \times 10^{-5} (< 0.4)$$

***Order of reaction w.r.t [SO]***

SO [M]	Average ( $k_{obs}$ ) ( $\text{min}^{-1}$ )	ln [SO]	ln ( $k_{obs}$ )
1.5	0.0044	0.405	-5.42
2.5	0.0067	0.916	-5.00
3.5	0.0097	1.252	-4.63
4.5	0.0127	1.504	-4.36
5.5	0.0148	1.704	-4.21

Table 9.16 Summary of the kinetic experiments to determine the order of reaction w.r.t. [SO], (reaction conditions: (1.5–5.5) M SO, 76 mM SiO<sub>2</sub>-PPI, 140 °C, 10 bar  $p$  (CO<sub>2</sub>)).

***Order of reaction w.r.t CO<sub>2</sub> pressure***

SO [M]	Average ( $k_{obs}$ ) ( $\text{min}^{-1}$ )	ln [SO]	ln ( $k_{obs}$ )
2.5	0.0004	0.916	-7.82
5	0.0008	1.609	-7.13
7.5	0.0015	2.014	-6.50
10	0.0018	2.302	-6.31

Table 9.17 Summary of the kinetic experiments to determine the order of reaction w.r.t. CO<sub>2</sub> (reaction conditions: SO, 76 mM SiO<sub>2</sub>-PPI, 140 °C, (2.5–10) bar  $p$  (CO<sub>2</sub>)).

**Order of reaction w.r.t [SiO<sub>2</sub>-PPI]**

SiO <sub>2</sub> -PPI (g)	SO [M]	Average ( <i>k<sub>obs</sub></i> ) (min <sup>-1</sup> )	ln [SO]	ln ( <i>k<sub>obs</sub></i> )
0.29	38	0.00385	3.637	-5.36
0.58	76	0.0073	4.330	-4.96
0.89	114	0.0106	4.736	-4.54
1.16	152	0.014	5.023	-4.16

Table 9.18 Summary of the kinetic experiments to determine the order of reaction w.r.t. [SiO<sub>2</sub>-PPI], (reaction conditions: 3.5 M SO, (38–152) mM SiO<sub>2</sub>-PPI, 140 °C, 10 bar *p* (CO<sub>2</sub>)).